Design of biodegradable soil moisture sensor powered by bacteria charged paper batteries

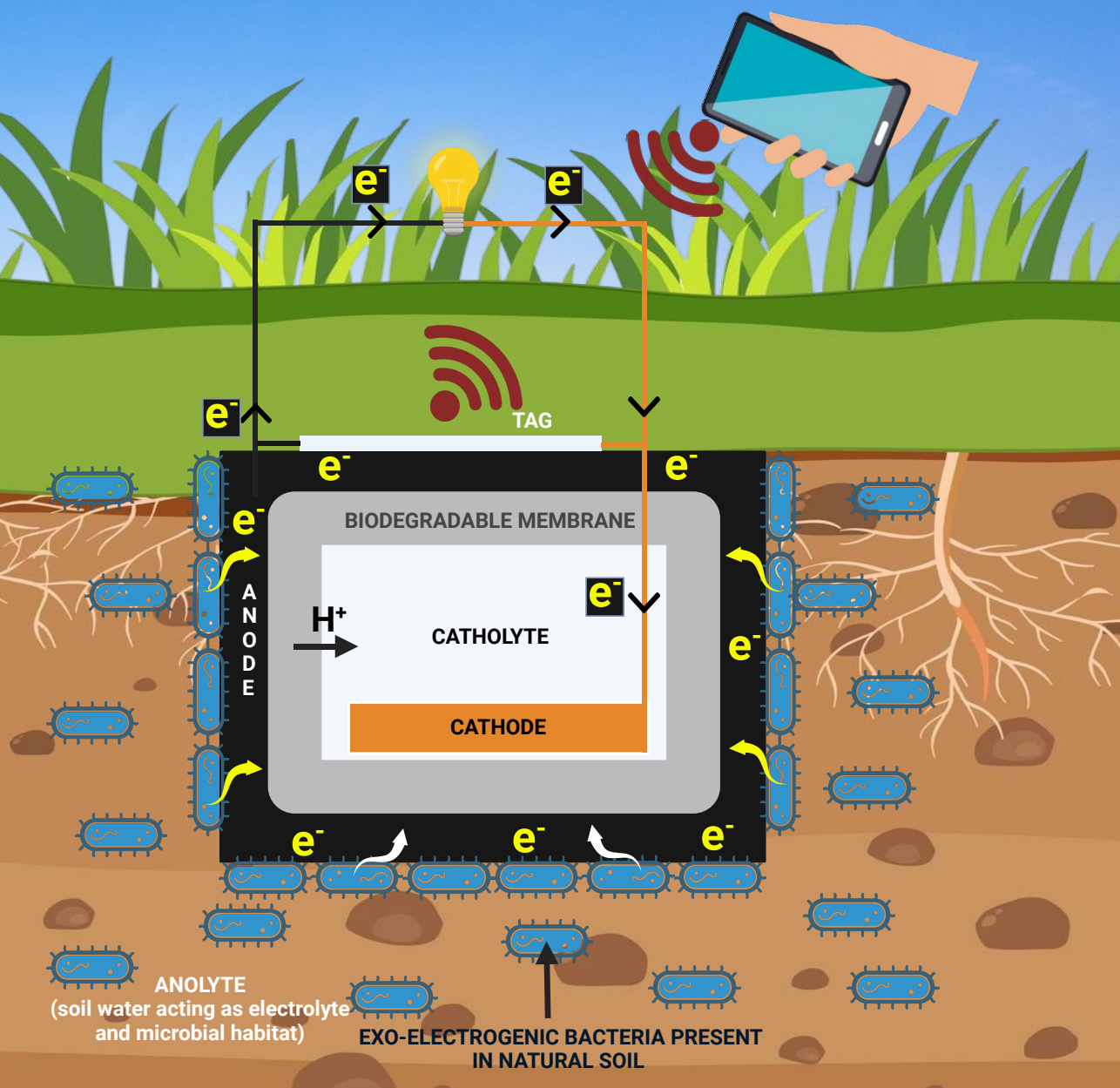

Sumit Moreshwar Meshram

Propositions

accompanying the dissertation

DESIGN OF SOIL MOISTURE SENSOR POWERED BY BACTERIA CHARGED PAPER BATTERIES

By

Sumit Moreshwar Meshram

1) Paper batteries offer feasible and biodegradable means to sense soil moisture for off-grid areas. [This thesis]

2) Electrode surface composed of Copper/Nickel (Cu/Ni) alloy reduces nitrate electrocatalytically better than Cu layer deposited on Ni. [This thesis]

3) Biopolymer-based foldable membranes can be used to build cheap, scalable Soil Moisture Sensing Systems (SMSSs). [This thesis]

4) A cubical battery design is optimal as it helps to maximize cathode surface area, minimizes anode-cathode distances, and enables efficient SMSSs orientation. [This thesis]

5) Like a kite in steady wind, innovators with all-black or all-white hair soar highest, mixed hair makes the ride bumpy.

6) Individual motivation can replace access to specialized resource needs for multidisciplinary research under one roof.

7) Today's water challenges need multidisciplinary solutions, but specialized labor market is still stuck in monodisciplinary frameworks.

8) Dreaming big and thinking beyond limits comes with its share of sacrifices and need to adapt.

9) Time is more valuable than money. You can get more money, but you cannot get more time.

10) A brain buffet is only possible when diverse cooks bring their own recipes to the table.

These propositions are regarded as opposable and defendable, and have been approved as such by the promotor Prof.dr.ir. N.C. van de Giesen and copromotor dr. S. Pande and copromotor dr.ir. L. Jourdin

DESIGN OF BIODEGRADABLE SOIL MOISTURE SENSOR POWERED BY BACTERIA CHARGED PAPER BATTERIES

Sumit Moreshwar MESHRAM

DESIGN OF BIODEGRADABLE SOIL MOISTURE SENSOR POWERED BY BACTERIA CHARGED PAPER BATTERIES

Dissertation

for the purpose of obtaining the degree of doctor

at Delft University of Technology

by the authority of the Rector Magnificus Prof.dr.ir. H. Bijl;

Chair of the Board for Doctorates to be defended publicly on

Tuesday 24, February 2026 at 15.00 o'clock

by

Sumit Moreshwar MESHRAM

Master of Technology in Civil Engineering, Indian Institute of Technology, Roorkee, India
born at Bhandara, Maharashtra, India

This dissertation has been approved by the promotors.

Composition of the doctoral committee:

Rector Magnificus	Chairperson
Prof. dr. ir. N.C. van de Giesen	Delft University of Technology, promotor
Dr. S. Pande	Delft University of Technology, co-promotor
Dr. L. Jourdin	Delft University of Technology, co-promotor

Independent members:

Prof. dr. ir. R. Uijlenhoet	Delft University of Technology
Prof. dr. ir. J. van Lier	Delft University of Technology
Prof. dr. A. Purushothaman Vellayani	University of Groningen
Dr. ir. D. Strik	Wageningen University and Research
Dr. ir. R. Lindeboom	Delft University of Technology, *reserve member*

TU Delft Delft University of Technology

महाराष्ट्र शासन
GOVERNMENT OF MAHARASHTRA
(INDIA)

This research was funded by the Ministry of Social Justice & Special Assistance Department, Government of Maharashtra, India. The opinions expressed in the document are of the authors only and in no way reflect the opinions of the Government of Maharashtra, India.

Keywords: Soil moisture sensing system, nitrate reduction, biodegradable membrane, origami, paper battery

Front & Back: Designed by Sumit Moreshwar Meshram using Biorender.com

ISBN/EAN: 978-94-6518-251-3 (for Ebook), 978-94-6384-909-8 (for Paperback/Softback)
An electronic version of this dissertation is available at
https://repository.tudelft.nl/

*Dedicated to **Dr. Babasaheb Ambedkar** (Social Reformer and Chief Architect of the Indian Constitution), to my late father **Mr. Moreshwar Madhav Meshram**, and to my mother **Mrs. Maya Moreshwar Meshram**.*

FOREWORD

This research began as more than an academic project, it was a personal mission. I grew up and worked in Maharashtra, the wealthiest state in India, which has the highest number of farmer suicides. From a young age, I read about these tragedies in newspapers. As part of the farming community, I witnessed the problems farmers faced and their decreasing interest in farming. The factors contributing to farmer suicides include inadequate irrigation, water scarcity, reliance on chemical fertilizers, crop failures, and lack of access to affordable modern technological tools.

During my time as an engineer in the Water Resources Department, impoverished and illiterate farmers approached me to transfer their farmland to a government project for compensation. They explained that agriculture had become unprofitable, citing the same reasons contributing to farmer suicides. Their educated descendants were reluctant to pursue farming as a career, so they no longer wished to continue agriculture. As an engineer and technocrat, I felt compelled to use my technical expertise for the farming community's welfare. I decided to resign from my government position and pursue agricultural research to improve farmers' lives and reduce suicides in my region.

When I arrived at TU Delft, I was motivated by a desire to assist farmers and advance environmental sustainability, which inspired the creation of an affordable, biodegradable system for sensing soil moisture. This project was based on the theory that soil moisture is linked to the activity of exo-electrogenic bacteria in the soil and is directly related to the current generated by these bacteria using soil microbial fuel cell technology. The goal of this research is not only to improve precision agriculture but also to reduce the environmental impact of deploying sensors. By incorporating concepts from materials science, biotechnology, electronics, and water resources engineering, this work reflects my commitment to merging scientific innovation with environmental responsibility. Throughout this journey, I faced moments of doubt and frustration due to the research's multidisciplinary nature, but I also felt hope and determination. Each experiment, setback, and progress reminded me that this work goes beyond personal ambition.

This thesis goes beyond its role as a mere technical document, embodying my belief that science can serve as an act of care. It is my aspiration that this work will not only advance the field of precision agriculture but also foster a profound respect for the delicate relationship we maintain with our planet. I extend my gratitude to all who have accompanied me on this journey - my supervisors, family, and friends for their steadfast support of this vision. This experience has been transformative, and I hope that, in some measure, this work will contribute to nurturing the future upon which we all rely. Furthermore, I trust that those who continue this research will remain mindful of its purpose, to enhance the well-being of smallholder farmers in developing countries, without seeking monetary gain.

Sumit Moreshwar Meshram

Delft, Netherlands, 2026

CONTENTS

SUMMARY

There is currently considerable global attention on improving the livelihoods of smallholder farmers, particularly in developing countries, through the adoption of sustainable water and soil management practices. This focus stems from the challenges these farmers encounter, including unpredictable rainfall, inadequate irrigation infrastructure, and limited access to essential agricultural technical equipment. Among various technical tools, soil moisture sensors are pivotal as they provide farmers with information on soil moisture levels, thereby facilitating the efficient use of water. However, existing sensors are often costly, unsustainable, and challenging to use in off-grid regions where most of these farms are situated. This study aims to develop low-cost, biodegradable, off-grid soil moisture sensing systems (SMSSs) for smallholder farmers of developing countries. It seeks to address the hypothesis that soil moisture sensors can be directly powered by electricity generated from the soil through soil microbial fuel cell (SMFC) technology, utilizing the bacteria present in the soil, with current production being directly proportional to the soil moisture.

The development of low-cost, biodegradable, off-grid SMSSs using soil moisture sensors for smallholder farmers represents a significant advancement in sustainable agriculture. Integrating SMFC to power these sensors address multiple challenges simultaneously. It not only provides farmers with crucial soil moisture data but also eliminates the need for external power sources, making it particularly suitable for remote and off-grid locations. It also provides uninterrupted power supply as it uses naturally available bacteria from soil. The biodegradable nature of these sensors aligns with environmental sustainability goals, reducing electronic waste and minimizing the ecological footprint of agricultural practices. Furthermore, it has the potential to revolutionize water management practices in smallholder farming. By providing soil moisture data, farmers can make informed decisions about irrigation, optimizing water usage and potentially increasing crop yields. This technology could improve water use efficiency, also the low-cost nature of these sensors makes it accessible to a broader range of farmers, potentially democratizing access to advanced agricultural technologies in developing regions..

This study explored the challenges faced by existing soil moisture sensing systems, with a particular emphasis on developing sensors that are low-cost, off-grid, biodegradable, and capable of autonomous in situ operation. The research aimed to determine the feasibility of designing a sensing system that incorporates all these desirable characteristics. By examining various aspects of soil moisture monitoring, the study sought to address the limitations of current technologies and propose innovative solutions. The investigation revealed that while individual design parameters could be met, creating a sensor that simultaneously satisfies all the desired criteria remains a significant challenge. Despite these challenges, the study identifies promising avenues for future development. Emerging technologies such as SMFC, paper batteries, origami, and papertronics offer potential pathways for creating more integrated and efficient SMSSs. These innovative approaches could potentially address multiple criteria simultaneously, paving the way for more sustainable, cost-effective, and autonomous soil moisture sensing solutions. As research in these areas progresses, it may become possible to overcome current limitations and develop SMSSs that more closely align with the ideal combination of features sought by researchers and practitioners in the field.

Paper batteries and SMFC represent a promising technological advancement with potential applications in various fields, including agriculture. However, it currently faces limitations in energy output and structural stability. Researchers are exploring innovative approaches to address these challenges, such as integrating multiple paper batteries using origami techniques with SMFC as both the paper batteries and SMFC are constructed based on similar concepts. They both have anode, cathode and a membrane in its construction. Protons move through the membrane, while electrons produced on anode travel externally to produce electricity. In addition SMFCs generate energy from microbes at an anaerobic anode, which break down organic material in the soil. This process enables electrons to be transferred to an aerobic cathode near the surface, with protons moving through the soil or a membrane. Although both systems use an anode–cathode–membrane configuration, they differ in their materials and energy sources. But by integrating both these technologies it can enhance both energy production and structural integrity. However several obstacles remain, including the fragility of stacked paper batteries, the risk of electrical short-circuits due to physical contact between the anode and cathode, toxic nature and design and practical complications associated with electron acceptors like potassium ferricyanide, and oxygen used in the preparation of these systems. To overcome these limitations, researchers are investigating alternative materials and designs which can overcome the issues associated with these electron acceptors.

One promising approach involves the incorporation of nitrates (NO_3^-) as electron acceptors in battery construction. Notably, NO_3^- that remain unutilized in these systems do not pose environmental harm, rather, they can be beneficial for agriculture, as unused NO_3^- may be repurposed as fertilizers for crops. However, the use of NO_3^- in battery construction necessitates specialized electrode (i.e. cathodes) capable of performing the electrocatalytic nitrate reduction (NO_3RR) reaction. To date, cathodes have been prepared using various metals and methods, specifically designed for the NO_3RR reaction. Various methods have been employed to design these electrodes for NO_3RR, but these methods are often costly, introduce contaminants, and require specialized technical expertise. To address these challenges, physical vapor deposition (PVD) methods were employed to prepare the electrode by depositing a thin copper (Cu) film on a nickel (Ni) surface. The study concluded that monometallic electrodes prepared using thin films are insufficient for effective NO_3RR. Instead, bimetallic Cu - Ni alloy electrodes are required to perform NO_3RR effectively.

In this study, the membranes, which are essential components of paper batteries and SMFCs, and which can be readily utilized in the design of SMSSs, were designed and manufactured. These membranes are pivotal in facilitating proton transfer across their structure, thereby enabling the efficient operation of these SMSSs. Although commercially available membranes such as Nafion are available, they pose several challenges that impede its widespread adoption. These challenges include high costs, susceptibility to biofouling, substrate losses, oxygen leakage, and complex manufacturing processes. To address these limitations, this study employed biodegradable biopolymers as alternative materials for membrane fabrication. Specifically, chitosan (CS) and polyvinyl alcohol (PVA) were selected as the primary biopolymers for this purpose. These materials offer several advantages over conventional membranes, including lower production costs and reduced environmental impact. By utilizing these biopolymers, the study aimed to develop membranes that can overcome the drawbacks associated with existing membranes while maintaining the necessary proton conductivity required for effective operation in paper batteries and SMFCs.

The development of paper battery using biodegradable membranes utilizing origami techniques signifies a substantial advancement in sustainable energy storage solutions,

particularly within the realm of SMFC technology. These innovative batteries, designed in both three-dimensional (3D) and two-dimensional (2D) configurations, present a promising approach to powering SMSSs in agriculture sector. The 3D cubical design was designed which is especially noteworthy, as it optimizes the surface area of both the anode and cathode and can be used with liquid catholyte, potentially enhancing the battery's power output and efficiency. The cubical shape of the 3D paper batteries offers additional benefits beyond increased surface area. Its geometric form allows for the seamless integration of wireless tags, which are crucial for wireless data transmission with the help of mobile phones. Moreover, the cubic structure facilitates the efficient stacking of multiple batteries, enabling scalable power solutions while maintaining proper orientation within the soil matrix. This design consideration is essential for ensuring optimal performance and longevity of the SMFC system across various soil conditions. The use of biodegradable materials in these paper batteries aligns with sustainable practices, minimizing environmental impact and potentially allowing for in-situ decomposition after the battery's useful life. These 3D paper batteries were tested using potassium ferro/ferricyanide as a redox couple and also in moist soil conditions. Additionally, 2D paper batteries were designed, utilizing oxygen as the electron acceptor.

The research demonstrates the feasibility of developing a cost-effective, off-grid, and biodegradable autonomous soil moisture sensing system using innovative technologies. This system combines paper battery and SMFC technologies, utilizing potassium ferricyanide, NO_3^-, or oxygen as electron acceptors. In the soil, organic molecules in the soil serve as electron donors and the exoelectrogenic bacteria in soil oxidize these molecules and facilitate the transfer of electrons to the anode, thereby transforming chemical energy into electrical energy. The system incorporates biodegradable CS/PVA membranes that function as proton exchange membranes, facilitating the movement of protons between the anode and cathode. This novel approach to soil moisture sensing offers several advantages over traditional methods. The use of biodegradable materials aligns with environmental sustainability goals, reducing the long-term impact of sensor deployment in agricultural and environmental monitoring applications. The off-grid nature of the system enables its use in remote locations without the need for external power sources, enhancing its versatility and applicability in various field conditions. Additionally, the low-cost aspect of this technology makes it accessible for widespread implementation, potentially revolutionizing soil moisture monitoring practices in agriculture, environmental science, and related fields.

SAMENVATTING

Er is momenteel aanzienlijke wereldwijde aandacht voor het verbeteren van het levensonderhoud van kleine boeren, vooral in ontwikkelingslanden, door de toepassing van duurzame water- en bodembeheerpraktijken. Deze focus komt voort uit de uitdagingen waarmee deze boeren worden geconfronteerd, zoals onvoorspelbare neerslag, inadequate irrigatie-infrastructuur en beperkte toegang tot essentiële agrarische technische apparatuur. Van de verschillende technische hulpmiddelen zijn bodemvochtensoren cruciaal, omdat deze boeren informatie geven over het bodemvochtgehalte en zo het waterverlies helpen verminderen. Bestaande sensoren zijn echter vaak duur, niet duurzaam en moeilijk te gebruiken in off-grid gebieden waar de meeste van deze boerderijen zich bevinden. Deze studie heeft tot doel goedkope, biologisch afbreekbare, off-grid bodemvochtdetectiesystemen (SMSSs) te ontwikkelen voor kleine boeren in ontwikkelingslanden. Men wil de hypothese onderzoeken dat bodemvochtensoren direct kunnen worden aangedreven door elektriciteit opgewekt uit de grond via bodem-microbiële brandstofceltechnologie (SMFC), waarbij de bacteriën in de bodem stroom opwekken die direct evenredig is met het bodemvocht.

De ontwikkeling van goedkope, biologisch afbreekbare, off-grid bodem vocht sensings systemen met bodemvochtensoren voor kleine boeren vertegenwoordigt een belangrijke vooruitgang in duurzame landbouw. Door SMFC te integreren om deze sensoren van stroom te voorzien, pakt de voorgestelde oplossing meerdere uitdagingen tegelijk aan. Deze aanpak biedt boeren niet alleen cruciale bodemvochtgegevens, maar elimineert ook de behoefte aan externe energiebronnen, wat bijzonder geschikt is voor afgelegen en off-grid locaties. Ze bieden bovendien een continu stroomvoorziening doordat natuurlijke bacteriën uit de bodem worden gebruikt. De biologisch afbreekbare aard van deze sensoren sluit aan bij milieudoelstellingen, vermindert elektronisch afval en verkleint de ecologische voetafdruk van landbouwpraktijken. Bovendien heeft deze innovatieve benadering het potentieel om irrigatiepraktijken in kleinschalige landbouw te revolutioneren. Door bodemvochtgegevens beschikbaar te stellen, kunnen boeren geïnformeerde beslissingen nemen over irrigatie, wat watergebruik optimaliseert en mogelijk de opbrengst verhoogt. Deze technologie kan waterverlies verminderen, en de lage kosten maken sensoren toegankelijk voor een breder scala aan boeren, wat de toegang tot geavanceerde agrarische technologieën in ontwikkelingsgebieden kan democratiseren. Deze studie pakt niet alleen directe landbouwproblemen aan, maar draagt ook bij aan bredere doelen van duurzame ontwikkeling en klimaatadaptatie in kwetsbare landbouwgemeenschappen.

In deze studie zijn de uitdagingen van bestaande bodemvochtsensorsystemen onderzocht, met bijzondere nadruk op het ontwikkelen van sensoren die goedkoop, off-grid, biologisch afbreekbaar en autonoom in situ kunnen functioneren. Het onderzoek had als doel de haalbaarheid te bepalen van een sensorsysteem dat al deze wenselijke kenmerken combineert. Door diverse aspecten van bodemvochtmonitoring te analyseren, poogde de studie de beperkingen van huidige technologieën aan te pakken en innovatieve oplossingen voor te stellen. De bevindingen tonen aan dat hoewel individuele ontwerpparameters haalbaar kunnen zijn, het creëren van een sensor die gelijktijdig aan alle gewenste criteria voldoet, een aanzienlijke uitdaging blijft. Ondanks deze obstakels identificeert de studie veelbelovende wegen voor verdere ontwikkeling. Opkomende technologieën zoals SMFC, papieren batterijen, origami-ontwerpen en papertronica bieden potentiële oplossingen voor meer geïntegreerde en efficiënte SMSSs. Deze innovatieve benaderingen kunnen meerdere criteria tegelijk

aanpakken, en zo de weg effenen naar duurzamere, kosteneffectievere en autonome bodemvochtsensoroplossingen. Naarmate het onderzoek op deze terreinen vordert, wordt het mogelijk om huidige beperkingen te overwinnen en SMSSs te ontwikkelen die beter aansluiten bij de ideale combinatie van kenmerken waar onderzoekers en praktijkmensen naar streven.

Papieren batterijen en SMFC vertegenwoordigen een veelbelovende technologische vooruitgang met toepassingen in diverse sectoren, waaronder de landbouw. Ze hebben echter momenteel beperkingen op het gebied van energie-output en structurele stabiliteit. Onderzoekers verkennen innovatieve benaderingen om deze uitdagingen aan te pakken, zoals het integreren van meerdere papieren batterijen via origamitechnieken met SMFC, aangezien zowel papieren batterijen als SMFC zijn opgebouwd volgens vergelijkbare principes. Beiden kennen een anode, kathode en membraan in hun constructie. In het systeem bewegen protonen door het membraan, terwijl elektronen die op de anode worden geproduceerd extern reizen om elektriciteit op te wekken. Bodem-microbiële brandstofcellen genereren energie van microben aan een anaerobe anode, die organisch materiaal in de bodem afbreken. Hierdoor kunnen elektronen worden overgedragen naar een aerobe kathode nabij het oppervlak, terwijl protonen door de bodem of een membraan bewegen. Hoewel beide systemen gebruikmaken van een anode–kathode–membrane configureuratie, verschillen zij in materialen en energiebronnen. Door beide technologieën te integreren kan zowel energieproductie als structurele integriteit verbeterd worden. Ondanks deze inspanningen blijven meerdere obstakels bestaan, zoals de kwetsbaarheid van gestapelde papieren batterijen, het risico van elektrische kortsluiting door fysieke aanraking tussen anode en kathode, het toxische karakter en ontwerp- en praktische complicaties rond elektronacceptoren zoals kalium ferricyanide en zuurstof bij de voorbereiding van deze systemen. Om deze beperkingen te overwinnen, onderzoeken onderzoekers alternatieve materialen en ontwerpen die de problemen rond electronacceptoren kunnen oplossen.

Een veelbelovende aanpak omvat de opname van nitraat (NO_3^-)als elektronacceptoren in batterijconstructie. NO_3^- fungeren als electronacceptoren en kunnen in deze context worden toegepast. Niet-gebruikte NO_3^- vormen geen milieuschade; ze kunnen zelfs gunstig zijn voor de landbouw, aangezien ongebruikte NO_3^- als meststof voor gewassen kunnen worden hergebruikt. Het gebruik van NO_3^- in batterijconstructie vereist echter gespecialiseerde elektroden (d.w.z. kathodes) die de electrocatalytische nitraat-reductiereactie (NO_3RR) kunnen uitvoeren. Tot nu toe zijn kathodes ontwikkeld met behulp van verschillende metalen en methoden, specifiek ontworpen voor NO_3RR, maar deze methoden zijn vaak kostbaar, brengen verontreinigingen met zich mee en vereisen gespecialiseerde technische expertise. Om deze uitdagingen aan te pakken, zijn fysieke dampafzettingsmethoden gebruikt om elektroden te bereiden door een dunne koperfilm op een nikkeloppervlak aan te brengen. De studie concludeerde dat monometallische elektroden, bereid met dunne films, onvoldoende effectief zijn voor NO_3RR; in plaats daarvan zijn bimetallische koper-nikkel legeringelektroden nodig om NO_3RR effectief uit te voeren.

In deze studie zijn membranen ontworpen - essentiële componenten van papieren batterijen en SMFCs - die direct kunnen worden toegepast in de constructie van SMSSs. Deze membranen zijn essentieel voor de protonoverdracht door hun structuur, wat een efficiënte werking van deze SMSSs mogelijk maakt. Hoewel commercieel verkrijgbare membranen zoals Nafion bestaan, vormen deze meerdere uitdagingen die hun brede toepassing belemmeren, zoals hoge kosten, gevoeligheid voor biofouling, verlies van substraten, zuurstoflekkage en complexe productieprocessen. Om deze beperkingen te overwinnen, heeft deze studie biologisch afbreekbare biopolymeren gebruikt als alternatieve membranen. Concreet werden

Chitosan en polyvinylalcohol geselecteerd als de primaire biopolymeren. Deze materialen bieden diverse voordelen ten opzichte van conventionele membranen, waaronder lagere productiekosten en verminderde milieu-impact. Door gebruik van deze biopolymeren streeft de studie ernaar membranen te ontwikkelen die de nadelen van bestaande membranen overwinnen, terwijl ze de noodzakelijke protongeleiding behouden voor effectieve werking in papieren batterijen en SMFCs.

De ontwikkeling van papieren batterijen met biologisch afbreekbare membranen onder gebruikmaking van origamitechnieken vormt een aanzienlijke vooruitgang in duurzame energieopslagoplossingen, met name binnen het domein van SMFC. Deze innovatieve batterijen-ontworpen in zowel driedimensionale (3D) als tweedimensionale (2D) configureuraties - bieden een veelbelovende aanpak voor het voeden van SMSSs voor bodembewaking in de landbouwsector. Het 3D-kubusontwerp is bijzonder opmerkelijk omdat het oppervlakte van zowel anode als kathode optimaliseert en kan worden gecombineerd met vloeibare catholyte, wat mogelijk de energie-output en efficiëntie verhoogt. De kubusvorm van de 3D-papieren batterijen biedt extra voordelen boven een groter oppervlak: de geometrie maakt naadloze integratie van draadloze tags mogelijk—cruciaal voor draadloze gegevensoverdracht via mobiele telefoons. Bovendien faciliteert de kubusstructuur efficiënte stapeling van meerdere batterijen, wat schaalbare energieoplossingen mogelijk maakt terwijl de juiste oriëntatie binnen de bodemmatrix behouden blijft. Dit ontwerpoverweging is essentieel voor het waarborgen van optimale prestaties en levensduur van het SMFC-systeem onder verschillende bodemcondities. Het gebruik van biologisch afbreekbaar materiaal in deze papieren batterijen sluit aan bij duurzame praktijken, vermindert milieueffecten en kan mogelijk afbraak op locatie toestaan nadat de batterij zijn levensduur heeft bereikt. Deze 3D-papieren batterijen zijn getest met kalium ferro/ferricyanide als redoxkoppel en ook in vochtige bodemomstandigheden, waarbij kalium ferricyanide dienstdoet als elektronacceptor. Daarnaast zijn 2D-papieren batterijen ontworpen waarbij zuurstof fungeert als elektronacceptor.

Het onderzoek toont de haalbaarheid aan van het ontwikkelen van een kosteneffectief, off-grid en biologisch afbreekbaar autonoom bodemvocht sensoring systeem met innovatieve technologieën. Dit systeem combineert papieren batterijen en SMFC-technologieën, waarbij kalium ferricyanide, nitraat of zuurstof dienen als elektronacceptoren. De elektrondonoren in deze opstelling zijn exo-electrogene bodem-bacteriën, die in staat zijn elektronen buiten hun cellen over te dragen. Het systeem maakt gebruik van biologisch afbreekbare chitosan/polyvinyl alcohol membranen die fungeren als proton-exchangemembranen, waardoor protonen tussen de anode en kathode kunnen bewegen. Deze nieuwe aanpak voor bodem bewaken biedt verschillende voordelen ten opzichte van traditionele methoden. Het gebruik van biologisch afbreekbare materialen sluit aan bij milieuduurzaamheidsdoelen, vermindert de impact van sensor deployments op lange termijn in landbouw- en milieumonitoringtoepassingen. Het off-grid karakter maakt het gebruik mogelijk op afgelegen locaties zonder externe stroombronnen, wat de veelzijdigheid en toepasbaarheid in diverse veldcondities vergroot. Bovendien maakt de lage kostprijs deze technologie toegankelijk voor brede implementatie, met potentieel om bodembewakingspraktijken in de landbouw, milieuwetenschappen en aanverwante gebieden te revolutioneren.

सारांश

सध्या जगभरात, विशेषतः विकसनशील देशांमध्ये, अल्पभूधारक शेतकऱ्यांचे जीवनमान सुधारण्याकडे मोठे लक्ष दिले जात आहे. या सुधारणांचा प्रयत्न शाश्वत पाणी आणि माती व्यवस्थापन पद्धती वापरून करण्यावर भर दिला जात आहे. यामागचे मुख्य कारण म्हणजे अल्पभूधारक शेतकऱ्यांना भेडसावणाऱ्या अनेक अडचणी. यामध्ये अनियमित पाऊस, अपुरी सिंचन व्यवस्था आणि शेतीसाठी आवश्यक तांत्रिक साधनांची मर्यादित उपलब्धता यांचा समावेश होतो. शेतीतील विविध तांत्रिक साधनांपैकी मातीतील ओलावा मोजणारे सेन्सर अत्यंत महत्त्वाचे आहेत. हे सेन्सर मातीतील ओलाव्याची माहिती शेतकऱ्यांना देतात, ज्यामुळे पाण्याचा योग्य आणि कार्यक्षम वापर करता येतो. मात्र सध्या उपलब्ध असलेले बहुतेक सेन्सर महागडे, पर्यावरणास अपायकारक आणि वीज नसलेल्या भागात वापरण्यास कठीण आहेत. बहुतेक लहान शेतजमिनी अशाच दुर्गम आणि वीजपुरवठा नसलेल्या भागात असतात. या संशोधनाचा मुख्य उद्देश विकसनशील देशांतील अल्पभूधारक शेतकऱ्यांसाठी स्वस्त, जैवविघटनशील आणि वीजेवर अवलंबून नसलेली मातीतील ओलावा मोजणारी प्रणाली विकसित करणे हा आहे. या संशोधनामागील मुख्य कल्पना अशी आहे की मातीतील ओलावा मोजणारे सेन्सर थेट मातीमधून तयार होणाऱ्या विजेवर चालू शकतात. ही वीज, मातीतील सूक्ष्मजीवांच्या मदतीने "माती सूक्ष्मजैव इंधन पेशी" या तंत्रज्ञानाद्वारे तयार होते. मातीतील ओलावा जितका जास्त, तितकी वीज निर्मिती जास्त हे या संकल्पनेचे मुख्य गृहितक आहे.

अल्पभूधारक शेतकऱ्यांसाठी स्वस्त, जैवविघटनशील आणि वीजेवर अवलंबून नसलेली मातीतील ओलावा मोजणारी प्रणाली विकसित करणे हे शाश्वत शेतीसाठी एक मोठे पाऊल आहे. या सेन्सरना ऊर्जा देण्यासाठी "माती सूक्ष्मजैव इंधन पेशी" तंत्रज्ञानाचा वापर केल्याने अनेक समस्या एकाच वेळी सोडवता येऊ शकतात . यामुळे शेतकऱ्यांना मातीतील ओलाव्याची महत्त्वाची माहिती मिळेल. तसेच बाह्य वीजपुरवठ्याची गरज नसल्यामुळे ही प्रणाली दूरच्या आणि वीज नसलेल्या भागांसाठी अतिशय उपयुक्त ठरेल. ही प्रणाली मातीतील नैसर्गिक जीवाणूंमुळे सतत वीज निर्माण करते, त्यामुळे अखंड वीजपुरवठा शक्य होतो. या सेन्सरचे जैवविघटनशील स्वरूप पर्यावरण संरक्षणाच्या दृष्टीने फायदेशीर आहे. यामुळे इलेक्ट्रॉनिक कचरा कमी होतो आणि शेतीमुळे होणारा पर्यावरणीय परिणामही कमी होतो. याशिवाय ही प्रणाली अल्पभूधारक शेतकऱ्यांच्या पाणी व्यवस्थापन पद्धतीत मोठा बदल घडवू शकते. मातीतील ओलाव्याची अचूक माहिती मिळाल्यामुळे शेतकरी सिंचनाबाबत योग्य निर्णय घेऊ शकतात. यामुळे पाण्याचा योग्य वापर होऊन पिकांचे उत्पादन वाढण्याची शक्यता आहे. तसेच हे तंत्रज्ञान पाण्याच्या वापराची कार्यक्षमता वाढवू शकते. तसेच हे सेन्सर स्वस्त असल्यामुळे अधिक शेतकरी याचा वापर करू शकतात. यामुळे विकसनशील देशांमध्ये आधुनिक शेती तंत्रज्ञान सर्वसामान्य शेतकऱ्यांसाठी उपलब्ध होऊ शकते.

या संशोधनात सध्याच्या मातीतील ओलावा मोजणाऱ्या प्रणालींच्या अडचणींचा सखोल अभ्यास करण्यात आला. विशेषतः स्वस्त, वीजेवर अवलंबून नसलेले, जैवविघटनशील आणि आपोआप कार्य करणारे सेन्सर विकसित करण्यावर भर देण्यात आला. या संशोधनाचा उद्देश असा होता की या सर्व गुणधर्मांचा समावेश असलेली एकच प्रणाली तयार करणे शक्य आहे का? हे तपासणे. मातीतील ओलावा मोजण्याच्या विविध पद्धतींचा अभ्यास करून विद्यमान तंत्रज्ञानातील मर्यादा ओळखण्यात आल्या. संशोधनातून असे आढळून आले की प्रत्येक गुणधर्म वेगवेगळा साध्य करता येतो. मात्र सर्व गुणधर्म एकाच सेन्सरमध्ये एकत्र आणणे हे अजूनही मोठे आव्हान आहे. तरीसुद्धा, भविष्यातील विकासासाठी काही आशादायक दिशा या संशोधनातून समोर आल्या आहेत. माती सूक्ष्मजैव इंधन पेशी, पेपर बॅटऱ्या, ओरिगामी आणि पेपरट्रॉनिक्ससारखी नवीन तंत्रज्ञाने यासाठी उपयुक्त ठरू शकतात. ही तंत्रज्ञाने एकत्र वापरल्यास अधिक कार्यक्षम, शाश्वत आणि स्वयंचलित माती ओलावा मोजणाऱ्या प्रणाली तयार होऊ शकतात.या क्षेत्रातील पुढील संशोधनामुळे सध्याच्या अडचणी दूर होऊन अधिक प्रभावी प्रणाली विकसित होऊ शकतील.

पेपर बॅटऱ्या आणि माती सूक्ष्मजैव इंधन पेशी ही तंत्रज्ञाने शेतीसह अनेक क्षेत्रांमध्ये वापरासाठी आशादायक मानली जात आहेत. मात्र सध्या या तंत्रज्ञानामध्ये वीज निर्मितीची क्षमता कमी असणे आणि रचनात्मक मजबुतीचा अभाव अशा मर्यादा आहेत. या अडचणी दूर करण्यासाठी संशोधक नवीन पद्धतींचा अभ्यास करत आहेत. यामध्ये ओरिगामी तंत्राचा वापर करून अनेक पेपर बॅटऱ्या एकत्र जोडणे आणि त्यांना माती सूक्ष्मजैव इंधन पेशी सोबत एकत्रित करणे याचा समावेश आहे. पेपर बॅटरी आणि माती सूक्ष्मजैव इंधन पेशी या दोन्हींची रचना जवळजवळ समान तत्त्वांवर आधारित असते. या दोन्ही प्रणालींमध्ये ॲनोड (धन अग्र), कॅथोड (ऋण अग्र) आणि मेम्ब्रेन (एक पडदा) असतो. या पडद्यामधून प्रोटॉन्स (धनायन) जातात. तर ॲनोडवर तयार झालेले इलेक्ट्रॉन्स (विद्युदणू) बाह्य मार्गाने प्रवास करून वीज निर्माण करतात. माती सूक्ष्मजैव इंधन पेशी मध्ये मातीतील सेंद्रिय पदार्थ विघटित करणारे सूक्ष्मजीव (जीवाणू) वीज निर्मितीसाठी वापरले जातात. हे जीवाणू ऑक्सिजन नसलेल्या ॲनोड भागात कार्य करतात आणि इलेक्ट्रॉन्स तयार करतात. हे इलेक्ट्रॉन्स जमिनीच्या वरच्या थरात असलेल्या कॅथोडपर्यंत पोहोचतात. त्याच वेळी प्रोटॉन्स मातीमधून किंवा पडद्यामधून प्रवास करतात. जरी दोन्ही प्रणालींमध्ये ॲनोड–कॅथोड–मेम्ब्रेन अशीच रचना असली, तरी त्यांचे साहित्य आणि ऊर्जा स्रोत वेगळे असतात. मात्र या दोन्ही तंत्रज्ञानांचे एकत्रीकरण केल्यास वीज निर्मिती आणि रचनात्मक मजबुती दोन्ही वाढू शकतात. तरीही काही महत्त्वाच्या

अडचणी अजूनही शिल्लक आहेत. उदा. अनेक पेपर बॅटऱ्या एकावर एक ठेवताना त्यांची नाजूकता वाढते. ॲनोड आणि कॅथोड एकमेकांच्या संपर्कात आल्यास शॉर्ट सर्किट होण्याचा धोका असतो. तसेच या मध्ये जे इलेक्ट्रॉन स्वीकारणारे घटक वापरतात उदाहरणार्थ पोटॅशियम फेरिसायनाइड विषारी असतात तर ऑक्सिजनचा वापर करताना रचना आणि प्रत्यक्ष वापरात अनेक अडचणी येतात. या अडचणी दूर करण्यासाठी संशोधक पर्यायी साहित्य आणि नवीन रचनांवर काम करत आहेत.

या समस्यांवर एक आशादायक उपाय म्हणजे बॅटरी तयार करताना नायट्रेट चा इलेक्ट्रॉन स्वीकारणारा घटक म्हणून वापर करणे. विशेष म्हणजे, वापरात न आलेले नायट्रेट पर्यावरणाला हानीकारक ठरत नाहीत. उलट, हे नायट्रेट शेतीसाठी उपयुक्त ठरू शकतात. उरलेले नायट्रेट पिकांसाठी खत म्हणून वापरता येतात. मात्र नायट्रेटचा वापर करण्यासाठी विशेष प्रकारच्या कॅथोडची आवश्यकता असते. हा कॅथोड "विद्युत-उत्प्रेरक नायट्रेट क्षपण अभिक्रिया" (म्हणजेच नायट्रेट कमी करण्याची) प्रक्रिया करू शकणारा असावा लागतो. आतापर्यंत या प्रक्रियेसाठी विविध धातू आणि पद्धती वापरून कॅथोड तयार करण्यात आले आहेत. मात्र या पद्धती महागड्या असून प्रदूषण निर्माण करतात आणि विशेष तांत्रिक कौशल्याची गरज भासते. या अडचणी दूर करण्यासाठी या अभ्यासात फिजिकल वेपर डिपॉझिशन तंत्राचा वापर करण्यात आला. या पद्धतीने निकेल च्या पृष्ठभागावर तांब्याचा अतिशय पातळ थर चढवण्यात आला. या संशोधनातून असे आढळून आले की फक्त एकाच धातूचा पातळ थर असलेले इलेक्ट्रोड विद्युत-उत्प्रेरक नायट्रेट क्षपण अभिक्रिया साठी पुरेसे ठरत नाहीत. त्याऐवजी तांबे–निकेल मिश्रधातूचे इलेक्ट्रोड अधिक परिणामकारक ठरतात.

या अभ्यासात पेपर बॅटरी आणि माती सूक्ष्मजैव इंधन पेशी साठी अत्यंत महत्त्वाचे असलेले पडदे (मेम्ब्रेन) देखील तयार करण्यात आले. हे पडदे मातीतील ओलावा मोजणाऱ्या प्रणालीमध्ये सहज वापरता येतात. हे पडदे प्रोटॉन्सच्या वहनासाठी महत्त्वाची भूमिका बजावतात. यामुळे प्रणाली कार्यक्षमपणे कार्य करू शकते. नॅफिऑनसारखे व्यापारी पडदे उपलब्ध असले तरी ते महागडे असतात. तसेच त्यामध्ये जीवाणूंमुळे घाण साचणे, साहित्याची झीज, ऑक्सिजन गळती आणि उत्पादनातील गुंतागुंत अशा समस्या असतात. या मर्यादा दूर करण्यासाठी या अभ्यासात जैवविघटनशील जैव-पॉलिमरचा वापर करण्यात आला. यासाठी विशेषतः चिटोसान आणि पॉलीव्हिनाइल अल्कोहोल यांची निवड करण्यात आली. हे पॉलिमर स्वस्त असून पर्यावरणाला कमी हानीकारक आहे. या जैव-पॉलिमरच्या मदतीने प्रभावी आणि पर्यावरणपूरक पडदे तयार करण्याचा उद्देश होता.

या संशोधनात ओरिगामी तंत्राचा वापर करून जैवविघटनशील पडद्यांपासून पेपर बॅटऱ्या विकसित करण्यात आल्या. हे शाश्वत ऊर्जा साठवण तंत्रज्ञानातील एक महत्त्वाचे पाऊल आहे, विशेषतः माती सूक्ष्मजैव इंधन पेशी प्रणालीसाठी. या बॅटऱ्या दोन प्रकारात तयार करण्यात आल्या - त्रिमितीय आणि द्विमितीय . या बॅटऱ्या शेती क्षेत्रातील माती ओलावा मोजणाऱ्या प्रणालीसाठी उपयुक्त ठरू शकतात. त्रिमितीय घनाकार (क्यूब) रचना विशेष महत्त्वाची आहे. या रचनेमुळे ॲनोड आणि कॅथोडचे पृष्ठफळ वाढते आणि जास्त वीज निर्मिती शक्य होते. या घनाकार रचनेत द्रव कॅथोलाइट वापरता येतो. यामुळे बॅटरीची कार्यक्षमता वाढते. या क्यूब आकाराच्या बॅटऱ्यांमध्ये वायरलेस टॅग सहज बसवता येतात. यामुळे टॅगमुळे मातीतील ओलाव्याची माहिती मोबाईल फोनद्वारे शेतकऱ्यांना पाठवणे शक्य होते. तसेच या बॅटऱ्या एकावर एक नीट रचता येतात. यामुळे मातीमध्ये योग्य दिशेने ठेवून अधिक वीज मिळवता येते. या बॅटऱ्या वापरानंतर मातीमध्येच विघटित होऊ शकतात. यामुळे पर्यावरणावर होणारा परिणाम कमी होतो. या त्रिमितीय पेपर बॅटऱ्यांची चाचणी पोटॅशियम फेरो/फेरिसायनाइड वापरून तसेच ओलसर मातीमध्ये करण्यात आली.तसेच द्विमितीय पेपर बॅटऱ्यांची रचना ऑक्सिजनचा इलेक्ट्रॉन स्वीकारक म्हणून वापर करून करण्यात आली.

या संशोधनातून स्वस्त, वीजेवर अवलंबून नसलेली आणि जैवविघटनशील अशी स्वयंचलित माती ओलावा मोजणारी प्रणाली तयार करणे शक्य आहे, हे सिद्ध झाले आहे. ही प्रणाली पेपर बॅटरी आणि माती सूक्ष्मजैव इंधन पेशी या दोन्ही तंत्रज्ञानांचा एकत्रित वापर करते. या प्रणालीमध्ये पोटॅशियम फेरिसायनाइड, नायट्रेट किंवा ऑक्सिजन हे इलेक्ट्रॉन स्वीकारक म्हणून वापरले जातात. मातीतील सेंद्रिय पदार्थ इलेक्ट्रॉन देणारे घटक म्हणून काम करतात. मातीतील जीवाणू हे सेंद्रिय पदार्थ विघटित करून इलेक्ट्रॉन्स ॲनोडपर्यंत पोहोचवतात. यामुळे रासायनिक ऊर्जा विद्युत ऊर्जेत रूपांतरित होते. या प्रणालीमध्ये चिटोसान/पॉलीव्हिनाइल अल्कोहोल चे जैवविघटनशील पडदे वापरण्यात आले आहेत. हे पडदे प्रोटॉन एक्सचेंज मेम्ब्रेन म्हणून काम करतात. ही पद्धत पारंपरिक माती ओलावा मोजण्याच्या पद्धतींपेक्षा अधिक फायदेशीर आहे. पर्यावरणपूरक साहित्य वापरल्यामुळे दीर्घकाळात पर्यावरणावर होणारा परिणाम कमी होतो. ही प्रणाली बाह्य वीजपुरवठ्यावर अवलंबून नसल्यामुळे दूरच्या भागात सहज वापरता येते. स्वस्त असल्यामुळे ही प्रणाली मोठ्या प्रमाणावर वापरता येऊ शकते. तसेच हे तंत्रज्ञान शेती, पर्यावरण विज्ञान आणि संबंधित क्षेत्रांमध्ये माती ओलावा मोजण्याच्या पद्धतींमध्ये आमूलाग्र बदल घडवू शकते.

1

INTRODUCTION

Parts of this chapter are based on :

Maya Moreshwar Meshram, S., Adla, S., Jourdin, L., Pande, S. (2024).Review of low-cost, off-grid, biodegradable, in situ autonomous soil moisture sensing systems: Is there a perfect solution? Computers and Electronics in Agriculture 225, 109289.

Maya Moreshwar Meshram, S., Gonugunta, P., Taheri, P., Jourdin, L., Pande, S. (2025). Investigating the influence of a thin copper film coated on nickel plates through physical vapor deposition for electrocatalytic nitrate reduction. Frontiers in Materials , Volume 12 - 2025.

Maya Moreshwar Meshram, S., Gonugunta, P., Taheri, P., Jourdin, L., Pande, S. (2025). Preparation of biodegradable membrane utilizing chitosan and polyvinyl alcohol, and assessment of its performance after coating with graphene conductive ink. Frontiers in Membrane Science and Technology , Volume 4 – 2025.

Maya Moreshwar Meshram, S., Pande, S. (2025). Design of origami-inspired paper batteries as a power source for soil moisture sensing system. (Submitted)

1.1. INTRODUCTION

Water is an essential resource for agriculture, availability of which significantly affects crop productivity, food security, and economic stability (Ingrao et al., 2023). Globally, agriculture is responsible for approximately 85 - 90% of freshwater withdrawals, rendering it the largest consumer of water across various sectors (Sui et al., 2021). Water, already scarce in numerous regions worldwide, is also recognized 1as one of the least efficiently utilized resources due to over-irrigation, deep percolation losses, leaky irrigation systems, and poor management practices, resulting in over 60% of irrigation water being wasted or lost (McNabb, 2019). The problem of water scarcity for irrigation becomes prominent in certain regions of the world, where the drought conditions arise due to uneven rainfall and inadequate water management practices. Consequently, in countries prone to drought, the efficient utilization of available water resources becomes essential for agricultural production (Alharbi et al., 2024).

The primary strategies for effectively using water in agriculture involve increasing the output per unit of water through engineering management, minimizing water losses, and mitigating water degradation from an environmental perspective (Howell, 2001). These strategies can be further refined by managing the precise timing and quantity of water application to the crops. This strategy can lead to water savings that may be utilized to irrigate additional land, a consideration of particular importance in regions where water availability is the limiting factor for agricultural production (Koech and Langat, 2018). Water saving through the monitoring of soil moisture is one of the techniques to use the available water in an effective manner.

Soil moisture is a critical variable in agricultural productivity, influencing plant health, crop yield, irrigation scheduling, and ultimately food security (Babaeian et al., 2019). Soil moisture refers to the volume of water contained within a given volume of soil (typically measured in m^3/m^3) (Dorigo et al., 2011). Particularly, capillary moisture held in the micropores of soil due to adhesive and cohesive forces has the greatest agronomic relevance (Filipović, 2020). This form of moisture determines the availability of water to plants, bridging the gap between rainfall or irrigation events and actual crop uptake. Consequently, monitoring soil moisture using soil moisture sensor's (SMS) allows for informed decision about the moisture content in the soil that enhances crop yield while conserving water. SMS has consequently become a crucial instrument in precision agriculture, facilitating farmers in making informed decisions regarding irrigation and land management (G. M. Iyer et al., 2022; Gopalakrishnan et al., 2022; Kasuga et al., 2024).

1.2 CHALLENGES OF CURRENTLY AVAILABLE SOIL MOISTURE SENSING SYSTEMS (SMSSs)

There are various SMSSs such as in-situ, invasive and non-invasive (Hardie, 2020; Rasheed et al., 2022; Zhang et al., 2024) which are used in precision agriculture. The adoption of such SMSSs remains limited in many regions globally, and especially among small scale (smallholder) farmers who frequently lack access to reliable, affordable, and sustainable technological solutions (Aarif K. O. et al., 2025). Additionally, the scarcity of accessible energy due to inadequate off- and on-grid infrastructure serves as a significant barrier to the scaling up of soil moisture sensing in off-grid areas (Durga et al., 2024). As a result, these farmers rely on non-technical moisture measuring techniques such as feel and appearance method and hand-push probe for their fields (Chauruka et al., 2023; Manevski and Andersen, 2024; Morris and Energy, 2006).

Currently available SMSSs in the market mostly use solar panels and batteries for powering the SMSSs in the off-grid regions of the world (Sajib and Sayem, 2025). These SMSSs are often made of plastic and powered by batteries containing hazardous substances such as Lead. Consequently, they pose environmental threats if they are not disposed of or maintained correctly (Mrozik et al., 2021). These SMSSs are usually constructed by integrating batteries and solar panels into its design (Han and Yun, 2024). Additionally, many commercially available sensors are expensive and rely on a steady electricity supply, which is often unavailable in rural, off-grid areas (Balendonck et al., 2013; Okasha et al., 2021). Without affordable, locally adaptable, and low-maintenance alternatives, the advantages of soil moisture monitoring remain inaccessible to many, especially, smallholder farmers, hindering their ability to optimize irrigation, conserve water, and sustainably boost productivity. There is, therefore, a critical need for SMSSs that are sustainable, off-grid, and cost-effective. These devices should be user-friendly, easy to construct, environmentally sustainable, and capable of autonomous operation in resource-limited areas. They should be able to utilize ambient energy (i.e. energy that is available in the surrounding environment) as an energy source while simultaneously minimizing electronic waste in the soil.

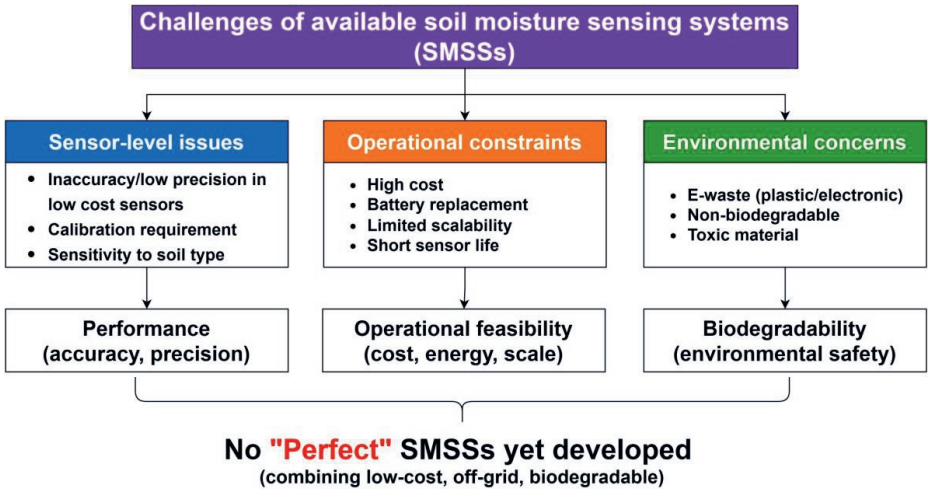

Figure 1.1: Various challenges of currently available soil moisture sensing systems.

To develop cost-effective, sustainable, and off-grid SMSSs, various ambient energy sources, such as solar energy, chemical reactions, etc. can be utilized (Chatterjee et al., 2023; Jawad et al., 2017; Mishu et al., 2020). Among these solar energy is actively developed and used in developing countries due to the abundance of solar radiation (Ahmed et al., 2024). Despite this it faces hurdles related to technology adoption, infrastructure, location, latitude, season, and time of day and financial constraints which affects the effectiveness of the solar energy (Ahmed et al., 2024; Caldwell et al., 2022; Ukoba et al., 2024). Also, integrating solar panels with SMSSs involves addressing challenges related to mounting, which are essential to resolve in order to prevent obstruction, ensure sensor functionality, and avoid damage during installation (Caldwell et al., 2022). Integrating batteries into the SMSSs increases the cost and necessitates maintenance, as they require regular replacement or recharging. This can be impractical in large-scale agricultural contexts (Le et al., 2023). Therefore, it is necessary to explore alternative ambient energy sources that can be easily integrated into the SMSSs to power these systems while simultaneously addressing the aforementioned challenges as depicted in Figure 1.1.

Soil moisture also plays a crucial role in plant growth by regulating the availability of water and nutrients (C. Wang et al., 2019) but also affects soil structure and temperature, thereby influencing various biological and chemical processes (Borowik and Wyszkowska, 2016). A significant biological process influenced by soil moisture is microbial activity (Brockett et al., 2012). Specifically, soil bacteria require adequate moisture levels to thrive and function optimally (Chen et al., 2024). These bacteria are essential for nutrient cycling, organic matter decomposition, and maintaining soil health, highlighting the importance of the relationship between moisture and microbial life in sustaining a balanced ecosystem (Chen et al., 2024). Among the diverse bacteria present in soil, some are capable of emitting electrons by oxidizing the organic matter within the soil (Rumora et al., 2023). This organic matter can serve as a promising alternative energy source in the development of sensing systems (Ivars-Barceló et al., 2018) using Microbial fuel cell (MFC) technology. This study aimed to test the hypothesis that increased soil moisture creates optimal environmental conditions for bacterial growth. Enhanced bacterial growth is hypothesized to result in a higher production of electrons, which in turn is expected to lead to increased signal strength. This hypothesis can be viewed as shown in following Figure 1.2.

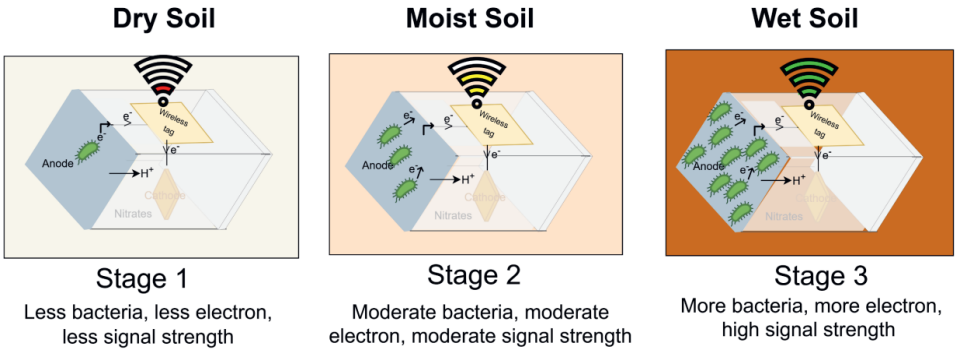

Figure 1.2: This illustrates the hypothesis concerning the interrelationship among soil moisture, electron production, and signal strength.

MFC is a bio-electrochemical system that facilitates the conversion of chemical energy stored in organic substrates into electrical energy through microbial activity (Obileke et al., 2021). A comprehensive explanation of the MFC is provided in Appendix 1.8.A. In MFCs in general, electrons are released by microbes through oxidation reactions at the anode (positive electrode) that are transferred via a conducting wire to cathode (negative electrode) where the electrons are accepted by certain reduction reactions. Protons exchanged between the two electrodes via an appropriate membrane through an aqueous solution thereby generating electric current and completing the circuit. There are various MFC available such as Plant, Sediment , Constructed Wetland, and Soil MFC (Toczyłowska-Mamińska et al., 2025). In Soil MFC the soil bacteria present in soil are employed for energy generation (Jiang et al., 2016). Another form of MFCs are paper based microbial fuel cell, which can be used in the construction of paper batteries.

A paper battery is a lightweight and flexible energy storage device that combines the functionalities of a conventional battery (Appendix 1.8.B.) and a supercapacitor. The process of harvesting electrical energy on paper involves the creation of MFC - based paper batteries (MFCPB). These MFCPBs, similar to other MFCs, generate energy by converting chemical energy from organics into electrical energy through the production of electrons via microbial

metabolism (Arwa Fraiwan et al., 2013; Y. Gao et al., 2019). The distinguishing features of MFCPB includes the utilization of a paper-based proton exchange membrane, use of cost-effective paper substrate (i.e a base layer or material upon which other components of the battery are built), rapid bacterial attachment, and immediate current generation. These batteries also feature integrated hollow space which can be used for anolyte and catholyte storage, they are highly portable, and possess the capability to generate power from biodegradable organic matter. They are characterized by shorter start-up times and can be configured in series or parallel to achieve desired voltage and current outputs. Additionally, they are compact, self-sustaining, used in intrinsic form without modifications, use capillary action (for fluid movement which facilitates easy expandability and integration of multiple MFCPB, making them suitable for low-power applications. These batteries then generate bioelectricity through microbial metabolism without the need for chemical treatments (A. Fraiwan et al., 2014, 2013; Fraiwan and Choi, 2014; Khan et al., 2021; S. H. Lee et al., 2016; Wagner et al., 2013).

Given that paper batteries are currently in the developmental phase, the present level of energy generation is relatively low. Consequently, research is being conducted on the integration of multiple paper batteries in a stack with perfect structural and dimensional stability using the origami technique to enhance energy production (Greenman et al., 2024; Mohammadifar and Choi, 2018). Origami is an ancient Japanese art of paper folding, through which 2D and 3D models with extensive surface areas can be developed (Dureisseix, 2012). In this process, paper is twisted, folded, crumpled, molded, cut, and sculpted, making it particularly suitable for applications in constrained spaces (H. Lee and Choi, 2015; Mohammadifar and Choi, 2018). However, when multiple MFCPBs are stacked using origami techniques, they are prone to breakage or tearing under pressure due to the fragile nature of paper (Khan et al., 2021). Such stacking can also disrupt electrical conductivity during bending and folding, potentially causing structural damage to the paper battery design. Also such folding and bending can cause stress, leading to wear and possible failure over time (Song et al., 2014). Complex folding patterns might cause energy loss, affecting battery performance (Mohammadifar et al., 2016a). Additionally, it is essential to ensure the separation and prevention of any physical contact between the anode and cathode when stacking MFCPBs to avoid electrical short-circuits (Walter et al., 2016). Furthermore, it is difficult to use liquid electron acceptor compounds at the cathode end, such as potassium ferricyanide and NO_3^-, which are typically used in liquid form, in such stacked MFCPBs. The incorporation of liquid compounds in the design of complex batteries may result in leakage if proper bonding is not achieved during the construction process. The use of liquid compounds can lead to a reduced lifespan, as they are rapidly depleted, and the replacement of these consumed compounds presents a significant challenge.

This motivates the design of MFCPBs that have a simple 3D and 2D origami design which can be easily stacked and joined together, are easy to use, and capable of generating sufficient energy using liquid electron acceptors such as potassium ferricyanide and NO_3^- in their design without undergoing any leakage. If the use of MFCPBs is required for an extended period, it is necessary to construct MFCPBs capable of utilizing alternative electron acceptors, such as oxygen, which is readily available in nature. Also at the end of the batteries lifecycle, they must decompose naturally without leaving harmful residues, thus mitigating environmental concerns related to traditional battery disposal.

1.3. SYNTHESIS OF BIMETALLIC ELECTRODE (CATHODE) FOR NO_3RR

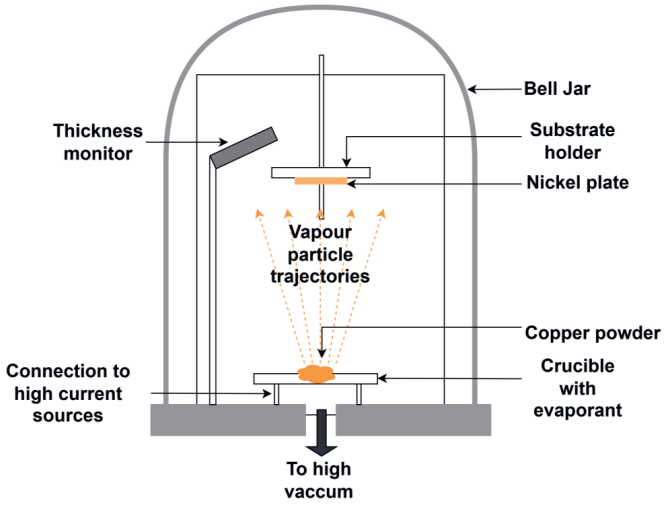

Figure 1.3: Schematic of the PVD equipment used for preparing bimetallic electrodes. It is used for depositing Cu on Ni plate

As discussed in Appendix 1.8.A. the oxidation and reduction reactions are integral parts of the MFC setup (Aghababaie et al., 2015; Roy et al., 2023). Oxidation reactions, which involve electron donors, are facilitated by exoelectrogenic bacteria at the anode as discussed above and utilize substrates such as acetate and glucose. In contrast, reduction reactions, which involve electron acceptors, have employed potassium ferricyanide, iron, nitrates, and oxygen in recent studies (Sun et al., 2016). As detailed in Appendix 1.8.A., MFC need electron-accepting compounds (also called electron acceptors) at the cathode that are capable of receiving electrons released by soil bacteria at the anode surface to complete the electrical circuit and facilitate current generation. Various studies are investigating different electron-accepting compounds in MFCs for different reasons (Ucar et al., 2017). These compounds exhibit diverse redox potentials (redox potential refers to the tendency of a chemical compounds to undergo reduction by accepting electrons or to undergo oxidation by donating electrons) (Mobilian and Craft, 2022), which can influence the energy output from a fuel cell (A detailed explanation of how the redox potential of the oxidation and reduction reactions influences the energy output of the MFC is given in Appendix 1.8.C.). Some of these compounds have slow reduction reaction rates and are less effective, necessitating the development of improved cathodic compounds (i.e reduction compounds at the cathode).

Amongst various compounds available (Ucar et al., 2017), oxygen and potassium ferricyanide are the most suitable electron accepting cathodic compounds. Potassium ferricyanide as an electron acceptor can generate higher power. However, the use of potassium ferricyanide as an electron acceptor poses environmental concerns due to its toxic nature, and has difficulty in chemical regeneration/recycling (Ucar et al., 2017), rendering it unsuitable for agricultural applications. Also, oxygen has an higher redox potential, yields a clean product (water) after reduction and is freely available in the environment. However using it as an electron acceptor has limitations such as poor contact angle with the electrode and the slow rate of reduction on normal electrodes (Ucar et al., 2017). Utilizing oxygen as the electron

acceptor, as in air cathodes, also necessitates a battery design with cathodes exposed to oxygen, which may not always be desirable because it may be obstruct farmers to cultivate their lands properly. Therefore, it is necessary to explore alternative electron acceptors that can address the challenges associated with oxygen and potassium ferricyanide.

NO_3^- are crucial in agriculture as they are a primary source of nitrogen for plant growth and are used in fertilizers to enhance crop yields. When used as fertilizers, NO_3^- in soil primarily undergo two main reactions: nitrification and denitrification (Giles et al., 2012). Nitrification is the biological conversion of ammonia (NH_3) or ammonium (NH_4^+) to nitrite (NO_2^-) and then to NO_3^-. Denitrification is the process where NO_3^- is converted back into gaseous forms of nitrogen, such as nitrous oxide (N_2O) and nitrogen gas (N_2), under anaerobic conditions. NO_3RR is a specific method of denitrification that uses electricity and catalysts to accelerate the reduction of NO_3^- by undergoing reduction reaction (Zhang et al., 2021).

NO_3RR has many advantages such as efficient and controllable synthesis of non-toxic nitrogen and other valuable products (so called selectivity - ability to favor the formation of a specific product) , such as ammonia and hydroxylamine, by selecting appropriate electrodes. Since the electrode material is the key in the NO_3RR (M. Li et al., 2019), it is necessary to design and construct efficient electrodes i.e. cathode for NO_3RR. In the past, noble metals, such as Pt, Rh, and Ru were used as electrodes and exhibited superior NO_3RR, but they have the corrosion problem affecting long term stability (Z. Chen et al., 2023), low selectivity and poor faradaic efficiency (measure of the efficiency with which the electrons participate in given electrochemical transformation) (Islam et al., 2025). Recent advancements have highlighted the frequent utilization of Cu in NO_3RR due to its remarkable activity and selectivity in converting NO_3^- to ammonia. However, certain limitations exist, such as the slow and inefficient reaction rate-determining step in the conversion of NO_3^- to NO_2^- (Hou et al., 2025), and the accumulation of NO_2^-, which poses environmental concerns due to its toxic nature (Zhu et al., 2020).

Monometallic Cu catalysts may not provide the optimal electronic environment for efficient NO_3^- reduction, necessitating the exploration of bimetallic or alloy systems to enhance performance (Hou et al., 2025). Bimetallic systems have been shown to improve NO_3^- reduction rates and selectivity by leveraging synergistic effects between different metals (Yuan et al., 2024). Consequently, bimetallic electrodes composed of a noble metal and a promoter metal, such as Palladium-Cu and Cu-platinum, have been developed (Meshram et al., 2025a). However, the high cost and scarcity of noble metals limit their practical applications (Zhang et al., 2021). Therefore, the development of new electrodes utilizing low-cost and readily available metals for NO_3RR is of significant importance.

Using bimetallic electrodes different reduction efficiencies and product selectivity can be obtained by adjusting the conditions of metal types, metal ratios and synthesis methods (Meng et al., 2023). There are various electrode synthesis methods such as electrodeposition (ED) (depositing a thin layer of a material onto a conductive surface using electrolysis) (Okoye et al., 2023), chemical vapor deposition (CVD) (this process involves creating films and coatings using chemical reactions of gases on or near a hot surface substrate) (Choy, 2003), and PVD (this is a vacuum-based technique in which a solid material is vaporized and subsequently deposited onto a substrate, resulting in the formation of a thin, durable coating as shown in Figure 1.3) (Rane et al., 2018) which can be used to prepare bimetallic electrodes (Long et al., 2025). Out of these, ED (Zhao et al., 2024) and CVD (X. Liu et al., 2024) have been used for preparing bimetallic electrode for NO_3RR. These methods present several challenges, including non-uniform coating, the potential for impurities in the deposited layer,

and limitations in scalability for large-scale applications. To address these issues in electrode preparation for NO_3RR, it is imperative to explore and test alternative electrode synthesis methods such as PVD and evaluate performance of these electrodes for NO_3RR.

1.4. TOWARD SUSTAINABLE BATTERY TECHNOLOGIES: THE NEED FOR BIODEGRADABLE MEMBRANES

As previously indicated, NO_3^- can be employed in battery construction, wherein the electrodes used for the NO_3RR function as the cathode. In the battery setup (detailed in Appendix 1.8.B.), however, NO_3RR cannot occur autonomously on the cathode surface without the movement of protons across a membrane and the flow of electrons through the external circuit (i.e. from anode to cathode through conducting wire). Various membranes, such as perfluorosulfonic acid-based polymers (Nafion) and sulfonated poly(ether ether ketone) (S-PEEK). (Ahmad et al., 2022; Nagao, 2024; Schmeisser, 2007), are available, with Nafion being predominantly used for NO_3RR (Mondol et al., 2022; Pirrone et al., 2024). Nevertheless, these membranes present several limitations, including high cost, vulnerability to biofouling, substrate losses, oxygen leakage (Ramirez-Nava et al., 2021; Tiwari et al., 2024), complex manufacturing processes, recycling challenges (Yang et al., 2024), and a lack of environmental sustainability (Gomaa et al., 2024). Also, the widely used Nafion exhibits other limitations, including a significant reduction in ionic conductivity under low humidity conditions, a decrease in mechanical strength at elevated temperatures, non- degradable and a high cost (Depuydt and Van der Bruggen, 2024; Safronova et al., 2022).

Nafion typically exhibits a flat structure, however, its morphology can be modified by factors such as mechanical stretching, temperature fluctuations, and humidity, which subsequently affect its uniformity and orientation (Melchior et al., 2015). Furthermore, the fabrication of various shapes or thicknesses using Nafion sheets presents significant challenges (Trabia et al., 2016), complicating their application in a 3D battery design that has a hollow interior for cathode and the catholyte (cathodic compound. Nafion also reverts to its original flat shape (Zhang et al., 2014), which can present challenges in the context of 3D battery design, where structural and dimensional stability are crucial. This stability is essential for maintaining structural integrity, preventing mechanical failure, ensuring consistent performance, and enhancing the battery's longevity by maintaining stable interfaces between components.(X. Liu et al., 2022) .

Therefore, there is a necessity for membranes that are cost-effective, biodegradable, and possess the potential for application in 3D battery systems which can provide better dimensional stability. These membranes could facilitate the NO_3RR by allowing the passage of protons from the outer surface of a 3D battery through the membrane to its interior catholyte compartment when used with electrodes designed to function as cathodes in the NO_3RR process as in Figure 1.4.Various biodegradable polymers, also referred to as biopolymers, are commercially available for the production of biodegradable membranes (Ehsani et al., 2022; Morales-Jiménez et al., 2023; Samir et al., 2022). These biopolymers are designed to function for a specified duration before degrading into easily disposable products through a controlled process (Samir et al., 2022). Membranes fabricated from biopolymers have numerous applications, including waste and wastewater treatment, gas separation, , drug delivery, food industry, and in fuel cells (Ehsani et al., 2022). Additionally, they provide an environmentally sustainable approach in energy production and battery technology (Bertaglia et al., 2024; Tiwari and Kumar Singh, 2024).

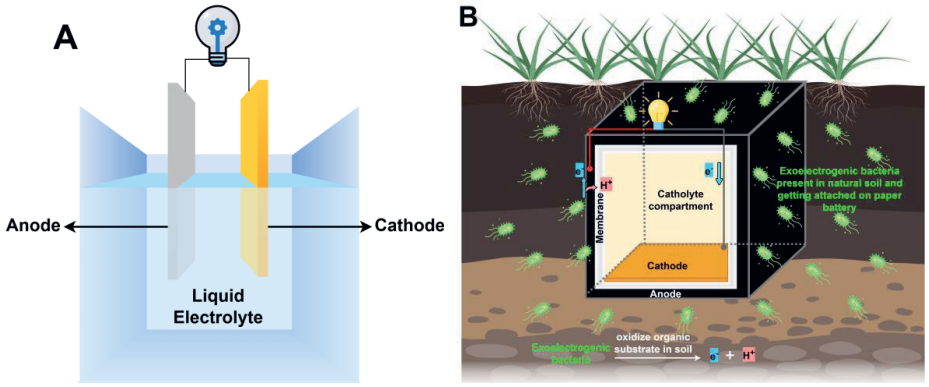

Figure 1.4: (A) A schematic representation of a conventional 3D membrane-less battery, illustrating the anode and cathode immersed in an electrolyte. **(B)** The schematic depicts a 3D paper battery system incorporating a membrane. In this configuration, electrons traverse the anode, while protons pass through the membrane, with both protons and electrons converging at the cathode within the catholyte compartment.

In the field of battery technology, these membranes function as separators, acting as a physical barrier that effectively isolates the cathode from the anode. As battery function as voltaic cells (an electrochemical cell that generates electricity through spontaneous redox (reduction-oxidation) reactions (reactions which occurs on its own naturally without any external energy)) the cathode acts as positive electrode and anode as negative electrode (Petrovic, 2021). This configuration facilitates ion movement while simultaneously preventing short circuits (Serra et al., 2023; Turossi et al., 2025). Additionally, some of these membranes are coated with catalysts to enhance the electrochemical reactions essential for energy conversion in fuel cell applications (H. Liu et al., 2024; Xie et al., 2021; Yingnakorn et al., 2025). Despite their advantages, these membranes exhibit low mechanical properties, which may lead to mechanical failure under stress. They also demonstrate higher shrinkage or degradation at elevated temperatures, potentially compromising battery safety and performance. Furthermore, they possess a rapid degradation rate, high hydrophilic capacity, and are brittle, with warping effects (Hasırcı et al., 2001; Rosseto et al., 2019; Sen Gupta et al., 2023). To ensure dimensional stability, enhanced moisture resistance, and increase mechanical strength, the introduction of a reinforcing structure through the creation of an interpenetrating network may be a viable approach for these applications (Abolhassani et al., 2017; Bhuvaneshwari et al., 2011; Boey et al., 2022; Hasırcı et al., 2001). Each polymer is characterized by distinct synthesis methods, properties, significance, degradation processes, and applications across various fields (Meghana et al., 2023). Consequently, it is imperative to identify suitable biodegradable polymers for the construction of biodegradable membranes. These membranes should function as proton exchange membranes, act as separators in battery construction, and be amenable to catalyst coating to enhance battery performance. Furthermore, these membranes must exhibit dimensional stability and effectively retard the rate of degradation.

1.5. PAPER BASED BATTERIES FOR SMSSs: STRUCTURAL COMPLEXITY AND PRACTICAL FUNCTIONALITY

3D batteries are energy storage devices made in a 3D shape to use space better and work more efficiently (Z. Wang et al., 2020). 3D batteries have several benefits. They can store more

energy because their design increases the surface area that holds more electrolyte. This larger surface area helps the battery work better by making reactions at the electrodes faster. The capacity of 3D batteries can be increased by making the electrodes longer without taking up more space. This means they can be made to fit different power needs without losing efficiency. Also, their small size makes them perfect for small devices such as SMSSs (Hart et al., 2003; Hyun et al., 2024; Long et al., 2004). Various 3D configuration of traditional batteries have been documented (Hummes et al., 2023; Hung et al., 2021; Lyu et al., 2021), which facilitate the preparation of conventional batteries. However, with the advancement of papertronics - a field that integrates paper-based materials with electronic circuits to create cost-effective, flexible, lightweight, and environmentally friendly devices (Landers et al., 2022; Z. Rafiee et al., 2024), and the application of origami techniques, it is possible to fabricate complex 3D paper battery shapes suitable for use in small-scale electronics. However, limited research has been conducted on paper-based batteries, where either the entire battery is designed in a 3D form (Gao and Choi, 2017; Gonzalez-Guerrero and Gomez, 2019; Mohammadifar and Choi, 2018; Xu et al., 2015) or the electrodes are fabricated in 3D form (Chen and Hu, 2018). The construction of this paper battery can be achieved through the application of origami and papertronics techniques, as illustrated in Figure 1.5.

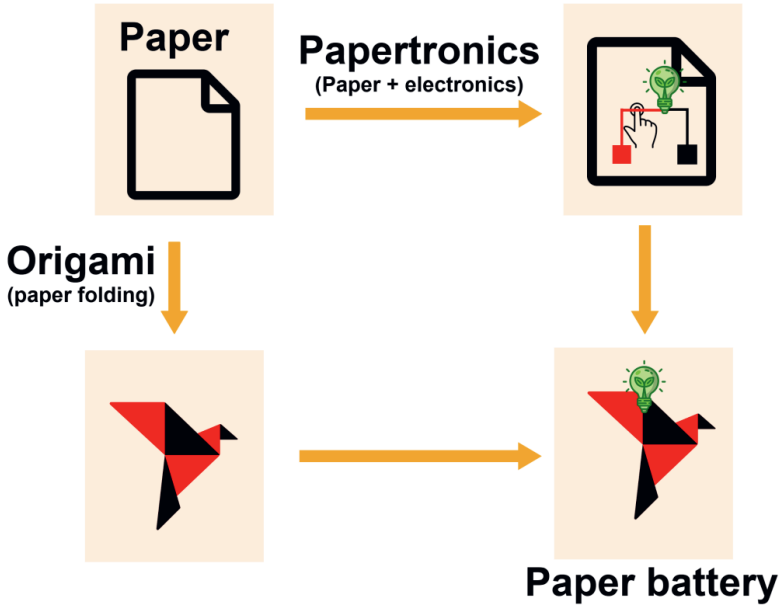

Figure 1.5: A flow diagram depicting the conversion of paper into a paper battery through the use of Origami and Papertronics.

As mentioned earlier in section 1.1 paper batteries can be prepared based on MFC technology, and taking motivation from this, researchers have been developing 3D MFCPB. The hollow spaces within these 3D MFCPB structures facilitate the use of thicker electrodes, particularly the cathode. This increase in electrode thickness is beneficial as it results in a higher energy output (Z. Wang et al., 2020). Additionally, these hollow spaces can serve as reservoirs for electrolyte storage. Furthermore, employing multifold folding techniques contributes to the reduction of ion transport by decreasing the distance between the electrodes (Gao et al., 2024; Shi et al., 2017). The distance between the electrodes can be further reduced by utilizing proton exchange membranes as both electrodes and membranes in a monolithic manner. This can be

achieved by directly coating conductive materials onto the membrane, thereby enhancing energy efficiency (Yang et al., 2020).

Some studies have developed complex-shaped batteries that offer an on-demand power supply tailored to specific applications (Mohammadifar and Choi, 2018). But making these batteries needs precise techniques, which can make mass production difficult (Chen et al., 2014). Also, adding these batteries to current SMSSs can be difficult because of their complex shapes and folding patterns (Song et al., 2014). Stacking 3D paper batteries with complex shapes poses significant challenges. Additionally, the positioning of the cathode in complex 3D configuration presents challenges, as both the orientation and surface area of the cathode are crucial determinants of power output performance (Dziegielowski et al., 2022; Papillon et al., 2021). One significant challenge associated with 3D battery design is the storage of liquid compounds, which serve as electrolytes within the hollow spaces of the batteries. As mentioned before, there is a risk of leakage if the 3D paper batteries are not adequately sealed. Furthermore, the replacement of these compounds becomes problematic once they are fully depleted. Current research indicates that the MFCPB has the potential to be utilized as an energy source in off-grid regions worldwide, which could worsen the issue of compound replacement. It is therefore essential to develop a simple 3D MFCPB. This design should facilitate the storage of catholyte, ensure optimal orientation of the cathode, allow for modifications to the cathode's surface area, enable easy stacking, and which can easily be integrated into SMSSs, all while maximizing power output. Additionally, in scenarios where the 3D MFCPB is not applicable, it is necessary to design alternative MFCPBs capable of operating for extended durations without the need for liquid compounds as electron acceptors, and also reducing uncertainties related to cathode orientation.

1.6. RESEARCH QUESTIONS

Considering the aforementioned imperative , this study focused on the design of a cost-effective biodegradable paper battery intended to serve as an energy source for autonomous soil moisture sensing systems in off-grid regions where commercially available systems are not feasible. Consequently, the following questions were formulated to guide the design of various components of the biodegradable paper battery.

1) What are the technological challenges and advancements in developing low-cost, off-grid, biodegradable in situ autonomous soil moisture sensing systems, and is a fully optimized solution feasible?

2) How does the electrodes prepared utilizing the environmentally friendly technique of physical vapor deposition affects the electrocatalytic nitrate reduction, and can NO_3^- be used as an electron acceptor for the battery construction.

3) How can a membrane be prepared for use in paper batteries, and what materials are suitable for its fabrication?

4) How can a 3D and 2D biodegradable paper battery be designed using origami technique, and what is its suitability for current generation in water saturated soils?

Based on the findings of this thesis, researchers will gain several insights, particularly 1) in the design of SMSSs for agricultural applications which will be powered by batteries that utilize NO_3^-, potassium ferricyanide, and oxygen as electron acceptors, thereby enabling their operation in off-grid regions without posing environmental threats, 2) in the development of a cost-effective SMS utilizing low-cost materials such as paper; 3) in the creation of

biodegradable membranes using biodegradable polymers such as CS and PVA, which can be employed in the design of biodegradable batteries through soil microbial fuel cell technology. These will be suitable for off-grid regions without reliance on external power sources like traditional batteries and solar power, thereby contributing to the reduction of electronic waste associated with battery and solar panel usage.

1.7. OUTLINE OF THE THESIS

The remaining thesis is organized as follows:

Chapter 2 investigates whether a "perfect" solution exists that not only performs effectively but is also cost-efficient, operates independently of conventional power sources, and minimizes environmental impact by naturally degrading over time. This critical review elucidates the necessity of low-cost, off-grid, biodegradable soil moisture sensing systems for remote areas. It also examines current technologies and identifies research gaps in soil moisture sensing. Additionally, it discusses the trade-offs between performance, feasibility, and biodegradability of these sensing systems.

Chapter 3 details the study in which Cu-Ni (bimetallic) electrodes were fabricated by depositing a thin Cu film onto a Ni plate using physical vapor deposition for NO_3RR reactions. The chapter further examines the impact of this thin Cu film on the electrocatalytic reduction of NO_3^-.

Chapter 4 details the methodology employed in the design of biodegradable membranes utilizing biopolymers such as CS and PVA, as well as the performance of these membranes in various tests.

Chapter 5 elucidates the methodology for designing a 3D and 2D paper battery utilizing a CS) based membrane, as well as its performance across various cathode positions in potassium ferricyanide under both aqueous and water saturated soil conditions. Additionally, it provides a detailed account of the design of an air cathode paper battery tested in fully saturated soil.

Chapter 6 concludes and offers a critical discussion of ways forward with recommendation for future research.

1.8. APPENDIX: BASIC CONCEPTS USED

This appendix explains the basic concepts used in the thesis. More details are discussed in the chapters that follow.

1.8.A. MICROBIAL FUEL CELL (MFC)

Definition: MFC is a bio-electrochemical system that converts chemical energy of organic compounds into electrical energy or bio-electrical energy through the microbial catalytic reaction at the anode under anaerobic conditions. The components of the MFC are similar to that of the battery explained in Appendix 1.8.B.

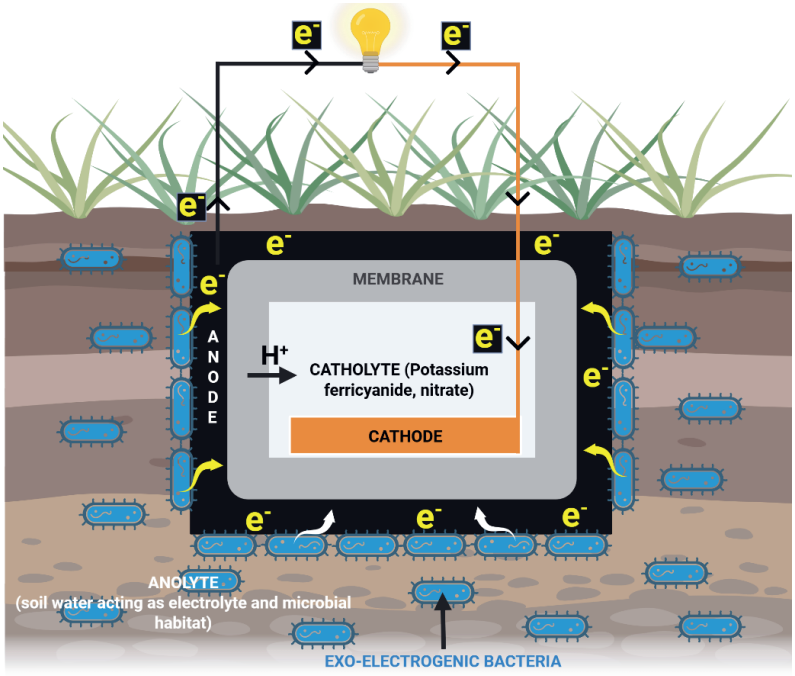

Figure 1.6: A schematic illustrates the integration of a microbial fuel cell within soil, depicting the movement of electrons and protons facilitated by the paper battery.

Working: MFC uses exo-electrogenic / electrocigenic / electroactive / electrogenic bacteria to convert chemical energy from organic matter directly into electrical energy. In the anaerobic anolyte chamber, these bacteria break down organic substances (electron donor) such as glucose, acetate, wastewater etc. by undergoing microbial oxidation reaction releasing electrons and protons on the anode surface. The electrons then travel through an external circuit to the cathode, generating electricity, while the protons pass through a proton exchange membrane to the catholyte chamber. In the catholyte chamber, the electron accepting compounds such as NO_3^-, potassium ferricyanide, oxygen etc. undergoes reduction reaction by accepting the electrons from the external circuit and proton through the proton exchange membrane. This process not only generates power but can also be used to treat waste, making MFCs a sustainable technology for both energy production and environmental management.

Based on natural environment or source of the substrate MFC are classified as SMFC (soil organic matter used as substrate), Sediment MFC (sediment organic matter from lakes, rivers, or marine environments), and Plant MFC (Plant root exudates from plant rhizosphere) (Gupta et al., 2023; Toczyłowska-Mamińska et al., 2025) which can be used as a ambient energy source in off-grid regions of the world.

1.8.B. BATTERY

Definition: A battery is a device that directly converts the chemical energy stored within its active materials into electrical energy through an electrochemical oxidation-reduction (redox) reaction. This reaction involves the transfer of electrons from one material to another via an electric circuit.

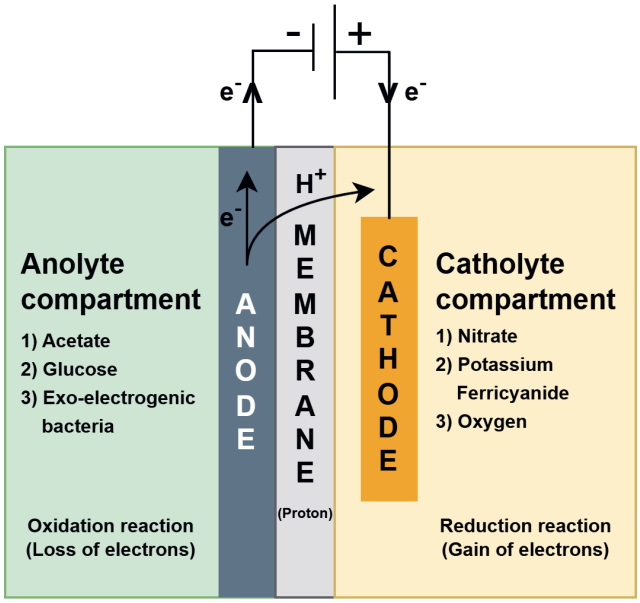

Figure 1.7: The schematic diagram illustrating the components of a battery, including the anode, membrane, and cathode, as well as the anolyte and catholyte compartments, demonstrates the movement of protons and electrons within the battery. (Sign convention: During discharging, the cathode is positive and the anode is negative; during charging, the polarity is reversed.)

Important components of battery: Batteries are composed by five important components

a) Anolyte: The anolyte is the liquid (electrolyte) that surrounds or contacts the anode in a battery or electrochemical cell. The place where this anolyte is present is called the anolyte compartment.

b) Anode: It is the negative or reducing electrode that releases electrons to the external circuit and oxidizes during and electrochemical reaction.

c) Separator/membrane: A separator is a thin, porous membrane placed between the anode and cathode in a battery. It keeps the two electrodes from touching (preventing short circuits)

while allowing ions to pass through, which is essential for the battery to function. The separator can be proton exchange membrane, anion exchange membrane or cation exchange membrane.

d) Cathode: is the positive or oxidizing electrode that acquires electrons from the external circuit and is reduced during the electrochemical reaction.

e) Catholyte: The catholyte is the electrolyte solution that surrounds or interacts with the cathode (the positive electrode) in batteries. The catholyte is stored in the catholyte compartment.

Working: A battery functions by facilitating the movement of electrons and protons (H^+ ions) through distinct pathways, thereby enabling the conversion of chemical energy into electrical energy. At the anode oxidation occurs, which involves the loss of electrons by atoms at the anode, often accompanied by the release of protons (H^+) or other positive ions into the surrounding anolyte. The electrons, unable to move through the separator, moves out of the anode and travel through an external circuit, generating an electric current that powers a device. Concurrently, the protons (or positive ions) released into the anolyte migrate through the separator porous membrane that permits only ions, not electrons, to pass toward the cathode. At the cathode, a reduction reaction occurs. Here, electrons returning from the external circuit combine with the incoming protons (H^+) from the anolyte and the reactive species present in the catholyte. This completes the redox reaction and balances the charge. The catholyte, which envelops the cathode, plays a pivotal role by facilitating the acceptance of incoming protons and supporting the chemical reactions that accommodate the arriving electrons. To conclude, a battery operates by differentiating the pathways of electrons (through the external circuit) and protons or positive ions (through the electrolyte and separator). This dual movement enables continuous charge flow and energy delivery until the chemical reactants are exhausted.

1.8.C. REDOX POTENTIAL

Definition: Redox potential, also known as oxidation–reduction or oxidoreduction potential or electrode potential or standard reduction potential (E^o), is a measure of the thermodynamic driving force for a chemical or biological species to either donate electrons (be oxidized) or accept electrons (be reduced) in chemical reactions (Hoehler, 2011).

Table 1.1: Redox potential of various reactions mostly used in MFC

Oxidation/reduction pairs E°	**mV**
$2H^+/H_2$	−420
NO_3^- / NO_2^-	+421
$[Fe(CN)_6]^{3+}/[Fe(CN)_6]^{4+}$	+430
NO_2^-/NH^{4+}	+440
O_2/H_2O	+820

A species with a higher reduction potential possesses a higher tendency to acquire electrons and be reduced. Conversely, a species with a higher oxidation potential possesses a higher tendency to lose electrons and be oxidized (Lu and Marshall, 2013). It indicates whether a substance is a strong oxidizer (has a high positive redox value) or a strong reducer (has a high negative redox value). The higher the redox value of a substance, the greater its ability to oxidize (donate electrons) or reduce (accept electrons). It is measured in volts (V) or millivolts (mV) .

The reduction potentials are measured under conditions of 25°C, 1 M concentration for reduced/oxidized species, or 1 atm pressure for gases. These potentials are compared to a standard hydrogen electrode (SHE) or normal hydrogen electrode (NHE) at 0 V. The difference between a compound's reduction potential and SHE is the standard reduction potential. The reduction potential difference between donor and acceptor determines electron transfer (ET) driving force, with electrons flowing from negative to positive potential. As redox reactions are equilibrium processes, electrons can flow in reverse depending on the equilibrium constant and reactant concentrations (Hoehler, 2011; Lu and Marshall, 2013).

In MFCs redox potential plays an important role in determining, efficiency of electron transfer from microbes to the anode (Aiyer, 2020), and selection of electron acceptors at the cathode (Chandrasekhar, 2019). A more negative anode redox potential enhances electron transfer from microbes, while a more positive redox potential at the cathode attracts electrons from the external circuit. The difference between the redox potential of the anode and cathode determines the theoretical voltage output of the MFC. The higher redox potential difference means greater driving force and ultimately higher power output. Various MFC electrode reactions and their corresponding redox potentials are given in (Du et al., 2007).

1.8.D. CYCLIC VOLTAMMETRY (CV)

Definition: In CV, the potential of the working electrode is swept at a constant rate in a forward direction (e.g., from a lower to a higher voltage) to induce an oxidation or reduction reaction, and then it is reversed to scan back to the starting potential. This forms a cyclic sweep, and the resulting current is plotted against the applied potential to produce a cyclic voltammogram.

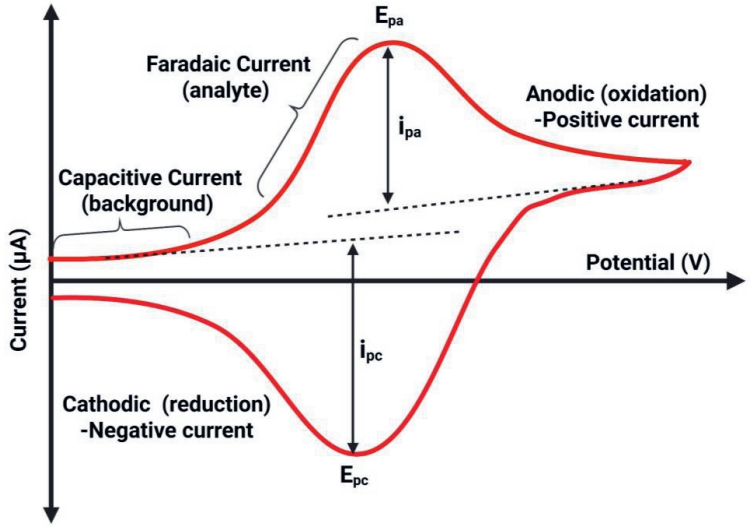

Figure 1.8: A typical cyclic voltammogram illustrates the oxidation and reduction curves, characterized by capacitive and oxidative currents, as well as distinct oxidation (i_{pa}) and reduction (i_{pc}) peak current.

CV is a powerful and popular electrochemical method commonly used to explore the reduction and oxidation processes of molecular species. CV is also valuable for studying chemical reactions initiated by electron transfer, including catalysis, providing insights into catalytic processes, and facilitating the understanding of redox mechanisms in various systems.

CV characterizes electrochemical systems by measuring the current response (i) as a function of applied voltage (E) (i vs. E), providing information on redox reactions, electron transfer kinetics, and stability of electroactive species (M. Rafiee et al., 2024). This technique involves linearly and cyclically sweeping the voltage while monitoring the resulting current response, allowing peak potentials, peak currents, and other electrochemical parameters to be determined (Elgrishi et al., 2018). In CV, the Butler–Volmer equation is often used to model the kinetics of electron transfer at the electrode interface as follows (Yammine et al., 2024).

As the potential reaches the redox potential of the analyte, electrons are transferred between the electrode and the analyte, generating a peak in current called anodic (oxidation)-positive current. During the reverse scan, the reverse redox process generates a second current peak called the cathodic (reduction) -negative current . The shape and position of these peaks provide detailed information about the electrochemical behavior of the species, such as its redox potential, reaction reversibility, diffusion coefficients, and kinetics.

In CV the capacitive current refers to the current generated by the charging and discharging of the electrical double layer at the electrode–electrolyte interface, rather than from any redox (electron transfer) reaction. When the potential of the working electrode is varied during the scan, ions in the solution rearrange at the surface of the electrode to maintain electrostatic balance, creating a double-layer capacitor. The continuous change in potential causes this capacitor to charge and discharge, resulting in a current known as the capacitive or non-faradaic current. This current is directly proportional to the scan rate and is symmetrical in both the forward and reverse scans. Unlike faradaic currents, which produce distinct peaks associated with redox reactions, capacitive currents appear as a background signal. While they do not provide direct information about the analyte's redox behavior, they can influence the overall shape of the voltammogram and must be accounted for, especially when analyzing small or fast redox signals or when using electrodes with high surface area (Elgrishi et al., 2018; Wang and Pilon, 2012).

1.8.E. CHRONOAMPEROMETRY

Definition: Chronoamperometry is an electrochemical technique that measures the electric current (i) as a function of time (i vs. t) when a constant electric potential (E) is applied to an electrode. chronoamperometry maintains a constant potential and measures the resulting electric current over time according to Cottrell's law. This technique is often used to study electrochemical reactions with specific electrode materials and to determine the kinetic constants of electrochemical reactions (Yammine et al., 2024).

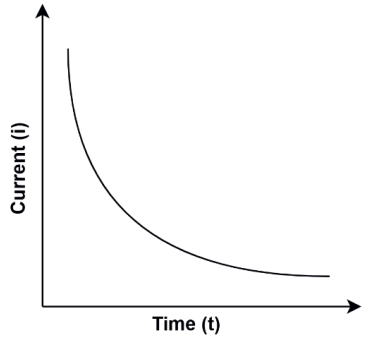

Figure 1.9: Typical graph of chronoamperometry showing the current changing with time

Chronoamperometry works by applying a sudden, constant voltage (known as a potential step) to an electrochemical cell and then monitoring how the resulting current changes over time. When the potential is applied, it drives a redox reaction at the working electrode surface, causing either oxidation or reduction of an electroactive species in the solution. Initially, the current is high due to the abundance of reactant molecules at the electrode surface. However, as the reaction proceeds, these molecules are consumed and must diffuse from the bulk solution to the electrode. This leads to a decrease in current over time, following a pattern described by the Cottrell equation, where current is inversely proportional to the square root of time. The shape and behavior of the current-time curve provide valuable information about the diffusion properties, reaction kinetics, and concentration of the species involved. Chronoamperometry is particularly useful for studying fast electron transfer processes and diffusion-controlled reactions in a simple and direct manner (M. Rafiee et al., 2024).

1.8.F. OPEN CIRCUIT POTENTIAL (OCP)

Definition: OCP also referred to as equilibrium potential or rest potential, is the voltage measured between two electrodes when no external current is applied, indicating an open circuit (Ghamsarizade et al., 2023). In a typical electrochemical cell, the OCP represents the difference in electrochemical potential between the working and reference electrodes, resulting from redox reactions at their surfaces. This potential reflects the thermodynamic tendency of electrons to move from one electrode to another, independent of any kinetic effects from an applied current . The OCP is influenced by the redox couple at the electrode interface and can be calculated using the Nernst equation. In the context of SMFCs the OCP signifies the potential difference between the anode, embedded in anaerobic soil, and the cathode, typically exposed to air or situated in oxygen-rich areas, when no external circuit is connected. At the anode, bio-electrochemical oxidation occurs as electroactive soil microbes decompose organic matter, releasing electrons and protons. These electrons accumulate at the anode, creating a negative potential relative to the cathode. The cathode, exposed to oxygen, is the site of the oxygen reduction reaction (ORR), resulting in a positive potential. Under open-circuit conditions, electrons cannot flow through the external circuit, causing the OCP to stabilize at a value that reflects the balance between microbial activity at the anode and electrochemical conditions at the cathode (Huang and Zhang, 2022). The OCP for an SMFC depends on factors such as soil composition, microbial community, oxygen availability, and substrate levels. A stable or increasing OCP generally indicates active microbial metabolism and effective redox separation between the anode and cathode environments (Barakat et al., 2024). Conversely, a decreasing OCP may suggest substrate depletion, microbial inactivity, biofilm degradation, or cathode fouling(Bhattacharya et al., 2023; Bimakr et al., 2018; Bird et al., 2021). Thus, OCP is a crucial diagnostic parameter for assessing the health and operational readiness of SMFCs for power generation.

2

CHALLENGES OF CURRENTLY AVAILABLE SOIL MOISTURE SENSING SYSTEMS (SMSSs)

Parts of this chapter are based on :

Maya Moreshwar Meshram, S., Adla, S., Jourdin, L., Pande, S. (2024).Review of low-cost, off-grid, biodegradable, in situ autonomous soil moisture sensing systems: Is there a perfect solution? Computers and Electronics in Agriculture 225, 109289.

2.1. INTRODUCTION

The agriculture sector is the highest consumer (~85 – 90 %) of freshwater (Sui et al., 2021) and is among the least efficient users. Agricultural water management using scientific methodologies can improve farm water management by reducing economic losses from over-/under-irrigation, excessive pumping costs, nutrient leaching, and greenhouse gas emissions (Abba et al., 2019; Neto et al., 2022).

Soil moisture, which is defined as the amount of water in a specific soil depth [m^3 water per m^3 soil] (Dorigo et al., 2011) and is categorized into gravitational, capillary, and hygroscopic forms, plays a critical role in agricultural water management (S.U. et al., 2014). Among the various forms of soil moisture, capillary moisture, which is held in micropores by cohesion and adhesion, is the most significant for agricultural purposes as it facilitates soil-environment interactions (S.U. et al., 2014). Capillary soil moisture, which is essential for comprehending soil-environment interactions, is typically categorized into field water capacity and wilting point. Field water capacity (FWC) refers to the water retained in the soil following the drainage of any excess gravitational water; however, this water may not always be accessible to plants. The wilting point, or permanent wilting point (PWP), is the soil moisture level below which plants begin to wilt. The amount of water available to plants was calculated by subtracting the permanent wilting point from the field water capacity (Widtsoe and McLaughlin, 1912). Understanding PWP, which exerts a substantial influence on plant growth, nutrient acquisition, disease and pest resistance, and crop production, is crucial for designing soil moisture sensors that guarantee plants receive adequate water without squandering resources. By doing so, these sensors optimize water usage in agriculture. Therefore, measuring and monitoring soil moisture is an essential component of the best management practices to improve agricultural sustainability (Mundewadi et al., 2023).

An appropriate choice of SMSS is essential for effective on-farm irrigation decision-making (Kojima et al., 2016). Although sensor suitability (e.g., to the type of soil and/or crop) is relevant to all users, performance accuracy and precision may be more important to scientific users, and operational feasibility may be more relevant for commercial agricultural users (Kukal et al., 2019). Operational feasibility includes cost and logistical aspects such as management, ease of operation, durability, life expectancy, and operational lifespan (Kukal et al., 2019; Schwamback et al., 2023). The utility of soil moisture sensing is challenged by i) sensor inaccuracy - some sensors may not provide accurate readings of soil moisture levels, especially if they are not properly calibrated or if the soil conditions are not suitable for the sensors (Adla et al., 2020; Kosasih et al., 2023). However, for some farmers and agronomists, precision is privileged over accuracy as consistent and reproducible outcomes facilitate better planning and resource allocation, which is especially crucial in areas with diverse hydrological regimes and distinct farming requirements (Gupta et al., 2024). By prioritizing precision, farmers can modify their strategies based on current data, identify discrepancies in field conditions, and optimize the utilization of resources, thereby emphasizing the value of precision in agricultural practices (Placidi et al., 2021); ii) sensor maintenance - some sensors may require frequent calibration, cleaning, or replacement, which can be time-consuming and expensive (Schwamback et al., 2023); iii) cost - high-quality soil moisture sensors can be expensive, which can limit their accessibility to low-income farmers (Schwamback et al., 2023); iv) environmental degradation through electrical and plastic waste in soil (Dahal et al., 2020); and v) replacement of sensor batteries - commercial environmental monitoring nodes are usually powered by batteries (Daskalakis et al., 2017). Addressing these challenges is critical for the widespread adoption of soil moisture sensors for agricultural water management, particularly in low-resource and remote areas.

This review is centrally motivated by the question of whether it is possible to have an SMSS that has all desirable attributes, i.e. it performs adequately, is operationally feasible (with respect to its cost and energy source) and is environmentally safe. This is necessary to overcome the problems of using SMSS due to lack of connectivity and resources (road, electricity, water resources) in remote or marginalized farms in developing countries, lack of material disposable facilities in developing countries, frequent climate fluctuations affecting efficiency of SMSS and lack of technical skills and financial conditions of smallholder farmers (Saleh et al., 2016). This review investigates the state-of-the-art in situ SMSS, highlighting the advances in low-cost sensors and sensing systems, off-grid ambient energy based SMSS, and biodegradable SMSS. The challenges and possibilities for the development and adoption of sensing systems that "has it all" in the agricultural water sector are then discussed, analyzing the trade-offs between sensor performance, operational feasibility, and environmental safety.

2.2. LITERATURE REVIEW AND SEARCH CRITERIA

A literature search was carried out using abstract and citation databases, including Scopus for peer-reviewed articles published in English and comprising the fields "article title"; "abstract"; and "keywords". The basic query structure used for searching articles was (("low cost") OR ("off grid") OR ("biodegrad*")) AND (("soil moisture sensor" OR "soil humidity sensor")) AND ("agricultur*" OR "farm*"). The eligibility criteria for studies covered by the review comprised journal articles and conference papers published in English within the last ten years (2014 - 2024) to ensure the inclusion of recent and up-to-date research findings. In total 130 articles were found in Scopus, 57 articles found in Web of Science and 60 articles were found in IEEE Xplore digital library. Zotero Software was used for managing the articles. After removing the duplicates and irrelevant articles 77 papers were selected for reviewing based on the above query. In total 115 articles were considered for this review paper.

The majority of the studies reviewed were conducted in Asia and Europe, with India and the United States of America leading the way in terms of the number of studies conducted on a country-by-country basis (as indicated in Table 2.1). However, it is important to note that the representation in the table below does not necessarily reflect the actual number of studies conducted in each region.

Table 2.1: Regions in which literature review studies were conducted (N=total number of studies in a region)

Region	**N**	**Specific countries**
Asia	91	India (51), China (8), Indonesia (5), Malaysia (5), Thailand (4), Bangladesh (3), Pakistan (3), Japan (2), Philippines (2), South Korea (2), Turkey (2), Iraq (1), Saudi Arabia (1), Sri Lanka (1), Lebanon (1)
Europe	33	Italy (7), Spain (6), Germany (5), Netherlands (4), France (2), Romania (2), Hungary (1), Bulgaria (1), Sweden (1), United Kingdom (1), Ireland (1), Austria (1), Serbia (1)
North America	20	United States of America (19), Canada (1)
South America	7	Brazil (5), Ecuador (2)
Africa	7	Nigeria (2), Tunisia (2), Morocco (1), Kenya (1), Egypt (1)
Australia/Oceania	4	Australia (4)

Given the study scope and data acquisition requirements, original studies with the following foci were eligible for inclusion: 1) low-cost sensors categorized based on their purchase prices, 2) sensors powered by renewable power sources, and 3) biodegradable sensors.

2.3. FUNDAMENTALS OF SOIL MOISTURE SENSING

Soil moisture sensing involves the understanding of physical, chemical, and biological processes that influence soil moisture content and the different techniques used to measure it (Kosasih et al., 2023). Physical factors such as soil texture, structure, porosity, compaction, and temperature influence the movement and storage of soil moisture, and the soil moisture sensor accuracy. Chemical factors, such as soil pH and salinity, can affect the electrical conductivity and dielectric properties of soil, which are important parameters for some soil moisture sensors. Biological factors, such as organic content, can also affect soil moisture sensing, as microbial activity and plant roots can influence soil water holding capacity and porosity. Additionally, plant residues and other organic matter in the soil can affect soil moisture sensing by altering the electrical conductivity and dielectric properties of soil (Topp et al., 2008; Wenwu et al., 2018; Zhu and Lin, 2011).

2.3.1. EXISTING SOIL MOISTURE SENSING TECHNIQUES

Soil moisture sensing can be categorized as gravimetric, volumetric, and potentiometric techniques (see Figure 2.1). Gravimetric and volumetric methods directly estimate the soil water content, whereas potentiometric methods measure the electrical potential difference between two electrodes inserted into the soil.

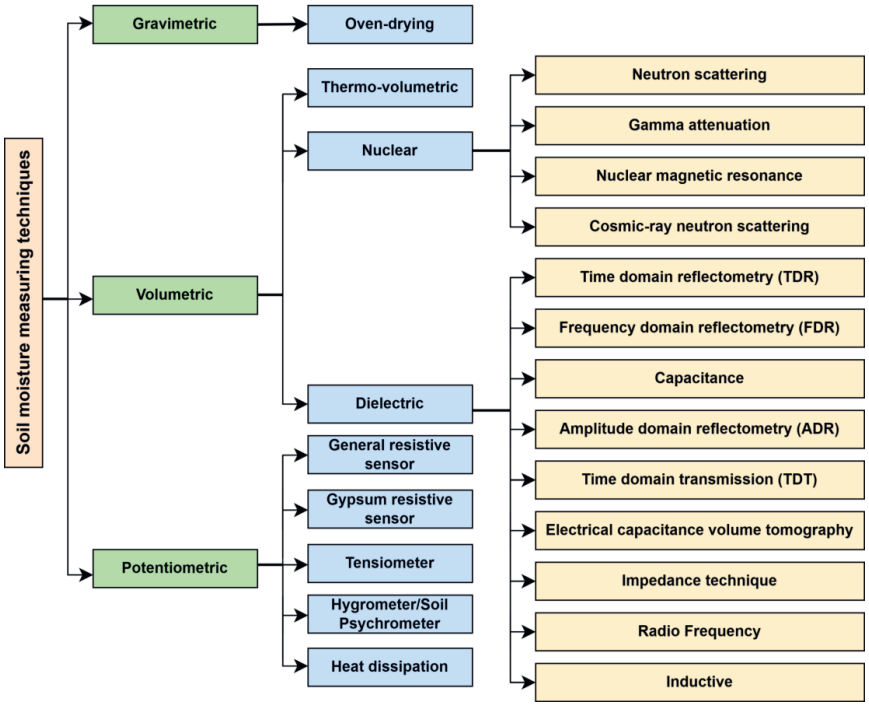

Figure 2.1: Soil moisture measuring techniques modified from Adla et al., (2020); Mukhlisin et al., (2021); Nikolov et al., (2021).

The gravimetric technique is the oldest technique, and involves weighing a soil sample before and after oven drying to determine the moisture content. The thermal volumetric technique directly measures the water content by measuring the water mass lost after oven-drying an undisturbed soil sample collected using a core sampler or tube auger. Nuclear techniques measure soil moisture indirectly by analyzing radiation-soil interactions. Neutron scattering techniques use a radioactive probe and helium-3 detector to estimate soil water by counting the thermal neutrons thermalized by hydrogen in the soil. The gamma ray transmission method uses a radioactive source, such as 137Cs, to emit γ-rays, and the energy of the γ-rays transmitted through the soil is used to estimate soil moisture content. Nuclear magnetic resonance (NMR) non-invasively estimates soil moisture by applying magnetic fields to the ground and detecting changes caused by hydrogen atoms in the soil. NMR logging can analyze hydrogen-containing fluid dynamics in porous media and detect soil moisture in situ. Cosmic-ray neutron sensing (CRNS) probes measure fast-moving neutrons in the soil and air to monitor soil moisture (Gianessi et al., 2021; Mukhlisin et al., 2021).

More recently, soil moisture sensing techniques have been developed to sense soil electrical properties (different from their electrochemical properties) including the natural electric field (electric potential), resistance (conductivity), electro-osmosis, and dielectric constants of soils (Yu et al., 2021). Dielectric techniques measure the dielectric constant of soil, a characteristic that changes with soil moisture (Zeni et al., 2015). Time-domain reflectometry (TDR) is a method of determining the apparent permittivity of soil by measuring the time it takes for an electromagnetic pulse to travel through parallel electrodes inserted into the soil. The apparent permittivity of water, which is approximately 80 (unitless), is significantly larger than that of other soil constituents, which typically range from 1 to 12 (unitless). As a result, the apparent permittivity of soil is strongly correlated with soil moisture (Kojima et al., 2016). Frequency Domain Reflectometry (FDR) based sensors, measures the frequency change of radio frequency (RF) signal in soil induced by moisture change (Chang et al., 2022; Oates et al., 2017). Capacitance sensors release electrical charge into the soil and measure the soil dielectric permittivity (Yuda Feng et al., 2022). Time domain transmission (TDT) measures electromagnetic wave propagation through soil to determine moisture content. Information obtained from the real and imaginary parts of the complex admittance, conductance, and susceptance can be used to determine material properties. Radio frequency (RF)-based sensors gauge soil moisture levels by assessing the attenuation or propagation velocity of radio frequency signals traversing the soil medium (Chen et al., 2022). Inductive sensors use electromagnetic induction to measure the soil moisture. They emit an oscillating electromagnetic field into the soil, which induces alternating currents. These currents generate a secondary electromagnetic field that is detected by the sensor. The characteristics of this secondary field provide information on the apparent electrical conductivity (ECa) of the soil, which is influenced by its moisture content (Basterrechea et al., 2021; Calamita et al., 2015; Tian et al., 2022). Potentiometric soil moisture monitoring measures the electrical potential difference between the electrodes, which is dependent on soil conductivity. Resistive sensors measure the electrical resistance of the soil, which is influenced by its water content (Kosasih et al., 2023). Electrical resistance blocks, often referred to as gypsum blocks, feature two embedded electrodes within the gypsum block itself. When these blocks are placed in soil, the resistance between the electrodes changes in response to the movement of water, which is influenced by soil moisture levels (Zeni et al., 2015). A tensiometer involves measuring the water movement in porous materials that are in contact with the soil to determine the soil moisture energy (Yu et al., 2021). Heat-dissipating sensors capitalize on the fact that wet soil is capable of dissipating heat more rapidly than dry soil, and they employ this phenomenon to quantify the rate of temperature increase when a heat source is applied (Ding and Chandra, 2019).

All the techniques mentioned above have their own set of advantages and disadvantages, which were thoroughly discussed in detail by Rasheed et al., (2022).

2.4. COMPONENTS OF SOIL MOISTURE SENSING SYSTEM (SMSS)

Monitoring and management of soil moisture influence resource management in agriculture (e.g., water and fertilizers). But its cost can be a major limiting factor for adoption among farmers (Ferrarezi et al., 2015; Schwamback et al., 2023). The design of affordable SMSS essentially implies the cost-effectiveness of each of its components. SMSS typically estimate soil moisture indirectly by detecting other soil properties (Zhou et al., 2019) and necessitates the inclusion of various components (Vandôme et al., 2023) in SMSS such as sensor, microcontroller, power source, communication module, software component and supporting hardware as shown in Figure 2.2 (Ferrarezi et al., 2015).

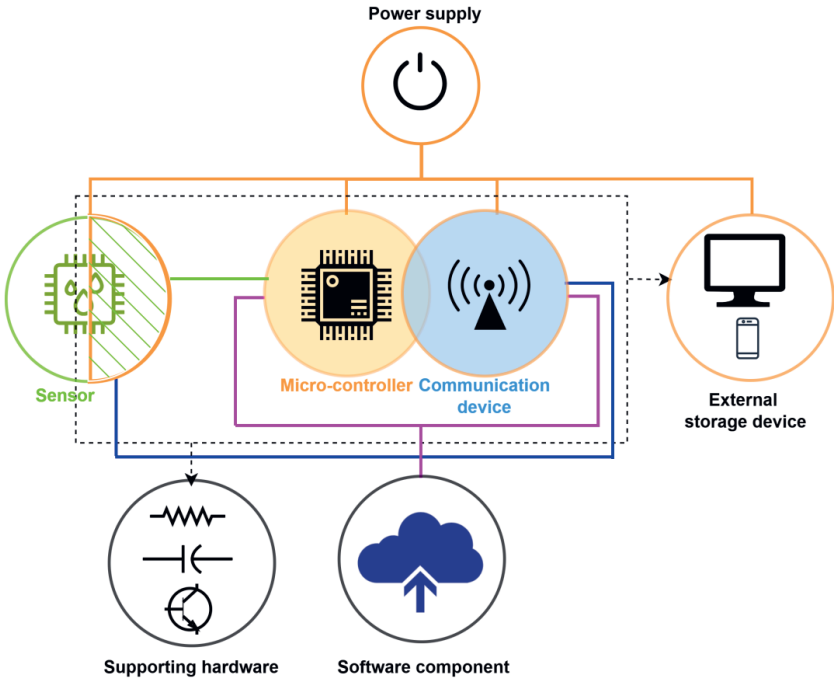

Figure 2.2: Various components of a SMSS modified (Ferrarezi et al., 2015).

A sensor is a device that measures a property that is linked to soil moisture. A microcontroller is a small, low-power computer that can control and read sensors, process sensor data, and control the operation of the system. A power source provides electricity to the system (e.g., batteries, solar panels, AC power, etc.). A communication module enables the system to transmit data to an external device such as a data logger, computer or smartphone (Josephson et al., 2020). The software component may include firmware and software for applications, such as data processing, database management, data (en-) coding, microcontroller unit, and sensor data processing. Additionally, software components can be involved in the user interface and cloud platforms to host data (Brinkhoff et al., 2018). The supporting hardware includes transistors, resistors, capacitors, and connecting wires, which can receive and display data from the system for later use (Ferrarezi et al., 2015).

Some of the available soil moisture sensor was connected to a microcontroller (light green line in Figure 2.2) and external data storage device. It may also be connected to a communication module that wirelessly transmits sensor data to the network server (blue line in Figure 2.2). Sensors, microcontrollers, and communication devices use hardware (black dotted line in Figure 2.2) to connect and store soil moisture data in external storage. Access to stored data and data communication is usually associated with software components. Components, such as sensors (with some exceptions depicted with green hatched lines in Figure 2.2), microcontrollers, and communication devices, require a power supply (shown with brown colour line in Figure 2.2). The specific components of an SMSS depend on its design and purpose. More accurate sensors and sensing systems tend to be costly and vice versa (Chang et al., 2022). When designing a low-cost SMSS, some important considerations include sensor and microcontroller selection while maintaining the accuracy and reliability of the data. The choice of data storage, such as cloud platforms and Secure Digital (SD) memory cards, also influences costs, particularly in harnessing the potential of big data in agriculture in a real-time manner. Furthermore, low-power sources and low-cost wireless communication modules can reduce operational and maintenance (O&M) costs and enable deployment in remote areas that lack adequate infrastructure (Yuda Feng et al., 2022; Mundewadi et al., 2023). O&M costs can also be lowered by reducing the need of technical expertise and skilled labor required in installing, operating, and maintaining SMSS (Placidi et al., 2023). Finally, capital is also required to deploy SMSS at larger spatial and temporal scale, to replicate and scale such solutions (Yuda Feng et al., 2022; Srbinovska et al., 2015).

2.4.1. LOW-COST SOIL MOISTURE SENSOR

The cost of a soil moisture sensor depends on factors, such as its measurement technique (Adla et al., 2020), accuracy (Schwamback et al., 2023), range of connectivity for wireless communication (Yuda Feng et al., 2022), durability (Schwamback et al., 2023), and manufacturing costs (Yu et al., 2020). More accurate soil moisture sensors tend to be more expensive owing to their high-quality sensor components (Mundewadi et al., 2023), fabrication methods (Farooqui and Kishk, 2018), and manufacturing processes (Biswas et al., 2022). Additionally, sensors that can measure soil moisture over a wider range of soil water content (Nagahage et al., 2019) have higher sensing volumes, longer life (Brinkhoff et al., 2018), faster response times, and shorter recovery times, and tend to be more expensive because they require more sophisticated calibration and validation processes (Jain et al., 2020). Sensors that can connect to the Internet or a wireless network to send data to a remote server or cloud-based system, or those that are built to withstand harsh environmental conditions (such as extreme temperatures and exposure to chemicals) can be more expensive than standalone sensors (Mundewadi et al., 2023). Finally, economies of scale achieved through higher production volumes also impact the overall costs (Manjakkal et al., 2021).

Current state-of-the-art commercially available soil moisture sensors may be cost-prohibitive, time-consuming to install, labor-intensive, and restrict the deployment density to approximately one device per field (Ferrarezi et al., 2015; Iqbal et al., 2020; Schwamback et al., 2023). Low-cost soil moisture sensors are often designed using less expensive materials, such as plastics, instead of more expensive materials, such as metals (Chanwattanapong et al., 2021; Iqbal et al., 2020). The term ‘low-cost sensor’ has been used subjectively in the literature in the context of the purchase prices of sensors, and a large variation in sensor costs has been reported (from < 1 USD to 300 USD per sensor) (Adla et al., 2020; Dahal et al., 2020; Yu et al., 2021; Zhou et al., 2019). According to Adla et al. (2020) and Biswas et al. (2022), capacitive sensors are classified as low-cost as they acquire soil water content at low cost with high precision and they also meet the requirements of wireless sensor network (WSN), and

resistive sensors are classified as very low-cost sensors. In addition, low-cost sensors have been developed based on TDR, electrical impedance spectroscopy (EIS) (Umar and Setiadi, 2015), mutual inductance (Parra et al., 2020, 2019; Tessmer and Aschenbruck, 2023), dual-probe heat pulses (Kalita et al., 2016), soil-moisture detection, and heat dissipation techniques (Saeed et al., 2019). They were also developed based on radio-frequency technology (Chang et al., 2022).

2.4.2. OTHER COMPONENTS IN LOW-COST SMSS

The other software and hardware components of SMSS (Figure 2.2) are interconnected; hence, their respective costs must also be considered to achieve overall cost-effectiveness. Table 2.2 provides information about the manufacturers and unit prices of various open-source and commercially available software and hardware components that can be used for designing low-cost soil moisture systems.

Table 2.2: Manufacturer and cost of hardware and software components used in low-cost sensing systems.

Index	Component	Manufacturer	Cost ($/unit)	Ref.
Hardware components				
A)	**Only microcontroller**			
1	Arduino	Arduino	12 –25	(Abba et al., 2019; Ferrarezi et al., 2015)
2	STC89C52RC	STC Micro	1.12	(Nagahage et al., 2019)
3	Raspberry Pi	Raspberry Pi Foundation	15	(Yuda Feng et al., 2022)
B)	**Only communication module**			
1	Wireless Fidelity (WiFi) (ESP8266)	Ai-Thinker	1.79	(Nagahage et al., 2019)
2	Long range (LoRa SX1276)	Semtech	20 Euro	(Placidi et al., 2023)
C)	**Both (Microcontroller + communication module)**			
1	ATMEGA328P	Microchip Technology (previously Atmel Corporation)	~3	(González-Teruel et al., 2019)
2	ESP32	Espressif Systems	~10	(S. Borah et al., 2020)
Software components				
1	Raspberry Pi OS	Raspberry Pi Foundation	Free	(Yuda Feng et al., 2022)
2	Arduino IDE	Arduino	Free	(de Melo et al., 2023)

2.4.2.1. HARDWARE COMPONENTS

2.4.2.1.1. MICROCONTROLLERS

Software and hardware components for microcontrollers are often developed as packages available under both commercial and open-source platforms (Bachuwar et al., 2018). These hardware may cost between approximately 3 USD (e.g., PIC, ATMEGA328P) and 11 USD (e.g., ARM Cortex M−4). Commercial microcontrollers, such as ESP32, can support Wi-

Fi and Bluetooth connectivity, consume low power, and still perform adequately in sensing soil moisture in automated solar irrigation pumping systems (Abba et al., 2019; S. Borah et al., 2020). The application of Internet of Things (IoT) technology in farms through Wireless Sensor Networks (WSNs) can substantially increase the adoption and upscaling of SMSS, by real-time communication of data from multiple interconnected sensors (Iqbal et al., 2020; Kumar et al., 2014; Placidi et al., 2023). The ARM Cortex M−4 core and ATMEGA328P software and hardware are proprietary microcontroller products that are also included in other commercial products. For instance, STM32 is a family of microcontroller chips based on the ARM Cortex-M cores, and is known for its versatility and extensive range of supported features in farming application (Sulthoni et al., 2016)and ATMEGA328P has been used for soil moisture applications in horticulture. (Abba et al., 2019; Bachuwar et al., 2018; S. Borah et al., 2020; Devapal, 2020; Saleh et al., 2016; Umar and Setiadi, 2015; Zeni et al., 2015).

However, commercial microcontroller products generally have proprietary designs that are unavailable for public access. The recent advent of open source as a disruptive phenomenon has improved the usage, modification, and distribution of such solutions. The Arduino is a microcontroller board based on the ATMEGA328P chip for sensing soil moisture (Abba et al., 2019; Chang et al., 2022; Iqbal et al., 2020; Jamroen et al., 2020; Schwamback et al., 2023; Vandôme et al., 2023; Zeni et al., 2015). Raspberry Pi is a primarily open-source single-board computer produced by the Raspberry Pi Foundation, which has been used to sense various parameters including soil moisture (Bachuwar et al., 2018; Yuda Feng et al., 2022; Iqbal et al., 2020; Kiv et al., 2022). Also, these microcontrollers provide a robust and versatile foundation for data logging technologies by interfacing with various sensors (Iribarren Anacona et al., 2023) and enabling accurate data acquisition and synchronization through real-time processing (Bhadola et al., 2022). Their low power consumption suits battery-operated, portable data logging systems in remote, off-grid locations (Bhadola et al., 2022). They can locally store data on SD cards and transmit it wirelessly for analysis. Additionally, microcontrollers can be tailored to specific data logging needs by adjusting sampling rates, data types, and the number of channels (Kerr and Rogers, 2023). Integration with components like amplifiers and analog-to-digital converters enhances functionality and accuracy. Their cost-effectiveness makes them accessible in developing and underdeveloped countries where expensive data loggers are unaffordable (Bhadola et al., 2022).

2.4.2.1.2. COMMUNICATION MODULES

Table 2.2 depicts various communication modules utilized in low-cost sensing systems. Notably, the table indicates that certain communication modules, such as ESP32 and ATMEGA328P, are integrated into microcontrollers. Two key factors in selecting a communication module are power consumption and range (of effective communication) (Briciu-Burghina et al., 2022). Other factors, such as the data transfer rate (of transmission and reception) (Kumar et al., 2014) and form factor (the module's physical shape and its dimensions) (Gonzalez-Teruel et al., 2022), along with the power consumption and range characteristics, contribute to the overall module cost (Vannieuwenborg et al., 2018). Based on their range, communication modules can be classified into contact range (0-10 m), short-range (10-100 m), short/medium-range (100-1000 m), medium-range (~5-10 km), and long-range (up to 100 km) modules (Brinkhoff et al., 2018; Chaudhari et al., 2020). Some SMSS may only require sensors to transmit over a relatively short range to the external storage device, for which short- and medium-range communication modules are sufficient.

More recently, communication devices have transcended their traditional roles and evolved into versatile sensors, transforming the interaction of humans with their surroundings.

Among contact and medium range solutions, Bluetooth Low Energy (BLE) is a low-power, wireless communication technology that is designed for devices that need to communicate with each other in sensing soil moisture (Bachuwar et al., 2018). ZigBee is a module frequently used in WSN applications (Abba et al., 2019; Briciu-Burghina et al., 2022; Brinkhoff et al., 2018; Deng et al., 2020; Lloret et al., 2021) and WiFi has also been used for soil moisture sensing (Abba et al., 2019; Ding and Chandra, 2019; Nagahage et al., 2019). Open-source integrated solutions such as Raspberry Pi and Arduino have already been discussed. Radio-Frequency Identification (RFID) and Near-field communication (NFC) tags are communication tags and use radio waves to identify and track objects equipped with tags containing microchips and antennas to collect and transmit data (S. Borah et al., 2020; Chang et al., 2022; Chen et al., 2022; Daskalakis et al., 2017; Dey et al., 2015; Iyer et al., 2022; Kim et al., 2014; Kiv et al., 2022; Zaccarin et al., 2023; Zeni et al., 2015). These tags have been used for measuring soil moisture sensor data. NFC tags are a form of RFID tags that communicate over relatively shorter ranges, enabling two-way communication between devices such as smartphones. NFC tags have advanced features and can interact with connected devices, and have been used widely in industries and in soil moisture sensing (Boada et al., 2018). Usually these tags are embedded in objects and RFID readers are used to retrieve soil moisture data from these tags. However, when these solutions need to be upscaled via WSNs and/or used in remote locations, a combination of long-, medium- and short-range communication modules may be required.

Cellular GSM modules are cellular modules from u-blox and other manufacturers that allow devices to access the internet to receive and transmit soil moisture data (Gianessi et al., 2021). By contrast, XBee is a wireless module known for its long-range capabilities (Kumar et al., 2014). LoRa is a low-power, low bandwidth wireless communication module that can communicate over ranges of 10 km, has a battery lifetime of months, and has been used for soil moisture sensing applications with strict power requirements (Bertocco et al., 2023; Chang et al., 2022; Chanwattanapong et al., 2021; Kiv et al., 2022; Vandôme et al., 2023; W. A. K. Afridi et al., 2023).

The selection of a communication module for low-cost sensing depends on the purpose, performance, and operational feasibility considerations of such a system.

2.4.2.2. SOFTWARE COMPONENTS

The aforementioned hardware requires software components for operation. Two significant examples of open-source products that combine both microcontrollers and communication capabilities are Raspberry Pi and Arduino (Schwamback et al., 2023). The Arduino Integrated Development Environment (IDE) is a cross-platform application that enables users to write and upload code to Arduino compatible microcontroller boards (S. Borah et al., 2020; González-Teruel et al., 2019). It provides a user-friendly interface and extensive community support for editing and debugging code, as well as a library of functions and examples to start with programming Arduino boards for designing SMSS (Vandôme et al., 2023). It can be used for the interface of various microcontrollers and for storing data. The Raspberry Pi OS (free and open-source Linux based operating system for Raspberry Pi microcontrollers) has also been used for soil moisture monitoring (Yuda Feng et al., 2022; Iqbal et al., 2020; Zeni et al., 2015).

2.5. OFF-GRID AMBIENT ENERGY BASED SMSS

The low-cost SMSS described in Section 4 rely on electronic components that require external energy sources, such as grid-based electricity (Abba et al., 2019; Chen et al., 2022).

Various advancements in energy generation and consumption hold promise for using such energy sources, including (i) improved battery technology resulting in longer battery life, (ii) lower power consumption because of optimized data communication via lightweight messaging protocols and low-power processors, and (iii) low-power processing technologies (Abba et al., 2019; McGrath et al., 2013; Zeni et al., 2015). However, access to energy grids is particularly limited in remotely located farms, off-grid homesteads, and mobile applications, where off-grid energy sources could be potentially useful (Lloret et al., 2021; Zeni et al., 2015). Additionally, recently developed wireless sensor networks used in SMSS require a continuous energy supply for continuous and lifetime operation for each node (Abba et al., 2019; Iqbal et al., 2020; Paz Silva et al., 2023; Sudarmaji et al., 2020). In addition to cost, the above factors limit the scalability of sensing systems. Hence, in situ energy generation by harvesting energy from ambient energy sources can be vital to power autonomous off-grid SMSS (Chatterjee et al., 2023; Faheem et al., 2019; Gill and Hasan Albaadani, 2021).

2.5.1. AMBIENT ENERGY SOURCES

The main ambient energy sources naturally or artificially present in the environment are: radiant, biochemical, thermal, magnetic, and mechanical (Chatterjee et al., 2023). This review focuses on chemical and radiant energy sources used in SMSS. Table 2.3 lists some relevant examples of ambient energy with their overall energy costs.

Table 2.3: Ambient energy sources used in review of SMSS and their overall energy cost.

Index	Ambient energy	Source	Renewable energy (Yes/No)	Examples	Cost	Ref.
1	Radiant	Solar radiation	Yes	Solar Photovoltaic	0.83 $/kW h	(Baurzhan and Jenkins, 2016)
		Radio Frequency	No	RFID	tag cost + reader cost	(Zare, 2010)
				NFC	tag cost + smartphone cost	(Arcese et al., 2014)
2	Chemical	Chemical reactions	Yes	Battery	273 $/kWh	(Curry, 2017)

2.5.2. AMBIENT ENERGY SOURCES FOR SOIL MOISTURE SENSING APPLICATIONS

2.5.2.1. RADIANT ENERGY

Radiant ambient energy encompasses electromagnetic radiation in the environment, such as visible light, infrared radiation, and radio waves, which can be converted into electricity for various uses. The sun, a major energy source, emits visible light, infrared, and ultraviolet radiation, harnessed through technologies like solar photovoltaic (PV) cells and radio frequency (RF) energy harvesters. RF radiation, with wavelengths longer than visible light, is also utilized in cellular communication (Tan and Panda, 2010).

2.5.2.1.1. SOLAR ENERGY

Radiant ambient energy applications, such as solar photovoltaic (PV) cells, are constructed from semiconductor materials that can absorb sunlight and generate electric

current. Solar PV energy has been extensively used to power wireless soil moisture sensors and in greenhouses. Solar photovoltaic (PV) systems require batteries to function effectively in off-grid regions, as solar energy is intermittent due to day-night cycles and weather conditions. These variations necessitate energy storage solutions to ensure a continuous power supply. The batteries within the solar panels store excess energy generated during peak sunlight hours, which can then be used during periods of low or no sunlight, thus maintaining the uninterrupted operation of wireless sensor networks (WSNs) (Dorel et al., 2023). Many studies have been conducted to measure soil moisture using solar energy, such as Brinkhoff et al., (2018); de Melo et al., (2023) ; Devapal, (2020) ; Schwamback et al., (2023); W. A. K. Afridi et al., (2023) and Zeni et al., (2015).

2.5.2.1.2. RADIO-FREQUENCY

In radio frequency ambient energy sources, RFID and NFC tags are utilized in SMSS. RFID devices comprise readers and tags. Readers emit magnetic fields or electromagnetic waves, and tags respond to reader commands. Tags can be either passive, powered by the reader (Kim et al., 2014), or active, with their own power sources. RFID tags can harvest energy to power external sensors or microcontrollers. Although low-powered, these tags can be used in WSN through wake-up signals that activate sensors only when needed, conserving energy (Jain and Vijaygopalan, 2010). WSN nodes can switch between active and sleep modes, allowing tag data to be read even when some nodes are inactive (Li et al., 2008). Tag reading protocols can be adjusted to involve multiple RFID-enhanced sensor nodes, distributing the energy load (Klair et al., 2008). RFID tags powered by renewable sources, such as solar panels, can efficiently drive low-power sensors (Ferdous et al., 2016). Previous studies have employed tags in SMSS (Chen et al., 2022; Daskalakis et al., 2017; Yuda Feng et al., 2022; Kim et al., 2014). The RFID reader has been identified as a potential radio frequency power source for sensors (Daskalakis et al., 2017)).

2.5.2.2. CHEMICAL AMBIENT ENERGY

Chemical ambient energy can be sourced from natural reactions in the environment, such as those in water, soil, and living organisms (Ahmed and Kakkar, 2017)offering significant potential for clean and sustainable applications (Mahmoud et al., 2022; Srikanth et al., 2018). Methods to harness this energy include fuel cells, batteries, and biological processes. Fuel cells convert chemical energy into electrical energy without combustion, making them a cost-effective alternative to traditional batteries, especially in remote and off-grid areas (Wilberforce et al., 2016). Microbial fuel cells, which generate electricity from waste products via certain bacteria, provides energy autonomy in off-grid regions (Rossi et al., 2017). Batteries generate energy by converting chemical energy into electrical energy, creating an electric current to power devices (Schmidt-Rohr, 2018). Additionally, electricity can be harnessed from the natural voltage differential in soil to convert chemical energy into electrical energy (Borno et al., 2021).

2.5.2.2.1. BATTERIES

Batteries are crucial in harnessing ambient energy sources such as solar to provide reliable and sustainable energy (Brinkhoff et al., 2018; Devapal, 2020; Sudarmaji et al., 2020). These batteries are energy storage systems, capturing excess energy generated during times of high solar or wind activity, and then releasing it when demand exceeds supply. This ability to store energy enables off-grid communities to maintain a consistent supply of electricity, regardless of the variability of ambient energy sources (de Melo et al., 2023). Various studies

have used batteries as energy source like Li-ion batteries (Bertocco et al., 2023; Paz Silva et al., 2023; Vandôme et al., 2023), solar (photovoltaic-PV) powered batteries (Patrizi et al., 2022), rechargeable batteries (Chen et al., 2022; de Melo et al., 2023; Yuda Feng et al., 2022; Ferrarezi et al., 2015; Vandôme et al., 2023), normal cell batteries (Schwamback et al., 2023) and 2000 mAh power bank (Kulmany et al., 2022). Moreover, solar panels can serve as a source of power to recharge battery chargers, or they can be integrated with inverters or other hardware devices (Brinkhoff et al., 2018, 2018). These low-power, battery operated SMSS work with various sensing techniques, including capacitance (Ferrarezi et al., 2015; Kojima et al., 2016; Vandôme et al., 2023). The operational life of battery operated sensors/transmitters is expected to be of the order of several years, with PV panels energizing the battery during the daytime (Zeni et al., 2015). Backscatter tags working on 4 AA size batteries have had battery lifetimes of upto 15 years (Josephson et al., 2020). Solar charged rechargeable batteries (even run off disposable batteries) within a SMSS with design choices to minimize power consumption have powered SDI-12 capacitance-based soil moisture probes for the duration of the entire growing season (González-Teruel et al., 2019).

The aforementioned ambient energy sources each have distinct advantages and limitations. Common benefits include their status as promising renewable and sustainable energy sources, requiring low maintenance, being non-toxic, and eco-friendly. However, the materials for construction are expensive. Solar radiation sources offer theoretically infinite power with no air and water pollution, but they require continuous sunlight and involve high initial storage or backup costs. Solar-powered batteries for SMSS are easy to install, provide high power output, and have long lifespans, yet they are not fully renewable, environmentally unfriendly, and need regular replacement. Radio frequency energy sources are cost-effective, compact, durable, and suitable for low-power devices like wireless sensor networks and RFID tags, but they deliver limited output power and can be disrupted by other electronic devices. NFC tags specifically have a short read range.

Ambient off-grid energy sources facilitate decentralized sensing systems but may increase overall costs. Key factors in selecting energy sources for SMSS include minimizing the levelized cost of electricity (LCOE), which compares power generation costs over time. High initial capital, installation, and maintenance costs for solar panels and generators are significant drawbacks. Their limited capacity also complicates charging multiple sensors simultaneously due to low power output. Despite favorable LCOE metrics, off-grid sources face institutional, regulatory, and human resource challenges. Weather variability, such as solar PV cells dependence on local radiation, further impacts reliability and applicability. Studies have reviewed and experimentally examined the energy needs of various soil moisture sensor modules with different microcontroller units, highlighting variations in energy consumption per measurement (mW.s), crucial for selecting energy sources in remote areas (Come Zebra et al., 2021; Shen et al., 2020).

In addition to the reliability and life expectancy of sensing systems, these considerations may thus trade off with scalability and hence influence the overall impact of such solutions.

2.6. BIODEGRADABLE SENSORS

Technological solutions such as SMSS including IoT systems offer promising improvements in water-use efficiency in precision agricultural systems. At the same time, they may cause environmental degradation (e.g., soil pollution via electrical and plastic waste) (Dahal et al., 2020). To reduce the impacts of these inherent contradictions, solutions need to be designed towards minimal ecological footprints. In this context, SMSS with biodegradable

sensors have the potential for more efficient agricultural input usage over entire cropping seasons and with lower detrimental impacts on the environment (Dahal et al., 2020). These sensors provide information about the moisture levels in the soil and are designed to degrade over time in the soil environment, which remain functional for extended periods in the presence of soil microbes, and then fail rapidly through electrode decomposition after the encapsulant (a covering that is applied to an electrode surface) sufficiently degrades (Dahal et al., 2020).

These sensors work through the interaction between soil water and sensing materials, such as electrolytes, semiconductor ceramics, and polymers. These sensing materials can be classified as biodegradable or nonbiodegradable. Biodegradable materials that naturally disappear in their respective environments can be used to manufacture biodegradable (or bioresorbable) sensors. These materials include polymers, co-polymers, silicon-based materials, proteins and metals. Biodegradable polymers can be either natural or synthetic. Natural biodegradable polymers, also called biopolymers, are further classified into biopolymers directly extracted from biomass (plant derived polymers and animal derived polymers) and biopolymers produced by natural or genetically modified organisms, whereas synthetic polymers are manufactured chemically (Samir et al., 2022). Plant derived polymers such as cellulose based materials, for example paper have been used as substrates for designing soil moisture sensors by Kim et al.(2014), balsa wood (Dahal et al., 2020; Sui et al., 2021) and animal derived polymers such as beeswax, soy wax, Poly(3-hydroxybutyrate-co-3-hydroxyvalerate) (PHBV) (Dahal et al., 2020).

Synthetic polymers are chemically synthesized from sources such as corn starch and cassava roots and are subdivided into polymers synthesized from bio-derived monomers (water-based monomers) and polymers synthesized from synthetic monomers (petroleum-based monomers) (Samir et al., 2022) (eg: wax blends and PHBV(Dahal et al., 2020)). Polylactic acid, which is a synthetic polymer, has been used to fabricate fully biodegradable capacitive soil moisture sensors by printable conductive pastes comprising poly(lactic acid) (PLA) as binder while Tungsten was used as a conductor (Atreya et al., 2020). Such composite conductors provide enhanced stability in various applications including agriculture (Atreya et al., 2020). It can be concluded from this study that the composite conductors give stability to the sensors. In addition to the above biodegradable polymers, Yu et al. (2020) proposed and demonstrated a novel corrosion-resistant, embeddable, open-end coaxial cable soil moisture sensors using moisture-sensitive PVA film on oxide-based thin-film transistors. In addition to the above soil moisture sensors, the utilization of certain humidity sensors has also been evaluated in this study, in light of the fact that they possess the potential for environmental application such as soil moisture (Abba et al., 2019; Kalita et al., 2016; Neto et al., 2022; Yu et al., 2020; Zaccarin et al., 2023). After designing a biodegradable sensor, it is also necessary to determine the biodegradation time of various sensors prepared using biopolymers. Different studies have described the various stages of degradation (Jain et al., 2020), tests for biodegradability (Kasuga et al., 2024), calculations about degradability rate (Dahal et al., 2020), and assessment of degradation kinetics of component materials (Dahal et al., 2020), all of which can help to design application-specific sensors.

2.7. SELECTING A "PERFECT" SOIL MOISTURE SENSING SOLUTION: LOW-COST, OFF GRID, BIODEGRADABLE

2.7.1. CURRENT CHALLENGES IN SOIL MOISTURE SENSING SYSTEMS

There are challenges in employing SMSSs associated with each of the reviewed factors. Low-cost SMSS have accuracy issues and generally need frequent soil- and site-specific calibration (Chang et al., 2022; González-Teruel et al., 2019; Mundewadi et al., 2023). Also, they either need continuous power supply or have recurrent battery and other maintenance costs (de Melo et al., 2023). Open-source components are generally available individually as commercial products and often need to be assembled in-house (Vandôme et al., 2023). The process of assembling these components restricts any optimization that can be done on the size of the overall system, as well as reduces system lifetime due to the lack of rigorous laboratory testing capabilities (Gopalakrishnan et al., 2021; Wu and Liu, 2012). This increases overall costs and reduces viability for wide-area distribution (Pal et al., 2022).

Remote solutions powered by off-grid ambient energy sources also tend to be challenged by the processes involved in the manufacture and disposal of the associated electronic components. In fact, such solutions may counterproductively harm environmental health to some extent while claiming to enhance environmental sustainability. Waste management infrastructure for collecting and recycling used lead-acid batteries, can have up to 50 % lead losses already in the recycling phase within the informal sector (Batteiger, 2015). In developing economies, disposal of batteries typically involve landfills and open garbage dumps (often associated with open waste burning) which adds to soil and air pollution (Hansen et al., 2022). The short (three to four years) working life of off-grid solar products leads to solar e-waste (Munro et al., 2023). Materials used in solar panels and batteries can have environmental and health impacts after use (Cross and Murray, 2018).

Biodegradable sensing systems are challenged by factors related to their degradation time as well as their degradability itself. There is a decrease in operational lifetimes in using laboratory tested sensors in complex biophysical environments and under mechanical stresses due to movements and deformations (Dahal et al., 2020; Zaccarin et al., 2023). Present day conductive traces used in these sensors also degrade through exposure to moisture, and research is needed to reduce this water-dependent degradation while maintaining adequate sensitivity to determine soil moisture (Atreya et al., 2020; Kojima et al., 2016). Surface roughness of cellulose paper creates challenge for sensor fabrication as it affects electrical properties (Iyer et al., 2022).

Many studies have combined one or more of the reviewed factors to design SMSSs, as outlined in Figure 2.3. This Venn diagram lists various studies classified on the basis of the SMSSs use of low-cost components, off grid energy sources or biodegradable material. It is evident that a significant number of cost-effective SMSSs are commercially available and can be manufactured using affordable hardware and/or software components (blue circle); this review identified 69 such studies. On the other hand, 17 studies have explored soil moisture sensing powered by off-grid ambient energy sources (orange circle). Since the development of biodegradable sensors is a recent phenomenon, a relatively lower number of such studies (8) have been included in this review (green circle).

Among the intersecting areas, studies have also developed and applied low-cost SMSS that can operate using off-grid energy sources such as solar power. 9 such studies have been

identified in the corresponding area of intersection. Also, low-cost biodegradable soil moisture sensing has seen recent advances, and this review includes 4 such publications.

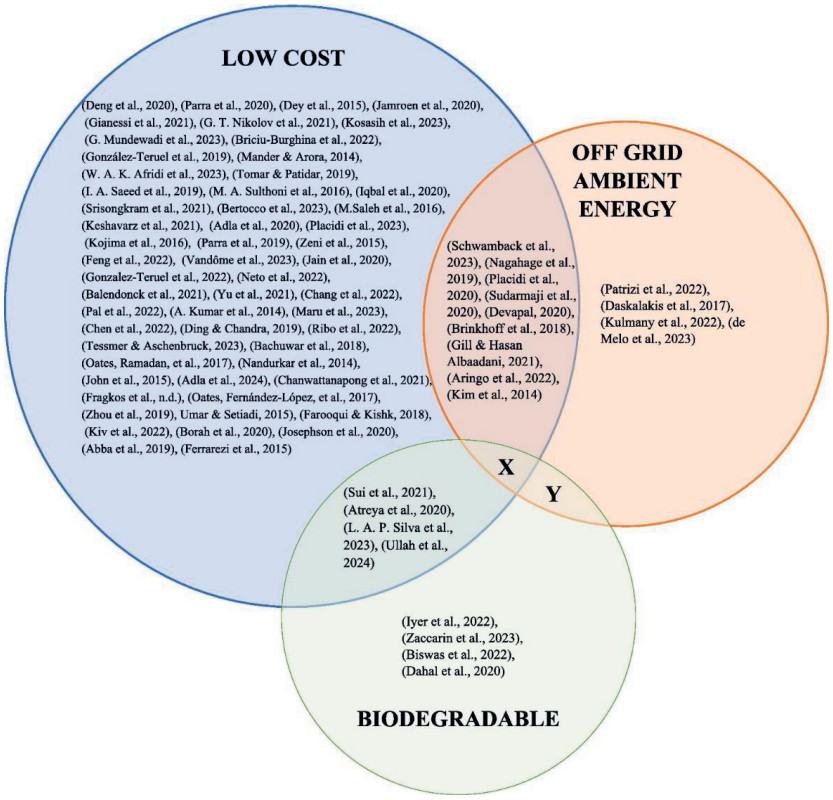

Figure 2.3: A Venn diagram representing the gaps in currently available literature on SMSS considering cost, off grid energy source-compatibility, and biodegradability.

However, no studies of biodegradable soil moisture sensing powered by off-grid energy sources could be identified in this review (region Y). Consequently, there are no published studies on SMSSs which capture all the three aspects highlighted in this review (region X). These gaps in the literature reveal the possibilities for research and development in SMSSs, accounting for cost effectiveness, remote applicability, and environmental safety.

2.7.2. SELECTING A "PERFECT" SOIL MOISTURE SENSING SYSTEM

The choice of sensing system depends on the tradeoffs between multiple attributes to 'balance' the overall system effectiveness. A commonly explored trade-off is between sensor cost and accuracy (Kojima et al., 2016). This tradeoff manifests from a larger, user-centric framework for selecting desirable SMSS that balance both sensor performance and operational feasibility (which subsumes cost considerations) (Kukal et al., 2019). Based on this review, a third aspect is suggested to be added to this trade-off – biodegradability. Figure 2.4 conceptualizes all these trade-offs as a three-way system to understand the multiple considerations when choosing an application specific SMSS. The arms represent sensor performance, operational feasibility, and biodegradability. Sensor performance involves

accuracy, precision, measurement range, environmental sensitivity, and response time (Ullah et al., 2024). Operational feasibility includes aspects such as cost, size, durability, and power requirements (with impacts on telemetry, sensing, and logging costs) (Kukal et al., 2019). Biodegradability is quantified by the biodegradation time taken for the system components to naturally break down in the environment.

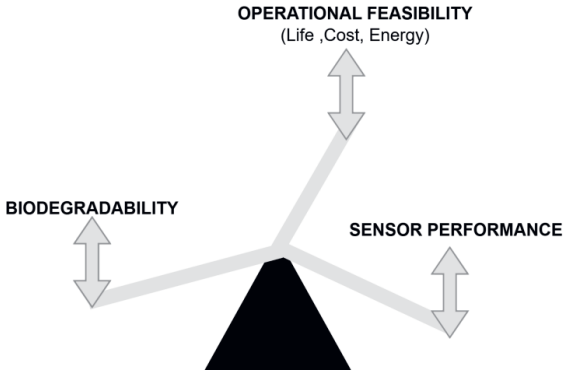

Figure 2.4: Conceptualizing the trade-offs based on operational feasibility (life, cost, energy requirement), sensor performance and biodegradability.

There is an indirect trade-off between biodegradability and sensor costs; a sensing system's life expectancy is reduced by its inherent biodegradable properties (of "disappearing naturally in its respective environment"), consequently impacting long-term monitoring (owing to more recurrent sensor costs). However, aspects such as life expectancy of SMSS have not been extensively explored much in the literature. Some studies may report the sensor life expectancy (Schwamback et al., 2023), nevertheless, any effort towards sensor development and testing would benefit from well-designed, application-oriented investigations into the life expectancies of the sensors themselves and the SMSS they are a part of. Sensor manufacturers may not release protocols for such testing because of the proprietary nature of the information, but in the age of open science (Vicente-Saez and Martinez-Fuentes, 2018), it is desirable that both peer-reviewed and non-refereed efforts test life expectancies and share their protocols.

This exemplifies the complexity of selecting a suitable sensing system because of the trade off "balance." These attributes must be deliberately weighed with respect to each other and can be used within existing frameworks (e.g., (Kukal et al., 2019)). Overall, there is no perfect solution and the decision of choosing a suitable SMSS is essentially context-specific, with a purposeful management of these trade offs. For example, small-scale farmers who may be rainfed and have no access to data about their farms' soil moisture status maybe practicing subsistence farming, and need to maximize yield rather than water use efficiency. A low-cost decentralized system which can detect water scarcity would be more applicable here. Whereas in developed countries, large-scale contract farmers may prioritize resource (including water) use efficiency, to give them a profitable proposition because of economies of scale of their own production. In this case, they would prefer high-precision agricultural solutions which demand accurate sensing systems, even if they provide marginal information. This review can help to assess the right SMSS for diverse applications in the agricultural sector.

The gaps as identified by regions X and Y (Figure 2.3) also imply that the corresponding trade offs have not been well explored. For example, if off-grid systems are not biodegradable then they may harm the environment as a result, disproportionately impacting

resource-poor farmers (gap is identified by region Y in Figure 2.3). Off-grid SMSSs use batteries and solar panels which contain harmful chemicals, and the disposal, recycling or reuse is a problem in developing countries, which is further accentuated by the diffused nature of the environmental harm (it being off-grid). Because of that these batteries are disposed of in landfills and open garbage dumps which cause soil pollution, soil erosion, and landscape change (Ellabban et al., 2014). Shorter (three to four years) working life of off-grid solar product leads to solar e-waste (Munro et al., 2023), which can have environmental and health impacts after use (Cross and Murray, 2018). All these should be considered before deciding the off grid ambient energy sources for SMSS. To enhance and ensure the accuracy of the perfect SMSS, various strategies can be implemented. These include universal and single-point calibration (Yuda Feng et al., 2022; Saito et al., 2022; Schwamback et al., 2023), integration of state-of-the-art sensor technologies, such as LTE signals (Kulmany et al., 2022), and utilization of LoRa signals, which have demonstrated an average error of 3.1 % (Chang et al., 2022). Additionally, a battery-free Wi-Fi tag system, such as SoilTAG, can be used to convert soil moisture changes into frequency responses, achieving an accuracy of 2 % within a 6-meter range and 3.64 % within a 10-meter range (Jiao et al., 2022). Furthermore, by improving the surface characteristics of sensor substrates (Iyer et al., 2022) and enhancing sensor trace quality (Iyer et al., 2022), as well as developing fully degradable intelligent radio transmitting sensors by encapsulating miniaturized resonating antennas in biodegradable materials, the accuracy of SMSS can be further improved (Gopalakrishnan et al., 2021).

2.8. CONCLUSIONS AND WAYS FORWARD

Commercially available low-cost SMSS may not provide accurate and reliable soil moisture estimates, leading to incorrect irrigation (and other) management decisions as it is influenced by soil characteristics, such as texture, temperature, bulk density, and salinity. The calibration functions provided by sensor manufacturers are typically developed under laboratory conditions and may not be accurate for field applications but can be improved by site-specific calibration. These sensors have shorter lifetimes owing to faster wear and tear of their sensing elements. This may limit their measurement ranges and reduce their suitability for all soil types and depths. This can be addressed to an extent by site-specific calibration and regular maintenance at the cost of other resources (e.g., time and human resources). Furthermore, low-cost sensing may be more susceptible to interference from other factors such as temperature, humidity, and soil salinity, which can affect data accuracy. This can be countered by rigorous laboratory and field testing and the corresponding methodological innovations to compensate for environmental sensitivity. As a result, although such methods can produce lower quality data than more expensive sensors, there are techniques to improve their utility in precision agriculture.

Off-grid power sources can generate or store a certain amount of energy; thus, they cannot power multiple devices or appliances simultaneously, thereby limiting their applicability in WSNs. The high initial cost of installing and maintaining off-grid power sources also makes them unaffordable. They are also unreliable sources and require specialized skills for maintenance and repair, which can be challenging for individuals without necessary expertise. However, they can enhance the scope of SMSS to regions that have yet to potentially benefit from WSNs. The current technological solution for powering IoT-based devices relies mainly on batteries. However, their lifetimes are generally much less than the expected lifetimes of the WSNs; hence, periodic replacement of batteries is required to keep the devices operational. This creates extra expenses and additional complications for remote sensors. Also, batteries are expensive, bulky, and contain harmful chemicals. Although efforts are currently being made to improve the energy storage capacity and, therefore, the lifetime of IoT devices,

the miniaturization of batteries remains a major technological challenge. Various energy sources like solar and RF can be used as energy harvesters to charge a sensor's super capacitor, indicating an interest in sustainable and off-grid power sources. There are other off-grid ambient energy sources which can be used as energy sources such as MFCs (e.g. Soil MFC, Plant MFC, Sediment MFC and Terrestrial MFC) in which bacteria's from soil generate electricity. Theoretically, sensor nodes powered by MFCs have eternal lifetimes.

Biodegradable sensors have been tested for their environmental biodegradability and corresponding effects on crop growth. However they have not been applied much in agricultural applications, and require substantial R&D support to enhance their capabilities. More research is needed to test the applicability of biodegradable sensors in soil moisture sensing, exploring their scope of applicability, accuracy (contextualized to their application), sensitivity to environmental factors (e.g., sensitivity to variations in temperature, salinity, and pH), and suitability across microbiome conditions (e.g., the effect of rhizosphere biological activity and organic matter in the soil zone). Studies to determine the scope of application would include investigations of the required accuracy, budget, qualified labor demand, sampling volume, and life expectancy. Furthermore, the sensor response time (to changes in the surrounding moisture conditions) is significantly longer in biodegradable sensors; this would require research to bring it to an acceptable limit useful for specific agricultural or other applications. To conclude, the challenges facing the design of truly biodegradable sensors include the fabrication of conductive biodegradable materials, wireless communication, power supply, power efficiency, quality of the substrate material and control of elimination rates.

Research and development in soil moisture sensing needs to be aligned towards specific applications and constrained by different contextual realities (e.g., costs, accessibility to the power grid, and environmental sustainability). Some applications may require soil moisture monitoring at finer observational scales of time or space (such as flood forecasting), while others may require observations at larger scales (such as drought monitoring). These would then influence relevant parameters for the design of the SMSS, such as sensor response time and whether a WSN is needed (and if yes, the spatial density of the sensors). Screening and pre-assessment of different components need to be tested individually and in combination with other biodegradable polymers. Experimental designs can be adapted from previous studies to test the accuracy of the sensors, develop appropriate calibration functions and quantify (and correct for) environmental sensitivity in laboratory conditions. Finally, field studies are required before full implementation of these solutions could be realized.

3

SYNTHESIS OF BIMETALLIC ELECTRODE (CATHODE) FOR NO_3RR

Parts of this chapter are based on:

Maya Moreshwar Meshram, S., Gonugunta, P., Taheri, P., Jourdin, L., Pande, S. (2025). Investigating the influence of a thin copper film coated on nickel plates through physical vapor deposition for electrocatalytic nitrate reduction. Frontiers in Materials , Volume 12 - 2025.

3.1. INTRODUCTION

NO_3^- is one of the most common toxic pollutants in groundwater (Li et al., 2015). NO_3^- contamination of groundwater is becoming increasingly serious in both developed and developing countries (Abba et al., 2023; Jia et al., 2020; Sancho et al., 2016). This problem is caused by a variety of activities, including agriculture, industry, sewage, septic tanks, and landfills, leading to an increase in NO_3^- levels in water sources (Abascal et al., 2022; Lockhart et al., 2013). The maximum amount of NO_3^- permitted in drinking water is 50 mg/L in Europe and 44.43 mg/L in the United States (Shen et al., 2009). Methemoglobinemia or "blue baby syndrome" can result from NO_3^- exposure above these levels and poses substantial health hazards, especially for young children and expectant mothers (Knobeloch et al., 2000). Additionally, NO_3^- poisoning of water used for agriculture has an impact on both ecosystems and human health (Della Rocca et al., 2007). Water bodies are also affected by excessive NO_3^- contamination, resulting in eutrophication, algal blooms, and disruption of the delicate balance of aquatic life (Moffat, 1998). Thus, to maintain the water quality, public health, and ecological integrity of agricultural watersheds, effective NO_3^- removal technologies are essential (Tomer et al., 2013).

Various methods have been developed to remove NO_3^- from water, including reverse osmosis (Ahn et al., 2008), ion exchange (Leaković et al., 2000), electrodialysis (El Midaoui et al., 2002), photocatalytic reduction (Varapragasam et al., 2021) and biological denitrification (Park and Yoo, 2009). In recent times, electrochemical methods, particularly NO_3RR, have gained recognition as a viable solution for the efficient elimination of low-concentration NO_3^- from water sources (de Groot and Koper, 2004). Although still in the developmental stage, this technology holds immense promise and, when fully realized, it can offer numerous advantages over conventional approaches, including environmental sustainability, compatibility, cost-effective energy consumption, high efficiency, satisfactory engineering compatibility, controllable operating conditions, selectivity to desired product, and potential integration with renewable energy sources (Jia et al., 2020; Lange et al., 2013; Wang et al., 2021). Two routes are involved in the NO_3RR (H. Wang et al., 2023): The indirect autocatalytic reduction pathway and the direct electrocatalytic reduction pathway. Indirect autocatalytic reduction occurs when NO_3^- is not involved in electron transfer processes (de Groot and Koper, 2004; Wang et al., 2021). This indirect autocatalytic reduction pathway usually occurs only at high NO_3^- concentrations and in strongly acidic media (Lange et al., 2013). Direct reductive chemical pathways are possible at low concentrations of NO_3^-. In the NO_3^- reduction process, N_2 and NH_3 are the main products, following reactions (Equations 1 – 5):

$$NO_3^- + H_2O + 2e^- \rightarrow NO_2^- + 2OH^- \quad \text{.....(1)}$$

$$NO_2^- + 2H_2O + 3e^- \rightarrow 1/2N_2 + 4OH^- \quad \text{.....(2)}$$

$$NO_2^- + 5H_2O + 6e^- \rightarrow 1/2NH_3 + 7OH^- \quad \text{.....(3)}$$

$$NO_2^- + 4H_2O + 6e^- \rightarrow NH_2OH + 5OH^- \quad \text{.....(4)}$$

$$NO_2^- + H_2O + 2e^- \rightarrow NO + 2OH^- \quad \text{.....(5)}$$

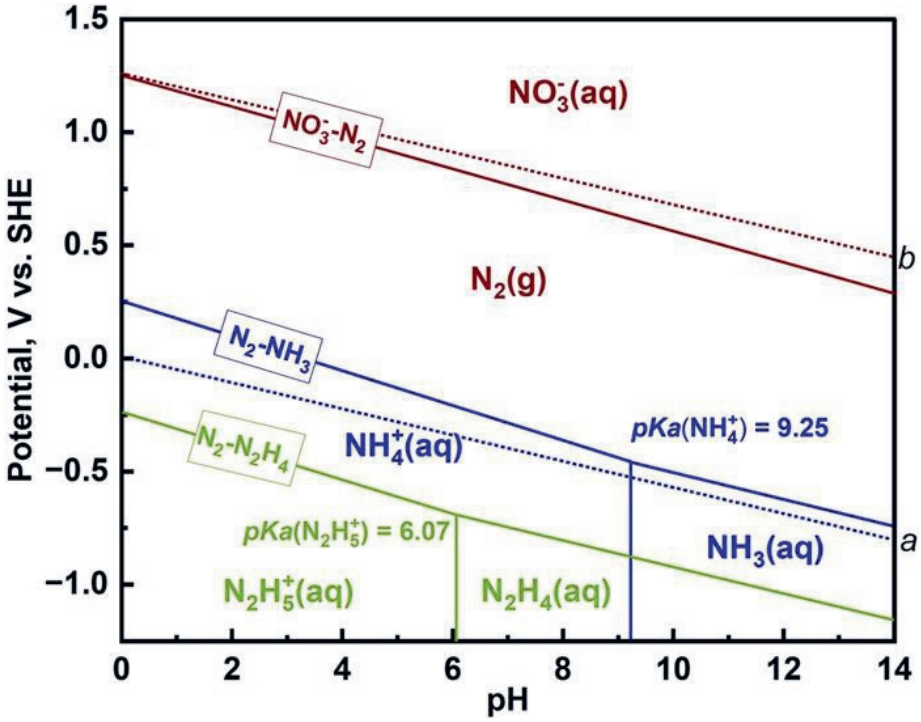

Figure 3.1: Pourbaix diagram of the N_2-H_2O system including N_2, NH_3, N_2H_4, and NO_3^-.

From the Pourbaix diagram shown in Figure 3.1, N_2 and NH_3 are the most thermodynamically stable forms of N_2 under standard conditions (Guo et al., 2019).

NO_3^- is more stable in alkaline solution. In alkaline solution, the reduction of NO_3^- will yield a series of products (e.g., dinitrogen tetraoxide (N_2O_4), hydrazine (N_2H_4), nitric oxide (NO), and hydroxylamine (NH_2OH)) which are not the primary products in NO_3^- reduction and may decompose into other species. The existing form of ammonia (NH_3) depends on the pH of the solution, where at pH ≥ 9.25, it exists in its molecular form, and at pH < 9.25, ionic NH_4^+ is the major form. For N_2H_4, the case is similar, where the pH boundary is 6.07. NO_3RR process involves the use of electrocatalysts, such as non-noble metals (e.g., Cu, Ni, Co, and Fe) or carbon-based materials, to reduce NO_3^- to N_2 gas or NH_3 (Liang et al., 2022; X. Zhang et al., 2022). The choice of electrocatalyst affects the reaction kinetics, selectivity, and efficiency (Xu et al., 2023). Cu and Cu-based materials are considered the most promising (He et al., 2022; Hu et al., 2021) because of their low cost, abundant availability (Yiyang Feng et al., 2022), high activity (Barrera et al., 2023; Hong et al., 2022; Hu et al., 2021), and excellent performance in producing NH_3 as the main electrolysis product (Abdallah et al., 2014; Karamad et al., 2023; Yuting Wang et al., 2020; Xu et al., 2023). Cu is an active monometallic electrocatalyst for the NO_3RR in acidic and alkaline electrolytes. It also exhibit good electrocatalytic activity in both acidic and alkaline media (Hasnat et al., 2015).

NO_3^- reduction on Cu is a pH-dependent reaction forming NO and NH_4^+ when an acidic electrolyte is used and NO_2^- and NH_2OH when the electrolyte is alkaline (Pérez-Gallent et al., 2017). Metallic Cu effectively attracts and retains oxygen (O) atoms from NO_3^-. This interaction weakens the N-O bonds in NO_3^-, creating a low energy point in the bond's profile. Consequently, this facilitates the conversion of NO_3^- into NO_2^- by easing the detachment of

one oxygen atom from N_2 (Liu et al., 2019). In the process of NO_3^- reduction, the movement of charge is typically slow due to the high energy present in the lowest unoccupied π molecular (LUMO) orbital of NO_3^-. This makes it difficult to inject charge into this orbital. However, the d-orbital energy levels of Cu-based materials are similar to the LUMO * of NO_3^- (Hao et al., 2021) allowing them to facilitate the electrochemical reduction of NO_3^-(aq) and transfer electrons more easily to the adsorbed NO_3^- (Beltrame et al., 2021; Reyter, 2014; Rezaei-Sameti and Zarei, 2018; Wei et al., 2024). Various studies have shown that Cu electrodes are used for NO_3^- reduction in a single chamber in acidic (Burke and Sharna, 2007; Lima et al., 2012), in neutral (Gao et al., 2018), and in alkaline media (Badea, 2009; Bouzek et al., 2001; Paidar et al., 1999), as well as in dual chambers in acidic (Beltrame et al., 2021), and alkaline media (Badea, 2009; Cattarin, 1992; Rajmohan and Chetty, 2014). In alkaline media, Cu electrodes produce fewer oxides of N_2 as byproducts, and are less corrosive than in acidic media (Badea, 2009). However, despite its advantages, there are some disadvantages with pure Cu catalysts, such as oxidative dissolution or irreversible surface poisoning, both of which lead to undesired catalyst degradation (Dima et al., 2003; Hou et al., 2018), as well as undesirable formation of unwanted by-products (Abdallah et al., 2014; Reyter et al., 2006), such as NO_2^- (He et al., 2022; Roy et al., 2016).

To overcome the disadvantages of Cu electrodes, various strategies have been developed including (i) engineering Cu into nanoscale or single reaction site (Zhao et al., 2023), (ii) doping Cu with other elements (Pd, P, Ni, etc.), and (iii) depositing Cu on a metal oxide support (X. Liu et al., 2023). Depositing Cu on a metal oxide support is the most preferred strategy, as it is simple to synthesize and provides considerable benefits from strong metal-support interactions (Smiljanić et al., 2022). There are various thin surface film deposition techniques (Abegunde et al., 2019; Jilani et al., 2017) for depositing or coating Cu such as electrochemical deposition (Alam et al., 2015; Chen and Chang, 2012; Couto et al., 2017, 2011; Epron et al., 2002, 2001; W. Gao et al., 2019; Hou et al., 2018; Lei et al., 2018; Liu and Zou, 2014; Mattarozzi et al., 2017; Molodkina et al., 2010; Rajmohan and Chetty, 2014; Ramos et al., 2001; C. Wang et al., 2023; Welch et al., 2005; Yin et al., 2019; Zhao et al., 2022; Zurita and Garcia, 2022; Zurita and García, 2023), photo-electrodeposition (Couto et al., 2012; Ribeiro et al., 2014), potentiostatic deposition (J.-Q. Chen et al., 2023; Lim et al., 2023; Roy et al., 2016), electro-crystallization (Hyusein and Tsakova, 2023) and dipping method (Hwang, 2012).

Using the above deposition techniques Cu has been deposited on many substrates such as palladium (Lim et al., 2023), graphene oxide (GO), modified graphite felt (Wang et al., 2022), polydopamine-derived nitrogen-doped hollow carbon spheres (Y. Liu et al., 2022), carbon nanotubes (Rajmohan and Chetty, 2017), Cu foil (Rajmohan and Chetty, 2014), and zinc oxide (Feng et al., 2024). Ni is also utilized as a substrate for catalyst preparation but mostly by forming an alloy with Cu. This approach is employed because Ni produces a homogeneous, stable, and highly active catalyst with Cu, exhibiting high chemical stability and good electron conductivity (Hou et al., 2018). Additionally, its site demonstrates strong adsorption for NO_2^- (He et al., 2022). The combination of Cu and Ni compensates for the low activity of pure Cu in mediating electron transfer between intermediates (Bai et al., 2023; Kobune et al., 2020; Shih et al., 2020b), and reduces the overpotential while improving the stability of the NO_3RR reaction (Bai et al., 2023). However, Cu deposition on Ni using electrochemical deposition, results in uneven film thicknesses due to variation in applied current densities (Goranova et al., 2016), electrolyte composition (Dejang et al., 2025), and temperature (Abdullah, 2017).

The film thickness and electrolyte concentration govern NO_3RR activity (J. Guo et al., 2023; Roy et al., 2016). The thickness of Cu film affects the activity and selectivity for NO_3^- reduction (Chen et al., 2004; Shih et al., 2020b). So, here PVD technique is adopted as it can provide coatings with high precision for various film thicknesses. In addition, PVD has several advantages over other coating techniques, such as high-purity coatings (Takahashi, 1998; Yanguas-Gil and Yanguas-Gil, 2017), low processing temperature (Shah et al., 2018), high deposition rates, better adhesion, denser microstructure, controllable material properties, the ability to use a larger choice of materials (Morgan et al., 2019; Savale, 2016), reduced production cost, improved productivity (Mubarak et al., 2005), and better quality films (O'Sullivan et al., 2002). Table 3.1 presents the state-of-the-art techniques for electrode preparation utilized in NO_3^- reduction, delineating the chemicals employed, electrolyte used, duration, and efficacy in NO_3^- reduction. It is significant to note that all previous investigations exclusively utilized Ni foam, with no studies exploring Ni plate as an alternative substrate for NO_3^- reduction. The Ni plate is chosen over Ni foam because it provides a more robust and stable structure compared to Ni foam, which helps maintain the catalyst's integrity during prolonged electrochemical operations. This enhanced stability reduces the likelihood of structural breakdown often seen in the more fragile foam configuration (Kabiraz et al., 2024). Also, when Cu is deposited on Ni using electrochemical deposition, it shows poor stability owing to the oxidation and detachment of the deposited Cu layer from the substrates during the course of NO_3^- electroreduction (Hou et al., 2018). Furthermore, Ni foam is prone to corrosion, resulting in the release of free Ni ions. This process alters the catalyst's composition and hinders the subsequent analysis of related catalytic mechanisms (Bu et al., 2021). Moreover, the utilization of PVD for electrode preparation has not been previously investigated in this field of research, as noted in (Yue et al., 2024).

Table 3.1: State-of-the-art electrode preparation techniques utilized for NO_3^- reduction employing Cu coated on Ni.

Sr. No	Electrode	Electrode preparation technique	Chemical composition	Electrolyte	Duration (hour)	NO_3^- reduction efficiency	Ref.
1	NiCu@N-C/Ni Foam	Co-assembly and carbothermic reduction	3.57 mM NO_3^-	50 mM SO_4^{2-}	8	98.63 %	(He et al., 2022)
2	$Cu_{0.66}Ni_{0.33}$ $Cu_{0.50}Ni_{0.50}$ $Cu_{0.33}Ni_{0.66}$	Electrodeposition	0.01 mol/L $NaNO_3$	0.1 mol/L Na_2SO_4	4	83.87 %	(Bai et al., 2023)
3	Cu-Ni Foam	Cold plasma jet printing	50 mg/L $NaNO_3$	0.05 mol Na_2SO_4	3	88.9 %	(Yue et al., 2024)
4	Cu_3P-Ni_2P/CP-x	Vapor-phase hydrothermal method	200 ppm $NaNO_3$ -N	0.5 M Na_2SO_4	2	—	(Jin et al., 2024)
5	Cu and NiO rod on Ni foam	Electrodeposition	0.1M KNO_3 -N	0.1M PBS	1	94 %	(X. Liu et al., 2023)
6	Cu/CoP/Ni Foam	Hydrothermal	15 mg/L NO_3 -N	0.05 M Na_2SO_4 and 0–2000 mg/L Cl^-	3.5	100 %	(S. Yang et al., 2022)
7	Cu on Ni Foam	Electrodeposition	200 ppm NO_3 -N	1M KOH	2	95.05 %	(J. Li et al., 2021)
8	CuNi alloy on mesoporous carbon	Evaporation induced self-assembly	30 mg/L NO_3^--N	0.1M Na_2SO_4	7	90 %	(Yao et al., 2021)

9	$Cu(OH)_2$ - Cu/Ni Foam	One-step hydrothermal method	50 mg/L NO_3^--N	50 mM Na_2SO_4	1.5	91.5 %	(Liang et al., 2023)
10	Cu nanoparticles on Ni plate	Physical vapour deposition	2.5 mM KNO_3	0.5 g/L of Na_2SO_4	6	10 %	This study

Therefore the primary objective of this research is to investigate the influence of thin Cu film coated on Ni plate using PVD technique for NO_3RR. Previous investigations that employed Cu coating for electrode preparation have deposited thin Cu films varying from 1 nm to 390 nm on various substrates that were used as electrodes for diverse applications except NO_3^- reduction (Ganchev et al., 2021; Gonzalez-Gallardo et al., 2024; Ince et al., 2012; Johnston et al., 2004; Kang et al., 2013; Löffler and Siewert, 2004; Nobili et al., 2009; Raaif and Mohamed, 2017; Salazar et al., 2015, 2016; Sun et al., 2015; Wu et al., 2010). Therefore, in this study thicknesses of 25, 50, and 100 nm were selected to encompass this range. Subsequently, the effect of Cu film on the NO_3RR was examined. Additionally, the effect of stirring on the NO_3^- reduction reaction was investigated. Further, the obtained Cu-Ni electrodes were analyzed using scanning electron microscopy (SEM) and X-ray photoelectron spectroscopy (XPS).

3.2. EXPERIMENTAL METHODS

3.2.1. CHEMICALS AND MATERIALS

All chemicals used in this study were of analytical grade and purchased from Sigma Aldrich. Potassium nitrate (KNO_3) and sodium sulphate (Na_2SO_4) were used to prepare the anolyte and catholyte. Pure Cu powder with a particle size < 425 µm, density of Cu = 8.930, Z-ratio = 0.437, and 99.5% purity was utilized for the deposition on Ni plates. These Ni plates served as substrates for the Cu films coating, which functioned as the cathodes in subsequent analysis. The Ni plates (purity = 99.96 %, thickness = 0.2 mm) were purchased from Haoxuan Metal Materials Ltd. Platinum mesh was used as anode. All solutions were prepared using milliQ water (water obtained from a Millipore system). pH of the solution was measured using a Multi9420 InoLab IDS multimeter. Spectrophotometer (model number: DR3900) was employed for determining the concentration of NO_3^-, NO_2^-, and NH_4^+. The LCK 340, LCK 342, and LCK (303 and304) Hach kits were utilized for measuring NO_3^-, NO_2^-, and NH_4^+, respectively.

3.2.2. SYNTHESIS OF THIN FILMS OF Cu ON Ni PLATE USING PHYSICAL VAPOR DEPOSITION

First, the Ni plate was sanded and polished with sandpaper of grit size 400 - 2000. To remove impurities, the Ni sheet (of purity > 99.8%) was ultrasonically degreased and cleaned in acetone and ethanol for 15 min. They were then immersed in a 1 $mol.L^{-1}$ aqueous hydrochloric acid (HCl) solution for 5 min and washed with milliQ water. 25, 50, and 100 nm thickness of the Cu was deposited on both sides of Ni plate using the PVD (VCM 600-SP3, rack-type vacuum evaporator) method by applying a current of ~80 A. The operation details of the PVD are: substrate temperature = 1,600 - 1,800°C, evaporation rate = 0.5 Å/s, current intensity = 150 Amp, base pressure = 2.8×10^{-7} mbar, and vacuum of 5.0×10^{-6} mbar was achieved. The PVD involves the condensation of vaporized Cu atoms onto a Ni substrate under vacuum conditions, resulting in the formation of a uniform and cohesive layer (Rossnagel,

2003). The Cu–Ni sheet of 2 cm × 1 cm was dried in air at room temperature. Figure 3.2 shows a schematic of the PVD equipment and the synthesis of Cu-Ni electrodes.

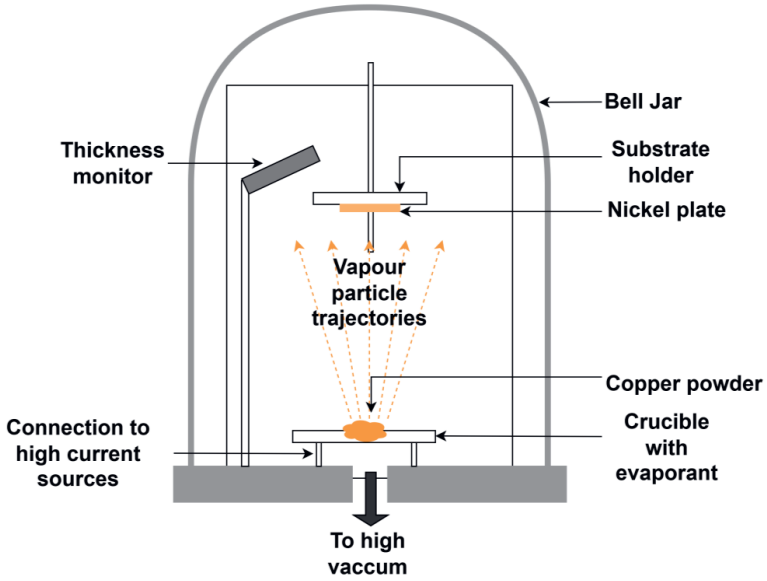

Figure 3.2: Schematic of the PVD equipment and Cu deposition process on a Ni plate.

3.2.3. ELECTROCHEMICAL NO_3^- REDUCTION

The NO_3^- electrochemical reduction experiments were carried out using a three-electrode system in a 300 mL dual-chamber H-type reactor, as shown in Supplementary Figure 3.S1 [Supplementary Material (SI)]. The anolyte was 3.5 mM Na_2SO_4, whereas the catholyte consisted of 2.5 mM KNO_3 and 0.5 g/L of Na_2SO_4 solution. 300 mL of catholyte was placed in the cathode chamber, which was then sparged with N_2 gas to remove oxygen from the solution to create anaerobic conditions. A Pt mesh (1 cm × 1 cm) was used as the counter (anode) electrode. A Cu-Ni plate (2 cm × 1 cm) was cut from a large Cu-Ni plate and used as the working electrode (cathode). The surface area of the working electrode was 4 cm^2. Ag/AgCl (3 M KCl) was used as the reference electrode. A titanium wire was connected to the Cu-Ni plate to form an external connection with the potentiostat (Admiral instrument's Squidstat Prime). A proton exchange membrane (Nafion 117) was used to separate anode and cathode chambers. A gas bag was attached to the anode and cathode chamber to collect any produced gases like H_2. All electrochemical experiments were performed by applying a constant current of −8.5 mA for 6 h. Approximately 10 mL of the solution was removed between two sampling points to determine the concentrations of NO_3^-, NO_2^-, and NH_4^+ ions and was replaced with fresh catholyte solution. NO_3^-, NO_2^-, and NH_4^+ in the solutions were measured using standard Hach kits with a UV-visible spectrophotometer (DR-3900, Lange). CV was performed at a potential scan rate of 1 mV/s under two conditions: with stirring at 500 rotation per minute (rpm) and without stirring.

The conversion rate $[C[NO_3^-]\%]$ of NO_3^- was calculated using Equation 6

$$C[NO_3^-]\% = \frac{\{C_0[NO_3^- - N] - C_t[NO_3^- - N]\}}{C_0[NO_3^- - N]} \times 100\% \quad \text{.....(6)}$$

The selectivity [S[NH_4^+]%] of NH_4^+ can be calculated based on Equation 7

$$S[NH_4^-]\% = \frac{C_t[NH_4^+ - N]}{C_0[NO_3^- - N] - C_t[NO_3^- - N]} \times 100\% \quad \text{.....(7)}$$

The concentration of gaseous compounds was calculated using mass balance Equation 8

$$C[Gaseous\ compounds] = \{C_0[NO_3^- - N] - (C_{nitrate\ remaining\ in\ solution} + C_{nitrite} + C_{ammonium}) \quad \text{.....(8)}$$

where, $C_0(NO_3^- - N)$ is initial the concentration of $NO_3^- - N$(mg/l), V is the volume of the electrolyte in the cathode compartment (L), where subscript '0' represents the initial condition whereas 't' represents the condition after time 't'.

3.2.4. ELECTRODE SURFACE CHARACTERIZATION

The morphologies of the samples were examined using field-emission scanning electron microscope (FE-SEM, JEOL JSM 6500F), which was equipped with an EDX detector. The surface chemistry of the samples was analyzed using a PHI-TFA XPS spectrometer from Physical Electronic Inc., which featured an Al Kα X-ray monochromatic source (hv = 1486.7 eV). The pass energy for the survey was set at 89.45 eV, and a vacuum of approximately 10^{-9} mbar was maintained during the XPS analysis (Cornet et al., 2024). Data was analyzed using Multipak version 8.0 software.

3.3. RESULTS AND DISCUSSIONS

3.3.1. CHARACTERIZATION

Supplementary Figure 3.S2 showcases SEM images of Cu-Ni electrodes, which were fabricated through PVD for the 25 nm thickness at 370x (Supplementary Figure 3.S2A), and 4,000x (Supplementary Figure 3.S2B) magnifications. Supplementary Figure 3.S3 shows the elemental EDX mapping and spectrum of 25 nm Cu-Ni electrode. The elemental EDX mapping of pristine Cu-Ni electrode demonstrates the complete coverage of the Ni plate with Cu, a finding that is consistent with the XPS results.

Supplementary Figures 3.S4 - S6 (shown in SI) depict the XPS of Ni plate, Cu-Ni electrode with 25 nm Cu coating (pristine) and (spent) after electrochemical reduction of NO_3^-, respectively. The detailed explanation about the XPS analysis given in SI. Supplementary Figure 3.S7 depicts a comparison of XPS spectra of Ni 2p of Ni plate without coating (Supplementary Figure 3.S7A), 25 nm Cu-Ni electrode (pristine) (Supplementary Figure 3.S7B), and 25 nm Cu-Ni electrode (spent) (Supplementary Figure 3.S7C). A noticeable difference in peaks can be observed for all three electrodes. The Ni plate without a coating exhibits the highest peaks, corresponding to Ni^0, Ni^{2+}, and Ni^{3+}, whereas no peaks were detected for the Cu-Ni electrode (pristine). For the Cu-Ni electrode (spent), Ni peaks are barely visible, indicating that some Cu has been removed, exposing the Ni surface during NO_3RR facilitating the NO_3^- reduction. A schematic diagram depicting the mechanism of Cu removal from the cathode during NO_3^- reduction is illustrated in Supplementary Figure 3.S8.

3.3.2. ELECTROCHEMICAL MEASUREMENTS

3.3.2.1. CYCLIC VOLTAMMETRY (CV) IN H-TYPE REACTOR

To assess the electrocatalytic performance of Cu deposition of different thicknesses on Ni plates, CV experiments were conducted. Figure 3.3 depicts the CV curves obtained for various concentrations of KNO_3 and Na_2SO_4 electrolyte solutions in the range of -1.8 to -0.4 V (versus Ag/AgCl (3 M KCl) reference electrode) at a scan rate of 1 mV/s.

From the cyclic voltammograms shown in Figure 3.3, an onset potential at ca. −0.603 ± 0.015 V (black curve), −0.617 ± 0.015 V (green curve), and −0.687 ± 0.031 V (red curve) was clearly visible for the experiments in which KNO_3 + Na_2SO_4 was fed and stirring was absent. No visible peak corresponding to NO_3^- reduction was detected under stirred conditions. The absence of a NO_3RR peak was anticipated, as mass transport is not limited under stirring which facilitates faster replenishment of NO_3^- at the cathode surface than it is consumed, and products are also removed faster from the surface. This is in contrast to the situation when stirring is ceased, resulting in the formation of a peak, in the −0.6 to −1 V range with a maximum at around −0.9 V vs. Ag/AgCl (where no or limited H_2 production was observed). For 5.9 mM KNO_3 + 3.5 mM Na_2SO_4, concentration in stirring conditions (red curves) the potential of the reductive peak shifted to slightly more negative potentials, ca. −1.03 ± 0.15 V vs Ag/AgCl. For the experiments that contained only for 3.5 mM Na_2SO_4 (pink curves), no peak was observed, and an onset in reductive current was only observed at ca. −0.85 ± 0.03 V (with stirring) and −0.88 ± 0.01 V (without stirring), is either corresponds to proton (H^+) and/or water reduction to H_2. The current densities at the NO_3RR peak in without stirring condition were ca. 1.48 ± 0.59 (black curve), 1.36 ± 0.68 (green curve), and 2.33 ± 0.11 mA cm^{-2} (red curve). Therefore, the presence of 5.9 mM KNO_3 (red curves) partially alleviated mass transport limitations (without stirring), resulting in a higher NO_3RR peak compared to 2.5 mM KNO_3 (black curves). No significant differences in peak height and onset were observed at varying Cu layer thicknesses without stirring, except for a slightly higher maximum peak current at 5.9 mM KNO_3 (red curve) and 100 nm Cu film thickness. With 25 and 100 nm thick Cu film and under stirring, a higher reductive current was recorded with 5.9 mM KNO_3 than with 2.5 mM KNO_3 in the −0.6 to −1 V range, which would indicate a higher rate of NO_3^- reduction, though this was not observed for 50 nm Cu film. As the Cu film thickness on the Ni plate is enhanced, a decrease in the current density is observed, as illustrated in Supplementary Figure 3.S9. This could be due to the evolution of microstructure and increased surface roughness (Lin et al., 2017), structural deterioration (Nguyen et al., 2024), and increased resistivity caused by variations in bonding mechanisms and interface voids in thicker films which impedes current flow (T.-F. Lu et al., 2024). Further investigation is necessary to elucidate these observations.

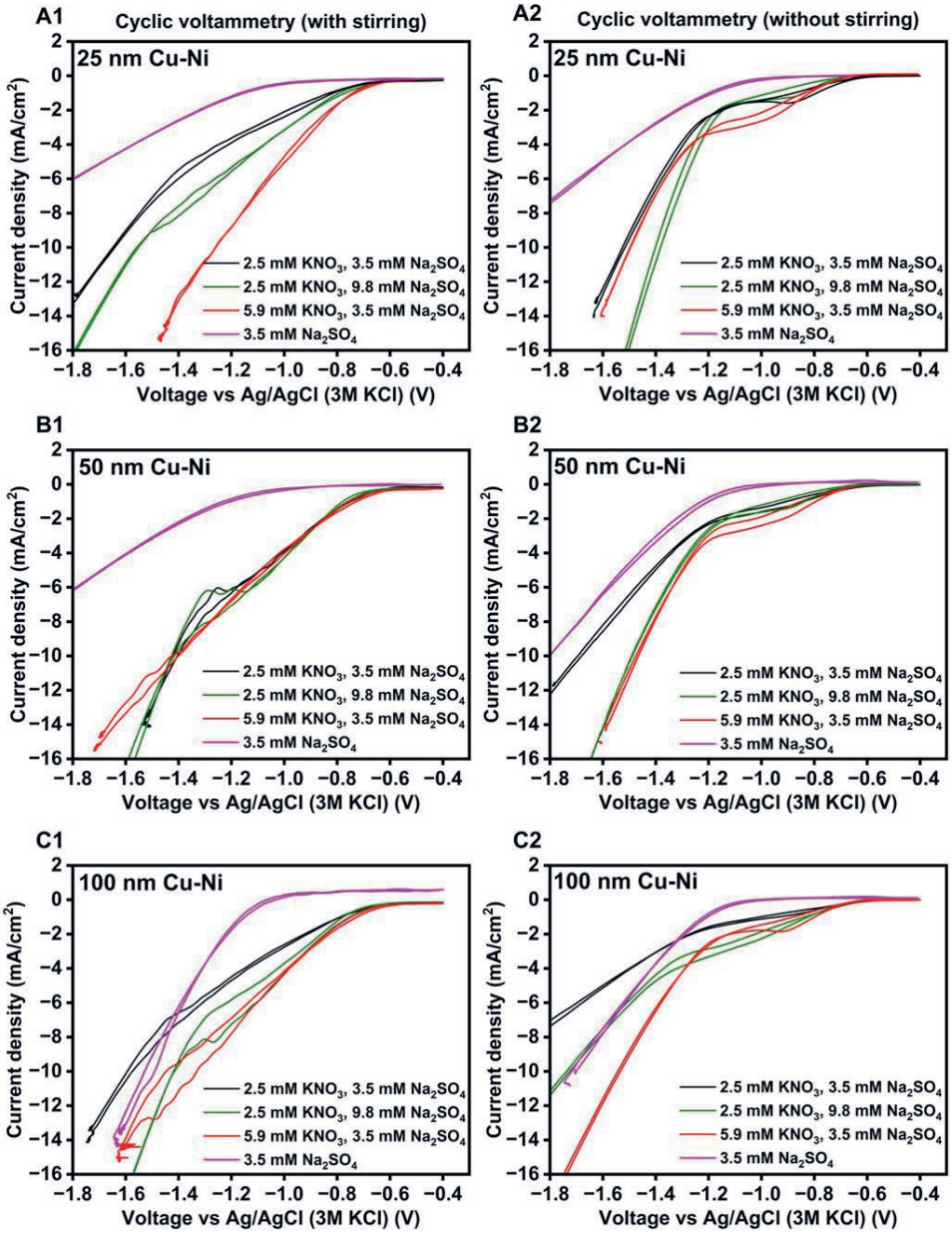

Figure 3.3: Cyclic voltammetry was recorded for Cu-Ni electrodes with varying Cu film thicknesses: **(A1,A2)** at 25 nm, **(B1,B2)** at 50 nm, and **(C1,C2)** at 100 nm, under N_2 sparging and with different concentrations of KNO_3 and Na_2SO_4 electrolyte. Additionally, **(A1,B1, and C1)** represent cyclic voltammetry measurements with stirring at 500 rpm, while **(A2,B2, and C2)** represent measurements without stirring, with a scan rate of 1 mV/s and an initial pH of 6.5.

3.3.3. NO_3RR USING 25 nm, 50 nm, AND 100 nm Cu-Ni PLATES

The performance of Cu-Ni electrodes of varying thicknesses for electrochemical NO_3^- reduction and product formation (NO_2^-, NH_4^+, and gaseous compounds (GC)) with time is shown in Figure 3.4.

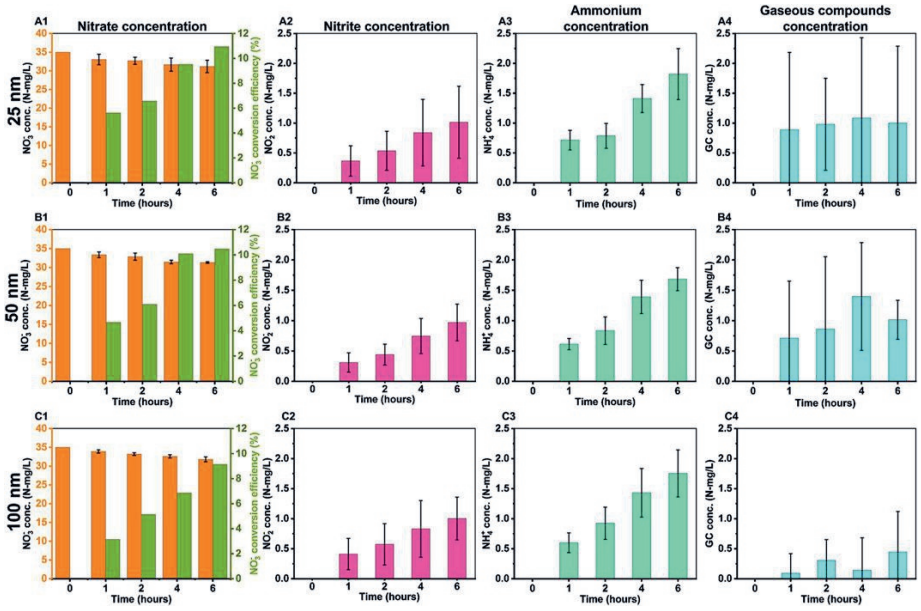

Figure 3.4: The concentrations (N-mg/L) of nitrate reduction reaction products were measured using a Cu-Ni electrode with varying Cu film thicknesses: **(A1–A4)** at 25 nm, **(B1–B4)** at 50 nm, and **(C1–C4)** at 100 nm. The experimental conditions included 2.5 mM KNO_3, 3.5 mM Na_2SO_4, an uncontrolled pH starting at 6.5, an applied current of −8.5 mA, and a duration of 6 h. The notations **(A1, B1, and C1)**, **(A2, B2, and C2)**, **(A3, B3, and C3)**, and **(A4, B4, and C4)** correspond to the concentrations of NO_3^-, NO_2^-, NH_4^+, and GC, respectively.

Figure 3.4 A1, B1, C1 shows that the concentration of NO_3^- decreased with reaction time. The concentration of NO_2^-, NH_4^+, and GC increased with time for all electrode as seen from Figure 3.4 A2, B2, C2 and Figure 3.4 A3, B3, C3, respectively, while the concentration of gaseous compounds (GC) remained relatively stable Figure 3.4 A4, B4, C4. The thickness of the Cu film on the Ni plate does not appear to have a substantial effect on NO_3^- conversion under the conditions that were tested. This can be attributed to the use of sodium sulfate (Na_2SO_4), which was employed as the electrolyte in NO_3^- reduction experiments. Because, it closely replicates the neutral, unbuffered environment of real-world NO_3^- contaminated water (Costa et al., 2024). However, the presence of SO_4^{2-} ions in the solution may hinder the adsorption of NO_3^- on the Cu active sites (De Vooys et al., 2000). Moreover, high concentration of OH^- (aq) can cause a poisoning effect on the electrode causing a decrease in NO_3^- reduction (Wang et al., 2007) as can be seen from Figure 3.5.

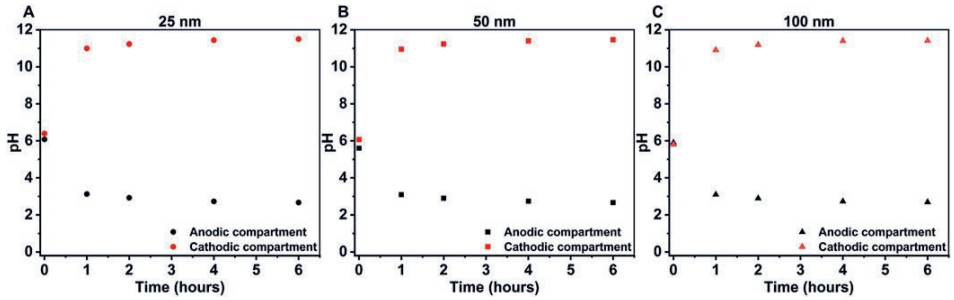

Figure 3.5: Changes in pH during NO_3^- reduction for **(A)** 25 nm Cu-Ni, **(B)** 50 nm Cu-Ni, and **(C)** 100 nm Cu-Ni at an applied current of −8.5 mA in 2.5 mM KNO_3 and 3.5 mM Na_2SO^4.

Figure 3.5 depicts the changes in the pH of the anolyte and catholyte solutions. Initially, the pH range of both solutions was approximately 5.5–6.5, for all experiments carried out with 25, 50, and 100 nm Cu-Ni electrodes. During the first hour of the experiment, the pH of the anolyte suddenly dropped and became acidic, while the pH of the catholyte rose rapidly and became alkaline. Thereafter, the pH of both solutions changed very slowly until the end of the experiment, indicating that NO_3^- reduction on the Cu-Ni electrode was possible in alkaline conditions as well (Beltrame et al., 2020). This behavior is attributed to the reactions that occur at the electrodes where OH^- (aq) formation in the cathodic compartment (reactions [1]-[5]) increases the pH over time and H^+ (aq) formation in the anodic compartment where water electrolysis occurs decreases the pH according to Equation 9.

$$Reaction\ at\ anode: H_2O \rightarrow 1/2O_2 + 2H^+ + 2e^- \quad \text{.....(9)}$$

The low NO_3^- reduction activity of Cu can be attributed to its unfavorable electronic state and the slow proton transfer at its surface, which is particularly significant in neutral or alkaline environment (X. Liu et al., 2023). The NO_3^- reduction activity can be increased by alloying Cu with Ni, which transform the unfavorable electronic state into a favorable one, resulting in an increased production of atomic hydrogen. Additionally, the 3D porous structure of the alloy enhances active sites, accelerates reaction kinetics, and boosts electrocatalytic activity (Z. Ma et al., 2024). The Cu-Ni alloy also changes the adsorption energies of intermediates like NO_3^-, NO_2^-, and NH_2, improving efficiency, selectivity, and reducing toxic NO_2^- buildup (Li R. et al., 2023; Ma et al., 2024). Compared to monometallic Cu, the Cu-Ni alloy exhibits higher initial currents and reduced current decay over time, making it more effective for NO_3^- reduction (Yuting Wang et al., 2020). In acidic media, Cu-Ni alloy electrodes outperform pure Cu or Ni electrodes, minimizing undesired side reactions like hydrogen evolution, and offering superior corrosion resistance and catalytic performance, essential for the long-term stability and efficiency of the NO_3^- reduction process (Lou et al., 2024). The Cu-Ni alloy's ability to reduce energy barriers for intermediate steps is crucial for efficient NO_3^- reduction in water treatment applications, and it performs well across various NO_3^- concentrations and in simulated wastewater, demonstrating its robustness and broad applicability in NO_3^- reduction (Li R. et al., 2023; Wei J. et al., 2024). Here, it has been demonstrated that PVD can effectively be used to synthesize catalysts for NO_3^- reduction but that further optimization of electrodes by coating Cu coatings as thin films along with Ni addition must be done to reach higher conversion efficiency, conversion rates, selectivity and product concentration. Table 3.2 shows the NO_3^- conversion rate of Cu-coated Ni electrodes, prepared on different Ni structures using various coating techniques. It also shows the

NO_3^- conversion rates for each study showing that these electrodes provides promising NO_3RR performance. As evidenced by Table 3.2 and from the literature (Meng et al., 2023), the conversion rate of NO_3^- is influenced by various factors, including the method of catalyst preparation, the structure of the Ni substrate, the surface area of the electrode, the amount of NO_3^- used, initial pH and the duration of the experiments conducted. In this study, only pure Cu was deposited on the Ni plate using PVD and ca.10.5% efficiency has been achieved. Use of PVD technique for electrode preparation is still promising because it can deposit up to 750 k atoms/min, making it suitable for rapid coating deposition, resulting in uniform film deposition which is confirmed from SEM analysis also. The evaporation process in PVD results in lower absorbed gas within the film, contributing to coatings' purity and quality which is confirmed from Supplementary Figure 3.S3 where the XPS of pristine 25 nm Cu-Ni electrode shows that no other metal impurities are present other than Cu, Ni, and oxygen. It is particularly versatile for industrial applications requiring thick films where surface morphology is not the primary quality requirement (Baptista et al., 2018).

Table 3.2: NO_3RR conversion rate with respect to preparation technique of Cu coating on Ni.

Preparation technique	**Ni structure**	**Surface area of working electrode (cm2)**	**Initial pH**	**Electrolyte composition**	**NO_3^-conversion rate**	**Ref**
Electrochemical deposition	Ni foils (0.2 mm thick)	15	NA	45 mg/L NO_3^--N + 0.1 M Na_2SO_4	29% after 48 h	(Hou et al., 2018)
Electrodeless plating	Ni foam (sheet thickness = 2 mm)	80	12.5	50 mg/L NO_3^--N + 0.1 M Na_2SO_4	For 4 h with Cu-Ni electrodes prepared using electrodeless Cu plating on Ni at different duration) a) Cu = 10% b) Cu/Ni/5 min = 60% c) Cu/Ni/10 min = 96% d) Cu/Ni/20 min = 92% e) Cu/Ni/40 min = 80% f) Cu/Ni/60 min = 50%	(Shih et al., 2020a)
Chemical deposition	Ni sponges	15	6.0-6.5	600 mg/L $NaNO_3$ + 1,400 mg/L Na_2SO_4	44% ± 5% after 6 h	(Beltrame et al., 2020)
Potentiostatic deposition	Polycrystalline Ni electrode	0.03	NA	5 mM $NaNO_3$ + 0.1 M NaOH	NA	(BADEA and BADEA, 2003)
Physical vapor deposition	Ni plate	5.2	5.5-6.5	2.5 mM KNO_3 + 3.5 mM Na_2SO_4	For 6 h with Cu-Ni electrode prepared using various thickness of Cu deposited on Ni by PVD a) Cu/Ni/25 nm = 10.9% b) Cu/Ni/50 nm = 10.5% c) Cu/Ni/100 nm = 10.0%	This study

3.4. FUTURE WORK AND SCOPE

In future work, reaction mechanisms must be investigated further, e.g., by employing advanced techniques such as in-situ spectroscopic methods (e.g., FTIR, Raman) to identify the reaction intermediates and elucidate the rate-determining steps involved in NO_3^- reduction. Further, systematic studies must be conducted to comprehend the synergistic effects between Cu and Ni, including the role of interfacial properties and electronic interactions in enhancing catalytic activity, and utilize computational modelling techniques (e.g., DFT) to gain insights into the adsorption and reaction pathways of NO_3^- on the Cu-Ni surface (Wang et al., 2021). Furthermore, rotating disk electrode experiments should be conducted on electrodes prepared using the PVD method to determine the kinetic current density and elucidate the electrocatalytic effect of Cu thin layers on Ni in the NO_3^- reduction reaction. The findings of this study, particularly the influence of Cu layer thickness on the NO_3RR performance, can inform the design of advanced electrodes for environmental remediation. Moreover, these electrodes could be employed in biosensors (Salazar et al., 2016), for energy storage as in supercapacitor (Madito et al., 2020), in microelectronic applications (Zhang et al., 2020), high-salt wastewater treatment (Tan et al., 2022), and in batteries (X. Liu et al., 2022; J. Lu et al., 2024; Pan et al., 2019). To further enhance the significance of this work, future studies should explore the durability and long-term performance of Cu-Ni electrodes under continuous operation and real-world conditions, investigate the synergistic effects of varying Cu deposition techniques, such as electrodeposition, alongside PVD, extend the approach to other electroactive species (e.g., NO_2^-, NH_3), to develop multi-functional electrocatalysts for broader environmental applications.

3.5. CONCLUSION

This study investigated the influence of the Cu layer thickness on NO_3^- electrochemical reduction using Cu-Ni composite electrodes produced by PVD. SEM and XPS analyses confirmed the uniform distribution of thin Cu film on the Ni plate, with small pits which played a critical role in NO_3^- reduction and NH_4^+ selectivity. Similar NO_3^- conversion and product formation rates were obtained on all electrodes regardless of the thickness of the Cu layer. Based on the experimental results, it can be concluded that the NO_3^- removal efficiency with respect to electrode preparation techniques achieved by the PVD method is approximately 10% for varying thicknesses of Cu on Ni plate after 6 h, which is lower compared to other electrode preparation techniques. Furthermore, a decrease in current density was observed with an increase in the thickness of Cu on the Ni plate. Noting the importance of both Cu and Ni, present in a Cu-Ni alloy, it is essential to conduct further investigation in order to deposit pure thin Cu and Ni films combinedly on a Ni plate through PVD for efficient NO_3RR.

3.6. APPENDIX

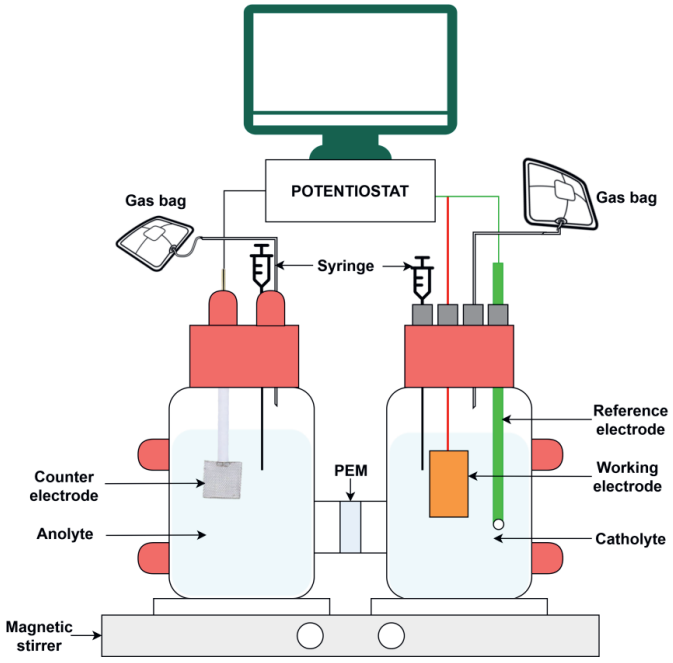

Supplementary Figure 3.S1: Schematic diagram of electrochemical setup for NO_3^- reduction

Figure 3.S2 displays the SEM images of pristine 25 nm Cu-Ni electrode at 370× and 4000× magnification. The images reveal the presence of pits on the Ni plate, with widths of ~1 µm.

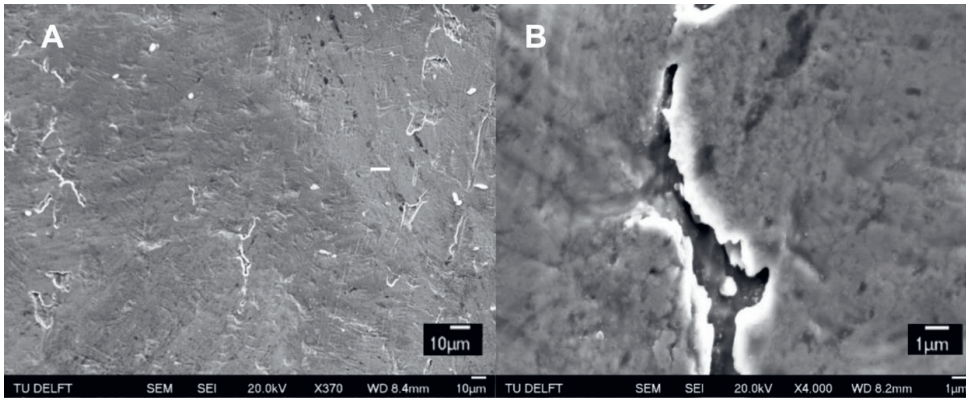

Supplementary Figure 3.S2: SEM micromorphology of 25 nm Cu-Ni electrode at **(A)** 370x, and **(B)** 4000x

Figure 3.S3 displays the elemental EDX mapping and EDX spectrum, which demonstrates the complete coverage of the Ni plate with Cu, a finding that is consistent with the XPS results (shown in the next section).

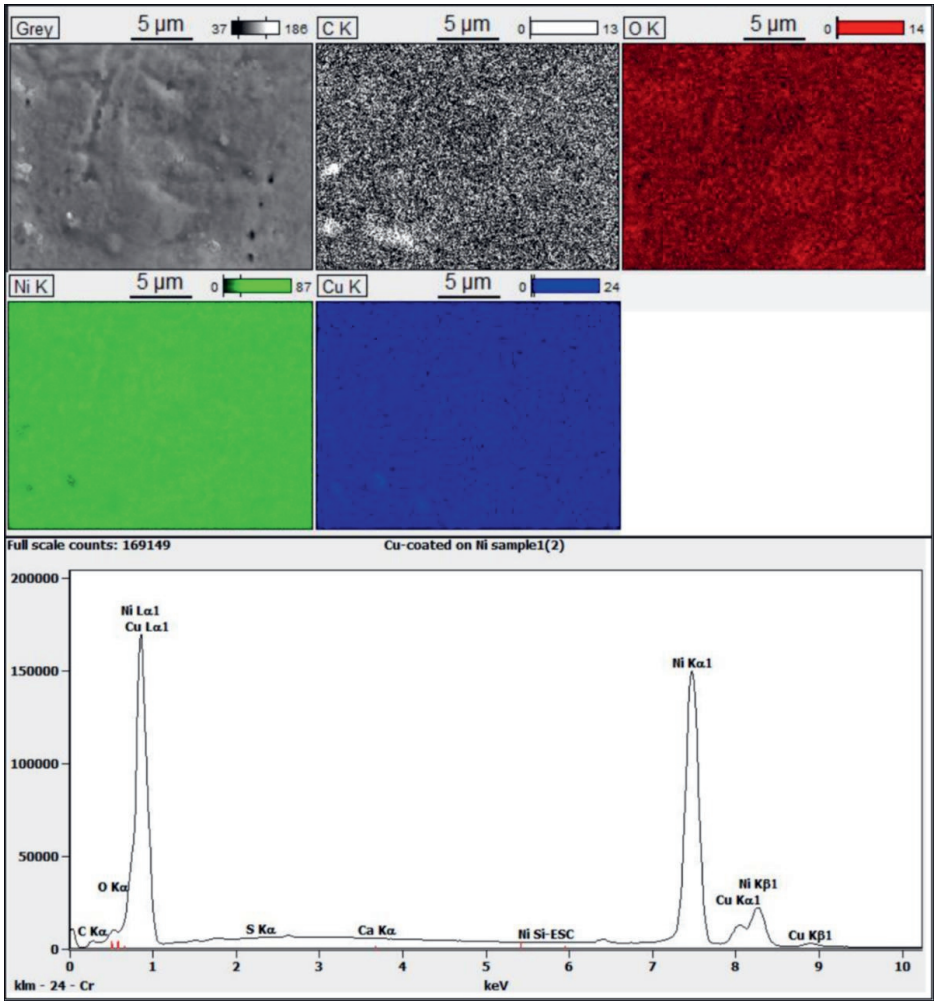

Supplementary Figure 3.S3: EDX images with elemental mapping and EDX spectrum of 25 nm Cu-Ni electrode

XPS spectra of the Ni plate used in this study is shown in Figure 3.S4. The survey spectrum of Ni plate showed the elements like C, Ni, O present on the surface (Figure 3.S4A). High resolution spectrum of Ni 2p is curve fitted as shown in Figure 3.S4B. In Ni 2p3/2 region, the peak at 852.39 eV corresponds to Ni metal (Ni^0) (Hu et al., 2019), the peaks at 855.13 eV and 857.14 eV correspond to Ni oxides, NiO and Ni_2O_3, respectively. The Ni 2p1/2 region, the peak at 870 eV corresponds to Ni metal (Ni^0), the peaks at 872.8 eV and 874.89 eV correspond to Ni oxides, NiO and Ni_2O_3, respectively (Cheng et al., 2017). All other peaks are satellite peaks. Figure 3.S4C shows the O 1s spectrum with three subpeaks at 529.09, 531.26 and 532.99

eV are corresponding to oxygen in Ni oxides (NiO and Ni_2O_3), $Ni(OH)_2$ and water adsorbed on Ni plate, respectively (Cheng et al., 2017).

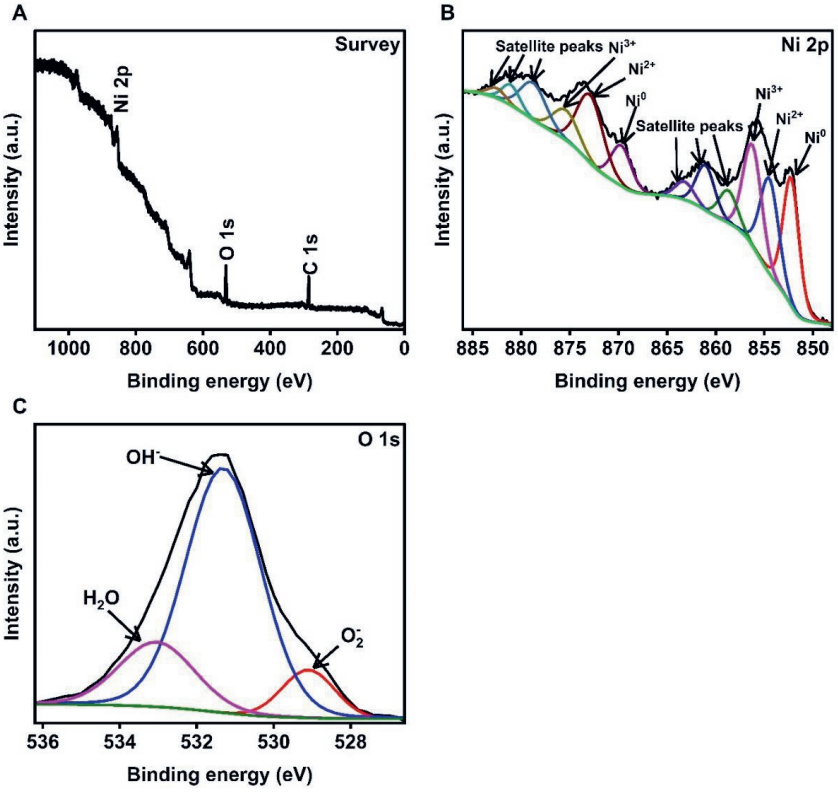

Supplementary Figure 3.S4: XPS spectra of Ni plate **(A)** Survey, **(B)** Ni 2p, **(C)** O 1s

XPS spectra of 25 nm thick Cu coated on Ni plate (Pristine) is shown in Figure 3.S5. The survey spectrum of 25 nm Cu-Ni plate showed the elements like C, Cu, and O present on the surface (Figure 3.S5A). The peaks corresponds Ni in high resolution Ni 2p spectrum (Figure 3.S5B) is negligible, due to complete coverage of Cu coating on Ni plate using PVD. High resolution spectrum of Cu 2p is curve fitted as shown in Figure 3.S5C. The peaks at 931.83 and 951.70 eV correspond to Cu metal (Cu^0), the peaks at 933.59 and 954.42 eV correspond to Cu^{2+} (Cu_2O), respectively (Jiang et al., 2021). Figure 3.S5D shows the O 1s spectrum with three subpeaks at 529.80, 531.87 and 534.0 eV are corresponding to oxygen in CuO, $Cu(OH)_2$ and adsorbed water molecules, respectively (Jiang et al., 2021).

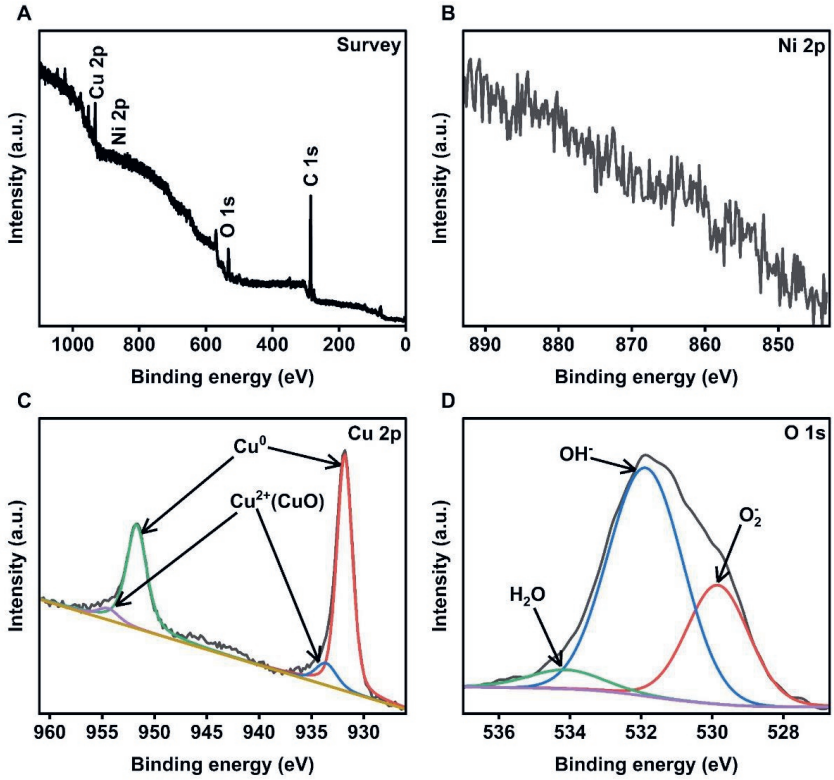

Supplementary Figure 3.S5: XPS spectra of pristine 25 nm Cu coated on Ni. **(A)** Survey, **(B)** Ni 2p, **(C)** Cu 2p, **(D)** O 1s

XPS spectra of spent 25 nm Cu-Ni cathode is shown in Figure 3.S6. The survey spectrum of spent 25 nm Cu-Ni cathode showed the elements like C, Ni, N, Cu, and O present on the surface (Figure 3.S6A). The Ni peaks in high resolution Ni 2p spectrum (Figure 3.S6B) is barely visible. This could be due the removal of Cu from cathode plate during NO_3^- reduction, most likely from the area of pits on the surface (Eiler et al., 2020). High resolution spectrum of Cu 2p is curve fitted as shown in Figure 3.S6C. The peaks at 933.59 and 951.70 eV correspond to Cu metal (Cu^0). The peaks at 933.59 and 954.42 eV correspond to Cu^{2+} (Cu_2O), respectively (Jiang et al., 2021). The small shift in the position of Cu^{2+} peaks is due to the adsorption of nitrogen compounds from the electrolyte on the surface of the cathode. Figure 3.S6D shows the O 1s spectrum with three subpeaks at 529.8, 531.87, and 534.0 eV correspond to oxygen in CuO, $Cu(OH)_2$, and adsorbed water, respectively (Jiang et al., 2021). Figure 3.S6E shows the N 1s spectrum with two subpeaks at 399.5 and 396.0 eV corresponding to $*NH_3$ and N^{3-} adsorbed on the Cu-Ni cathode plate, respectively (Baltrusaitis et al., 2009; Kehrer et al., 2019; Yoon et al., 2019).

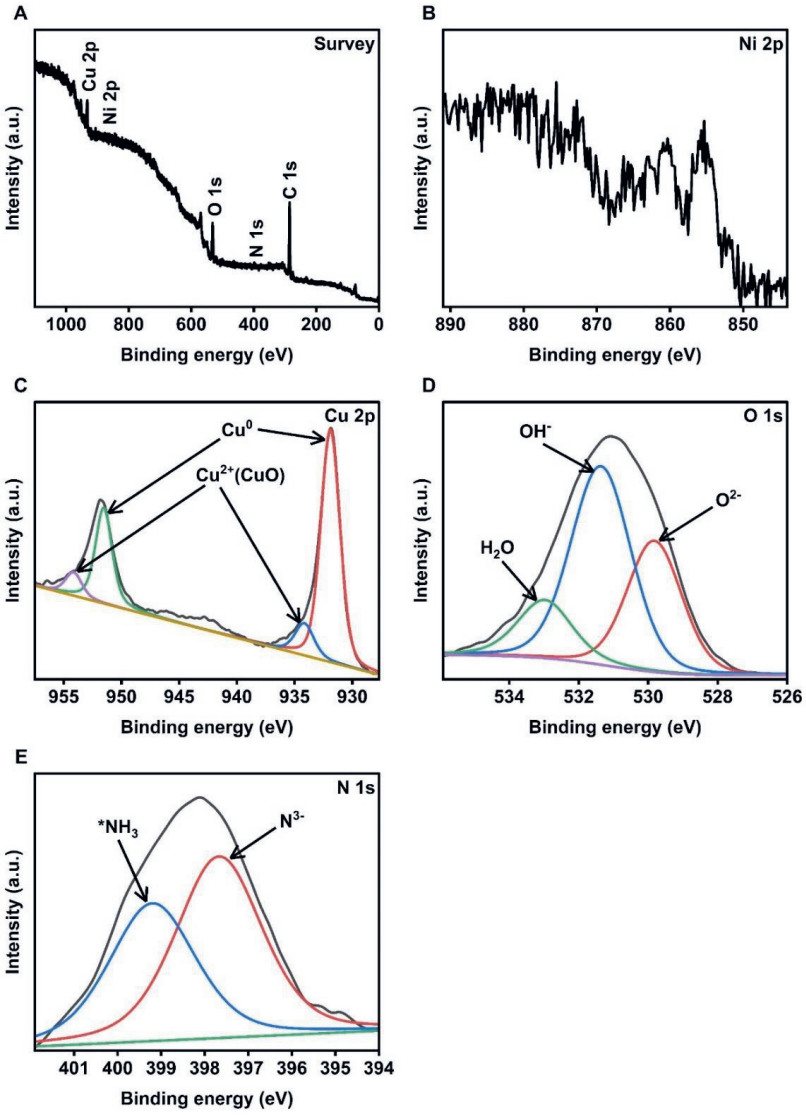

Supplementary Figure 3.S6: XPS spectra of spent 25 nm Cu coated on Ni. (A) Survey, (B) Ni 2p, (C) Cu 2p, (D) O 1s, (E) N 1s

Figure 3.S7 depicts a comparison of XPS spectra of Ni 2p for Ni plate without coating (Figure 3.S7A), 25 nm Cu-Ni electrode (pristine) (Figure 3.S7B), and 25 nm Cu-Ni electrode (spent) (Figure 3.S7C). A noticeable difference in peaks can be observed for all three electrodes. The Ni plate without a coating exhibits the highest peaks, corresponding to Ni^0, Ni^{2+}, and Ni^{3+}, whereas no peaks were detected for the Cu-Ni electrode (pristine). For the Cu-Ni electrode (spent), Ni peaks are barely visible, indicating that some Cu has been removed, exposing the Ni surface during NO_3RR facilitating the NO_3^- reduction.

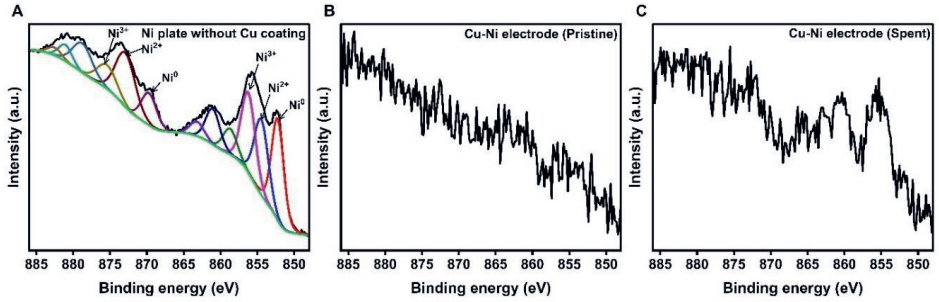

Supplementary Figure 3.S7: XPS spectra of Ni 2p of **(A)** Ni plate without coating, **(B)** 25 nm Cu-Ni electrode (pristine), **(C)** 25 nm Cu-Ni electrode (spent)

A schematic diagram depicting the mechanism of Cu removal from the cathode during NO_3^- reduction is illustrated in Figure 3.S8. The Cu particles detach from the electrode during the electrocatalytic process of NO_3^- reduction, revealing the Ni plate and forming pits.

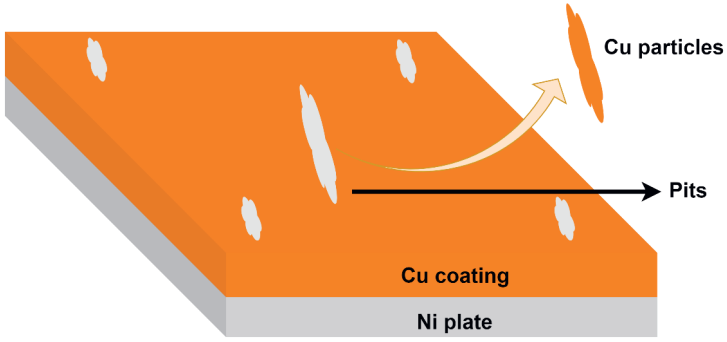

Supplementary Figure 3.S8: Schematic of Cu removal mechanism on Cu-Ni cathode during NO_3^- reduction

The comparison of reduction curves for 25 nm, 50 nm, and 100 nm Cu-Ni electrodes is illustrated in Figure 3.S9. It is evident from the Figure 3.S9 that as the thickness of Cu is increased, the current density decreases because as film thickness increases there is a evolution of microstructure and increased surface roughness (Lin et al., 2017), structural deterioration (Nguyen et al., 2024), and increased resistivity caused due to variations in bonding mechanisms and interface voids in thicker films which impedes current flow (T.-F. Lu et al., 2024).

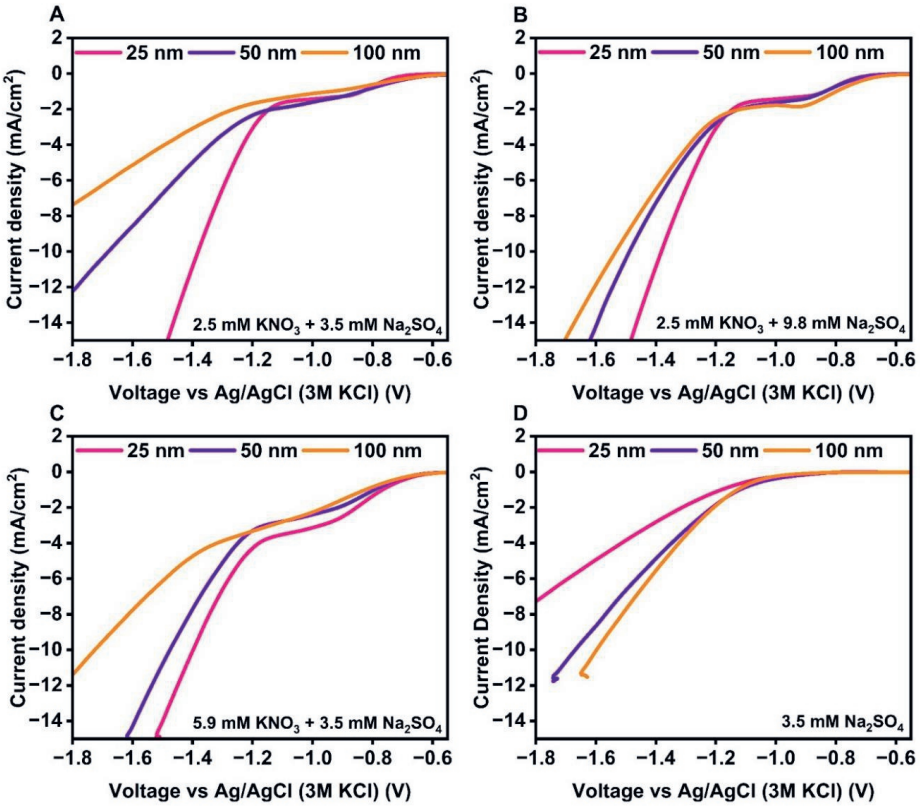

Supplementary Figure 3.S9: Comparison of reduction curves for 25 nm, 50 nm, and 100 nm Cu-Ni electrodes with different catholyte concentration of **(A)**: 2.5 mM KNO_3 + 3.5 mM Na_2SO_4 , **(B)**: 2.5 mM KNO_3 + 9.8 mM Na_2SO_4 , **(C)**: 5.9 mM KNO_3 + 9.8 mM Na_2SO_4, and **(D)**: 3.5 mM Na_2SO_4

4

TOWARD SUSTAINABLE BATTERY TECHNOLOGIES: THE NEED FOR BIODEGRADABLE MEMBRANES

Parts of this chapter are based on:

Maya Moreshwar Meshram, S., Gonugunta, P., Taheri, P., Jourdin, L., Pande, S. (2025). Preparation of biodegradable membrane utilizing chitosan and polyvinyl alcohol, and assessment of its performance after coating with graphene conductive ink. Frontiers in Membrane Science and Technology , Volume 4 – 2025.

4.1. INTRODUCTION

For environmental applications, biodegradable membranes are crucial, as they offer an environmentally sustainable approach for addressing pollution, while conserving natural resources (Janakiraman et al., 2024). Applications include water electrolysis and wastewater treatment, gas separation, bioenergy, and biobatteries production (Ehsani et al., 2022; Osman et al., 2024). Biobatteries are part of the broader initiative to develop environmentally sustainable energy storage solutions, which are essential for supporting renewable energy systems (Bertaglia et al., 2024). They represent a promising avenue in sustainable energy technology, utilizing biological processes to generate electrical energy (Fraiwan et al., 2016). These biobatteries harness the power of microorganisms or enzymes to convert organic matter into electricity through biochemical reactions (Gao et al., 2020). Biobatteries consist of an anode, a cathode, an electrolyte, and a membrane (Hassanzadeh and Choi, 2015; Hassanzadeh and Langdon, 2023). Membranes serve to keep the positive and negative half-cells apart, preventing the mixing of electrochemically active ions. At the same time, they allow the necessary ionic conductivity for specific ions that are not electrochemically active, such as H^+ (Fraiwan and Choi, 2014; Long Doan et al., 2015; Yogesh and Srivastava, 2022). Also, they are impermeable to fuel and oxidizing gases (Vilela et al., 2019). Proton exchange membranes (PEM) are specialized membranes that facilitate the passage of protons across their surfaces(Fraiwan and Choi, 2014). This proton transfer through the PEM, occurring between the anode and cathode, is essential for maintaining electroneutrality (H. Lee and Choi, 2015). Commercially available PEMs are costly and non-degradable (González-Pabón et al., 2019), because they are fabricated using nafion, sulfonated polybenzimidazole, polysulfone, and sulfonated poly(ether ketone) (A. Sharma et al., 2024; L. Wang et al., 2019). In addition, nafion exhibits poor durability and low power density, and upon disposal, it releases numerous perfluorinated compounds, including toxic perfluorocarboxylic acids and other environmentally persistent and bioaccumulative substances (Brito dos Santos et al., 2024). Due to these aforementioned limitations, these membranes are not suitable for biobattery construction (Akshat Sharma et al., 2024). Hence there is a need of alternate membranes which can be suitable in the construction of such biobatteries.

Biopolymers can be utilized for membranes preparation in biobatteries, owing to their sustainability, environmental benefits, and functional properties (Galiano et al., 2018; Joshi et al., 2024; Muhamaruesa and Isa, 2020; Patra et al., 2024). These biopolymers also provide a low-cost alternative to traditional membranes, contributing to cost reduction, biodegradability, and high strength owing to their robust intramolecular and intermolecular hydrogen-bonding networks. These properties makes them as valuable materials for applications requiring durability and stability (Cox and Litwinski, 1979; D.-C. Wang et al., 2023; L. Wang et al., 2019). Various biopolymers are available in market, such as CS, PVA, Polylactic acid (PLA) etc., as described in (Alday et al., 2020; Ghanbarzadeh et al., 2013; Reddy et al., 2021), which can be employed for the preparation of membranes. CS is a naturally occurring polysaccharide in animal based biomass resources that has various advantages, such as an eco-friendly nature, flexibility for structural modification, high hydrophilicity, cost efficiency, improved and chemical stability, and the ability to form a membrane (Dharmadhikari et al., 2018; Muhmed et al., 2020; Mukoma et al., 2004; Sheth et al., 2024; Zhao et al., 2020). CS based membrane has been fabricated by blending with nanocellulose (nanoscale fibers of cellulose) and also by combining two or more polymer layers, particularly with a solid support layer for dimensional stability (Zhao et al., 2020). For example, Song et al. (2024) has fabricated CS nanofiber paper membrane via a papermaking process to use in lithium-ion batteries, Yang et al. (2022) designed CS modified filter paper separator for aqueous zinc batteries, Guo et al. (2023) used CS hydrogel polyelectrolyte-modified cotton pad as dendrite-inhibiting separators in aqueous

zinc-ion batteries. Also, Tian et al. (2024) fabricated a multifunctional membrane from polydopamine-modified waste paper and hydrothermal carbonized CS, through simple vacuum filtration for separating oil-in-water emulsions and for in situ dye removal under controllable pH conditions.

PVA is a biodegradable and water-soluble synthetic polymer with reactive chemical functionalities (Halima, 2016). Through appropriate modifications, in the chemical features of the PVA, it can be used as membrane (Maiti et al., 2012; Surti et al., 2024). Raja et al. (2022) has developed a paper-based ceramic separator using a low-cost paper substrate functionalized by the wet-coating method using duo-polymer (CS and PVA) and ceramic barium titanate nanopowder. Ridwan et al. (2024) made conductive solid electrolyte membranes by mixing potassium hydroxide (KOH), PVA, and glycerol with the addition of nanocrystalline cellulose paper. Li et al. (2017) prepare the membrane by mixing cotton pulp with nylon (polyamide fiber), vinylon (acetalized PVA fiber), and polypropylene fiber for zinc-silver battery. Wang et al. (2020) fabricated a PVA/lyocell dual-layer paper-based separator by dual-layer forming papermaking process for using in Zinc -air batteries.

However, the incorporation of the above biopolymers into cellulose paper, whether through impregnation or other methods, results in increased vulnerability to swelling, water absorption, and deterioration (Mohammed et al., 2023; Sahu and Gupta, 2022). This susceptibility is particularly pronounced when the paper is stored in highly humid environments or exposed to conditions of elevated moisture making it not suitable for biobattery construction. To address these issues, surface treatments such as sizing and coating are often employed to enhance the water resistance properties of cellulose paper. Modifying the wettability of the cellulose paper surface with sizing agents or by applying hydrophobic coatings such as, a water barrier can be created to protect the paper from moisture damage (Rhim et al., 2006). Several significant studies have recently explored the use of hydrophobic coatings. These coatings have been crafted from lignin-based carbon nanospheres (Wen et al., 2024), ORMOCER, which are inorganic–organic polymers (Solberg et al., 2023), the diblock copolymer PMMA-b-P(MA-FPOSS) (Pan et al., 2021), Photothiol-X Ligations (Bretel et al., 2018), emulsions made from carnauba wax and alcohol with Nano-TiO_2 particles (Wang et al., 2017), polyvinylidene fluoride (PVDF)/SiO_2 microspheres (Gao et al., 2017), polyhydroxybutyrate (PHB) particles mixed with nanofibrillated cellulose (NFC) and plant wax (Rastogi and Samyn, 2017), and catechol (adhesive) moieties (García et al., 2014). Coated paper can provide enhanced features by reducing the porosity and roughness and improve the moisture barrier properties. If a barrier coating layer is applied, the cellulose substrate becomes resistant to humidity changes and as well as to dimensional instability (Agate et al., 2018). However, only a limited number of studies have investigated the application of conductive hydrophobic coatings on cellulose paper. Coatings are often employed as a simple and cost-effective method to improve the properties of paper substrates used in membrane preparation. Some studies has coated membranes using conductive inks such as by Li et al. (2022) where they have utilized carbon-based conductive inks as coatings on membranes. Veerubhotla et al. (2017) have applied coatings on Whatman filter paper, which served not only as a support for electrode fabrication but also as a membrane in the biobattery. They employed commercially available eyeliner containing carbon nanoparticles and Fe_3O_4 as a conductive ink without any binder for the preparation of the membrane. Jenkins et al. (2012) have used filter paper coated with conducting carbon ink in the biobattery setup. As can be seen that there are a few studies done in which membrane has been prepared using biopolymers impregnated with cellulose paper coated with conductive ink. The cellulose filter paper is utilized as reinforcement because it serves as a porous base for membranes, providing a structure that can be easily saturated and coated with casting solutions. The fibrous nature of filter paper results in a complex and uneven

surface, which is beneficial for membrane applications. It improves lamination strength and membrane performance without causing the support to swell or dissolve. Additionally, the high crystallinity of filter paper ensures a stable and durable structure for reinforcement (Prambauer et al., 2015; Tran and Ulbricht, 2023). Also, the graphene conductive ink provides exceptional electrical conductivity, flexibility, and potential for environmentally sustainable formulations. In comparison to other coatings, it demonstrates superior adhesion, high printing resolution, and the ability to enhance conductivity (Ashok Kumar et al., 2022; Saidina et al., 2019).

While biodegradable polymers like CS and PVA have been widely studied, the integration of cellulose filter paper as a reinforcing scaffold for these membranes remains underexplored. Notably, the application of water-resistant graphene conductive ink as a coating on biodegradable polymer membranes has not been previously reported. Hence, in this study, eco-friendly and sustainable biodegradable membranes were synthesized from cellulose filter paper by impregnation with CS, PVA and 1:1 CS/PVA, followed by the coating with the mixture of graphene conductive ink and respective polymer CS, PVA and 1:1 CS/PVA. This study will help create a membrane for biobatteries. They can power low-energy devices like soil moisture sensors. They can also be used in fuel cells that conduct protons, in water treatment to clean or remove salt, in eco-friendly packaging because they break down naturally, and in medical devices like temporary implants or systems that deliver drugs.

4.2. EXPERIMENTAL MATERIALS AND METHODS

4.2.1. MATERIALS AND CHEMICALS

All chemicals were analytically pure and used without further purification. Cellulose filter paper, with a 7.5 cm diameter, and an average pore size of 1.5 µm, was purchased from Ahlstrom (Helsinki, Finland), PVA (molecular weight - 146,000-186,000, 99+% hydrolyzed), and CS (high molecular weight) were purchased from Sigma-Aldrich. Conductive ink with graphene was purchased from FWG Limited, United Kingdom. PK booster compost tea was purchased from Biotabs (The Netherlands).

4.2.2. MEMBRANE SYNTHESIS

Membranes were prepared using the solution casting method. Initially, the polymers were dissolved in the solution, subsequently, the filter paper was immersed in it, and then dried in an oven at 60 °C. Following this, the conductive ink was applied on the membrane using a paint brush. The detailed procedure is described in the subsequent subsections. Figure 4.1 illustrates the schematic of the membrane preparation method.

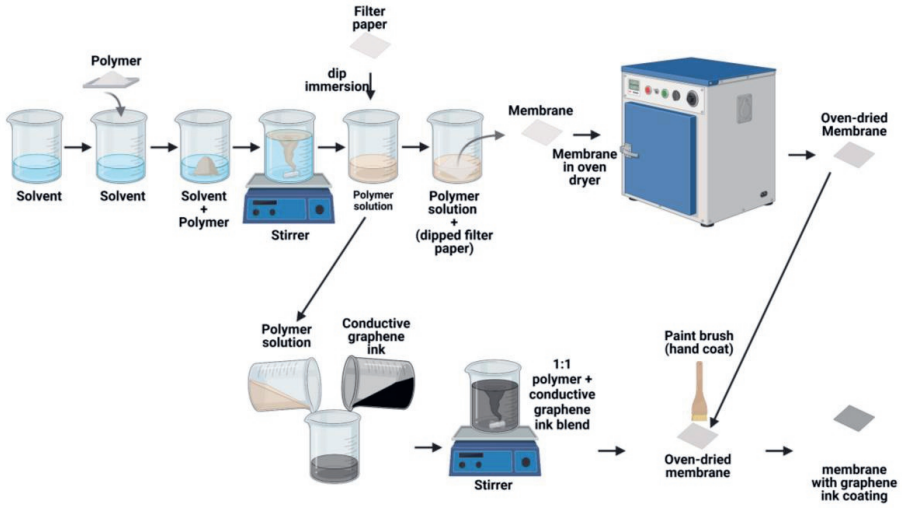

Figure 4.1: Schematic diagram of CS, PVA, and CS/PVA membranes prepared by solution-casting method

4.2.2.1. CS MEMBRANE

An aqueous solution of CS at a concentration of 2% (w/v) was prepared by dissolving 4 g of CS in 200 mL of acetic acid aqueous solution containing 2% (v/v). The mixture was stirred for 12 h at room temperature at 1000 rpm. To reduce the thickness of the solution, 150 mL of acetic acid was added to the previously prepared solution, and the mixture was stirred for one more hour. The solution was then filtered and stored at 4 °C for 24 h. Subsequently, a 6 cm × 6 cm filter paper was immersed in the CS solution for 2 minutes to allow the CS solution to be absorbed by the filter paper, which was then left to dry at room temperature for 24 h. The filter paper was then dehydrated at 60 °C for 6 h in oven. The dry weight of the membrane was then measured to determine the amount of solution that had been absorbed by the filter paper.

The membrane was neutralized with 2 M NaOH for 5 minutes and washed with Milli-Q water. It was then crosslinked by immersion in 0.5 M H_2SO_4 for 24 h at room temperature. To remove excess cross-linking agent, the membrane was dipped in Milli-Q water and allowed to dry for 24 h at room temperature. The weights of the membranes were measured after cross-linking.

4.2.2.2. PVA MEMBRANE

PVA (10 g) was added to 100 mL of Milli-Q water (10% w/v aqueous PVA solution) and allowed to hydrate for 24 h. PVA was then dissolved by stirring at 500 rpm at 80 °C for 2 h. The filter paper of size 6 cm × 6 cm, was then dipped in the PVA solution for 2 minutes, allowing the PVA solution to be absorbed by the filter paper. The filter paper was left to dry at room temperature for 24 h, and then at 60 °C for another 6 h. The dry weight of the membranes was measured to determine the amount of solution absorbed by the filter paper.

The membranes were then treated with a 10 % (v/v) solution of hydrogen peroxide for 1 h, washed, and crosslinked with a 10 % (v/v) solution of sulfuric acid for 12 h. The weights of the membranes were measured after crosslinking.

4.2.2.3. CS/PVA MEMBRANE

Aqueous solutions of PVA and CS were mixed at a 1:1 (v/v) ratio (Ambili et al., 2019) and stirred for 2 h at 500 rpm. After mixing, the solution was stored at 4 °C for 24 h. Filter paper, measuring 6 cm × 6 cm, was dipped in the CS/PVA solution for 2 minutes to allow the CS/PVA solution to be absorbed. The filter paper was left to dry at room temperature for 24 h and then dehydrated for 6 h in an oven at 60 °C. The dry weights of the membranes were measured to determine the amount of solution absorbed by the filter paper.

The obtained membranes were neutralized with 2 M NaOH for 5 minutes and washed with Milli-Q water. Cross-linking was performed by immersing the membrane in 0.5 M H_2SO_4 for 24 h at room temperature, followed by dipping in Milli-Q water to remove excess cross-linking agent. The membranes were then allowed to dry at room temperature for 24 h. After crosslinking, the membrane weights were measured.

4.2.2.4. GRAPHENE CONDUCTIVE INK SOLUTION

5 g of conductive graphene ink is mixed with 5 g of polymer solution of CS, PVA, and CS/PVA to prepare the conductive ink solution. The conductive ink solution mixture was stirred for 24 h at 200 rpm using a magnetic stirrer which results in 1:1 (Graphene ink: of CS, PVA, and CS/PVA) conductive ink solution. Subsequently, these 1:1 mixtures were coated onto the polymer membranes using paint brush in two layers on one side of the membranes.

4.2.3. MEMBRANE PERFORMANCE STUDIES

4.2.3.1. SWELLING RATIO AND WATER UPTAKE CAPACITY

Swelling ratio: The swelling ratios of the prepared membranes were calculated using the procedure described by González-Pabón et al. (2019) and the following equation:

$$Swelling\ ratio\ (\%) = \frac{T_{wet} - T_{dry}}{T_{dry}} \times 100 \quad \text{.....(1)}$$

where T_{wet} represents the thickness of the wet membranes obtained after soaking in Milli-Q water for 24 h and T_{dry} is the thickness of the respective dry membranes. The thickness of the membranes was measured using a digital vernier caliper (range: 0 to 150 mm; accuracy: 0.2 mm; resolution: 0.1 mm). Measurements were taken at various locations on the membranes, and the average thickness was subsequently calculated.

Water uptake capacity: The water uptake capacity was determined by measuring membrane weight changes during the hydration process (González-Pabón et al., 2019). The membranes were first dried in an oven at 30 °C for 15 h, and then weighed (W_{dry}). After drying, the membranes were immersed in Milli-Q water for an initial period of 1 minute, wiped with tissue paper, and immediately weighed (W_{wet}). The procedure was repeated for several times. Finally, the membranes were stored in Milli-Q water and maintained at room temperature for 24 h to avoid the warping of the membrane and use them for subsequent experiments. The water uptake (W %) was calculated using the following equation:

$$Water\ uptake\ capacity\ (\%) = \frac{W_{wet} - W_{dry}}{W_{dry}} \times 100 \quad \text{.....(2)}$$

where W_{wet} represents the weight of the wet membranes obtained after soaking in Milli-Q water for 24 h and W_{dry} is the weight of the respective dry membrane.

4.2.3.2. ION EXCHANGE CAPACITY (IEC)

IEC is a measure of the number of ions that a material can exchange. IEC was calculated using an acid-base titration method according to the procedure described by González-Pabón et al. (2019). Circular membrane pieces (12.57 cm^2) were weighed and subsequently immersed in 1 M H_2SO_4 aqueous solution for 24 h to saturate the ion-exchange sites of the membrane with hydrogen ions (H^+). Subsequently, the membranes were thoroughly washed with Milli-Q water to eliminate any residual H_2SO_4 and retain only the H^+ ions bound to the ion exchange sites on the membrane. Then the obtained membranes were subsequently immersed in 50 mL of 1 M NaCl solution for 24 h. Throughout this time frame, the H^+ ions within the membrane were substituted with Na^+ (sodium ions) from the NaCl solution, thereby allowing H^+ ions to be released into the solution and acidic solution. The solution containing the released H^+ was then titrated with a 0.01 M NaOH basic solution using phenolphthalein as an indicator. Phenolphthalein indicator was prepared by adding 1 g of Phenolphthalein powder in 100 mL solution containing 50 mL of ethanol and 50 mL of Milli-Q water. This indicator is commonly employed to evaluate the electrochemical properties (Li et al., 2022). This colorless indicator underwent a change to pink upon titration as a result of the H^+ ions released from the membrane being neutralized by the OH^- ions from the NaOH solution. When the pH of the solution reaches 8.2 or above, a color change occurred, resulting in a pink solution. The IEC (meq/g) values of the dry membranes were calculated using the following equation.

$$IEC = \frac{V_{NaOH} \times S_{NaOH}}{W_{dry}} \quad \text{.....(3)}$$

where V_{NaOH} is the volume of NaOH spent during titration and W_{dry} is the dry weight of the membrane (g).

IEC specifies the number of ions that a membrane can exchange within a solution. A higher IEC signifies that the membrane can exchange a larger quantity of ions.

4.2.3.3. CONDUCTIVITY DETERMINATION

Understanding the proton conductivity is essential for designing batteries that ensure efficient energy transfer for improved performance and higher energy efficiency. The mechanisms to describe proton transfer across the membranes (usually the main charge transporter) are related to the 'Grotthuss mechanism,' where protons flow from one proton carrier to another. In this case, the proton moves through proton carrier molecules with functional groups, such as $-NH_2$, $-NH_3^+$, or $-SO_3H$, which dissociate H^+ and form hydrogen bonds. There is also a second mechanism called the 'vehicle mechanism.' In this mechanism, protons combine with water molecules to produce hydronium ions (e.g., H_3O^+, $H_5O_2^+$, and $H_9O_4^+$), which can migrate through a stream of water (González-Pabón et al., 2021).

Electrochemical impedance spectroscopy (EIS) measurements were carried out using 3 electrode system setup to obtain the specific conductivities of all the synthesized membranes (Panawong et al., 2022) and to determine the effect of the conductive ink coating on proton conduction compared to uncoated membranes. EIS experiments were performed using an Autolab PGSTAT302N potentiostat equipped with an FRA impedance module at open-circuit potential (Magar et al., 2021; Rezaei Niya and Hoorfar, 2013). The impedance of a material, which is a measure of its opposition to alternating current (AC), is composed of two components: resistance (real impedance) and reactance (imaginary impedance). Conductivity measurements were performed on the coated and non-coated membranes. The analysis was performed in the frequency range of 0.1 Hz and 10^5 Hz with an amplitude of 0.01 V at room

temperature under 100% relative humidity (RH) by immersing the membranes in Milli-Q water before each measurement. Conductivity was calculated using the following equation:

$$\sigma\left(\frac{S}{cm}\right) = \frac{d}{R_S \times S} \quad \text{.....(4)}$$

where σ is the conductivity (S/cm), d is the electrode distance (cm), R_S is the resistance obtained from the impedance data (Ω), and S is the membrane area (cm^2) (Tabata et al., 2022).

4.2.3.4. OXYGEN DIFFUSIVITY DETERMINATION

Oxygen diffusivity play a significant role in battery design because oxygen is an electron acceptor (Ucar et al., 2017). It is essential to avoid competition between the electron acceptor used in the battery and oxygen. The tests were performed in an H-type reactor. Oxygen concentrations were measured in the anode chamber using a dissolved oxygen (DO) probe (G1610, Greisinger, Germany) (precision ± 0.2 mg/L). Prior to the measurement, the DO probe was inserted into the anode chamber containing water (250 mL) and was made airtight after purging with pure N_2 gas to remove dissolved oxygen from the anode chamber. The concentration of dissolved oxygen in the anodic chamber was periodically recorded to observe oxygen diffusivity from the cathode chamber to the anode chamber.

The oxygen mass transfer coefficient k_{O_2}(cm/s), which characterizes oxygen permeability, was calculated from the cathode to the anode chamber over time using the mass balance in Equation 5 (González-Pabón et al., 2019):

$$k_{O_2} = \frac{-V}{A \times T} \times ln\left[\left(\frac{C_{O_2} - C}{C_{O_2}}\right)\right] \quad \text{.....(5)}$$

where V is the volume of the anode chamber (300 mL i.e 300 cm^3), A is the cross-sectional area of the membrane (12.57 cm^2), C_{O_2} is the saturation concentration of oxygen in the water (assumed to be 7.8 mg/L), and C is the concentration of oxygen in the anode chamber at time 'T (sec)' (mg/L).

The oxygen diffusion coefficient (D_0, cm^2/s) was calculated using the wet membrane thickness (T_{wet}) (González-Pabón et al., 2019):

$$D_0 = k_{O_2} \times T_{wet} \quad \text{.....(6)}$$

4.2.3.5. LINEAR SWEEP VOLTAMMETRY (LSV) STUDIES

The performance of the membrane circles (12.57 cm^2) were evaluated by polarization studies. The membrane were used as a separator in an H-type reactor, where the anodic and cathodic compartments were 300 mL each, respectively. Platinum electrode (1 cm × 1 cm) and carbon felt (1 cm × 2 cm) were used as anode and cathode, respectively. The anode compartment was filled with 300 mL of Milli-Q water, whereas the cathode compartment was filled with 150 mL of a phosphate buffered (0.1 M, pH 7) solution containing potassium ferricyanide (150 mL, 0.1 M), in order to avoid cathodic limitations. Linear sweep voltammetry (LSV) was performed in the potential range of 0 to 2 V at a scan rate of 1 mV/s using a Squidstat Potentiostat.

4.2.3.6. DEGRADATION TESTING IN COMPOST TEA

Biodegradation tests of membranes were performed in 100 % composted tea. First, compost tea was prepared according to (Atreya et al., 2023; Marín et al., 2013), with a 1:3 (v:v) compost: water ratio in a 0.9 L PET flask. Non-aerated compost tea was used, in which the compost was suspended in Milli-Q water at the proportion indicated and stored at 20 °C for seven days in the dark with periodic homogenization. After seven days, the compost tea was filtered through a sieve and used for testing. In total 6 samples of size 2 cm × 1 cm were cut from the main membrane. They were then dried in an oven at 50 °C for 1 h, and their initial weight was measured (m_i), after which two samples were immersed in three bottles, each of 25 mL of compost tea, for the desired days under airtight conditions. After 5, 50, and 100 days, the samples were removed and dried at 50 °C, and the final weight (m_f) of the membranes were measured. The degradation is calculated by finding out the percentage weight loss by the formula,

$$Percentage\ weight\ loss = \left[\frac{(m_i - m_f)}{m_i}\right] \times 100 \quad \text{.....(7)}$$

where m_i is the initial weight and m_f is the weight remaining after immersing the membranes in the compost tea.

4.2.3.7. CHARACTERIZATION OF MEMBRANES

The hydrophobicity/hydrophilicity of the prepared membranes was quantified by measuring the contact angle of a water droplet with an optical tensiometer (Theta Lite, TL100-TL101) by using the sessile drop method. The contact angle was measured immediately after putting water droplet on the membrane surface (t = 0). The water droplet was left undisturbed for 5 minutes on the CS membrane and 10 minutes for PVA and CS/PVA membranes before remeasuring the another contact angle. The surface morphology and microstructure characteristics of membranes were studied using a scanning electron microscope (SEM, JSM-IT800). The thermal stability of membranes was investigated using thermogravimetric analyzer (TGA, Netzsch STA 409 C/CD) instrument under argon (Ar) atmosphere, in the range of 25 °C - 600 °C and heating rate was 20 °C min^{-1}. The mechanical properties of the membranes were assessed using a Z010 Universal Testing Machine (Zwick, Ulm, Germany). Test specimens were excised from membranes that had been immersed in MilliQ water for 7 days, with dimensions of 60 mm in length and 10 mm in width. Prior to testing, the specimens were dried using tissue paper. The tensile measurement were performed on strips with dimensions of 10 mm × 60 mm at room temperature with a crosshead speed of 2 mm/min. Subsequently, the mechanical properties (tensile strength, young's modulus, and elongation at break) were determined.

All experiments were performed in triplicate, and descriptive statistics were applied using Origin software to calculate the mean and standard deviation values.

4.3. RESULTS AND DISCUSSION

4.3.1. SWELLING RATIO AND WATER UPTAKE CAPACITY

Figure 4.2A, 2B, and 2C illustrate the water uptake capacity (%), swelling ratio (%) (based on thickness), swelling based on area **(i.e.** in-plane direction) of the CS, PVA, and CS/PVA membranes, wherein uncoated samples are represented as plain and ink coated samples as hatched. These values were calculated using Equation 1 and Equation 2 and has

been shown in Table 4.1. The CS membrane exhibited the highest water uptake capacity (94.10 %), followed by PVA (63.87 %) and CS/PVA (54.44 %) in uncoated samples. CS membrane exhibits significantly higher water absorption capacity than PVA membrane because of its distinctive structure and the presence of ionotropic cross-links, whereas PVA membrane exhibits lower water absorption owing to its differing chemical structure and cross-linking behavior, which constrains its hydrophilicity relative to CS-based materials (Sangeetha et al., 2022). In addition, the absorption of water in PVA membrane is lower due to the formation of intramolecular hydrogen bonds between adjacent hydroxyl (OH) groups, which effectively reduces the number of water molecules that can be hydrated per -OH group. While each -OH group can attract water, PVAs retain only approximately 2 to 2.2 water molecules in aqueous solution (Satokawa and Shikata, 2008).

PVA membrane (150 %) showed the highest swelling ratio compared with CS membrane (2 %) and CS/PVA membrane (111.67 %) in the uncoated samples. Interestingly, the swelling ratio of the CS uncoated membrane was found to be almost negligible in comparison to the other membranes. This phenomenon can be attributed to the cellulose filter paper in CS, which, when exposed, exhibits a robust network structure formed by extensive hydrogen bonding among cellulose fibers. This structure effectively prevents swelling despite significant water uptake. The cellulose filter paper fibers are clearly depicted in Supplementary Figure 4.S2A1. Also, the compact arrangement ensures mechanical integrity and stability, enabling the membrane to function efficiently without excessive expansion (Z. Li et al., 2021). The data depicted in Figure 4.2A and Figure 4.2B indicate that the ink coated membrane (hatched lines) exhibited a lower water uptake capacity for CS (59.62 %), PVA (59.06 %), and CS/PVA (17.08 %), and a lower swelling ratio for CS (1.50 %), PVA (127.27 %), and CS/PVA (10 %) compared to the uncoated samples (plain lines).This suggested that the ink coating impeded the ability of the samples to absorb water. The water uptake and swelling ratio are low in the coated membranes because graphene is hydrophobic and repels water (Sun et al., 2023), creating a physical barrier on the cellulose fibers. This makes it harder for water molecules to penetrate (Jingfeng Wang et al., 2019) and acts as a structural reinforcement for this study. As the ink dries, it forms a network of interconnected flakes that strengthen the paper matrix. This reinforcement helps the paper to resist the internal pressure caused by the absorbed water, thereby reducing swelling (Gambhir et al., 2015).

To assess the swelling of the membrane based on area (i.e., in the plane direction), a rectangular strip of membrane measuring 10 mm in width and 60 mm in length was excised from the membrane, and the rectangular area was calculated. The swelling area of the membrane was observed to be negligible, potentially due to the cellulose paper, which restricts the membrane's swelling in both length and width directions (i.e. in-plane) (M. Lee et al., 2016). Cellulose fibers in filter paper exhibit anisotropic swelling behavior, with greater expansion in the thickness direction than in-plane. This structural arrangement of aligned and bonded fibers restricts the membrane's swelling in the in-plane direction (Bloch et al., 2024; Hubbe et al., 2024).

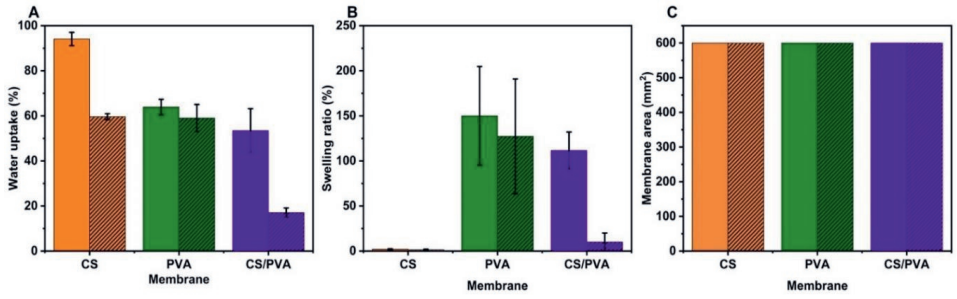

Figure 4.2: (A) Water uptake capacity, **(B)** Swelling ratio (based on thickness), and **(C)** Swelling area (in in-plane) of the membrane (plain graph - uncoated, hatched graph - ink coated)

4.3.2. ION EXCHANGE CAPACITY (IEC)

Figure 4.3 illustrates the IEC of the uncoated (plain) and ink coated (hatched) CS, PVA, and CS/PVA membranes in terms of milliequivalents per gram (meq/g). The IEC values were calculated using Equation 3 and are shown in Table 4.1. In the bar graph, the x-axis represents the membrane, and the y-axis represents the IEC. The plot indicates that the uncoated PVA (3.94 meq/g) membrane has the highest IEC, followed by the CS (1.82 meq/g) and CS/PVA (1.50 meq/g) membranes. While for the coated membranes, IEC values decreased for all the three membranes: CS (0.61 meq/g), PVA (2.88 meq/g) and CS/PVA (0.71 meq/g). This could be because the ink coating acted as a barrier, preventing the ions from reaching the exchange sites on the membrane. The difference in performance between the coated and uncoated membranes was minimal for the PVA membranes. The IEC values in theory are approximately 3.1 meq/g for CS, around 11.6 meq/g for PVA, and about 7.36 meq/g for the CS/PVA combination.

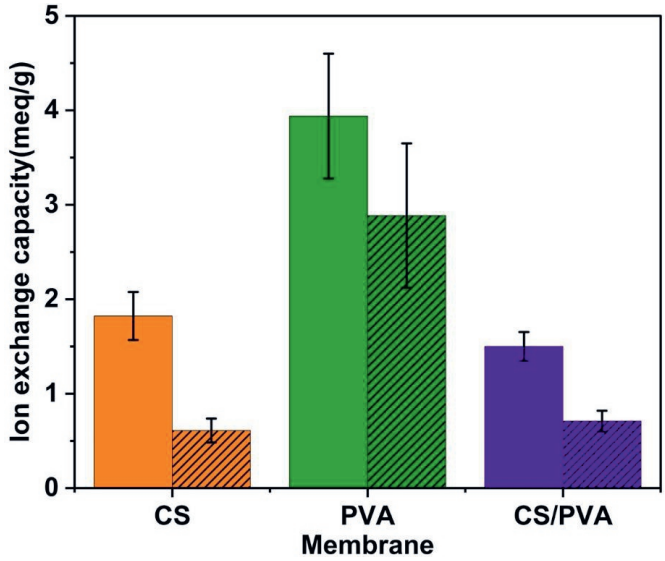

Figure 4.3: Ion exchange capacity of CS, PVA, and CS/PVA membranes (plain graph – uncoated samples, hatched graph - ink coated samples)

Among the uncoated membranes, PVA exhibited the highest IEC at 3.94 meq/g, followed by CS at 1.82 meq/g, and the CS/PVA at 1.50 meq/g. The application of a graphene ink coating resulted in a reduction of IEC across all membrane types: CS decreased from 1.82 to 0.61 meq/g, for PVA from 3.94 to 2.88 meq/g, and for CS/PVA from 1.50 to 0.71 meq/g. This coating likely acted as a barrier, impeding ions from accessing the exchange sites on the membrane, potentially obstructing pores or functional groups involved in ion exchange. Other factors influencing IEC include the chemical structure, where PVA's configuration provides more ion exchange sites than CS, crosslinking, which can affect the availability of these sites, and hydrophilicity, as more hydrophilic materials generally exhibit higher IEC. Additionally, graphene's hydrophobic nature might reduce the water uptake necessary for ion transport. The smallest difference between coated and uncoated membranes was observed in PVA, suggesting its structure might still permit ion exchange despite the coating. Theoretical IEC values exceeded measured ones, indicating that not all potential exchange sites are accessible. Further experiments are necessary to gain a deeper understanding of the behaviour of these membranes. This could involve measuring IEC with different coating thicknesses, examining the membrane surface chemistry before and after coating, testing various coating materials to evaluate their effects, and investigating ion movement through coated membranes.

Table 4.1: Average water uptake, swelling ratio, ion exchange capacity and proton conductivities of CS, PVA, and CS/PVA membranes

Membrane	**Water uptake (%)**		**Swelling ratio (%)**		**Ion exchange capacity (meq/g)**		**Proton conductivity (S/cm)**	
	uncoated	coated	uncoated	coated	uncoated	coated	uncoated	coated
CS	94.10	59.62	2.00	1.50	1.82	0.61	7.8 µ	0.73 m
PVA	63.87	59.06	150.00	127.27	3.94	2.88	31.8 µ	1.51 m
CS/PVA	53.44	17.08	111.67	10.00	1.50	0.71	5.87 µ	1.74 m

4.3.3. CONDUCTIVITY DETERMINATION

Supplementary Figure 4.S3A,and Figure 4.S3B shows the electrochemical impedance spectra of the CS, PVA, and CS/PVA membranes for both uncoated and ink coated respectively. The real impedance, represented on the x-axis in ohms, and imaginary impedance, represented on the y-axis in ohms, are illustrated Supplementary Figure 4.S3. The EIS spectra indicated that the real impedances of all three membranes were higher at lower frequencies. This is because, at lower frequencies, the ions in the electrolyte have more time to diffuse into the membrane, which increases the resistance. At higher frequencies, the ions have less time to diffuse and the impedance decreases (Saghafi et al., 2023). The CS/PVA membrane exhibited the highest impedance among the uncoated membrane samples, whereas the CS membrane showed the highest impedance for the coated samples. The utilization of ink coating has a profound impact on the impedance of the membranes. Notably, the impedance of the coated membrane was lower than that of the uncoated membrane. This can be attributed to the fact that the graphene-based conductive ink applied to membranes improves the electrochemical properties, generates more interconnected channels for proton transfer, and facilitates efficient proton transfer across the membrane (Ahmed et al., 2023; Kushwaha et al., 2023; Muhmed et al., 2023).

The proton conductivities of the membranes were calculated using Equation 4 and are illustrated in Figure 4.4 and are reported in Table 4.1. The PVA membranes exhibited higher conductivities than the CS and CS/PVA membranes. These results are in agreement with the IEC data, where the highest IEC values were obtained with PVA membrane as the IEC and the

proton conductivity was directly related (Wei et al., 2023). As reported in a previous study (Maiti et al., 2012), the proton permeability of the CS/PVA membranes was 11.2 mS/cm. However, in our study, the proton conductivity was found to be significantly lower 5.87 µS/cm when uncoated . This difference may be due to the cellulose filter paper used as reinforcement in the membranes, which may have impeded the proton flow. However, when coated, the conductivity increased to 1.74 mS/cm, even when cellulose filter paper was used as the reinforcement. This is in agreement with the study performed by Khan et al. (2015), where they have shown that the graphene enhances proton conductivity when blended with polymer. However in case of PVA these values are 31.8 µS/cm in uncoated and 1.51 mS/cm in coated condition. The reduction in proton conductivity in the PVA membrane after coating with graphene can attributed to the high content of graphene nanofillers blocking ionic channels, which restricts the free movement of ions, thus hindering conductivity (Das et al., 2019). The IEC of a membrane depends on its material composition, structure, and surface treatments (Haldrup et al., 2016). CS membrane with abundant amine groups and hydrophilic properties, offers moderate proton exchange potential but has low density of exchangeable sites, resulting in reduced conductivity when uncoated (Palanisamy et al., 2023). When coated with ink containing acidic groups, the IEC improves, increasing conductivity. PVA forms flexible, water-retaining films but lacks strong acidic groups for high IEC. Its high conductivity indicates effective proton mobility, with coating providing slight enhancement. The CS/PVA membrane shows decreased conductivity when uncoated, likely due to phase separation (Aziz et al., 2017). However, coating significantly improves performance by introducing ion-exchange functionality and enhancing proton transport. The coating boosts IEC by adding proton-conducting groups and improving hydration, particularly in membranes with lower intrinsic ion exchange potential, demonstrating the importance of surface engineering for proton exchange applications.

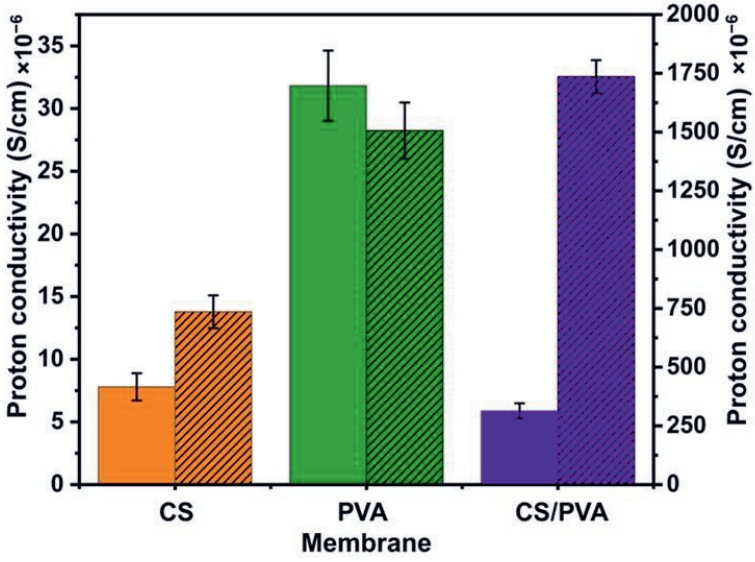

Figure 4.4: Proton conductivities attained for CS, PVA and CS/PVA membranes (plain graph - uncoated (left y-axis), hatched graph - ink coated (right y-axis))

4.3.4. OXYGEN DIFFUSIVITY MEASUREMENT

The average oxygen concentration (mg/L) in the anode chamber, measured for 5 h, is shown in Figure 4.5A (uncoated) and Figure 4.5B (ink coated). These data are also given in Table 4.2, along with the oxygen diffusion, oxygen mass transfer coefficient, and oxygen diffusion coefficient which were calculated using Equation 5 and Equation 6, respectively. The average membrane thickness for the uncoated membranes is 0.01 cm for CS, 0.0183 cm for PVA, and 0.01 cm for CS/PVA. On the other hand, for the coated membranes, the thickness is 0.01 cm for CS, 0.025 cm for PVA, and 0.0125 cm for CS/PVA. The average oxygen concentration in the anode at the end of 5 h was the highest for PVA membrane (0.167 mg/L), whereas CS and CS/PVA membranes exhibited the same value of 0.100 mg/L when uncoated. However, in the coated membranes, these values were 0.100 mg/L, 0.067 mg/L, and 0.033 mg/L for CS, PVA, and CS/PVA, respectively. It can be seen that when the proton membranes are coated, the oxygen concentration in the anode chamber is less than that when uncoated because the graphene ink coating reduces oxygen diffusion (Topsakal et al., 2012). This is because the graphene coating create a high-energy barrier that impedes the movement of oxygen atoms, making it difficult for them to penetrate through the membrane (Topsakal et al., 2012). The accuracy range of the oxygen diffusion probe was found to encompass the oxygen diffusion rates for all membranes, which was ± 0.2 mg/L. Hence, no definitive conclusions could be drawn regarding the accuracy of the membranes based on data collected over a period of 5 h. To draw any meaningful conclusions regarding the accuracy of the membranes, it is necessary to conduct oxygen diffusion experiments over an extended period of time or utilize an instrument that can measure significant variations in the oxygen diffusion rates more precisely.

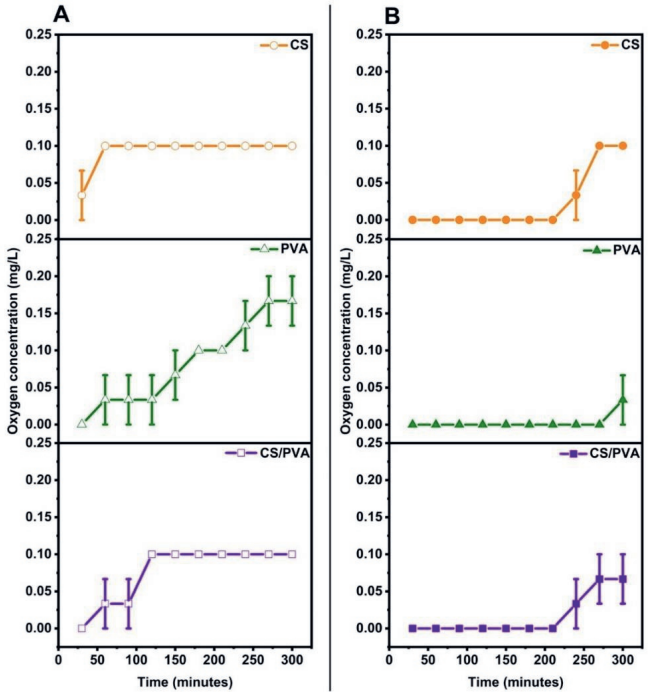

Figure 4.5: Average oxygen concentration (mg/L) of CS, PVA, and CS/PVA membranes. **(A)** uncoated, and **(B)** ink coated

When uncoated, PVA membrane has the highest value for the oxygen mass transfer coefficient, which is 2.391 x 10^{-5} cm/s followed by CS and CS/PVA membranes having the same value of 1.425 x 10^{-5} cm/s. Compared to the uncoated membranes, the coated membranes showed lower values for PVA (0.953 x 10^{-5} cm/s) and CS/PVA (0.468 x 10^{-5} cm/s), but for CS, it was the same as for uncoated membranes, which was 1.425 x 10^{-5} cm/s. The oxygen diffusion coefficient was the highest in PVA membrane (0.437 x 10^{-5} cm^2/s) under uncoated and coated conditions (0.238 x 10^{-5} cm^2/s). In general, the coating reduces the oxygen mass transfer and diffusion coefficients, with coated CS/PVA membrane demonstrating the lowest values.

It is noteworthy that although the viscosity of the polymer solutions (CS, PVA, and CS/PVA) likely affected the membrane coating and thickness (Zong et al., 2021), quantitative viscosity measurements were not conducted during membrane preparation. This constitutes a limitation of the present study, and future research will incorporate systematic viscosity characterization to more accurately correlate solution properties with membrane performance.

Table 4.2: Oxygen diffusion, oxygen mass transfer coefficient and oxygen diffusion coefficient of CS, PVA, and CS/PVA membranes

Membrane	Oxygen diffusion (avg at t = 5 hours) (mg/L)		Oxygen mass transfer coefficient k_{O_2} (cm/s) (10^{-5})		Oxygen diffusion coefficient D_o (cm^2/s) (10^{-5})	
	uncoated	coated	uncoated	coated	uncoated	coated
CS	0.100	0.100	1.425	1.425	0.142	0.142
PVA	0.167	0.067	2.391	0.953	0.437	0.238
CS/PVA	0.100	0.033	1.425	0.468	0.142	0.058

4.3.5. LINEAR SWEEP VOLTAMMETRY (LSV)

The findings from the LSV curves, as illustrated in Figure 4.6A (uncoated) and Figure 6B (ink coated), reveal that there is a negligible current density between 0 and 1 V, indicating an electrochemical reaction in which no electrons are involved within this potential range for both the uncoated and coated membranes (i.e., CS, PVA, and CS/PVA). However, when the voltage was increased to more than 1 V, a considerable increase in the current flow was observed for the membranes, suggesting the onset of an electrochemical reaction.

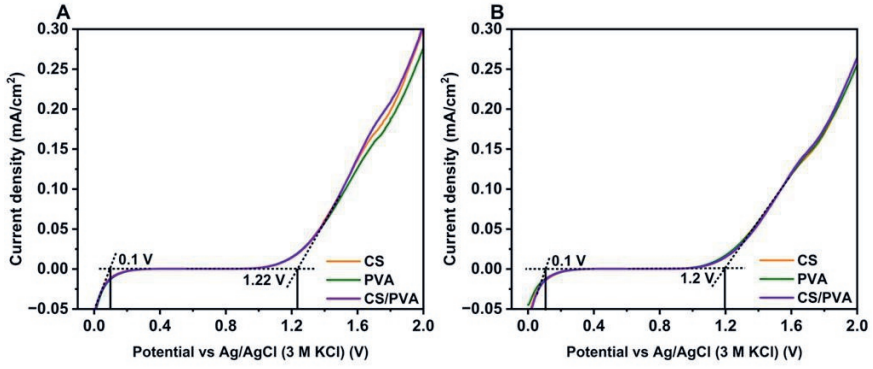

Figure 4.6: H-type reactor performance LSV curves of CS, PVA and CS/PVA membranes. (A) uncoated, (B) ink coated.

Previous studies have shown varied potential levels at which the current starts increasing, around the values reported here. For example, CS (1 - 1.3 V) (Shukur and Kadir,

2015), PVA (4.5 V) (Xiao et al., 2015), PVA - CS (1.70 V) (Kadir and Arof, 2011), CS - PVA and potassium hydroxide (KOH) (2 V) (Poosapati et al., 2021), CS with NH_4SCN and glycerol (2.09 V) (Aziz et al., 2021b), CS with DXN3 (1.54 V) (Aziz et al., 2021a), PVA - CS with NH_4I (1.33 V) (Shahab Marf et al., 2020), CS with NH_4NO_3 and ethylene carbonate (1.8 V) (Ng and Mohamad, 2008), and PVA with dextran and NH_4I (1.3 V) (Aziz et al., 2020) were noted. If the current remains stable below 1 V, without any sudden increase in current density, it can be considered as a positive indicator because it helps to minimize solvent evaporation and leakage within the electrochemical system. This is particularly beneficial for preventing any potential issues that may arise owing to solvent loss (Aziz et al., 2021a). For the uncoated and coated membranes, there was no variation in the current density between 0 and 1 V. For all the membranes (uncoated and coated), the current started rising after 1 V, hence it can be concluded that these membranes can be used in practical applications without undergoing any damage. These results suggest that the coating does not have a significant impact on the current density of the membranes, as there is only a slight decrease in the highest current density achieved by the coated membranes at a final potential of 2 V.

4.3.6. DEGRADATION TEST

To create biodegradable batteries suitable for soil moisture sensors, it is essential that they have a functional lifespan of at least 100 days, as the typical growth period for crops ranges from 100 to 120 days (Wang et al., 2010). Given the significance of biodegradable membrane as a crucial component of batteries, it is vital to be aware of its degradation time. The study conducted on degradation of the membranes yielded degradation values, in terms of percentage of mass loss are listed in Table 4.3. These values were found out using Equation 7. It can be seen that the membranes degrade very slowly in 100 days at room temperature in compost tea (in between 2 wt % - 5 wt %), which is in agreement with the results shown in (Chiellini et al., 2003). Multiple factors may be responsible for the reduced degradation of these membranes, such as the polymer morphology, structure, chemical treatment, environmental conditions, and molecular weight (Chiellini et al., 2003; Samir et al., 2022). Previous studies have tested the degradation of CS, PVA, and CS/PVA membranes at various temperatures (Murmu et al., 2022; Vera et al., 2022) and have shown that degradation occurs beyond 250 °C (Ambili et al., 2019; Vera et al., 2022). The degradation of CS occurs in the temperature range of 200° C–300° C and 500° C–600° C (Schaffer et al., 2018), and for PVA, it occurs at more than 50 °C with a 99.9 % degree of hydrolysis (Zhu and Ge, 2021). Based on these results, it can be inferred that the CS, PVA, and CS/PVA membranes exhibit stability at room temperature and in the presence of compost tea membranes are not going under any degradation. Consequently, these membranes can be utilized for extended periods under normal environmental conditions without any degradation.

Table 4.3: Degradation of CS, PVA, and CS/PVA membranes in compost tea (100 % concentration)

Time (days)	Membranes	CS			PVA			CS/PVA		
		m_i (avg)	m_f (avg)	% mass loss	m_i (avg)	m_f (avg)	% mass loss	m_i (avg)	m_f (avg)	% mass loss
5	Coated	0.0255	0.0255	0.00	0.0545	0.0545	0.00	0.0295	0.0295	0.00
50		0.0265	0.0260	1.92	0.0565	0.0560	0.89	0.0280	0.0275	1.82
100		0.0255	0.0250	2.00	0.0555	0.0545	1.83	0.0290	0.0280	3.57
5	Uncoated	0.0240	0.0240	0.00	0.0510	0.0510	0.00	0.026	0.026	0.00
50		0.0265	0.0255	3.92	0.0510	0.0495	3.03	0.027	0.0265	1.89
100		0.0245	0.0235	4.26	0.0475	0.0450	5.56	0.026	0.025	4.00

4.3.7. CHARACTERIZATION

Contact angle: Contact angle measurements were conducted to determine whether the membranes exhibit hydrophobic or hydrophilic properties. Figure 4.7 shows the mean contact angle versus time of all the three membranes at beginning and after 5/10 minutes waiting time.

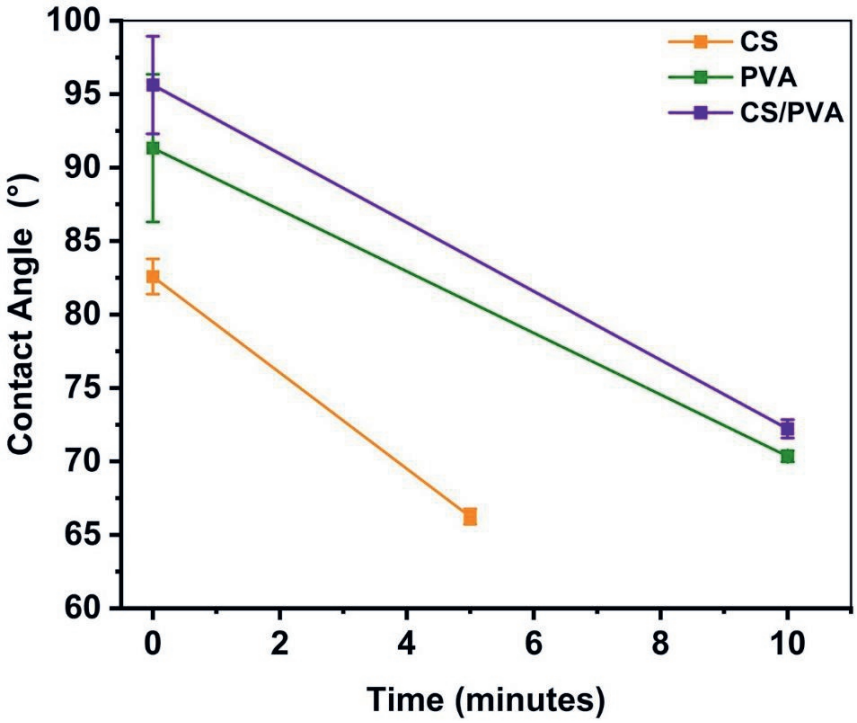

Figure 4.7: Mean contact angle vs time for CS, PVA, and CS/PVA membranes.

Figure 4.8 shows photographs of contact angle measurements of all the three membranes. It was observed that the water droplet was gradually absorbed by the membranes, resulting in decreasing contact angles after waiting time. The absorption rate was found to be higher on CS membrane compared to on PVA and CS/PVA, membranes. The hydrophobicity of the membranes exhibited the following order for the membrane: CS/PVA > PVA > CS. The lower contact angle of CS membrane is attributed to the water uptake observation (Figure 4.2A), which illustrates that CS membrane exhibits a higher water uptake capacity compared to PVA and CS/PVA membranes. Study done by Tran et al. (2025) shows that the contact angle of the CS/PVA composite blended with graphene is significantly higher than the pure PVA, indicating the improved hydrophobicity in the composite films. Notably, the contact angle of all membranes decreased with time, regardless of the polymers used. Increasing the PVA percentage reduces the contact angle and hydrophilic characteristic of PVA in comparison to CS (Campa-Siqueiros et al., 2020).

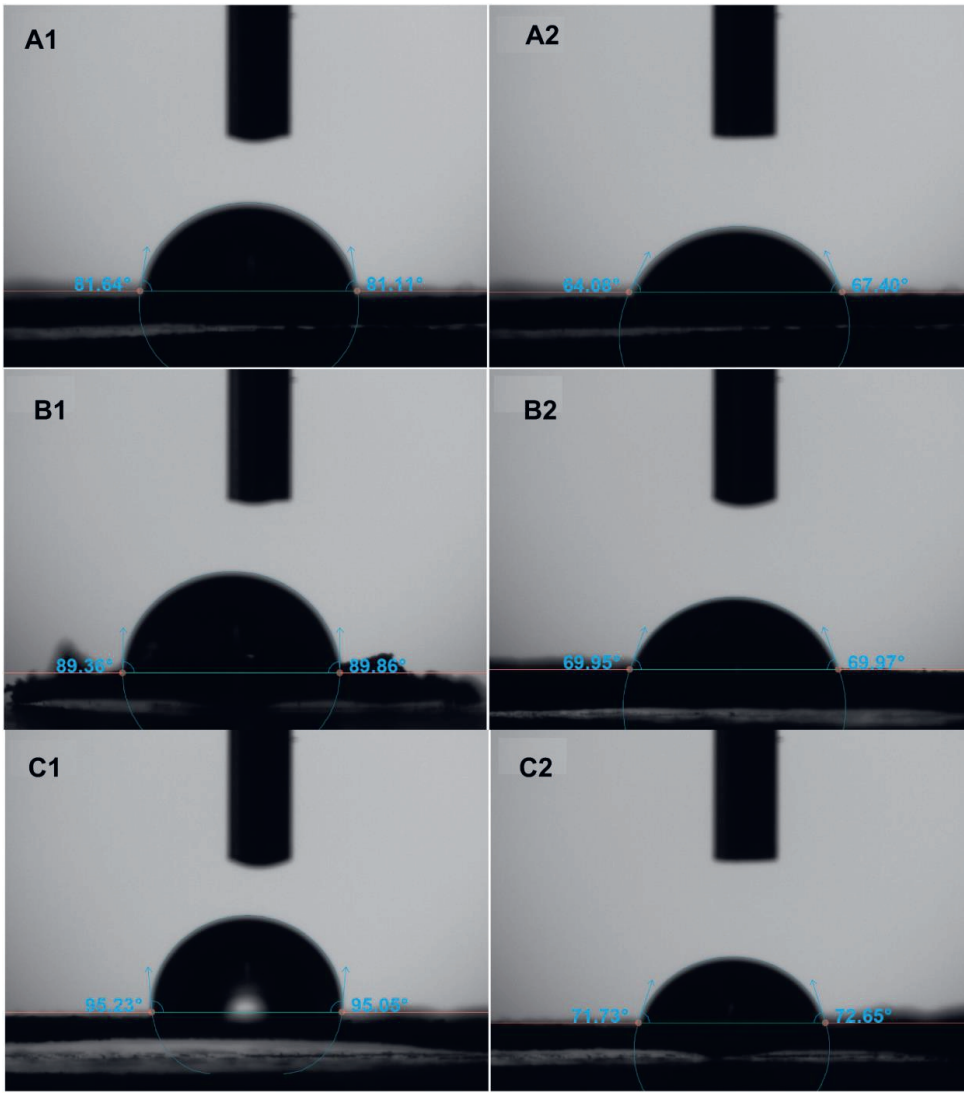

Figure 4.8: Mean contact angle measurements of CS, PVA, and CS/PVA membranes. **(A1):** CS, t = 0 min, **(B1):** PVA, t = 0 min, **(C1):** CS/ PVA, t = 0 min. **(A2):** CS, t = 5 min, **(B2):** PVA, t = 10 min, **(C2):** CS/ PVA, t = 10 min.

SEM: Figure 4.9 presents the SEM images of CS, PVA, and CS/PVA membranes, each coated with a mixture of graphene ink and the corresponding polymer blend. The SEM images of CS membrane (Figure 4.9 A1, A2) reveal that graphene flakes are readily observable. The graphene dispersed within the CS solution exhibits irregularly wrinkled like structures. It can been that there are some uncovered areas, where cellulose of filter paper is exposed. Long Cellulose fibers are clearly visible in SEM images of CS shown in Supplementary Figure 4.S2A1. The SEM images of PVA membrane demonstrate that a layer of graphene nanoparticles adheres to the surface of PVA molecules, where a smooth surface can be seen suggesting that the ink is uniformly distributed on the surface of the PVA membrane. The SEM images of CS/PVA

membrane display a rough surface. Similar to CS membrane, there are some uncovered areas on CS/PVA membrane as seen in Figure 4.9C1, but smaller in area. Nano cellulose fibers are visible in both the CS and CS/PVA membranes as observed by (T.-T. Li et al., 2019; Younas et al., 2019). To assess the coating thickness of the ink, SEM images were takes on the cross section of membranes. Upon examining the cross-section of the membranes, two distinct morphologies are evident: one associated with the ink and the other with the polymer. The absorption of ink into the CS membrane is observed to be non-uniform. This variation is attributed to the thickness of the graphene layer, where a thinner layer appears brighter and a thicker layer appears darker (Park et al., 2012). The thin layer of graphene ink exposes the underlying cellulose fiber, which is seen as brighter areas in the cross-section. In the case of PVA, the absence of bright areas indicates that the graphene ink blend is evenly distributed on the PVA membrane, forming a large dense layer (Eljaddi et al., 2021). In the CS/PVA membrane, two distinct, evenly distributed layers are visible, the upper darker layer is due to the graphene ink blend, while the lower brighter layer is attributed to the CS/PVA membrane. The absorption of the ink into the filter paper follows an increasing order: CS < CS/PVA < PVA. Analysis of the SEM images indicates that a uniform ink coating layer cannot be achieved by manually applying the ink on the membranes. Therefore, it is necessary to employ the specialized coating technologies for applying graphene. Furthermore, observations of the PVA membranes reveal that the graphene ink is absorbed into the PVA. To prevent this absorption, an additional coating is required between the graphene ink and the PVA membrane, which will serve as a barrier to avoid ink absorption.

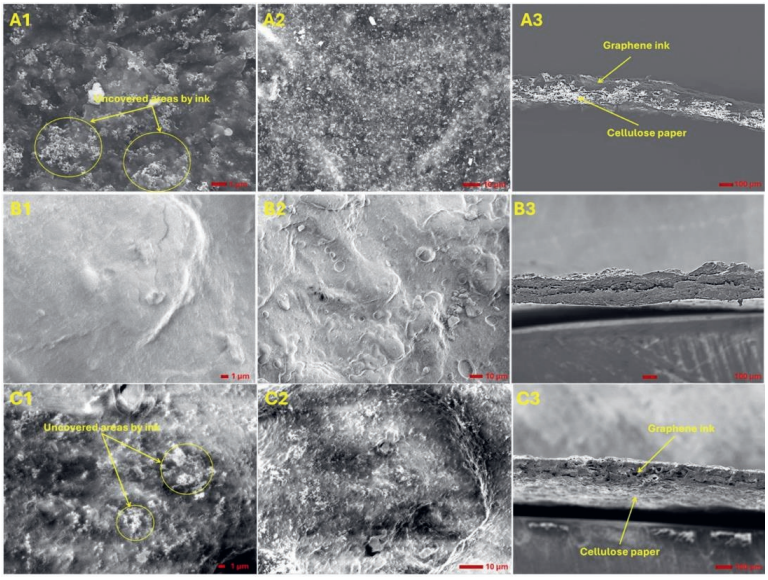

Figure 4.9: SEM images of CS, PVA, and CS/PVA membranes after coating with graphene ink. Panels **(A1, A2), (B1, B2),** and **(C1, C2)** depict the surface morphologies of the CS, PVA, and CS/PVA membranes, respectively, while panels **(A3, B3, C3)** shows the cross-sectional morphologies of these membranes.

TGA: Figure 4.10 shows TGA curves of CS, PVA, and CS/PVA membranes coated with graphene ink. For CS, PVA, and CS/PVA the TGA curves showed that at about 100 °C, the weight loss was about 1.5 % which could be due to the loss of free water trapped in the CS, PVA, and CS/PVA molecules. A significant mass loss occurred at about 235 °C, indicating the

beginning of degradation, which was due to with the loss of amino and hydroxyl groups on CS membranes (Yang et al., 2018), and, due to the degradation of the main chain of the PVA polymers (Kandile and Nasr, 2023). At about 410 °C, the weight loss was about 30 % and the rate of degradation decreased due to the rigid and regular ring structure of CS (Yang et al., 2018). Generally, the temperatures where the biobatteries were used ranges from 4–90°C maximum. The examples of the reported temperature ranges of biobatteries are 4°C–25°C (Adekunle et al., 2019), 30 - 40 °C (Mohammadifar and Choi, 2019), 65 °C (Chen et al., 2016), and 90 °C (Cheng et al., 2015). From the TGA curves, it can be seen that the three membranes investigated are stable below 100 °C, hence these membranes can be used in the biobattery applications.

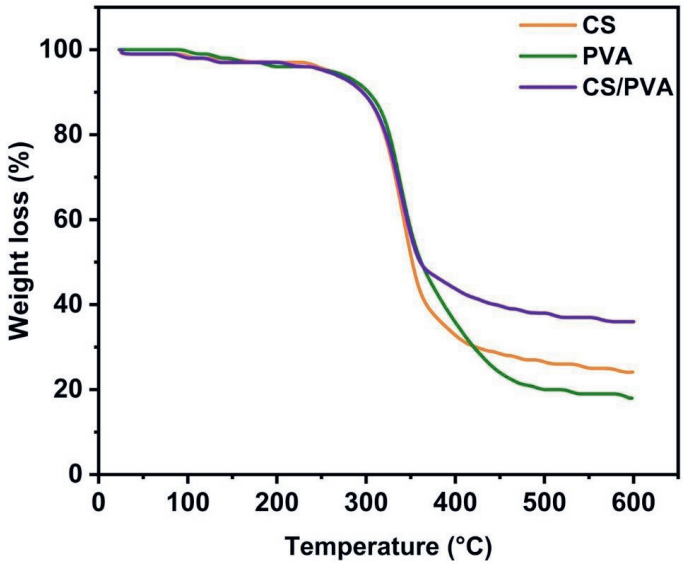

Figure 4.10: TGA analysis of CS, PVA, and CS/PVA membranes coated with graphene ink

Mechanical properties: Figure 4.11A, 11B, 11C, and 11D shows the Stress-strain curve, Young's modulus, tensile strength, and elongation at break respectively which were extracted from the stress–strain curves of CS, PVA, and CS/PVA membranes, while the Supplementary Table 4.S1 shows the exact calculated values from the test. The tensile measurements were performed on strips with dimensions of 10 mm × 60 mm at room temperature with a crosshead speed of 2 mm/min. The CS membrane exhibited a tensile strength of approximately 1.28 ± 0.29 MPa, a tensile strain of 6.48 ± 2.47 %, and a Young's modulus of 0.38 ± 0.23 MPa. The PVA membrane demonstrated a tensile strength of about 0.58 ± 0.04 MPa, a tensile strain of 11.43 ± 1.14 %, and a Young's modulus of 0.07 ± 0.01 MPa. The CS/PVA membrane, showed a tensile strength of approximately 3.73 ± 1.30 MPa, a tensile strain of 12.22 ± 0.29 %, and a Young's modulus of 0.33 ± 0.08 MPa. The CS/PVA membrane showed the highest tensile strength values compared to CS and PVA membranes. The tensile strength of the CS, and PVA is lower which shows that it has higher flexibility and hence the CS and PVA membranes can be used in flexible biobattery design, as it was shown that the flexibility and tensile strength has a inverse relationship (Arpa et al., 2021). CS/PVA membranes showed the highest elongation at break values compared to CS and PVA membranes. Analysis of the data indicates that the selection of membranes should be tailored to the specific requirements of the

applications. This is due to the absence of a consistent detectable trend in the various tensile strength, stress-strain, and elongation at break values.

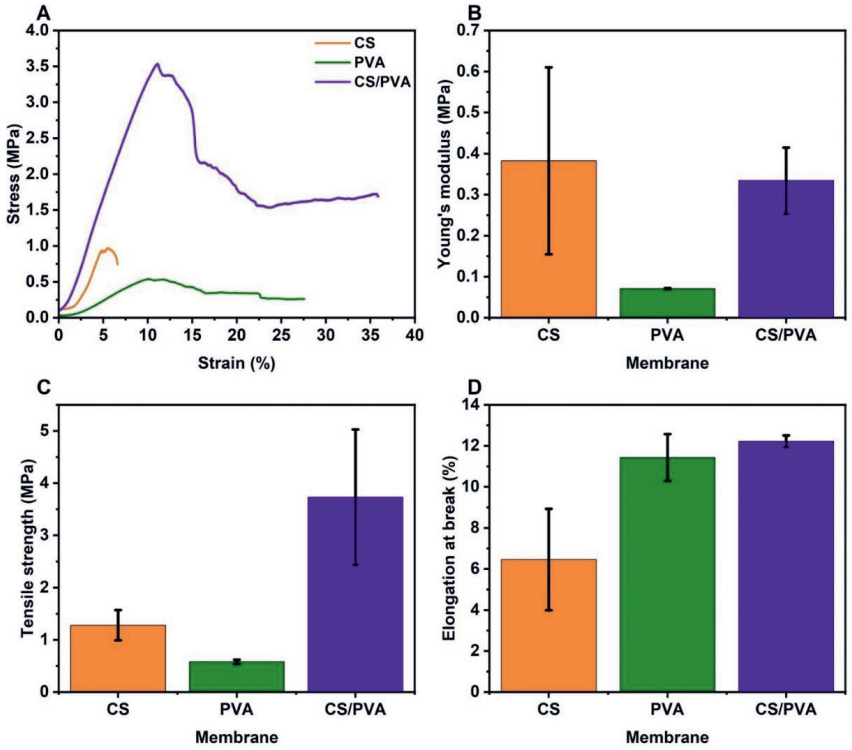

Figure 4.11: (A) Stress–strain curve, **(B)** Young's modulus plot, **(C)** tensile strength plot, and **(D)** elongation at break plot of CS, PVA, and CS/PVA membranes

4.4. CONCLUSIONS

This study illustrates the feasibility of fabricating biodegradable membranes utilizing CS, PVA, and CS/PVA composites reinforced with cellulose filter paper via the solution casting method. These membranes were subsequently coated with a water-resistant, conductive graphene ink to enhance their performance. The uncoated CS membrane exhibited the highest water uptake capacity at 94.10 %, whereas the uncoated PVA membrane demonstrated the highest swelling ratio (150 %) and ion exchange capacity (3.94 meq/g). Among all samples, the coated CS/PVA membrane exhibited the lowest oxygen diffusion coefficient (0.058×10^{-5} cm^2/s) and the highest proton conductivity (1.74 mS/cm). These findings suggest that the graphene-coated membranes possess superior electrochemical properties compared to their uncoated counterparts. All three membrane types exhibited slow degradation over 100 days at room temperature in compost tea, underscoring their potential for medium-term stability in water-rich environments. The integration of cellulose filter paper reinforcement and conductive graphene coating offers a promising strategy for the development of biobatteries and other biodegradable electronic devices. Characterization techniques such as SEM, thermogravimetric analysis (TGA), and contact angle measurements provided valuable insights into membrane morphology, thermal stability, and surface properties. Expanding the range of characterization tools could further enhance the understanding of membrane behaviour and

performance. Future research should focus on optimizing membrane composition by exploring different CS/PVA ratios, alternative crosslinking methods, and modifications to improve specific properties such as proton conductivity and mechanical strength. The coating process could be refined to ensure more uniform graphene ink distribution, potentially through techniques such as spray coating, screen printing, or spin coating. Additionally, varying the properties of the cellulose filter paper (e.g., thickness, pore size) and incorporating additives could further tailor membrane characteristics. Potential applications of these biodegradable membranes include biobatteries for low-power devices such as soil moisture sensors, fuel cells leveraging proton-conducting capabilities, water treatment utilizing selective permeability for purification or desalination, eco-friendly packaging due to their biodegradable nature, and biomedical devices, including temporary implants or drug delivery systems. Overall, this research opens promising avenues for the development of sustainable materials and energy technologies. Balancing key membrane properties such as water uptake, swelling, and conductivity will be essential for optimizing performance in targeted applications.

4.5. APPENDIX

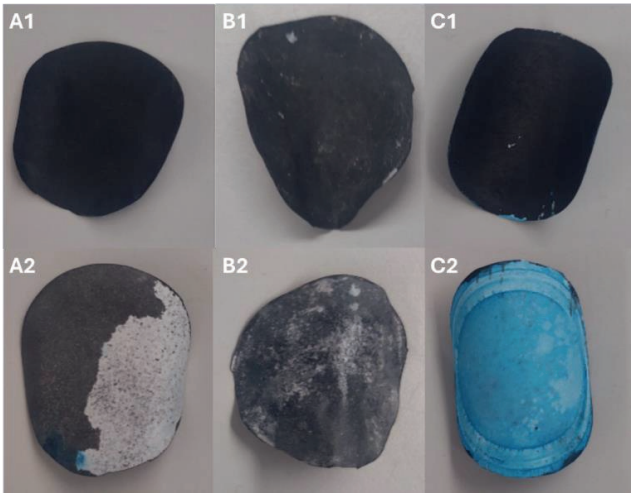

Figure 4.S1: CS, PVA, and CS/PVA membranes after the electrochemical experiments. **(A1, B1, C1)** are ink-coated side of CS, PVA, and CS/PVA membranes and **(A2, B2, C2)** are uncoated side of CS, PVA, and CS/PVA membranes

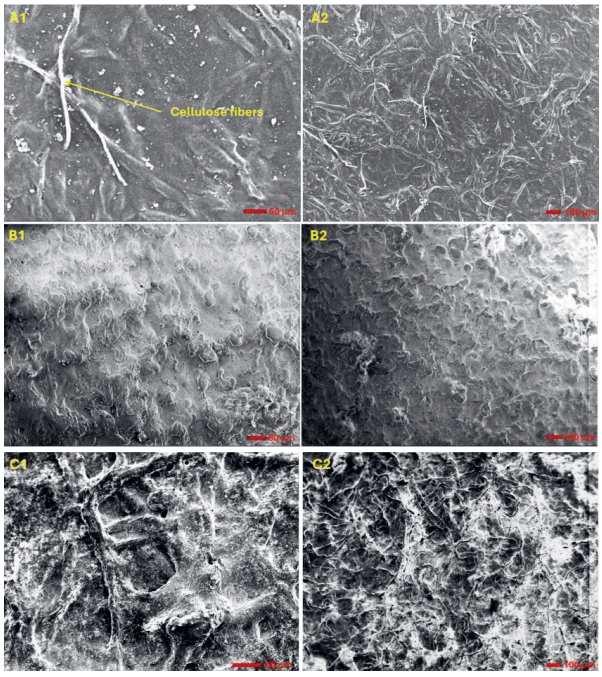

Figure 4.S2: SEM images of CS, PVA, and CS/PVA membranes after coating with graphene ink. Panels **(A1, A2)**, **(B1, B2)**, and **(C1, C2)** depict the surface morphologies of the CS, PVA, and CS/PVA membranes.

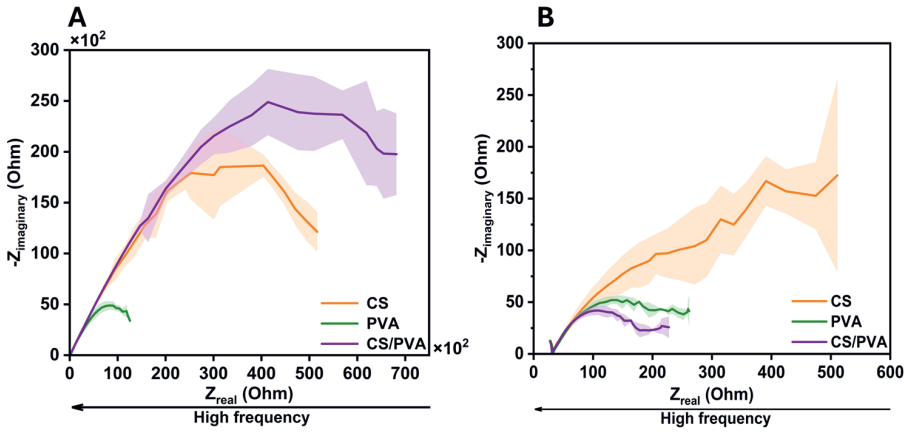

Figure 4.S3: Electrochemical impedance spectroscopy (EIS diagram) of CS, PVA and CS/PVA membranes. A - uncoated samples, B - ink coated samples (0.01V amplitude and 0.01 Hz frequency).Shaded area shows the standard deviation of the EIS values

Table 4. S1: Youngs modulus, tensile strength and elongation at break values of CS, PVA, and CS/PVA membranes

Membrane	Young's modulus (MPa)	Tensile strength (MPa)	Elongation at break (%)
CS	0.38 ± 0.23	1.28 ± 0.29	6.46 ± 2.47
PVA	0.07 ± 0.01	0.58 ± 0.04	11.43 ± 1.14
CS/PVA	0.33 ± 0.08	3.73 ± 1.30	12.22 ± 0.29

5

DESIGN OF ORIGAMI-INSPIRED PAPER BATTERIES AS A POWER SOURCE FOR SOIL MOISTURE SENSING SYSTEM

Parts of this chapter are based on:

Maya Moreshwar Meshram, S., Pande, S., (2025). Design of origami-inspired paper batteries as a power source for soil moisture sensing system. **(Submitted)**

5.1. INTRODUCTION

The increasing demand for eco-friendly and sustainable energy solutions has sparked increased interest in the development of biodegradable batteries (Juqu et al., 2022). In contexts such as remote agricultural or environmental monitoring, sustainable energy options such as MFC (especially SMFC) (Donovan et al., 2008) and small-scale batteries are ideal for powering soil moisture sensors. However the conventional batteries pose significant environmental hazards owing to their reliance on toxic components (Melchor-Martínez et al., 2021) and complex recycling processes (Y. Li et al., 2021). To address these challenges, research on alternative materials and designs for energy producing systems that are both efficient and environmentally friendly has intensified (Bertaglia et al., 2024). One promising approach to overcome this challenge is the development of paper-based batteries (Economou et al., 2018; Z. Rafiee et al., 2024). It is also easy to design the SMSS by combining the concepts of a MFC with a paper battery, as they can be self-powered with no need for external traditional batteries, are environmentally sustainable, low-cost, and capable of long-term moisture monitoring.

In SMSS, the SMFC can functions both as a power source and a primary sensor (Doglioni et al., 2024) because it generates electricity through the metabolic activities of soil microbes, which are directly affected by the soil's moisture level. In the SMFC, electrodes (i.e. anodes) are placed strategically deeper in the soil anaerobic layers and a cathode near the surface (Toczyłowska-Mamińska et al., 2025). When the soil is wet, microbial activity and ionic conductivity rise, leading to increased electrical output, whereas in dry conditions, both decrease, resulting in lower voltage (Nguyen and Nitisoravut, 2019). This characteristic makes the SMFC particularly suitable for the continuous monitoring of long-term soil moisture variations. The paper battery component serves as a rapid-response moisture indicator (Korotcenkov, 2023). When the soil is wet, the paper absorbs moisture and facilitates ionic conduction between electrodes, rapidly generating a voltage. In dry soil, the paper battery produces minimal or no output, making it ideal for swiftly detecting moisture changes. However, the limitation of conventional SMFCs is the low power output because of the distance between the cathode and the buried anode, soil resistance, and the electrode materials (Yu et al., 2017). These limits hinder their practical applications due to their complex installation and field operation (Hsu et al., 2017). In addition paper batteries have lower power which can be attributed to the limitations of electrochemical reactions, material degradation, and current manufacturing complexities (Juqu et al., 2022). Nevertheless, the power source, specifically the SMFC, can be directly integrated into paper via a paper battery utilizing papertronics, wherein electrical circuits are printed on paper for the design of SMSSs which can help to increases the power output and use SMFC for longer time. This is easy because SMFC and paper batteries work on same principle and they rely on similar electrode-based architectures, typically involving an anode and cathode, which can be made from compatible materials such as graphite or carbon felt, facilitating potential shared or hybrid electrode designs. Additionally, both systems depend on ion movement through an electrolyte medium soil in SMFCs and liquid or gel electrolytes in batteries suggesting the feasibility of integrated or co-functional electrolyte environments, especially in moisture-rich conditions. In addition, the structural properties of paper, such as rough and porous surfaces, facilitate ion and electron transportation through the entire structure to attain high power performance, distinctively within the electrode (Juqu et al., 2022). In addition the SMFC itself can be used as a soil moisture sensors, where the bacteria are used as living sensors (Nakamoto et al., 2024).

Paper as the primary substrate material for batteries offers advantages including porosity, permeability for water and electrolyte ions, adsorption capacity, abundance, cost-effectiveness, lightweight nature, and biodegradability (Khan et al., 2021; Pandey et al., 2022;

Peng et al., 2023; Thom et al., 2012; Yang et al., 2021). Paper facilitates fluid transportation through capillary action, eliminating the need for additional pumps (Shen et al., 2019). It also serves as a microfluidic channel that enables laminar electrolyte flow, which is crucial for battery efficiency and addresses electrode passivation (Shen et al., 2019).

Paper batteries are flexible, allowing them to be seamlessly molded into any desired form or dimensions without compromising their structural integrity (Agrawal et al., 2015). Hence, when divided in half, their energy output declines, however, when stacked, their power output is enhanced.

However, the durability of filter paper decreases under wet conditions (Fan et al., 2018). Using CS, the durability of the filter paper can be improved under wet conditions (700% increase in the tensile strength compared to when there is no CS coating) (Fan et al., 2018). CS is a slowly degradable biopolymer and is responsible for the sustainable power production (Karthikeyan et al., 2017). P. Yang et al. (2021) conducted research in which they reinforced hydrogel with cellulose paper for printable zinc batteries and paper electronics. By combining the characteristics of cellulose paper and hydrogel, the composite paper presented favorable mechanical and ion conductivity properties that are suitable for its function as a membrane and electrolyte in quasi-solid zinc batteries (Yang et al., 2021). These batteries exhibit high volumetric capacity (i.e. the amount of energy a battery can hold within a given space) and energy density (i.e. the amount of energy the device can store per mass or volume), which surpass those of other paper-based or thin-film energy storage units (R. Borah et al., 2020; Yang et al., 2021). They also reported that the printed micro batteries delivered limited areal capacity and volumetric energy density (up to ≈10 mWh cm^{-3}).

As previously noted, both SMFC and paper batteries operate on the same principle and utilize similar electrode-based architectures. The design of these systems is crucial and may involve configuring the entire paper battery in either a 3D or 2D format, or alternatively, designing the electrodes in 2D or 3D. However, limited research has been conducted on paper-based batteries, where either the entire battery is designed in a 3D form (Gao and Choi, 2017; Gonzalez-Guerrero and Gomez, 2019; Mohammadifar and Choi, 2018; Xu et al., 2015) or the electrodes are fabricated in 3D form (Chen and Hu, 2018). Researchers have used 3D paper electrodes for constructing battery. Xu et al. (2015) introduced a flexible 3D Si/C fiber paper electrode, synthesized through electro spraying of nano-Si-PAN clusters and electrospinning of PAN fibers, followed by carbonization for Li-ion batteries. The electrode exhibited a capacity of 1600 mAh g−1 and excellent cycling stability with capacity loss below 0.079% per cycle over 600 cycles. Gonzalez-Guerrero and Gomez (2019) developed a 3D alkaline Zn/Fe_3O_4 origami battery using printed wax for hydrophobic and hydrophilic barriers. The 3D battery, shaped like a boat, comprised of two screen-printed Zn/Fe_3O_4 batteries in series. It used 6M KOH electrolyte, activated by water through dry KOH redissolution. The battery achieved a current of 22 mA and a power output of 7.5 mW, demonstrating the potential of 3D origami-based Zn/Fe_3O_4 batteries as energy sources. Cho et al. (2015) introduced hetero-nanonet (HN) rechargeable paper batteries using cellulose nanofibrils (CNFs) and multiwall carbon nanotubes (MWNTs) electrodes. These provided a 3D bicontinuous electron/ion transport pathway, enhancing electrochemical performance and flexibility. HN paper batteries achieved an energy density of 226 Wh kg^{-1}. Mohammadifar et al. (2018) developed a scalable 3D biobattery stack using origami techniques. A 2D paper sheet with functional components was folded to form nine 3D MFC. Pseudomonas aeruginosa PAO1 was introduced into areas that formed the MFCs. The biobattery stack generated a maximum power of 20 µW and current of 25 µA. Wang et al. (2018) introduced a design for lithium metal batteries (LMBs) using nanocellulose fibers (NCFs). They created a 3D porous conducting cellulose paper (CCP)

current collector by combining NCFs with carbon nanofibers. The porous CCP structure enabled dendrite-free lithium deposition. Lithium electrodes were formed by electrodeposition on CCP substrates. The LMB showed excellent cycling stability, retaining 91% capacity after 800 cycles and 85% after 1000 cycles at 2 C (L. Wang et al., 2023) (1.27 mA cm^{-2}).

These studies have used complex shapes to design the battery that require multifold folding and bending of the paper. This folding and bending can induce stresses folding and bending can cause stress, leading to wear and possible failure over time (Song et al., 2014). Complex folding patterns might cause energy loss, affecting battery performance (Mohammadifar et al., 2016b). In addition, the production of these batteries needs precise techniques, which can make mass production difficult (Chen et al., 2014). In addition, adding these batteries to current SMSSs can be difficult because of their complex shapes and folding patterns (Song et al., 2014). Additionally, the positioning of the cathode in complex 3D configurations is difficult, as both the orientation and surface area of the cathode are crucial determinants of power output performance (Dziegielowski et al., 2022; Papillon et al., 2021). One significant challenge associated with 3D configuration is the storage of liquid compounds, which serve as electrolytes within the hollow spaces of the batteries. There is a risk of leakage if the 3D paper batteries are not sealed adequately. Furthermore, the replacement of these compounds becomes problematic once they are fully depleted. Integrating complex 3D paper batteries into SMSSs presents significant challenges, particularly in embedding wireless tags, which are integral components of SMSSs. Additionally, managing the orientation of these wireless tags poses a considerable challenge. Hence there is a need to design 3D paper battery that should facilitate the storage of catholyte, ensure optimal orientation of the cathode and wireless tag, allow for modifications to the cathode's surface area, enables easy stacking, and can easily be integrated into SMSSs, all while maximizing power output.

Alternatively, a 2D paper battery utilizing MFC technology may also offer a viable solution to the aforementioned challenges while also generating energy. Several studies have explored the use of 2D designs for energy production applications. Shimohata, Nakamoto, and Taguchi et. al. (2023) developed a 2D vertical MFC employing Bokuju (drawing ink used in Japan) and smoked charcoal. This configuration indicates that the vertical arrangement enhances both the installation process and the electrode replacement. Nguyen, Nguyen, and Taguchi (2022) employed multiwalled carbon nanotube paper for SMFCs, demonstrating that these systems can be activated on demand by insertion into wet soil. They found that a cathode floating on water outperformed a non-floating cathode. Chang et al. (2020) developed a novel biochar air cathode utilizing the naturally porous structure of Balsa wood chips, concluding that biochar chips can be used to create binder-free air cathodes, which exhibited a 45% increase in power density compared to carbon felt cathodes. Md Khudzari et al. (2019) utilized biochar granules as an anode, demonstrating that biochar can serve as an electrode in place of carbon felt in MFCs, provided that its electrical conductivity is enhanced (Li et al., 2016). The 2D design can be utilized for extended periods because of the availability of oxygen in the environment, which serves as an electron acceptor. In addition, the 2D design can be easily integrated with wireless tags in SMSSs. However, none of the aforementioned studies have incorporated the biodegradable polymer CS alongside cellulose filter paper in the design of 3D or 2D paper battery structure. Moreover, no research has yet investigated the impact of crosslinking on the performance of paper batteries, despite evidence suggesting that crosslinking enhances dimensional stability, electrolyte uptake, wet strength, and ionic conductivity (Davis et al., 2024; Selinger et al., 2024; Zeng et al., 2022).

The primary objective of this research is to assess the feasibility of integrating the SMFC as both a power source and a sensor within the framework of paper batteries. This

integration aims to facilitate the development of SMSSs by employing a 3D paper battery structure incorporating origami techniques and biopolymers. In addition, a 2D paper battery structure was also evaluated. The study involved testing the performance of the prepared 3D biodegradable paper battery using a potassium ferri/ferrocyanide redox couple. Additionally, the research aimed to examine the effects of crosslinking and cathode placement on the battery's performance using methodologies such as CV, OCP, chronoamperometry, and electrochemical impedance spectroscopy. Furthermore, a 2D air cathode paper battery was designed using a CS membrane, and its performance was tested under fully saturated soil conditions. This study seeks to contribute to the development of more environmentally sustainable off-grid energy producing solutions that align with environmental sustainability goals and can serve as power sources for small devices in the agricultural sector.

5.2. MATERIALS AND METHODS

5.2.1. EQUIPMENT AND CHEMICALS

All chemicals utilized were of analytical grade and employed without additional purification. Cellulose filter paper, designated as #610, with a diameter of 7.5 cm, grade5, was procured from Ahlstrom (Helsinki, Finland). CS, which is characterized by a high molecular weight, was obtained from Sigma-Aldrich. Conductive ink containing graphene was sourced from FWG Limited, United Kingdom. Both Potassium Ferricyanide and Potassium Ferrocyanide were supplied by Sigma-Aldrich, which also provided Sodium Hydroxide. MiliQ water was employed for the preparation of solutions. A Squidstat potentiostat was utilized for conducting OCP, chronoamperometry, and CV tests, while an Autolab potentiostat was used for executing electrochemical impedance spectroscopy (EIS). The thermal stability of CS membrane was investigated using thermogravimetric analyzer (TGA, Netzsch STA 409 C/CD) instrument under argon (Ar) atmosphere, in the range of 25 °C - 600 °C and heating rate was 20 °C min^{-1}.

5.2.2. COLLECTION OF SOIL SAMPLES

For this study, soil specimens were extracted from the grounds of Delft University of Technology in South Holland, Netherlands as it is shown that the exo-electrogenic bacteria exist in soils of different land types, including arid farmlands, woodlands, grasslands, paddy fields, lakeshore, and coastal areas, accounting for 0.26% - 7.70% of total bacterial abundance (Jiang et al., 2016; Rumora et al., 2024, 2023; Jun Wang et al., 2019). The aforementioned studies demonstrate that these bacteria are present in soil regardless of location, soil type, contamination in the soil, and soil classification. However, to enhance the performance of SMFC, the presence of compost in soil was found to augment microbial activity and electricity generation, suggesting that soil amendments can improve SMFC performance without the need for external bacterial addition (Gagliardi et al., 2024) Consequently, a small quantity of compost is incorporated into the soil for conducting the experiments. Also, in the aforementioned studies, it was observed that soil samples were extracted from depths ranging from 0 to 50 cm. The extraction process involved collecting samples at a depth 10 cm below the surface. The soil was then turn into mud by adding tap water and then subsequently passed through a 2 mm sieve to achieve particle homogeneity (Li et al., 2016). In SMFC, exoelectrogenic bacteria, such as Geobacter species, adhere to the anode embedded in anaerobic soil. These bacteria migrate towards the electrode in response to electrochemical gradients, subsequently forming a biofilm on its surface. This process involves the utilization of structures such as pili, adhesion proteins, and extracellular polymeric substances (EPS) (Rumora et al., 2023). To expedite the process of bacterial attachment, bacteria from Plant-e

(Wageningen University) were applied to the anode side. However, the primary application of this SMFC system is intended for the agricultural sector, where the compost will be used by the farmers for the growing their crops. Hence, 10% of organic compost was incorporated into the soil, serving as a source of microorganisms for the operation of the SMFC in addition to bacteria from Plant-e.

5.2.3. PRODUCTION OF THE BATTERIES

5.2.3.1. MEMBRANE PREPARATION

An aqueous solution of CS at a concentration of 2% (w/v) was prepared by dissolving 4 g of CS in 200 mL of an acetic acid aqueous solution containing 2% v/v. The mixture was stirred for 12h at room temperature at 1000 rpm. To make the solution thinner, 150 mL of acetic acid was added to the previously prepared solution, and the mixture was stirred for another hour. The solution was then filtered and stored at 4 °C for 24 h. Afterward, a filter paper was fashioned into the 3D shape depicted in the Figure 5.1 (A). The incorporation of 3D shapes in battery design presents a methodology for enhancing the areal energy density by decoupling the electrode thickness from the ion-transport distance. This geometric configuration enables more efficient utilization of materials without increasing the ion transport distance. Optimization of the electrode spatial configuration might improve the battery performance, resulting in improved power and energy densities. This approach increases the capacity per unit area (i.e. the amount of charge a battery can store per unit area of the electrode) (Arandhakar et al., 2024) by utilizing vertical space and enhances the performance through expanded active surface areas and improved electrolyte infiltration, thereby leading to greater overall efficiency. Moreover, the design flexibility afforded by various substrate geometries facilitates the optimization of battery performance and integration into diverse devices (J. Ma et al., 2024; Miyamoto, 2024; Miyamoto et al., 2020; Roberts et al., 2011).

Subsequently, the CS solution was poured onto a filter paper, which was laid horizontally on a steel plate. The filter paper along with CS solution was left at room temperature for 24 h, allowing the CS solution to permeate through the filter paper and dry completely. Subsequently, the filter paper was turned upside down and the CS solution was poured onto it again. The filter paper was then left to sit at room temperature for an additional 24 h, enabling the CS solution to seep thoroughly into the filter paper. The filter paper was then dehydrated at 60 °C for 6 h. The dry weight of the membrane was then measured to determine the amount of solution that had been absorbed by the filter paper.

The membrane was neutralized with 2M NaOH for 5 min and washed with Milli-Q water. It was then crosslinked by immersion in 0.5M H_2SO_4 for 24 h at room temperature. To remove excess crosslinking agent, the membrane was dipped in Milli-Q water and allowed to dry for 24 h at room temperature.

5.2.3.2. PROPERTIES OF CS MEMBRANE

The various properties of the biodegradable CS membrane, as prepared using the method detailed in Section 2.3.1, are presented in Table 5.1 and is adopted from the previous work (Meshram et al., 2025b). Understanding the properties outlined in Table 5.1 is crucial, as they have a significant impact on the system's efficiency, stability, and viability (Banerjee et al., 2022). These property values are dependent upon the membrane's applications. In the context of SMFC and paper batteries used in the design of SMSSs, a higher water retention capacity is advantageous for maintaining consistent operation despite variations in moisture

levels. The swelling ratio, which indicates membrane expansion during water absorption, must be regulated to ensure durability in environments with varying mechanical stress. The ion exchange capacity, indicative of proton transport ability, is directly correlated with electrical performance; therefore, to achieve increased current production, it should be enhanced. A low oxygen transfer coefficient is essential for anaerobic electron acceptors, such as NO_3^-, as it prevents oxygen diffusion through membranes and supports the reduction reaction of NO_3^- used in 3D batteries. The contact angle reflects membrane wettability, with more hydrophilic membranes (characterized by a low contact angle) promoting better microbial adhesion and proton transport, thereby enhancing SMFC power generation. Furthermore, the membrane should exhibit lower fouling and degradation rates to ensure longevity (Banerjee et al., 2022; Jenani et al., 2024).The contact angle property of the membrane can be adjusted according to the specific application in which the membranes are utilized, as outlined by (Cherian et al., 2022).

Table 5.1: Properties of CS membrane used in the construction of paper battery

Properties	**Water Uptake (%)**	**Swelling ratio (%)**	**Ion exchange capacity (meq/g)**	**Proton conductivity (µS/cm)**	**Oxygen diffusion coefficient (cm^2 /s)**	**Contact angle (^{0})**	**Degradation rate (%) after 100 days**
CS coated with graphene ink	59.62	1.50	0.61	735.5	0.142×10^{-5}	c.a. 82.5	2.00

5.2.3.3. PAPER BATTERY PREPARATION

5.2.3.3.1. 3D BATTERY

In Section 2.2.1, a membrane was prepared using filter paper, which was subsequently shaped into a 3D cubic form using the origami technique and superglue, as illustrated in Figure 5.1 (E). A mixture of water-resistant graphene conductive ink and CS polymer (1:1, w/w) was prepared. The electrodes were fabricated using water-resistant graphene ink owing to its superior conductivity, larger specific surface area, and enhanced pore structure. Furthermore, graphene contributes to improved electrode stability in terms of both the structure and composition (Li et al., 2023). The mixture was stirred for 24 h at 200 rpm using a magnetic stirrer. A 1:1 mixture was applied to the three sides of the paper battery, namely surfaces 4, 5, and 6, using a hand brush in five coating layers to facilitate proton movement through the surface and increase the durability of the paper.

A conductive ink layer is essential to enable paper batteries to store and transmit electrical charges. This is because cellulose, the primary component of paper, is non-conductive and electrochemically inactive (Isacsson et al., 2024). Hence, surfaces 1, 2, and 3 of the paper battery were coated with water-resistant graphene conductive ink, which functioned as an electron carrier and served as the anode. The coating was performed on the outer surface because printing electrode inks on both sides may cause the battery to short-circuit owing to the rough and permeable surface of the paper (Yang et al., 2021).

A graphite felt cathode, measuring 4 cm x 4 cm x 0.3 cm, was also prepared for the battery and utilized as the cathode. The total active area of the anode (surfaces 1, 2, and 3) is 16 cm^2, whereas the total surface area of the cathode is 36.8 cm^2. Also, the cathode were placed in different position to see the effects of the cathode placement on the performance of the 3D

paper battery, as previous studies has shown that the position of cathode affects the performance of the battery (Lee and Huang, 2013).

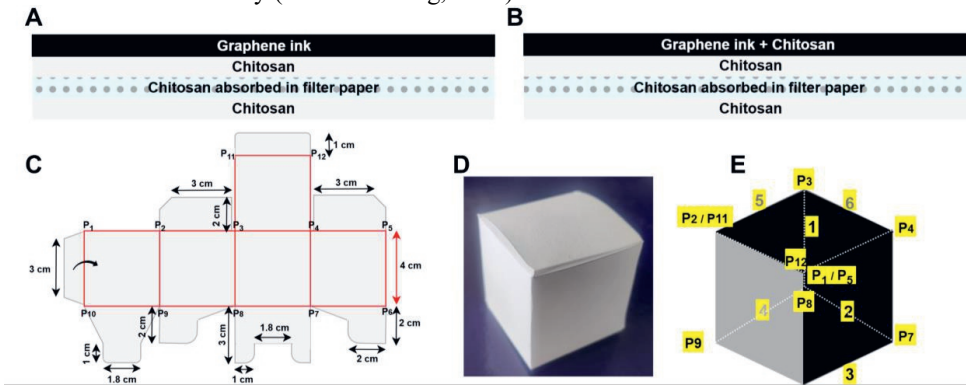

Figure 5.1: (A) Cross-section of the electron conductive electrode acts as anode i.e. surfaces 1,2,3, (B) Cross-section of the proton conductive surface i.e. surfaces 4,5,6, (C) Dimensions and folding pattern of origami structure is shown, where solid red lines represent the valley folds with 40 mm length of 3D paper battery, (D) Final shape of the prototype after folding, (E) 3D model of paper battery designed using origami technique after coating, where "P" represents the various points used for folding .

Figure 5.2 depicts the configuration of the electrode setup, which comprises three cathodes: two vertical (2V) positioned at the back and left side, and one horizontal (1H) situated at the bottom, with all three cathodes interconnected. In contrast, the setup designated as 1H employs only the bottom electrode. Henceforth, 2V1H will refer to the three electrode configuration, while 1H will denote the single horizontal electrode setup. Figure 5.2 also provides detailed dimensions of the cathode and indicates the specific locations where the cathode was folded to facilitate its integration into the paper battery.

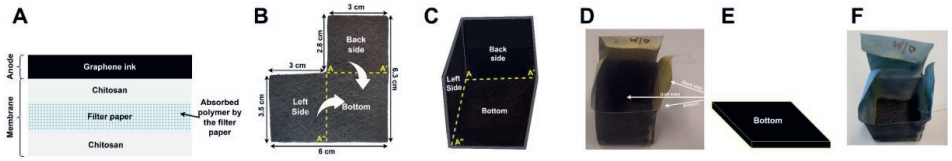

Figure 5.2: Configuration for 3 electrode (2V1H) setup: **(A)** Cross section of anode, **(B)** Dimensions of the cathode, **(C)** Folding of the cathode in 3 cathode setup, **(D)** 3 cathode placement inside the paper battery, **(E)** 1 horizontal cathode, and **(F)** 1 horizontal cathode placement inside the 3D paper battery

Figure 5.3 shows the reactor setup for testing the 3D paper battery using potassium ferro/ferricyanide and moist soil/potassium ferricyanide as anolyte and catholyte respectively. The first set up as shown in Figure 5.3A used potassium ferrocyanide as anolyte and potassium ferricyanide as catholyte. Potassium ferrocyanide functions as an electron donor by undergoing an oxidation reaction within the anolyte compartment and on the anode surfaces. The electrons generated then travels through the external circuit and reach the catholyte chamber, where they encounter the cathode. In the presence of potassium ferricyanide within the catholyte chamber, these electrons are accepted through a reduction process (Koç et al., 2021). In Figure 5.3B,

moist soil functions as an anolyte, wherein bacteria oxidize organic matter present in the soil, thereby releasing electrons. These electrons subsequently travel towards the cathode through an external circuit, where potassium ferricyanide present in catholyte chamber is reduced by accepting the electrons.

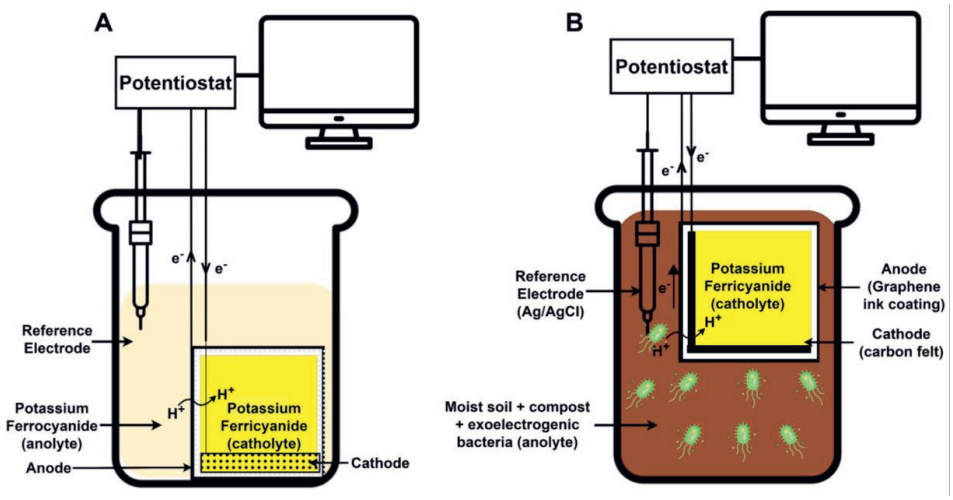

Figure 5.3: Reactor setup for testing 3D paper battery **(A)** in potassium ferro/ferricyanide **(B)** in moist soil/potassium ferricyanide

Initially, electrochemical investigations were conducted to evaluate the influence of crosslinking on the membranes, employing a single horizontal electrode configuration within a 3D paper battery setup as shown in Figure 5.3A. The potassium ferro/ferricyanide redox couple was used in this setup. Subsequently, electrochemical analyses were performed to investigate the effect of cathode orientation with crosslinked membranes, initially utilizing a configuration of 3 cathode (2V1H) setup, followed by a 1 horizontal cathode setup in the potassium ferro/ferricyanide redox couple. Finally, electrochemical studies were conducted using 3 cathode , with crosslinked membranes under moist soil conditions, as depicted in Figure 3B. Further electrochemical studies were conducted to evaluate the electron acceptors, potassium ferricyanide and oxygen, using a 3 cathode setup. In these studies, the anode was exposed to moist soil, while the cathode was initially exposed to potassium ferricyanide. Subsequently, the potassium ferricyanide was removed from the catholyte chamber, and the cathodes were exposed to oxygen to assess the effect of the electron acceptor in moist soil.

5.2.3.3.2. 2D BATTERY

The 2D air-cathode configuration is the most practical and extensively utilized cathode design in MFCs. This configuration effectively addresses the challenges posed by the low solubility of oxygen in water, thereby facilitating the attainment of higher current densities (Chen et al., 2018). Also, the vertical design of the battery ensures contact between the cathode electrode and the air, easing the installation of the device and the replacement of the electrode (Shimohata et al., 2023). Schematic representation of the 2D air cathode paper battery is shown in Figure 5.4.

The anode was prepared using graphene conducting ink because reducing the distance between soil and anode results in the decrease of remediated medium quantity. The cathode

composed of carbon felt was employed as an air cathode due to its porous structure, which enhances the electrochemically active surface area and facilitates improved oxygen reduction reactions (ORR) (Kosimaningrum, 2018), good electrical conductivity, and lower cost (Deng et al., 2010).Titanium wires were used to connect anode and cathode.

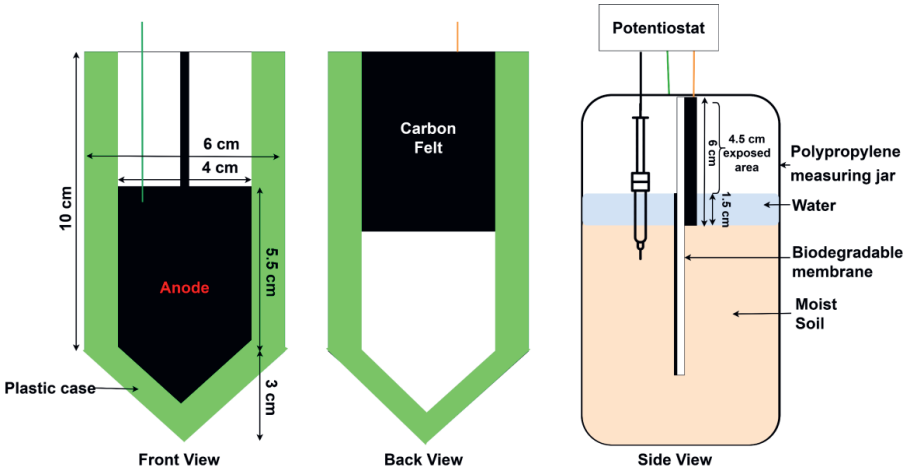

Figure 5.4: Schematic representation of the 2D air cathode paper battery showing the front, back, and side view

5.2.4. ELECTROCHEMICAL CHARACTERIZATION OF PAPER BATTERY

To evaluate the performance of the 3D paper battery prepared in Section 2.3.2.1 (Figure 5.3) was tested for using electrochemical experiments under crosslinked and non-crosslinked conditions. OCP (i.e. the potential difference between two electrodes in an electrochemical cell when no current is flowing), electrochemical impedance spectroscopy (EIS), and CV, were performed to assess the electrochemical stability of the system under study.

The experiment utilized a three-electrode setup consisting of working (anode), reference (Ag/AgCl,3M KCl), and counter electrodes (carbon felt) submerged in potassium ferrocyanide electrolyte as shown in Figure 5.3. For OCP, the potential was tracked for a predetermined period without applying any external current to the system, ensuring accurate determination of the natural equilibrium potential of the working electrode. CV experiments were performed to examine the cyclic redox behavior and electrochemical characteristics of the system. The potential was swept between the 0 and 0.8 V and at different scan rates, and data were collected using a potentiostat. The resulting data were evaluated to determine crucial parameters, including the peak current, peak potential, and reversibility of the redox reactions. Electrochemical Impedance Spectroscopy (EIS) was performed to evaluate the electrochemical properties of the system. Impedance spectra were recorded over a frequency range of 0.01 Hz to 100 kHz, with an AC amplitude of 0.01V with frequency decreasing from left to right. Nyquist plots were constructed by plotting the real part (Z′) of the impedance against the negative imaginary part (−Z′). The high-frequency semicircle is attributed to the charge transfer resistance (R_{ct}) and double-layer capacitance at the electrode-electrolyte interface. The low-frequency linear tail is associated with diffusion-controlled processes and is often described using the Warburg impedance as shown in Figure 5.5A. The Bode plots as shown in Figure

5.5B represent the impedance magnitude |Z| and phase angle (ϕ) as functions of the logarithmic frequency. All the above experiments were performed at room temperature.

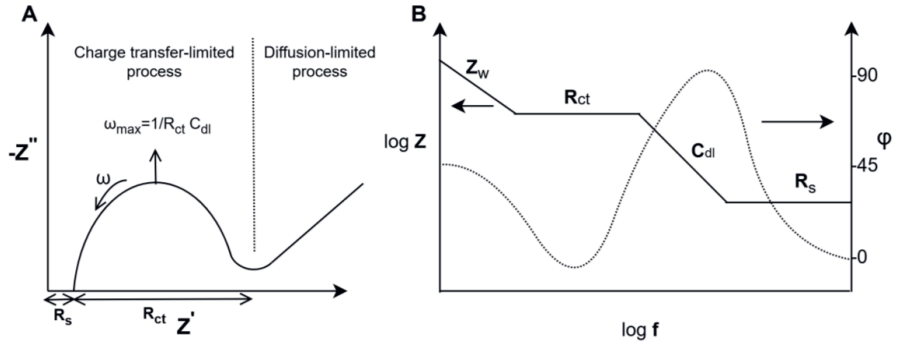

Figure 5.5: (A) Nyquist plot and **(B)** Bode plot; ω=2πf is angular frequency, R_s is solution resistance, R_{ct} is charge-transfer resistance, C_{dl} is double-layer capacitance and Z_w is infinite diffusion Ref: (Mohd Said, 2014).

First, OCP was measured for 18 h. Then the CV were performed, followed by the potentiostatic electrochemical impedance spectroscopy (EIS) test at a frequency range from 100 kHz to 0.1 Hz and an amplitude of 0.01 V. The reactions occurring at the anode and cathode are (Koç et al., 2021; Logan et al., 2006).

Oxidation reaction (at anode): $[Fe(CN)_6]^{4-} \rightarrow [Fe(CN)_6]^{3-} + e^-$ .....(1)

Reduction reaction (at cathode): $[Fe(CN)_6]^{3-} + e^- \rightarrow [Fe(CN)_6]^{4-}, E^0 = 0.361$ V vs SHE .....(2)

Whereas the reactions occurring at the anode and cathode in soil are (Kacmaz and Eczacioglu, 2024) .

Oxidation reaction (at anode): $(CH_2O)_n + H_2O \rightarrow CO_2 + H^+ + e^-$ .....(3)

Reduction reaction (at cathode) :

a) for 3D paper battery – $[Fe(CN)_6]^{3-} + e^- \rightarrow [Fe(CN)_6]^{4-}, E^0 = 0.361$ V vs SHE .(4)

b) for 2D paper battery – $O_2 + H^+ + 4e^- \rightarrow 2H_2O$ ..... (5)

5.3. RESULTS AND DISCUSSION

5.3.1.TGA ANALYSIS FOR CROSSLINKED MEMBRANE

In the case of a 2D paper battery, the section of the battery situated above the soil is exposed to environmental conditions, resulting in temperature variations between the portions above and below the soil. Consequently, it is essential to assess the thermal stability of the membranes. Figure 5.6 shows the TGA curve of CS membrane coated with graphene ink adopted from (Meshram et al., 2025b). It shows that at about 100 °C, the weight loss was about 1.5 % which could be concerned with the loss of free water in the molecules. A significant mass loss occurred at about 235 °C, indicating the beginning of degradation, which was concerned with the loss of amino and hydroxyl groups in the CS membrane (Yang et al., 2018). At about

410 °C, the weight loss was about 70% and the rate of degradation decreased due to the rigid and regular ring structure of CS (Yang et al., 2018). From the TGA curve, it can be seen that the membrane investigated was stable below 100 °C.

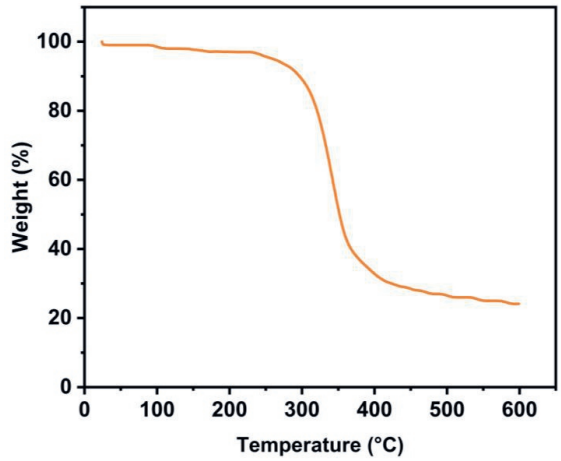

Figure 5.6: TGA curve for CS and crosslinked membrane

5.3.2. OCP FOR 3D PAPER BATTERY PREPARED USING CROSSLINKED AND NON-CROSSLINKED MEMBRANE

The OCP vs. time behaviour of the crosslinked and non-crosslinked paper-battery samples is shown in Figure 5.7. It has two curves, one representing crosslinked samples (black) and one representing non-crosslinked samples (red). Non-crosslinked curves initiated at c.a. 0.195 V, whereas the crosslinked curves were initiated at 0.18V.

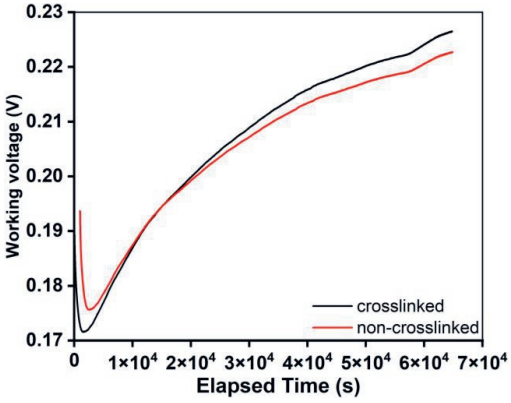

Figure 5.7: OCP for paper batteries prepared using crosslinked and non-crosslinked membrane

As can be seen, the potential first decreased in samples and approached a minimum value. Subsequently, it gradually increased to ~ c.a. 0.22 V for the non-crosslinked and c.a. 0.225 V for crosslinked at the end of exposure time of 18 h. First decrease in OCP c.a. 0.172 V

(crosslinked) and ~ 0.176 V (non-crosslinked) can be attributed to the removal of the air-formed oxide film on the electrode surface (Salahinejad et al., 2013), as well as to the transient phenomenon associated with stabilization or initial equilibration. Then, there was an increase in the OCP with time after passing through the minima, where a new surface film might have developed. This increase reflects the stabilization and potential development of the electrochemical properties of the material under open-circuit conditions. The crosslinked membrane exhibits a lower OCP compared to non-crosslinked membranes until approximately 1.45 x 10^4 seconds (i.e., 4 hours). Subsequently, the OCP increases continuously. This observation suggests that crosslinking enhances the performance of the material by increasing voltage after the initial phase. The disparity becomes more pronounced as time progresses, indicating that crosslinking enhances the stability or efficiency of the system over time. Crosslinking is likely to improve the structural integrity or electrochemical properties of the material, resulting in enhanced voltage output and stability in the system. The graph elucidates the beneficial effects of crosslinking on performance over time.

5.3.3. EIS FOR 3D PAPER BATTERY PREPARED USING CROSSLINKED AND NON-CROSSLINKED MEMBRANE

Figure 5.8A and 5.8B shows Nyquist plots (left panels) and Bode plots (right panels) for crosslinked and non-crosslinked paper batteries plotted using electrochemical impedance spectroscopy (EIS) data respectively. In Figure 5.8A the Nyquist Plots (Left Panels) depict the real impedance (Z′) on the x-axis, and imaginary impedance (−Z″) on the y-axis (Laschuk et al., 2021; Mei et al., 2018). A semicircular arc was observed at lower Z′ values, representing the charge-transfer resistance (Rct). The linear portion at higher Z′ in the crosslinked region indicates Warburg impedance, which is associated with ion diffusion within the battery. The arc for the crosslinked system is smaller, indicating a lower charge transfer resistance, suggesting improved ionic conductivity or enhanced electrode-electrolyte interactions. The Rct value for the crosslinked sample was c.a. 1000 Ohms. For the non-crosslinked system, similar trends are observed, however, the semicircular arc is larger than that in the crosslinked system, implying a higher charge transfer resistance, which is c.a. 2300 Ω, likely due to reduced structural integrity or less effective ionic transport in the absence of crosslinking.

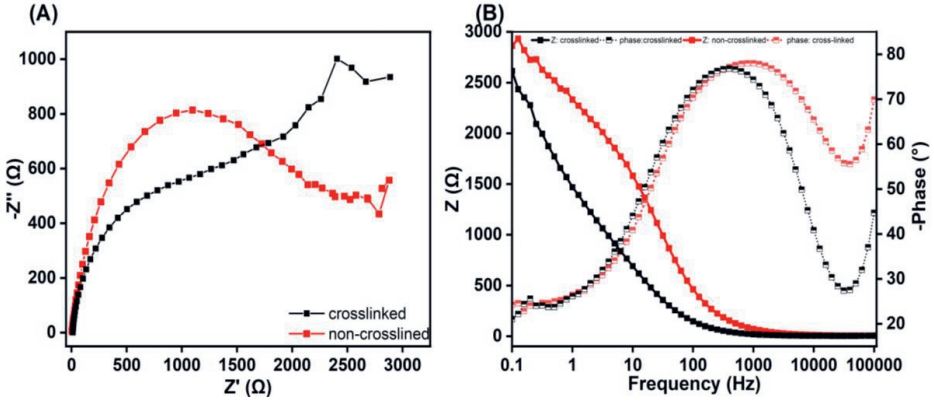

Figure 5.8: Nyquist plot **(A)** and Bode plot **(B)** for paper batteries

Figure 5.8 (B) shows the Bode Plots in which the impedance magnitude (Z) is shown on the left y-axis, the phase angle (ϕ) on the right y-axis, and the frequency (in Hz) on the x-axis (log scale). The phase angle attains a maximum at intermediate frequencies (c.a. 500 Hz),

indicating the predominant relaxation process associated with charge transfer. The magnitude of impedance for the crosslinked film is lower than that of the non-crosslinked film, which shows higher conductivity. The phase angle in the case of crosslinking was lower c.a. -30° compared of the non-crosslinked c.a. -55°. This difference suggests less efficient charge transfer and slower ion dynamics owing to the absence of crosslinking. In conclusion, crosslinked paper batteries demonstrate superior electrochemical behavior, rendering it a more effective for paper batteries.

5.3.4. CV FOR 3D PAPER BATTERY PREPARED USING CROSSLINKED AND NON-CROSSLINKED MEMBRANE

Figure 5.9 presents CV curves, which are electrochemical measurements utilized to investigate the redox behaviour and electrode properties of the paper battery for crosslinked and non-crosslinked configuration.

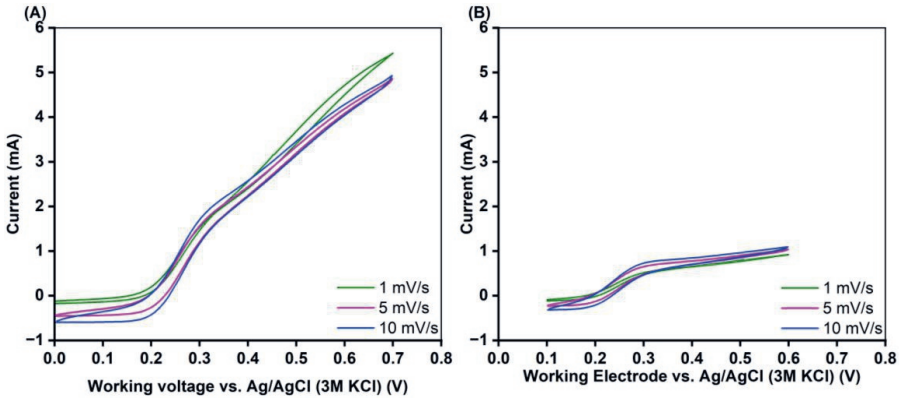

Figure 5.9: Cyclic voltammetry of paper batteries for various scan rates 1,5 and 10 mV/s, **(A)** crosslinked **(B)** non-crosslinked, voltage range 0 to 0.8 V.

In case of the crosslinked system, the current increases significantly with increasing voltage, reaching 5.5 mA at 0.7 V, demonstrating electrochemical oxidation activity. The curves are well defined and vary with the scan rates (1, 5, and 10 mV/s). Whereas, in non-crosslinked system, the current response was substantially lower than that of the crosslinked batteries, and the curves were less distinct across scan rates, as shown in Figure 5.9 (B). The maximum current reached at 0.6 V is c.a. 1 mA. Reductive current was observed at c.a. 0.17 V whereas an oxidation peak was observed at c.a. 0.28 V. It can be concluded that the crosslinked electrode exhibited enhanced electrochemical activity and improved conductivity, stability, and active surface area, enabling a higher current response. This observation indicates that the absence of crosslinking reduces the electrochemical activity of the material, likely due to poor conductivity, reduced surface area, or limited electron transfer pathways. Additionally, the nearly overlapping curves suggest slower kinetics or a less efficient charge transfer. Therefore, it can be concluded that crosslinked paper batteries exhibit a significantly higher current, indicating superior performance in terms of electron transfer and redox activity. Ultimately, it can be concluded that crosslinking is crucial for enhancing the electrochemical properties of the paper battery under investigation, owing to the improved current response, kinetics, and redox activity.

5.3.5. CV FOR CATHODE PLACEMENT ACROSS VARIOUS CONFIGUREURATIONS AND SURFACE TREATMENTS USING CROSS-LINKED MEMBRANE

Figure 5.10 represents the CV for the set up with 3 electrodes (2V1H) and paper coated with ink + CS and without coating under multiple cycles, highlighting the effect of surface modification and coatings for crosslinked membranes. It was observed that the current increased significantly as the working voltage increased, and the current also decreased with the number of cycles (3 cycle < 2 cycle < 1 cycle). The peak current was approximately 61 mA at the highest working voltage (~2.9 V). No distinct oxidation peak was observed for coated samples, while a reduction peak was observed at c.a. 0.4 V for the 1st cycle. The maximum current peaks moved slightly towards a higher potential as the number of cycles increased. It is interpreted that the ink + CS coating enhances electrode performance, likely by improving conductivity, adhesion, and stability.

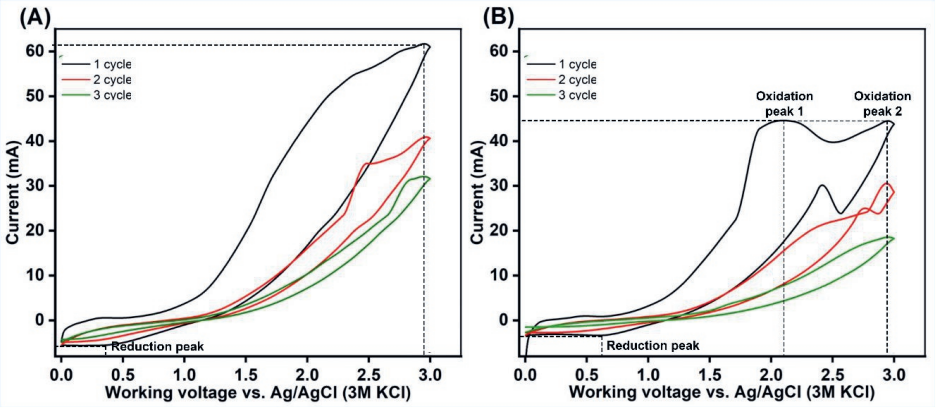

Figure 5.10: CV for 3 cathodes using cross-linked membrane : **(A)** coated and **(B)** uncoated

Figure 5.10 (B) shows that the current response is lower than that shown in Figure 5.10 (A). Two oxidation peaks were observed at c.a 2.1 V and c.a. 2.9 V. The maximum current observed was c.a.45 mA. The reduction peak was observed at 0.6 V. Here, the current also decreased as the number of cycles increased. The absence of a CS coating results in reduced electrochemical activity, likely owing to poor surface properties (e.g., lower conductivity or stability). Both systems exhibited activity across the same voltage range, but the higher current of the coated electrode implies improved kinetics or electron transfer efficiency. Hence, it is concluded that the ink + CS coating enhances the electrochemical performance, demonstrating its potential for improving electrode properties, such as conductivity, stability, and redox activity.

Figure 5.11 presents CV for 1 horizontal electrode setup and for two surfaces of paper battery coated with ink + CS and without coating under multiple cycles, highlighting the effect of surface modification and coatings for the crosslinked paper batteries. It is observed that the current increases significantly as the working voltage increases, also the current decreases with the number of cycles (3 cycle < 2 cycle < 1 cycle). The current reaches c.a. 40 mA at the highest working voltage (c.a. 3.0 V). Two oxidation peaks are observed first at c.a. 2.1 V and second at c.a. 2.7 V for the 1st cycle, whereas a reduction peak was observed at c.a. 0.5 V for

all the cycles. The oxidation peaks moved towards a higher potential as the number of cycles increased.

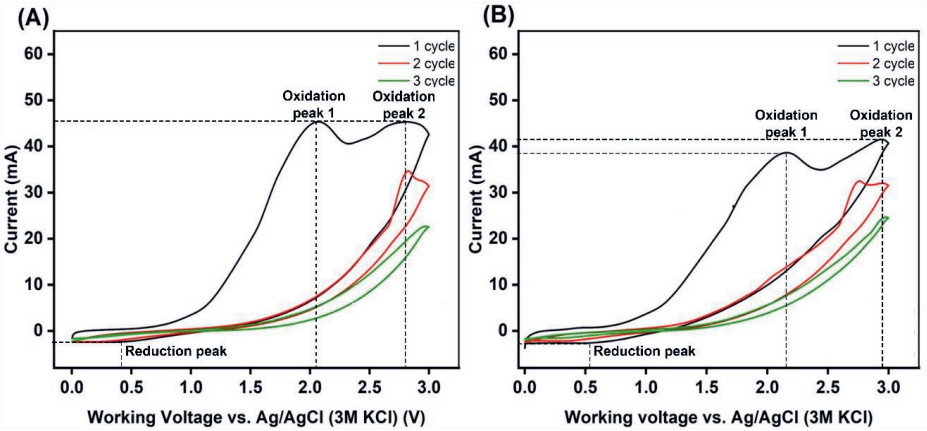

Figure 5.11: CV for 1 horizontal cathode using cross-linked membrane : **(A)** with ink + CS coating and **(B)** without coating

It was observed that the current response for paper battery without coating also shows two oxidation peak current of 39 mA and 41 mA at 2.2 V and 2.9 V respectively. The reached a current of 40 mA whereas in coated the current continuously increasing and reached the maximum current of 60 mA at 3 V. Here, the current also decreased as the number of cycles increased. The absence of a CS coating results in reduced electrochemical activity, likely owing to poor surface properties (e.g., lower conductivity or stability). Both systems exhibited activity across the same voltage range, but the higher current of the coated electrode implied improved kinetics or electron transfer efficiency.

In conclusion, membrane coatings can significantly enhance the performance of electrochemical systems. These coatings facilitated ion transport and stabilized the system over multiple cycles, thereby reducing energy losses and ensuring reproducibility. These findings validate the importance of surface modifications in optimizing energy storage devices and illustrate how material engineering can affect device performance. Based on these results, 3D design with 3 electrodes and membranes coated with graphene conductive ink was chosen for experiments with moist soils.

5.3.6. TESTING OF 3D PAPER BATTERY WITH 3 ELECTRODES IN MOIST (100% SATURATED) SOIL

5.3.6.1. OCP MEASUREMENT

Figure 5.12 presents the open-circuit potential (OCP) of a 3D paper battery configured with three electrodes under moist soil conditions, utilizing potassium ferricyanide as the electron acceptor over a period of approximately 70 hours prior to the introduction of acetate.

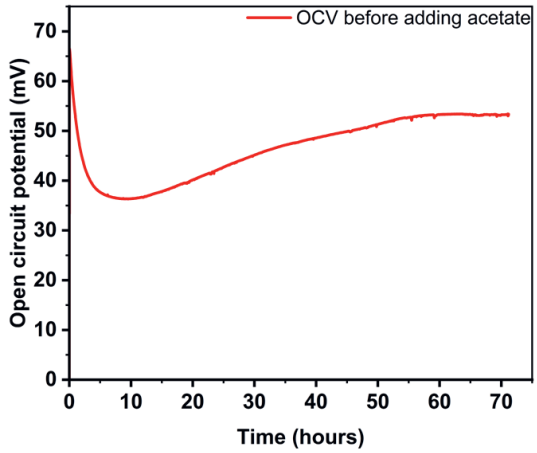

Figure 5.12: OCP of 3D paper battery using 3 electrodes in moist soil conditions

Initially, the OCP experiences a rapid decline from approximately 65 mV to nearly 36 mV within the first 10 hours. This swift reduction likely reflects early electrochemical adjustments on the electrode surface, such as the formation of a double layer, initial microbial attachment, or redox reactions occurring in the absence of a carbon source. Following this initial decrease, the OCP gradually increased over time, indicating a progressive stabilization of the system. This trend suggests the establishment of a quasi-equilibrium state, potentially due to the gradual formation of a biofilm or microbial community on the electrode surface in systems involving microbial activity. At approximately 60 hours, the OCP stabilizes at around 54–55 mV, signifying that the system has reached a relatively stable electrochemical state. This stabilized OCP serves as a baseline measurement before the addition of acetate, a common electron donor, which is expected to alter the potential due to enhanced microbial metabolic activity and electron transfer processes.

5.3.6.2. OUTPUT VOLTAGE ACROSS DIFFERENT EXTERNAL RESISTANCES

Figure 5.13 illustrates the output voltage profile of the 3D paper battery equipped with 3 cathodes in moist soil over a duration of approximately 150 hours, subjected to three distinct external resistances (1000 Ω, 560 Ω, and 220 Ω). The data indicate a continuous decline in performance over time. Initially, at 1000 Ω, the MFC generated a relatively higher voltage at 2 mV, which gradually decreased to 0.75 mV, likely due to substrate depletion or diminished microbial activity. When the resistance was reduced to 560 Ω, the voltage decreased more rapidly from 0.75 mV to 0.1 mV, suggesting that the system struggled to accommodate the increased current demand. In the final phase, with an applied resistance of 220 Ω, the voltage approached zero, indicating that the MFC could no longer sustain power generation under 220 Ω load conditions. This overall decline suggests a progressive weakening of electrochemical activity, potentially due to limited substrate availability, microbial inactivity, or increased internal resistance within the system.

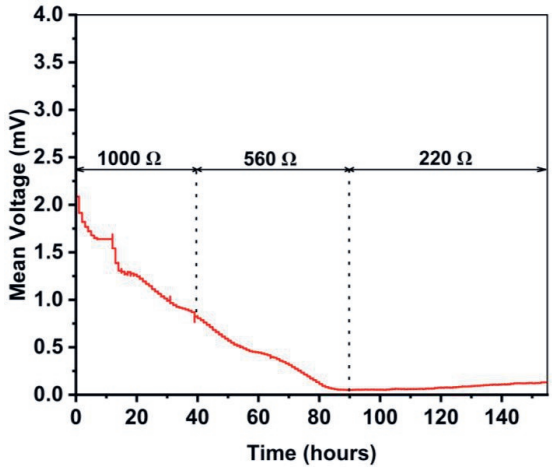

Figure 5.13: Output voltage of 3D paper battery using 3 electrodes across different external resistances.

5.3.6.3. CURRENT AND POWER DENSITY CURVES

Figure 5.14 presents the power and current density outputs of a system over approximately 150 hours, evaluated under three distinct external resistances: 1000 Ω, 560 Ω, and 220 Ω.

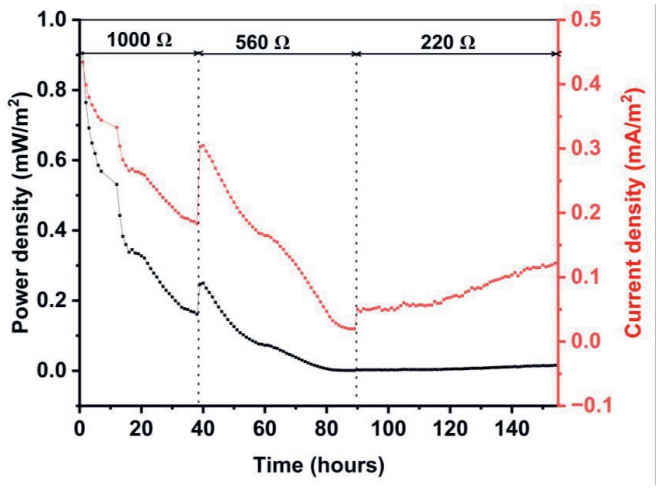

Figure 5.14: Current and power densities monitoring for 140 days across different external resistances

Initially, at a resistance of 1000 Ω, the MFC exhibits relatively high power of 0.8 mW/m^2 and current densities 0.4 mA/m^2. However, both metrics gradually decline, likely due to substrate depletion or reduced microbial activity. Upon reducing the resistance to 560 Ω, there is a sudden increase in power density and current density, but it both power and current densities is decreased as the time passes, indicating that the MFC struggles to accommodate the increased current demand, possibly due to limited electron availability or stress on the biofilm. In the final phase, at 220 Ω, the current density shows a slight improvement, while the power

density remains low. This suggests a minor recovery in microbial activity or electron transfer, yet the low voltage associated with the reduced resistance impedes efficient power generation. Overall, these patterns indicate a consistent decline in MFC performance under increased electrical load and prolonged operation, likely attributable to biological and electrochemical constraints within the system.

5.3.6.4. CV FOR 3D PAPER BATTERY WITH 3 ELECTRODES

CV curves depicted in Figure 5.15 illustrate the electrochemical performance of the cathode under three distinct conditions associated with the presence of the redox mediator potassium ferricyanide. Initially, when the cathode is immersed in a fresh ferricyanide solution (black curve), a pronounced redox response is observed, characterized by distinct anodic and cathodic peaks and elevated current levels, indicative of efficient electron transfer and active electrochemical reactions.

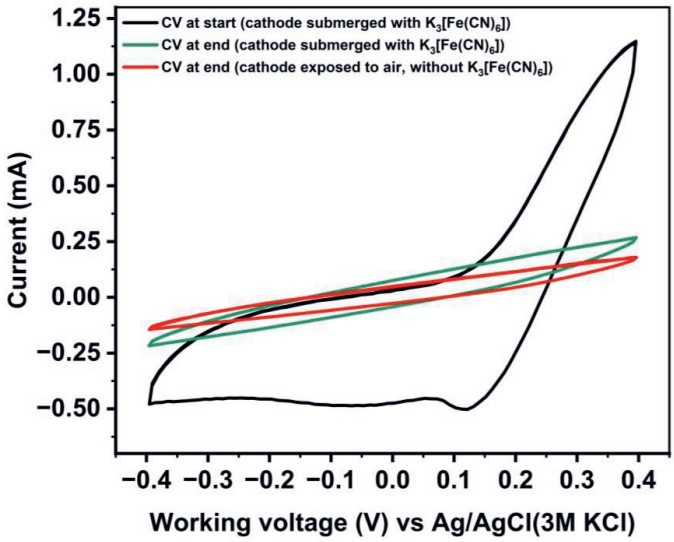

Figure 5.15: CV for 3D paper battery with 3 cathodes in moist soil

By the conclusion of the experiment, with the cathode still immersed in the same ferricyanide solution (green curve), the redox peaks are significantly diminished, suggesting a notable decline in electrochemical activity, likely attributable to mediator degradation, electrode fouling, or a reduction in reactive surface area. Finally, when the cathode is exposed to air in the absence of ferricyanide (red curve), the CV profile exhibits minimal current and lacks distinct redox peaks, reflecting poor electron transfer and limited oxygen reduction activity. This progression underscores the critical role of the ferricyanide mediator in maintaining cathodic performance and highlights how its degradation or absence results in reduced electrochemical efficiency.

5.3.7. FAILURE OF 3D PAPER BATTERY DESIGN

During the experimental procedures, it was observed that potassium ferricyanide migrated from the catholyte chamber to the anolyte chamber. This might have been caused by the CS membrane or due to weak bonding of the paper substrate. This migration has the

potential to impact both the structural integrity and the performance of the system (Sun et al., 2025), aspects which were not examined in this study. The inherent porosity of the paper facilitates ion movement but also permits electrolyte leakage. Such leakage could result in a short circuit between the electrodes (C. Zhang et al., 2022). These findings highlight the necessity for robust sealing, binder or coating techniques to enhance the stability and longevity of paper-based energy storage devices. An alternative approach to mitigate electrolyte seepage involves employing an air cathode 2D paper battery configuration, which utilizes naturally available oxygen in the environment as an electron acceptor instead of potassium ferricyanide in the design of the paper battery.

5.3.8. EFFECT OF 2D AIR CATHODE ON THE CURRENT PRODUCTION IN SOIL MFC

5.3.8.1. CHRONOAMPEROMETRY TEST FOR 2D AIR CATHODE IN SOIL MFC

Chronoamperometry tests were conducted and it can be seen that the 2D air cathode battery could consistently generate electricity for up to six cycles when sodium acetate was utilized as a carbon source as shown in Figure 5.16. This efficient repetitive operation is beneficial in environments containing atypical microorganisms (Choi et al., 2004), such as those found in typical soil conditions. It is also seen that the current increased as soon as the sodium acetate was added (spikes in current) but the current gradually decreased as the time passed. It was observed that increasing the concentration of sodium acetate did not enhance current production in the air battery setup, resulting in a decline in current production over time. Other factors contributing to the reduced current production may include the limited anode surface area available for exo-electrogenic bacteria to form biofilms and the biofouling of the cathode and of the water layer.

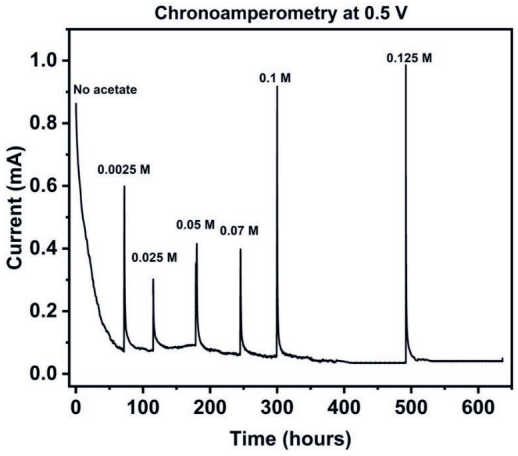

Figure 5.16: Current generation at 0.5 V anode potential and with spikes of different concentration of sodium acetate.

This biofouling covered the catalytic-layer side after prolonged operation, leading to performance degradation primarily by obstructing the transfer of OH^- ions and reducing the effective cathode surface available for O_2 oxidation, thereby resulting in decreased current production (Al Lawati et al., 2019; Chen et al., 2018; Jadhav et al., 2021; Kolajo et al., 2022;

Pasternak et al., 2022). Previous research indicated that biofouling begins after seven days (Baranitharan et al., 2015; Haupt et al., 2022), initially without impacting battery performance. However, after 10 days, biofouling significantly diminishes the battery's performance. Water-resistant graphene ink might also have contributed to decreased current production due to its ability to repel water, preventing bacteria from adhering to the surface (Uneputty et al., 2022). The CS has both the hydrophilic (amine and hydroxyl groups) and hydrophobic (acetyl groups) sites and these properties could be controlled by adjusting pH (X.-Y. Wang et al., 2023). At pH = 7 (i.e. in neutral condition) where most of the exoelectrogenic bacteria's are active (Guang et al., 2020), the CS shows hydrophobic nature (X.-Y. Wang et al., 2023), which could be one of the reason for the reduced performance. This hydrophobic nature could discourage the biofilm growth on the anode surface, and hence the performance. Hence, it can be concluded that the optimum concentration of sodium acetate is necessary to maximize the performance of the air cathode for prolonged experimental runs without biofouling or adapting other strategies to avoid detrimental biofouling. It is essential to decrease the hydrophobicity of CS membranes at pH 7 to optimize their performance in MFCs.

5.3.8.2. EFFECT OF SCAN RATE AND SODIUM ACETATE CONCENTRATION

Figure 5.17 shows the CV curves for the various concentration of sodium acetate and for different scan rates.

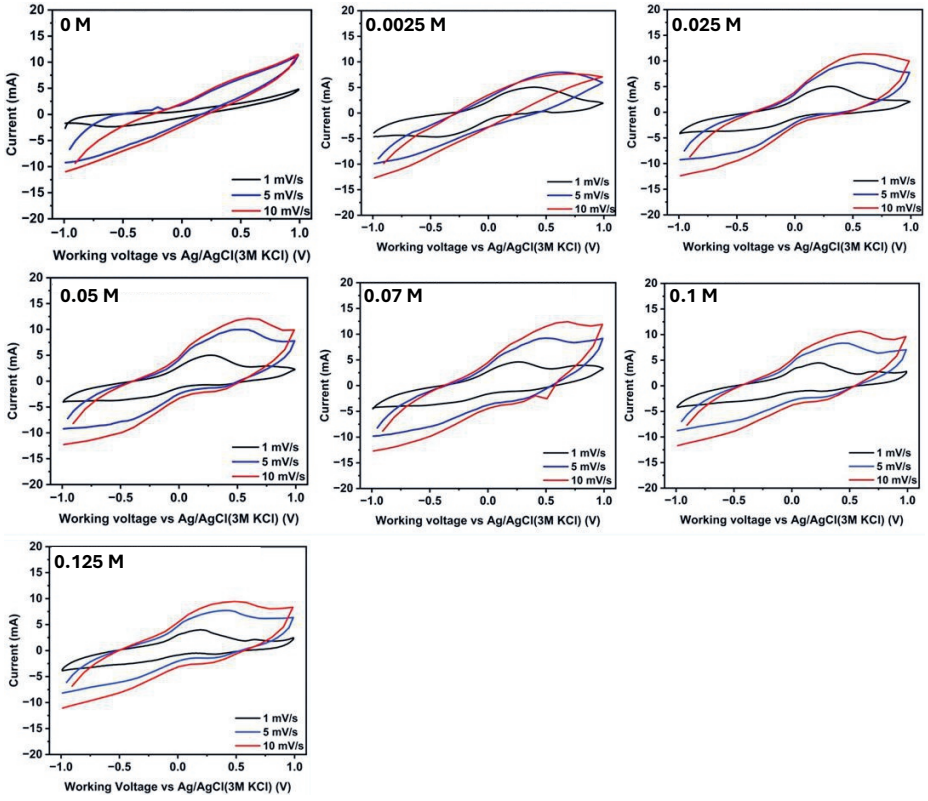

Figure 5.17: CV curves for various concentration of sodium acetate and scan rates.

CV measurements were performed on a 2D air cathode paper battery within a SMFC setup, utilizing varying concentrations of sodium acetate and different scan rates. The CV for 0 M sodium acetate did not exhibit the classical S-curve, whereas the CVs for other concentrations of sodium acetate displayed the classical S-curve, indicating biological and electrochemical activity in the presence of sodium acetate. It was observed that all paper batteries demonstrated similar peaks at 0.6 V for a scan rate of 1 mV/s, 0.5 V for 5 mV/s, and 0.25 V for 10 mV/s (versus Ag/AgCl,3M KCl). The peak potential was also similar for the different concentration of sodium acetate. It can be concluded that the concentration of sodium acetate has little affect on the current production, in these given conditions. Upon increasing the scan rate, the oxidation peak shifted towards more positive potentials, accompanied by an increase in peak-to-peak separation. This observation suggests that the electron transfer process is not fully reversible, likely being quasi-reversible or irreversible (Randviir, 2018). This behavior is attributed to ohmic polarization or IR-drop, which refers to the resistance of the electrolyte and other cell components during the flow of electrical current (Y. Liu et al., 2023). The shift indicates slower electron transfer kinetics, implying that the reaction cannot match the increasing scan rate and requires more energy to proceed. Previous studies have demonstrated that the current should increase with the concentration of acetate (Lóránt et al., 2015). However, in this study the current does not increase, which may be attributed to biofouling of the cathode surface. This biofouling results in a reduction of the effective cathode area and decreases the power output of the microbial fuel cell, as observed in this study (Kolajo et al., 2022). .

5.4. FUTURE SCOPE AND WORK

Future research directions include evaluating the performance of the proposed 3D and 2D paper battery designs using various crosslinking agents and electron acceptors. Further investigation is needed to develop a 3D paper battery that incorporates a binder, ensuring secure adhesion of paper components and making the entire design leakage-proof to prevent electrolyte leakage. Further research is necessary to fully comprehend the charge transfer resistance exhibited by paper batteries and to minimize it in order to enhance the operational lifespan of these batteries. Moreover, additional research is necessary to incorporate alternative biodegradable polymers into the design of 2D paper batteries to mitigate biofouling, thereby optimizing the performance of the paper battery. It is essential to determine the optimal concentration of sodium acetate to generate a sustained current under moist conditions without depleting the sodium acetate.

5.5. CONCLUSIONS

This study describes a 3D and 2D paper battery design prepared using origami technique. Paper-based batteries are characterized by simplicity, low cost, lightweight nature, and ease of fabrication using Whatman 1 paper. The battery was constructed using a CS polymer, and conductive graphene ink was manually applied and used as the electrode. The 3D battery was evaluated using a potassium ferro/ferricyanide redox couple. Crosslinking the paper battery results in reduced resistance to ion flow and enhanced electrochemical behaviour. These results indicate that the ink and CS coatings facilitate higher current generation. It was observed that an increased cathode area (3 electrodes) yielded higher current generation than a single horizontal electrode. However the performance of these batteries reduced after some time, this can be due to the electrolyte leakage in 3D paper battery , which negatively impacted its performance. To enhance performance, it is essential to employ effective binders to secure the corners of the surfaces. Biofouling was observed in both the 3D and 2D paper battery designs, contributing to the reduced performance of the batteries. Therefore, improved

biofouling treatments should be applied to the electrodes to address this issue. Finally it can be concluded that biodegradable CS membranes are suitable for the design of 3D and 2D paper battery for current generation. It is also concluded that the cubical shape of 3D paper battery can be used as SMSSs construction with this the anode and cathode surface areas can be maximized, it will be easy to keep the orientation of the cathode and the SMMSs on a whole in correct position and use them as an low-cost energy sources for powering small portable devices under saturated soil conditions in off-grid regions of the world, provided that the issues related to leakage and biofouling are resolved.

6

CONCLUSIONS

Parts of this chapter are based on :

Maya Moreshwar Meshram,S.,Adla,S.,Jourdin,L., Pande,S. (2024).Review of low-cost,off-grid,biodegradable, in situ autonomous soil moisture sensing systems: Is there a perfect solution? Computers and Electronics in Agriculture 225, 109289.

Maya Moreshwar Meshram, S., Gonugunta, P., Taheri, P., Jourdin, L., Pande, S. (2025). Investigating the influence of a thin copper film coated on nickel plates through physical vapor deposition for electrocatalytic nitrate reduction. Frontiers in Materials , Volume 12 - 2025.

Maya Moreshwar Meshram, S., Gonugunta, P., Taheri, P., Jourdin, L., Pande, S. (2025). Preparation of biodegradable membrane utilizing chitosan and polyvinyl alcohol, and assessment of its performance after coating with graphene conductive ink. Frontiers in Membrane Science and Technology , Volume 4 – 2025.

Maya Moreshwar Meshram, S., Pande, S. (2025). Design of origami-inspired paper batteries as a power source for soil moisture sensing system. (Submitted)

6.1. CONCLUSIONS

The thesis objectives and research questions are reflected upon in this chapter. The overall objective of the thesis was to "Design a soil moisture sensor powered by bacteria charged paper batteries". The objective was assessed through the four research questions. The following section summarizes the findings corresponding to each of the four research questions.

6.1.1. FINDINGS OF THE RESEARCH QUESTIONS

6.1.1.1. RESEARCH QUESTION 1

The first research questions was '*What are the technological challenges and advancements in developing low-cost, off-grid, biodegradable in situ autonomous soil moisture sensing systems, and is a fully optimized solution feasible?'* .

This was examined in Chapter 2 by analyzing the challenges, technical difficulties and factors associated with employing affordable soil moisture sensors in off-grid regions of the world. The study concluded that while low-cost soil moisture sensors offer a more economical alternative, they often yield less accurate results compared to high-cost currently available soil moisture sensors. The study emphasized that the calibration functions provided by manufacturers are typically developed under laboratory conditions, which may not be accurate when the sensors are deployed in diverse, remote and off-grid field conditions. Low-cost sensors tend to have shorter operational lifespans due to the accelerated wear and tear of their components, which diminishes their effective measurement range and suitability across different soil types. Currently available sensors, including both low and high cost, require periodic maintenance and recalibration, which can increase overall costs in terms of time, labor, and resources. The research highlighted that current soil moisture sensors rely on off-grid energy sources such as batteries and solar panels. Although these alternatives eliminate the need for grid-powered electricity, they present their own challenges, including limited energy output, higher initial costs, dependance on climatic conditions and the necessity for periodic replacements, which can be hurdles for smallholder farmers with limited technical resources. This indicated that while off-grid solutions extend the reach of soil moisture sensing, particularly in remote locations, they also require specialized skills for maintenance and repair, rendering them less ideal for users with limited resources. The study discussed how traditional electrical components generate environmental waste, including plastic and heavy metal residues from batteries and solar panels and mentioned that biodegradable sensors are emerging as a promising solution to reduce environmental impacts, however, these are still in the early stages of research and require further development to become a viable alternative for agricultural use.

The study emphasized that there is no single 'perfect' soil moisture sensing system that meets criteria studied (namely low- cost, off-grid, autonomous, and biodegradable). Instead, the selection of a system depends on balancing sensor performance, operational feasibility (such as cost, size, durability, and power requirements), and biodegradability. This trade-off necessitates users to consider their specific application context, such as small-scale versus large-scale farming, where decisions will differ based on whether the focus is on water use efficiency, yield maximization, or sustainable practices.

6.1.1.2. RESEARCH QUESTION 2

The second research question was *'How does the electrodes prepared utilizing the environmentally friendly technique of physical vapor deposition affects the electrocatalytic NO_3^- reduction, and how the NO_3^- can be used as an electron acceptor for the battery construction?'*

This was addressed in Chapter 3 by preparing bimetallic Cu-Ni electrodes using the PVD technique. The study highlighted that PVD can be used as one of the green technologies in which bimetallic electrodes can be prepared without any other chemical contamination. The study examined how the thickness of a Cu film deposited on Ni plates influences the performance in NO_3RR. The findings demonstrated that employing a Cu-Ni bimetallic electrode can enhance NO_3^- reduction by modifying the thickness of the Cu layer on the Ni plate. Various thicknesses (25, 50, and 100 nm) were tested, revealing that although the Cu film was uniformly distributed, the current density decreased as the thickness increased, indicating a complex relationship between thickness and catalytic performance. It was thus concluded that the thickness of the Cu layer impacts NO_3RR when using Cu-Ni bimetallic electrodes. It showed that careful control of film thickness allows for better management of reaction conditions, which is essential in practical applications. Electrochemical studies, such as CV, indicated that the onset potential for NO_3^- reduction varied with Cu thickness. The study checked the influence of stirring on NO_3RR and found out that under non-stirred conditions, distinct peaks were observed, suggesting that the Cu-Ni electrodes facilitated effective electron transfer under non-stirring conditions. However, under stirred conditions, the absence of a NO_3^- reduction peak was noted, indicating that mass transport limitations were alleviated, which is crucial for practical applications. The study emphasized that thin Cu films deposited using PVD enable the formation of uniform, well-adhered layers, ensuring minimal impurities, and defect-free surface to promote effective catalysis. This approach was noted to be underexplored in the context of NO_3RR, making the findings significant for future research and applications.

Finally, it was concluded that further studies are needed to clearly understand the underlying reaction mechanisms. Future research might explore advanced in-situ spectroscopic methods to pinpoint intermediates and elaborately model how Cu and Ni interact at the atomic level. This underscores the ongoing commitment to optimizing electrode design and improving reaction efficiencies in practical applications. These points collectively demonstrate that the research not only advances the technical understanding of thin film deposition and electrochemical performance but also provides practical guidelines for designing more effective electrodes for energy storage devices and NO_3^- removal.

6.1.1.3. RESEARCH QUESTION 3

The third research question was '*How can a membrane be prepared for use in paper batteries, and what materials are suitable for its fabrication?'*

In response to the question, Chapter 4 demonstrated the feasibility of preparing biodegradable membranes using CS and PVA polymers, reinforced with cellulose filter paper and coated with graphene conductive ink. The membranes were synthesized through a solution-casting method using CS, PVA, and a 1:1 CS/PVA composite, reinforced with cellulose filter paper. A water-resistant graphene conductive ink was applied as a coating to study the membranes' performance. The graphene-coated membranes exhibited superior electrochemical properties compared to their uncoated counterparts. Specifically, the coated CS/PVA membrane showed the lowest oxygen diffusion coefficient and the highest proton conductivity among all

samples. This improvement is attributed to the graphene-based conductive ink creating more interconnected channels for proton transfer and acting as a barrier to impede oxygen diffusion. Uncoated CS membranes had the highest water uptake capacity, while uncoated PVA membrane showed the highest swelling ratio and ion exchange capacity. The graphene coating significantly reduced both water uptake and swelling ratios, as graphene is hydrophobic and repels water, forming a physical barrier. All three membrane types (CS, PVA, and CS/PVA membranes) demonstrated slow degradation over 100 days when exposed to compost tea at room temperature. The observed long-term stability indicates the membranes' appropriateness for medium-term applications in aqueous environments, such as biobatteries used in soil moisture sensors, which generally necessitate a functional lifespan of at least 100 days.

Chapter 4 thus underscored the potential of these membranes as a sustainable and cost-effective alternative for various applications, particularly in biobatteries and other low-power electronic devices.

6.1.1.4. RESEARCH QUESTION 4

The fourth research question was '*How can a 3D paper-based battery be designed through the application of origami techniques, in comparison to a 2D paper-based battery without origami, and what is the relative suitability of each design for current generation in water-saturated soils?'*

Chapter 5 successfully designed and prepared both 3D and 2D paper batteries using origami techniques. These batteries were constructed using CS polymer and conductive graphene ink, which was manually applied to serve as electrodes. Paper-based batteries were characterized by their simplicity, low cost, lightweight nature, and ease of fabrication using Whatman 1 paper. The performance of the 3D battery was assessed initially through the use of a potassium ferrocyanide reaction at the anode and a potassium ferricyanide reaction at the cathode. Subsequently, the evaluation was conducted under moist soil conditions at the anode, while maintaining the potassium ferricyanide reaction at the cathode. Crosslinking which refers to the creation of tiny links or bridges between polymer chains so they form a strong interconnected network in the paper battery which significantly reduce resistance to ion flow and enhanced electrochemical behavior. The ink and CS coatings were found to facilitate higher current generation. An increased cathode area, specifically using three vertical electrodes, yielded higher current generation compared to a single horizontal electrode.

The 2D air cathode paper battery was designed using a CS membrane, and its performance was tested under fully saturated soil conditions. The CS membranes can be effectively used in the design of 2D air cathode paper batteries for current generation in saturated soil conditions. The findings demonstrate that origami-based paper batteries, prepared with CS and graphene conductive ink, hold potential for use as alternative low-cost energy sources for powering small portable devices. The 3D battery was observed to generate a significantly lower current when utilizing both the potassium ferrocyanide (anolyte) and potassium ferricyanide (catholyte) redox couple, as well as in the soil environment where natural soil combined with sodium acetate served as the anolyte and potassium ferricyanide as the catholyte.

The chapter concludes that biodegradable, origami-inspired paper batteries, particularly those incorporating CS and graphene, present a promising, cost-effective, and environmentally sustainable solution for portable energy applications. The study highlights that crosslinking and cathode configuration are critical factors for enhancing performance. Furthermore, it

emphasizes the necessity for additional research on both 3D and 2D paper batteries before they can be effectively utilized as energy sources.

In conclusion, this thesis investigated the development of a biodegradable soil moisture sensor powered by a paper-based, bacteria-charged battery. Although the device examined and tested in this study utilized the principles of a microbial fuel cell, the term "paper battery" was employed to highlight its structural and functional resemblance to small electrochemical power sources, as well as its biodegradable and accessible nature. Biodegradable membranes, reinforced with cellulose filter paper and coated with graphene, exhibited promising electrochemical properties and stability, while 3D origami-inspired batteries showcased the potential of foldable designs for enhanced functionality in soil environments. The origami-inspired design involved folding paper to create a 3D (cuboid) functional structure, with a binder used solely for stabilization to preserve the folding concept. This project provided various insights and laid the foundation for future advancements by examining different aspects of cost-effective, off-grid biodegradable soil moisture sensing systems, including electrode performance, membrane fabrication, and battery design, by identifying areas for improvement. These findings offer guidance for advancing paper based, microbial energy-harvesting devices towards practical and sustainable applications in agriculture.

6.2. LIMITATIONS IDENTIFIED

It is crucial to recognize the limitations identified in this thesis, including the assumptions and uncertainties associated with the employed design, as well as the complexities involved in integrating all pertinent factors into the study, as discussed below.

This study highlighted that low-cost SMSSs often face accuracy issues. These inaccuracies are influenced by various soil properties, such as texture and salinity, making these sensors less reliable for a range of agricultural applications. Such SMSSs necessitate site-specific calibration, which can be both time-consuming and resource-intensive, complicating their practical use. The sensors analyzed in this thesis generally have shorter operational lifespans due to the rapid degradation of their components. This limitation requires frequent replacements, thereby increasing overall costs and reducing the practicality of these sensors over time. Factors such as degradation time and sensitivity to moisture can limit their operational capabilities. The reliance of SMSSs on off-grid power sources, like exo-electrogenic bacteria, can be challenging, as these bacteria depend on various factors for survival, and need periodic replacement, complicating the maintenance of remote sensors. Although biodegradable sensors that are used in SMSSs can be a solution to reduce environmental impacts, it can be seen that their effectiveness in complex biophysical environments is still under investigation. The thesis emphasizes that there is no "perfect" SMSS, and users has to navigate trade-offs between performance, operational feasibility, and biodegradability as per their application requirements. This complexity can pose challenges for users in selecting the most suitable sensor for their specific needs. These limitations underscore the challenges in developing effective, sustainable soil moisture sensing systems, highlighting the need for further research and innovation in this field.

The study highlighted that the degradation of Cu layer can significantly reduce the effectiveness and lifespan of the catalyst during the NO_3RR.The performance of the Cu-Ni electrodes is sensitive to pH changes in the solution, and if the pH is not maintained in the solution it can affect the NO_3RR and thus hindering the reaction.

Chapter 3 discussed how the reduction of NO_3^- can yield various products depending on the pH, which complicates the reaction pathways and may lead to the formation of undesired byproducts. It pointed out that while the Cu-Ni alloy improves the electronic state for NO_3^- reduction and selectivity towards desired product, the detailed mechanisms of how these alloys interact with reaction intermediates remain poorly understood. This lack of clarity can hinder the optimization of the catalyst for specific applications. Although the Cu-Ni alloy showed improved performance and selectivity compared to monometallic Cu, the long-term stability and performance of these electrodes in real-world conditions were not fully addressed. Cu-Ni alloy also has the potential for side reactions, such as hydrogen evolution, which could also affect the overall efficiency of the NO_3^- reduction process. It found that varying the thickness of the Cu layer impacted the electrochemical performance, but the optimal thickness for maximum efficiency was not definitively established. This presents a challenge for scaling up the technology for industrial applications. These limitations underscore the need for further research to address the challenges associated with Cu-Ni alloy electrodes and to enhance their performance in electrocatalytic applications.

Chapter 4 highlighted specific limitations in the design of biodegradable membranes, particularly noting that these membranes cannot be fabricated using any type of cellulose paper. For the preparation of these membranes with polymers, it is crucial that the cellulose paper exhibit a porous structure. The polymers must possess sufficient viscosity to ensure absorption into the filter paper. Prolonged use of the membranes results in the diffusion of electrolytes across the membranes. Manual coating presents limitations, as it cannot ensure uniform coatings. In certain polymers, the conductive ink is entirely absorbed into their structure.

Chapter 5 identified several limitations and challenges associated with the design and performance of origami-inspired paper batteries. The complex folding and bending required for 3D battery designs can induce stresses, leading to wear and potential failure over time. Complex folding patterns may cause energy loss, negatively affecting battery performance. Because of the complex 3D patterns of these batteries they require precise techniques for mass production, making mass production challenging. Integrating complex 3D paper batteries into existing systems, such as SMFC systems, is difficult due to their intricate shapes and folding patterns. The current output from a single 3D paper battery is limited due to the reduced anode surface area available for bacterial growth and oxidation reactions, as well as the diminished cathode surface area available for reduction reactions. The positioning of the cathode in complex 3D configuration presents difficulties, as both its orientation and surface area are critical for power output performance. A significant challenge for 3D configuration in soil is the storage of liquid compounds (electrolytes) within the hollow spaces of the batteries, posing a risk of leakage. Replacing depleted liquid compounds becomes problematic once they are fully consumed. The studied 3D cubical shapes can deform under pressure and can easily become parallelograms. The inherent porosity of the paper, while facilitating ion movement, also permits electrolyte leakage, which could result in a short circuit between the electrodes. This highlights the necessity for robust sealing, binding, or coating techniques to enhance stability and longevity.

While 2D air cathode paper batteries can serve as alternatives to 3D paper batteries, they possess inherent limitations. The study observed that in 2D batteries, biofouling on the cathode surface, particularly after extended operation (e.g., seven to fifteen days), can significantly impair battery performance by obstructing ion transfer and reducing the effective cathode surface area. The 2D batteries are inserted into the soil such that half portion of these 2D batteries are exposed to the environment and are positioned partially in the soil and half partially above it, the section above the soil is susceptible to damage during various agricultural

activities. The 2D battery which is used in vertical position provides a limitation for keeping the embedded wireless tags (such as RFID, NFC) in horizontal direction if the 2D battery is intended to be used in SMSSs. These batteries are intended for use during the cropping season, and since crops require a near-neutral pH (6-7.5), the CS membranes, especially at neutral pH, exhibit a hydrophobic nature, which can inhibit biofilm growth on the anode surface, potentially reducing performance in microbial fuel cells. In the context of 2D paper batteries, water passes through the minute pores of the membranes employed in the battery's construction through capillary action. Simultaneously, water is lost to the atmosphere via evaporation from the portion of the battery exposed to the environment. A challenge emerges when the rate of evaporation exceeds the membrane's capacity to draw water upward, a situation further complicated by the gravitational resistance encountered in a vertical orientation. Consequently, the membrane's surface may become desiccated despite the presence of water at its base. In short the rate of capillary action in the membrane can be lower than the rate of evaporation.

Overall, while the thesis demonstrated the potential of origami-inspired paper batteries, it also clearly outlined several areas that require further research and development to overcome current limitations related to mechanical stability, energy efficiency, production scalability, and long-term operational performance, particularly concerning biofouling and electrolyte management.

6.3. WAYS FORWARD AND RECOMMENDATIONS

The development of biodegradable soil moisture sensing systems offers a promising route for sustainable agriculture and environmental conservation. This study explains the integration of biodegradable materials into the design of paper batteries, which can serve as an energy source in off-grid regions. The research addressed some of the challenges posed by conventional electronic waste used in soil moisture sensors, particularly in large-scale or short-term agricultural applications. However, while current research emphasized the potential of biodegradable sensors in SMSSs, several areas necessitate further investigation to ensure their practical applicability and widespread adoption.

The bioanode is integral to the development of SMSSs that employ bacteria-powered paper batteries. However, bioanodes encounter several challenges, including low and unstable current densities due to environmental variability, microbial competition that diminishes coulombic efficiency, mass transport limitations in compact soils, fouling or passivation of electrode surfaces, and prolonged biofilm start-up times. These factors collectively obstruct the provision of a reliable long-term power supply under field conditions. It is therefore advisable to employ high surface area materials that can be modified with nanomaterials such as graphene for the anode. Graphene possesses unique properties that can enhance soil health, including nutrient availability and soil physical and chemical properties, if it leached into the soil. It is also advised to position the anode in the moist anoxic zone. The anodes should be activated by inoculating them with electrogenic microbes such as Geobacter or Shewanella immediately prior to use to expedite the biofilm startup time. Furthermore, the anode substrates should be prepared by incorporating nutrients to facilitate rapid utilization by the bacteria.

It is recommended to develop specific calibration method which can be used across different soil types and different field conditions. The reliability of these sensors can then be significantly improved, leading to better water management decisions among smallholder farmers. It is recommended to comprehensively test paper degradation under real field conditions, and share testing protocols openly to help improve future designs.

It is recommended to explore other methodologies to coat Cu and Ni onto filter paper as a composite, as it is difficult to coat Cu and Ni on filter paper with PVD. This can help evaluate NO_3RR using biodegradable electrodes. Also, it is recommended to identify the optimal composition of Cu and Ni while preparing Cu-Ni alloy for NO_3RR applications in soil batteries. Additionally, determining the appropriate thickness of the Cu-Ni composite is crucial for the effective functioning of NO_3RR, given that these batteries will be deployed in soil environments where stirring is not feasible.

It is advisable to determine the optimal viscosity of biodegradable polymers to facilitate their impregnation into filter paper. Additionally, it is recommended to investigate various cellulose papers that offer greater strength than filter paper and can effectively absorb biodegradable polymers. Furthermore, it is suggested to explore methods or instruments suitable for applying conductive inks, intended for use as anodes, onto biodegradable membranes to achieve uniform thickness without compromising the integrity of the membranes. The use of molds for casting the membranes using polymers as per the shape of the battery is also recommended during the polymer impregnation process into filter paper to ensure uniform membrane thickness. Conductive ink is fully absorbed by certain polymers; therefore, an additional barrier layer is necessary to prevent ink absorption and ensure a more uniform coating. The investigation of the capillary movement of water through membranes is essential, and it is recommended to explore methods to enhance this capillary movement using 3-D microfluidic pathways within the paper layers.

It is recommended to explore alternative 3D structures capable of maintaining stability in uneven soil conditions, demonstrating resistance to collapse or deformation when buried or partially embedded. These structures should be designed to withstand the weight and pressure exerted by the soil. Appropriate binding materials should be incorporated into the 3D design, employing origami techniques to secure the edges. The folding and binding processes should be executed with precision using machinery. The 3D design must ensure robust support for the electrode, specifically the cathode, when utilized in the catholyte compartment. If the design of the 3D battery is not airtight, then the electrodes used in the design are susceptible to fungal growth on their surfaces. Consequently, once the entire SMSSs is embedded in the soil with a defective design, replacing these electrodes becomes impractical.

Therefore, it is imperative to apply an anti-fouling treatment prior to their use. It is recommended to incorporate antifouling agents to ensure longevity and prevent damage during extended use. Additionally, it is essential to investigate the duration for which the electrodes can function in such a system without experiencing biofouling. Thin, flexible connecting wires are advised for establishing connections, or conductive ink may be utilized for connecting the electrodes of the paper battery. In light of the observation that a single 3D paper battery has generated a lower current in this study, it is advisable to arrange multiple 3D paper batteries in parallel to enhance current output and to increase electrode areas. Additionally, arranging multiple 3D paper batteries in series is recommended to achieve higher voltage generation. Standard electrochemical equations are available to calculate or predict current and voltage generation, taking into account electrode kinetics, ohmic losses, and mass transport.

The shape of the 3D battery should ensure that the embedded tags remain in a horizontal direction (i.e., parallel to the soil surface) as shown in Figure 1 and can be captured by mobile phones used in SMSSs.

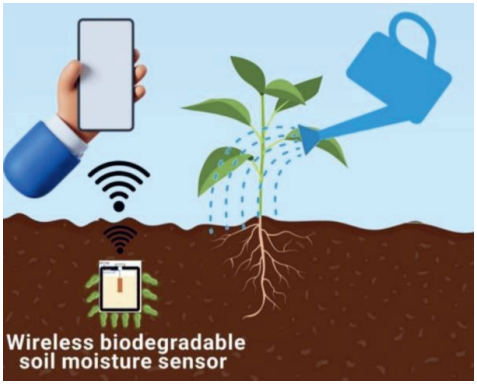

Figure 6.1: Placement of paper battery in the soil as discussed in Chapter 5 and the detection of signal using SMSSs with the help of mobile phones.

This orientation is crucial because, in developed countries with the necessary infrastructure, including readers and satellites, the direction of signal-emitting tags significantly influences their detection by readers, thereby facilitating farmers' access to soil moisture information. In contrast, while scaling up in developing countries where such infrastructure is absent and are in need of such SMSSs, inadequate orientation may impede farmers ability to accurately measure soil moisture. Figure 6.2 illustrates signal detection via satellite in developed countries and through handheld mobile phones in developing countries.

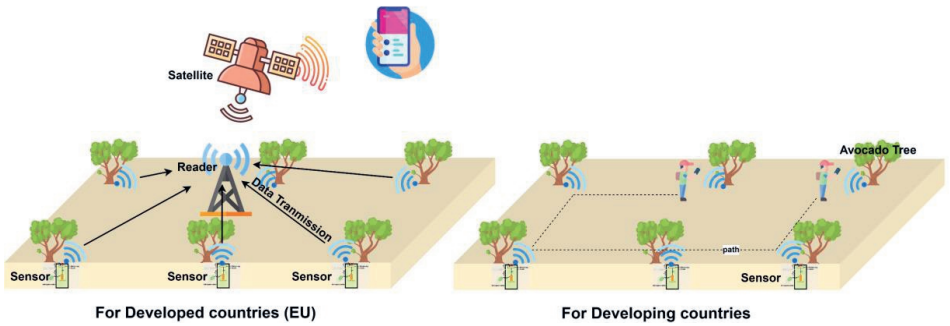

Figure 6.2: demonstrates the process by which signals are detected by the reader, subsequently by the satellite in developed countries and by the farmers in developing countries

In the case of 2D paper batteries, it is essential that the rate of capillary water movement through the membranes is higher than the rate of water evaporation from these membranes. This is critical because the portion of the battery exposed above the soil may dry out, thereby compromising the performance of the 2D paper battery. Achieving this balance requires an understanding of the relationship between the evaporation rate and the capillary movement rate of water within the membranes. This can be accomplished by modifying the microfluidic pathways within the membranes. Additionally, this can be achieved by designing the pore size of the membrane (i.e., increasing the porosity of the membranes) and determining the height to which the water must travel within the membrane using the Lucas-Washburn equation. It is also advisable to design the 2D battery in such a way that it can be easily inserted into the soil while maintaining the wireless tags in a horizontal position if used in SMSSs.

7

BIBLIOGRAPHY

A. Fraiwan, H. Lee, S. Choi, 2014. A Multianode Paper-Based Microbial Fuel Cell: A Potential Power Source for Disposable Biosensors. IEEE Sensors Journal 14, 3385–3390. https://doi.org/10.1109/JSEN.2014.2332075

Aarif K. O., M., Alam, A., Hotak, Y., 2025. Smart Sensor Technologies Shaping the Future of Precision Agriculture: Recent Advances and Future Outlooks. Journal of Sensors 2025, 2460098. https://doi.org/10.1155/js/2460098

Abascal, E., Gómez-Coma, L., Ortiz, I., Ortiz, A., 2022. Global diagnosis of nitrate pollution in groundwater and review of removal technologies. Science of the total environment 810, 152233.

Abba, Namkusong, Lee, Crespo, 2019. Design and Performance Evaluation of a Low-Cost Autonomous Sensor Interface for a Smart IoT-Based Irrigation Monitoring and Control System. Sensors 19, 3643. https://doi.org/10.3390/s19173643

Abba, S.I., Egbueri, J.C., Benaafi, M., Usman, J., Usman, A.G., Aljundi, I.H., 2023. Fluoride and nitrate enrichment in coastal aquifers of the Eastern Province, Saudi Arabia: The influencing factors, toxicity, and human health risks. Chemosphere 336, 139083. https://doi.org/10.1016/j.chemosphere.2023.139083

Abdallah, R., Geneste, F., Labasque, T., Djelal, H., Fourcade, F., Amrane, A., Taha, S., Floner, D., 2014. Selective and quantitative nitrate electroreduction to ammonium using a porous copper electrode in an electrochemical flow cell. Journal of Electroanalytical Chemistry 727, 148–153.

Abdullah, S.S., 2017. Electrodeposition of nickel/copper multi-nanolayer by dual bath technique at ambient temperature.

Abegunde, O.O., Akinlabi, E.T., Oladijo, O.P., Akinlabi, S., Ude, A.U., 2019. Overview of thin film deposition techniques. AIMS Materials Science 6, 174–199.

Abolhassani, M., Griggs, C.S., Gurtowski, L.A., Mattei-Sosa, J.A., Nevins, M., Medina, V.F., Morgan, T.A., Greenlee, L.F., 2017. Scalable Chitosan-Graphene Oxide Membranes: The Effect of GO Size on Properties and Cross-Flow Filtration Performance. ACS Omega 2, 8751–8759. https://doi.org/10.1021/acsomega.7b01266

Adekunle, A., Raghavan, V., Tartakovsky, B., 2019. Real-Time Performance Optimization and Diagnostics during Long-Term Operation of a Solid Anolyte Microbial Fuel Cell Biobattery. Batteries 5, 9. https://doi.org/10.3390/batteries5010009

Adla, S., Rai, N.K., Karumanchi, S.H., Tripathi, S., Disse, M., Pande, S., 2020. Laboratory calibration and performance evaluation of low-cost capacitive and very low-cost resistive soil moisture sensors. Sensors (Switzerland) 20. https://doi.org/10.3390/s20020363

Agate, S., Joyce, M., Lucia, L., Pal, L., 2018. Cellulose and nanocellulose-based flexible-hybrid printed electronics and conductive composites – A review. Carbohydrate Polymers 198, 249–260. https://doi.org/10.1016/j.carbpol.2018.06.045

Aghababaie, M., Farhadian, M., Jeihanipour, A., Biria, D., 2015. Effective factors on the performance of microbial fuel cells in wastewater treatment – a review. Environmental Technology Reviews 4, 71–89. https://doi.org/10.1080/09593330.2015.1077896

Agrawal, C., Sharma, B., Bhojwani, D., Rajawat, S., 2015. Paper Batteries, in: Vijay, V., Yadav, S.K., Adhikari, B., Seshadri, H., Fulwani, D.K. (Eds.), Systems Thinking Approach for Social Problems. Springer India, New Delhi, pp. 231–237.

Ahmad, S., Nawaz, T., Ali, A., Orhan, M.F., Samreen, A., Kannan, A.M., 2022. An overview of proton exchange membranes for fuel cells: Materials and manufacturing. International Journal of Hydrogen Energy 47, 19086–19131. https://doi.org/10.1016/j.ijhydene.2022.04.099

Ahmed, M.R., Mirihanage, W., Potluri, P., Fernando, A., 2023. Highly Stable Graphene Inks Based on Organic Binary Solvents. Particle & Particle Systems Characterization 40, 2200153. https://doi.org/10.1002/ppsc.202200153

Ahmed, N.T., Bentaher, H.A., Al-Mahammedi, M.T.F., 2024. Using the Erratic Application of Solar Photovoltaic Panel Installations to Power Agricultural Submersible Pumps in Deep Wells in Order to Extend Productive Times and Boost Water Production. Applied Sciences 14, 29. https://doi.org/10.3390/app14010029

Ahmed, S., Kakkar, V., 2017. An electret-based angular electrostatic energy harvester for battery-less cardiac and neural implants. IEEE Access 5, 19631–19643.

Ahn, J.-H., Choo, K.-H., Park, H.-S., 2008. Reverse osmosis membrane treatment of acidic etchant wastewater: Effect of neutralization and polyelectrolyte coating on nitrate removal. Journal of Membrane Science 310, 296–302. https://doi.org/10.1016/j.memsci.2007.11.010

Aiyer, K.S., 2020. How does electron transfer occur in microbial fuel cells? World J Microbiol Biotechnol 36, 19. https://doi.org/10.1007/s11274-020-2801-z

Al Lawati, M.J., Jafary, T., Baawain, M.S., Al-Mamun, A., 2019. A mini review on biofouling on air cathode of single chamber microbial fuel cell; prevention and mitigation strategies. Biocatalysis and Agricultural Biotechnology 22, 101370. https://doi.org/10.1016/j.bcab.2019.101370

Alam, M.M., Hasnat, M.A., Rashed, M.A., Uddin, S.M.N., Rahman, M.M., Amertharaj, S., Ahmed, N., Mohamed, N., 2015. Nitrate detection activity of Cu particles deposited on pencil graphite by fast scan cyclic voltammetry. J Anal Chem 70, 60–66. https://doi.org/10.1134/S1061934815010037

Alday, P.P., Barros, S.C., Alves, R., Esperança, J.M.S.S., Navarro-Segarra, M., Sabaté, N., Silva, M.M., Esquivel, J.P., 2020. Biopolymer Electrolyte Membranes (BioPEMs) for Sustainable Primary Redox Batteries. Advanced Sustainable Systems 4. https://doi.org/10.1002/adsu.201900110

Alharbi, S., Felemban, A., Abdelrahim, A., Al-Dakhil, M., 2024. Agricultural and Technology-Based Strategies to Improve Water-Use Efficiency in Arid and Semiarid Areas. Water 16, 1842. https://doi.org/10.3390/w16131842

Ambili, K., Joseph, S., Sidharthan, A., 2019. A polyvinyl alcohol/chitosan blend proton exchange membrane for direct methanol fuel cell. AIP Conference Proceedings 2162, 020051. https://doi.org/10.1063/1.5130261

Arandhakar, S., Nakka, J., Krishna, V.B.M., 2024. A comprehensive analysis and future prospects on battery energy storage systems for electric vehicle applications. Energy Sources, Part A: Recovery, Utilization, and Environmental Effects 46, 13004–13031. https://doi.org/10.1080/15567036.2024.2401118

Arcese, G., Campagna, G., Flammini, S., Martucci, O., 2014. Near Field Communication: Technology and Market Trends. Technologies 2, 143–163. https://doi.org/10.3390/technologies2030143

Arpa, M.D., Ünükür, M.Z., Erim, Ü.C., 2021. Formulation, characterization and in vitro release studies of terbinafine hydrochloride loaded buccal films. Journal of Research in Pharmacy.

Ashok Kumar, S.S., Bashir, S., Ramesh, K., Ramesh, S., 2022. A comprehensive review: Super hydrophobic graphene nanocomposite coatings for underwater and wet applications to enhance corrosion resistance. FlatChem 31, 100326. https://doi.org/10.1016/j.flatc.2021.100326

Atreya, M., Desousa, S., Kauzya, J.-B., Williams, E., Hayes, A., Dikshit, K., Nielson, J., Palmgren, A., Khorchidian, S., Liu, S., Gopalakrishnan, A., Bihar, E., Bruns, C.J., Bardgett, R., Quinton, J.N., Davies, J., Neff, J.C., Whiting, G.L., 2023. A Transient Printed Soil Decomposition Sensor Based on a Biopolymer Composite Conductor. Advanced Science 10, 2205785. https://doi.org/10.1002/advs.202205785

Atreya, M., Dikshit, K., Marinick, G., Nielson, J., Bruns, C., Whiting, G.L., 2020. Poly(lactic acid)-Based Ink for Biodegradable Printed Electronics with Conductivity Enhanced through Solvent Aging. ACS Applied Materials and Interfaces 12, 23494–23501. https://doi.org/10.1021/acsami.0c05196

Aziz, S.B., Abdullah, O.G., Hussein, S.A., Ahmed, H.M., 2017. Effect of PVA Blending on Structural and Ion Transport Properties of CS:AgNt-Based Polymer Electrolyte Membrane. Polymers 9, 622. https://doi.org/10.3390/polym9110622

Aziz, S.B., Brza, M.A., Hamsan, H.M., Kadir, M.F.Z., Abdulwahid, R.T., 2021a. Electrochemical characteristics of solid state double-layer capacitor constructed from proton conducting chitosan-based polymer blend electrolytes. Polym. Bull. 78, 3149–3167. https://doi.org/10.1007/s00289-020-03278-1

Aziz, S.B., Brza, M.A., Hamsan, M.H., Kadir, M.F.Z., Muzakir, S.K., Abdulwahid, R.T., 2020. Effect of ohmic-drop on electrochemical performance of EDLC fabricated from PVA:dextran:NH4I based polymer blend electrolytes. Journal of Materials Research and Technology 9, 3734–3745. https://doi.org/10.1016/j.jmrt.2020.01.110

Aziz, S.B., Nofal, M.M., Abdulwahid, R.T., Kadir, M.F.Z., Hadi, J.M., Hessien, M.M., Kareem, W.O., Dannoun, E.M.A., Saeed, S.R., 2021b. Impedance, FTIR and transport properties of

plasticized proton conducting biopolymer electrolyte based on chitosan for electrochemical device application. Results in Physics 29, 104770. https://doi.org/10.1016/j.rinp.2021.104770

Babaeian, E., Sadeghi, M., Jones, S.B., Montzka, C., Vereecken, H., Tuller, M., 2019. Ground, Proximal, and Satellite Remote Sensing of Soil Moisture. Reviews of Geophysics 57, 530–616. https://doi.org/10.1029/2018RG000618

Bachuwar, V.D., Ghodake, U.R., Lakhssassi, A., Suryavanshi, S.S., 2018. WSN/Wi-Fi Microchip-Based Agriculture Parameter Monitoring using IoT, in: 2018 International Conference on Smart Systems and Inventive Technology (ICSSIT). Presented at the 2018 International Conference on Smart Systems and Inventive Technology (ICSSIT), pp. 214–219. https://doi.org/10.1109/ICSSIT.2018.8748638

Badea, G.E., 2009. Electrocatalytic reduction of nitrate on copper electrode in alkaline solution. Electrochimica Acta 54, 996–1001. https://doi.org/10.1016/j.electacta.2008.08.003

BADEA, G.E., BADEA, T., 2003. Nitrate reduction in alkaline solutions mediated by Cu and Cd underpotential deposition on Au and Ni substrates. Rev. roum. chim 48, 843.

Bai, Z., Li, X., Ding, L., Qu, Y., Chang, X., 2023. Artificial Cu-Ni catalyst towards highly efficient nitrate-to-ammonia conversion. Sci. China Mater. 66, 2329–2338. https://doi.org/10.1007/s40843-022-2392-8

Balendonck, J., Hilhorst, M., Kroese, W.S., Meijer, G., 2013. A wireless passive soil water content sensor tag. Presented at the 10th Int. Conf. on Electromagnetic Wave Interaction with Water and Moist Substances (ISEMA2013), Weimar (D), pp. 25–27.

Baltrusaitis, J., Jayaweera, P.M., Grassian, V.H., 2009. XPS study of nitrogen dioxide adsorption on metal oxide particle surfaces under different environmental conditions. Phys. Chem. Chem. Phys. 11, 8295–8305. https://doi.org/10.1039/B907584D

Banerjee, A., Calay, R.K., Eregno, F.E., 2022. Role and Important Properties of a Membrane with Its Recent Advancement in a Microbial Fuel Cell. Energies 15, 444. https://doi.org/10.3390/en15020444

Baptista, A., Silva, F.J.G., Porteiro, J., Míguez, J.L., Pinto, G., Fernandes, L., 2018. On the Physical Vapour Deposition (PVD): Evolution of Magnetron Sputtering Processes for Industrial Applications. Procedia Manufacturing, 28th International Conference on Flexible Automation and Intelligent Manufacturing (FAIM2018), June 11-14, 2018, Columbus, OH, USAGlobal Integration of Intelligent Manufacturing and Smart Industry for Good of Humanity 17, 746–757. https://doi.org/10.1016/j.promfg.2018.10.125

Barakat, N.A.M., Gamal, S., Ghouri, Z.K., Fadali, O.A., Abdelraheem, O.H., Hashem, M., Moustafa, H.M., 2024. Graphitized mango seed as an effective 3D anode in batch and continuous mode microbial fuel cells for sustainable wastewater treatment and power generation. RSC Adv. 14, 3163–3177. https://doi.org/10.1039/D3RA05084J

Baranitharan, E., Khan, M.R., Prasad, D.M.R., Teo, W.F.A., Tan, G.Y.A., Jose, R., 2015. Effect of biofilm formation on the performance of microbial fuel cell for the treatment of palm oil mill effluent. Bioprocess Biosyst Eng 38, 15–24. https://doi.org/10.1007/s00449-014-1239-9

Barrera, L., Silcox, R., Giammalvo, K., Brower, E., Isip, E., Bala Chandran, R., 2023. Combined Effects of Concentration, pH, and Polycrystalline Copper Surfaces on Electrocatalytic Nitrate-to-Ammonia Activity and Selectivity. ACS Catal. 13, 4178–4192. https://doi.org/10.1021/acscatal.2c05136

Basterrechea, D.A., Rocher, J., Parra, M., Parra, L., Marin, J.F., Mauri, P.V., Lloret, J., 2021. Design and Calibration of Moisture Sensor Based on Electromagnetic Field Measurement for Irrigation Monitoring. Chemosensors 9, 251. https://doi.org/10.3390/chemosensors9090251

Batteiger, A., 2015. Off-grid electrification and its impacts on the waste management system–the case of Bangladesh. UCL STEaPP.

Baurzhan, S., Jenkins, G.P., 2016. Off-grid solar PV: Is it an affordable or appropriate solution for rural electrification in Sub-Saharan African countries? Renewable and Sustainable Energy Reviews 60, 1405–1418.

Beltrame, T.F., Carvalho, D., Marder, L., Ulla, M.A., Marchesini, F.A., Bernardes, A.M., 2020. Comparison of different electrode materials for the nitrate electrocatalytic reduction in a dual-chamber cell. Journal of Environmental Chemical Engineering 8, 104120. https://doi.org/10.1016/j.jece.2020.104120

Beltrame, T.F., Zoppas, F.M., Gomes, M.C., Ferreira, J.Z., Marchesini, F.A., Bernardes, A.M., 2021. Electrochemical nitrate reduction of brines: Improving selectivity to N2 by the use of Pd/activated carbon fiber catalyst. Chemosphere 279, 130832. https://doi.org/10.1016/j.chemosphere.2021.130832

Bertaglia, T., M. Costa, C., Lanceros-Méndez, S., N. Crespilho, F., 2024. Eco-friendly, sustainable, and safe energy storage: a nature-inspired materials paradigm shift. Materials Advances. https://doi.org/10.1039/D4MA00363B

Bertocco, M., Parrino, S., Peruzzi, G., Pozzebon, A., 2023. Estimating volumetric water content in soil for IoUT contexts by exploiting RSSI-based augmented sensors via machine learning. Sensors 23, 2033.

Bhadola, P., Kunakhonnuruk, B., Kongbangkerd, A., Gupta, Y.M., 2022. Analysis of Microenvironment Data Using Low-Cost Portable Data Logger Based on a Microcontroller. ECS Trans. 107, 15099. https://doi.org/10.1149/10701.15099ecst

Bhattacharya, R., Bose, D., Yadav, J., Sharma, B., Sangli, E., Patel, A., Mukherjee, A., Ashutosh Singh, A., 2023. Bioremediation and bioelectricity from Himalayan rock soil in sediment-microbial fuel cell using carbon rich substrates. Fuel 341, 127019. https://doi.org/10.1016/j.fuel.2022.127019

Bhuvaneshwari, S., Sruthi, D., Sivasubramanian, V., Niranjana, K., Sugunabai, J., 2011. Development and characterization of chitosan film. Int. J. Eng. Res. Appl 1, 292–299.

Bimakr, F., Ginige, M.P., Kaksonen, A.H., Sutton, D.C., Puzon, G.J., Cheng, K.Y., 2018. Assessing graphite and stainless-steel for electrochemical sensing of biofilm growth in chlorinated drinking water systems. Sensors and Actuators B: Chemical 277, 526–534. https://doi.org/10.1016/j.snb.2018.09.005

Bird, L.J., Tender, L.M., Eddie, B., Oh, E., Phillips, D.A., Glaven, S.M., 2021. Microbial survival and growth on non-corrodible conductive materials. Environmental Microbiology 23, 7231–7244. https://doi.org/10.1111/1462-2920.15810

Biswas, A., Yin, S., Tursunniyaz, M., Karamimohammadi, N., Huang, J., Andrews, J., 2022. Geometrical Optimization of Printed Interdigitated Electrode Sensors to Improve Soil Moisture Sensitivity. IEEE Sensors Journal 22, 19162–19169. https://doi.org/10.1109/JSEN.2022.3200008

Bloch, P.-Y., Bloch, J.-F., Olejnik, K., Brissaud, D., 2024. Anisotropy and Fiber Orientation: A Key Player in the Lateral Imbibition of Cellulose Paper. Fibers 12, 56. https://doi.org/10.3390/fib12070056

Boada, M., Lázaro, A., Villarino, R., Girbau, D., 2018. Battery-Less Soil Moisture Measurement System Based on a NFC Device With Energy Harvesting Capability. IEEE Sensors Journal 18, 5541–5549. https://doi.org/10.1109/JSEN.2018.2837388

Boey, J.Y., Lee, C.K., Tay, G.S., 2022. Factors Affecting Mechanical Properties of Reinforced Bioplastics: A Review. Polymers 14, 3737. https://doi.org/10.3390/polym14183737

Borah, R., Hughson, F.R., Johnston, J., Nann, T., 2020. On battery materials and methods. Materials Today Advances 6, 100046. https://doi.org/10.1016/j.mtadv.2019.100046

Borah, S., Kumar, R., Pakhira, W., Mukherjee, S., 2020. Design and Analysis of Power Efficient IoT Based Capacitive Sensor System to Measure Soil Moisture, in: Paul, S., Verma, J. (Eds.), . Presented at the 2020 INTERNATIONAL CONFERENCE ON COMPUTATIONAL PERFORMANCE EVALUATION (COMPE-2020), pp. 182–188.

Borno, M.S.I., Sayeduzzaman, M., Elme, K.M., Islam, M.H., Rahman, M.A., 2021. An empirical analysis of Sustainable Earth-Battery. Energy Reports 7, 144–151.

Borowik, A., Wyszkowska, J., 2016. Soil moisture as a factor affecting the microbiological and biochemical activity of soil. Plant, Soil and Environment 62 (2016), 250–255. https://doi.org/10.17221/158/2016-PSE

Bouzek, K., Paidar, M., Sadilkova, A., Bergmann, H., 2001. Electrochemical reduction of nitrate in weakly alkaline solutions. Journal of Applied Electrochemistry 31, 1185–1193.

Bretel, G., Rull-Barrull, J., Nongbe, M.C., Terrier, J.-P., Le Grognec, E., Felpin, F.-X., 2018. Hydrophobic Covalent Patterns on Cellulose Paper through Photothiol-X Ligations. ACS Omega 3, 9155–9159. https://doi.org/10.1021/acsomega.8b01317

Briciu-Burghina, C., Zhou, J., Ali, M.I., Regan, F., 2022. Demonstrating the potential of a low-cost soil moisture sensor network. Sensors 22, 987.

Brinkhoff, J., Hornbuckle, J., Quayle, W., Lurbe, C.B., Dowling, T., 2018. WiField, an IEEE 802.11-based agricultural sensor data gathering and logging platform. Presented at the Proceedings of the International Conference on Sensing Technology, ICST, pp. 1–6. https://doi.org/10.1109/ICSensT.2017.8304434

Brito dos Santos, F., Kaschuk, J., Banvillet, G., Jalaee, A., Rojas, O.J., Foster, E.J., 2024. Alternative proton exchange membrane based on a bicomponent anionic nanocellulose system. Carbohydrate Polymers 340, 122299. https://doi.org/10.1016/j.carbpol.2024.122299

Brockett, B.F.T., Prescott, C.E., Grayston, S.J., 2012. Soil moisture is the major factor influencing microbial community structure and enzyme activities across seven biogeoclimatic zones in western Canada. Soil Biology and Biochemistry 44, 9–20. https://doi.org/10.1016/j.soilbio.2011.09.003

Bu, X., Wei, R., Cai, Z., Quan, Q., Zhang, H., Wang, W., Li, F., Yip, S.P., Meng, Y., Chan, K.S., Wang, X., Ho, J.C., 2021. More than physical support: The effect of nickel foam corrosion on electrocatalytic performance. Applied Surface Science 538, 147977. https://doi.org/10.1016/j.apsusc.2020.147977

Burke, L.D., Sharna, R., 2007. Surface active state involvement in electrocatalytic reductions at copper in acid solution. J Appl Electrochem 37, 1119–1128. https://doi.org/10.1007/s10800-007-9370-9

Calamita, G., Perrone, A., Brocca, L., Onorati, B., Manfreda, S., 2015. Field test of a multi-frequency electromagnetic induction sensor for soil moisture monitoring in southern Italy test sites. Journal of Hydrology 529, 316–329. https://doi.org/10.1016/j.jhydrol.2015.07.023

Caldwell, T.G., Cosh, M.H., Evett, S.R., Edwards, N., Hofman, H., Illston, B.G., Meyers, T., Skumanich, M., Sutcliffe, K., 2022. In situ Soil Moisture Sensors in Undisturbed Soils. Journal of Visualized Experiments 2022. https://doi.org/10.3791/64498

Campa-Siqueiros, P., Madera-Santana, T.J., Ayala-Zavala, J.F., López-Cervantes, J., Castillo-Ortega, M.M., Herrera-Franco, P.J., 2020. Nanofibers of gelatin and polivinyl-alcohol-chitosan for wound dressing application: fabrication and characterization. Polímeros 30, e2020006. https://doi.org/10.1590/0104-1428.07919

Cattarin, S., 1992. Electrochemical reduction of nitrogen oxyanions in 1 M sodium hydroxide solutions at silver, copper and CuInSe2 electrodes. J Appl Electrochem 22, 1077–1081. https://doi.org/10.1007/BF01029588

Chandrasekhar, K., 2019. Chapter 3.5 - Effective and Nonprecious Cathode Catalysts for Oxygen Reduction Reaction in Microbial Fuel Cells, in: Mohan, S.V., Varjani, S., Pandey, A. (Eds.), Microbial Electrochemical Technology, Biomass, Biofuels and Biochemicals. Elsevier, pp. 485–501. https://doi.org/10.1016/B978-0-444-64052-9.00019-4

Chang, H.-C., Gustave, W., Yuan, Z.-F., Xiao, Y., Chen, Z., 2020. One-step fabrication of binder-free air cathode for microbial fuel cells by using balsa wood biochar. Environmental Technology & Innovation 18, 100615. https://doi.org/10.1016/j.eti.2020.100615

Chang, Z., Zhang, F., Xiong, J., Ma, J., Jin, B., Zhang, D., 2022. Sensor-free Soil Moisture Sensing Using LoRa Signals. Proc. ACM Interact. Mob. Wearable Ubiquitous Technol. 6, 1–27. https://doi.org/10.1145/3534608

Chanwattanapong, W., Hongdumnuen, S., Kumkhet, B., Junon, S., Sangmahamad, P., 2021. LoRa Network Based Multi-Wireless Sensor Nodes and LoRa Gateway for Agriculture Application. Presented at the Proceedings - 2021 Research, Invention, and Innovation

Congress: Innovation Electricals and Electronics, RI2C 2021, pp. 133–136. https://doi.org/10.1109/RI2C51727.2021.9559804

Chatterjee, A., Lobato, C.N., Zhang, H., Bergne, A., Esposito, V., Yun, S., Insinga, A.R., Christensen, D.V., Imbaquingo, C., Bjørk, R., Ahmed, H., Ahmad, M., Ho, C.Y., Madsen, M., Chen, J., Norby, P., Chiabrera, F.M., Gunkel, F., Ouyang, Z., Pryds, N., 2023. Powering internet-of-things from ambient energy: a review. J. Phys. Energy 5, 022001. https://doi.org/10.1088/2515-7655/acb5e6

Chaudhari, B.S., Zennaro, M., Borkar, S., 2020. LPWAN Technologies: Emerging Application Characteristics, Requirements, and Design Considerations. Future Internet 12, 46. https://doi.org/10.3390/fi12030046

Chauruka, M., Duker, A., Prasad, P., Zaag, P.V. der, 2023. Endogenous irrigation in arid Zimbabwe: farmer perceptions of livelihood benefits and barriers to scaling. Water SA 49, 355–362.

Chen, C., Hu, L., 2018. Nanocellulose toward Advanced Energy Storage Devices: Structure and Electrochemistry. Accounts of Chemical Research 51, 3154–3165. https://doi.org/10.1021/acs.accounts.8b00391

Chen, H., Zhu, Z., Huang, R., Zhang, Y.-H.P., 2016. Coenzyme Engineering of a Hyperthermophilic 6-Phosphogluconate Dehydrogenase from NADP+ to NAD+ with Its Application to Biobatteries. Sci Rep 6, 36311. https://doi.org/10.1038/srep36311

Chen, J.-Q., Ye, X.-X., Zhou, D., Chen, Y.-X., 2023. Roles of Copper in Nitrate Reduction at Copper-Modified Ru/C Catalysts. Journal of Physical Chemistry C 127, 2918–2928. https://doi.org/10.1021/acs.jpcc.2c07813

Chen, P.-Y., Chang, Y.-T., 2012. Voltammetric study and electrodeposition of copper in 1-butyl-3- methylimidazolium salicylate ionic liquid. Electrochimica Acta 75, 339–346. https://doi.org/10.1016/j.electacta.2012.05.024

Chen, Q., Song, Y., An, Y., Lu, Y., Zhong, G., 2024. Soil Microorganisms: Their Role in Enhancing Crop Nutrition and Health. Diversity 16, 734. https://doi.org/10.3390/d16120734

Chen, S., Patil, S.A., Schröder, U., 2018. Substrate Crossover Effect and Performance Regeneration of the Biofouled Rotating Air-Cathode in Microbial Fuel Cell. Front. Energy Res. 6. https://doi.org/10.3389/fenrg.2018.00085

Chen, S.-S., Hu, C.-W., Yu, I.-F., Liao, Y.-C., Yang, J.-T., 2014. Origami paper-based fluidic batteries for portable electrophoretic devices. Lab Chip 14, 2124–2130. https://doi.org/10.1039/C4LC00091A

Chen, W., Feng, Y., Cardamis, M., Jiang, C., Song, W., Ghannoum, O., Hu, W., 2022. Soil moisture sensing with mmWave radar. Presented at the mmNets 2022 - Proceedings of the Millimeter-Wave Networks and Sensing Systems, Part of MobiCom 2022, pp. 19–24. https://doi.org/10.1145/3555077.3556472

Chen, Y.X., Zhang, Y., Liu, H.Y., Sharma, K.R., Chen, G.H., 2004. Hydrogen-based tubular catalytic membrane for removing nitrate from groundwater. Environmental Technology 25, 227–234. https://doi.org/10.1080/09593330409355456

Chen, Z., Zhang, Y., Cao, T., Yao, K., 2023. Electrochemical removal of nitrate using Co/Ni bimetallic electrode: High N2 selectivity and long-term stability. Process Safety and Environmental Protection 179, 384–393. https://doi.org/10.1016/j.psep.2023.09.035

Cheng, K., Zhang, F., Sun, F., Chen, H., Percival Zhang, Y.-H., 2015. Doubling Power Output of Starch Biobattery Treated by the Most Thermostable Isoamylase from an Archaeon Sulfolobus tokodaii. Sci Rep 5, 13184. https://doi.org/10.1038/srep13184

Cheng, M., Fan, H., Song, Y., Cui, Y., Wang, R., 2017. Interconnected hierarchical NiCo2O4 microspheres as high-performance electrode materials for supercapacitors. Dalton Trans. 46, 9201–9209. https://doi.org/10.1039/C7DT01289F

Cherian, R.M., Kargarzadeh, H., Rosli, N.A., Jose, C., Thomas, S., 2022. Tuning the Hydrophilic/Hydrophobic Behavior of Biopolymers, in: Handbook of Biopolymers. Springer, Singapore, pp. 1–35. https://doi.org/10.1007/978-981-16-6603-2_14-1

Chiellini, E., Corti, A., D'Antone, S., Solaro, R., 2003. Biodegradation of poly (vinyl alcohol) based materials. Progress in Polymer Science 28, 963–1014. https://doi.org/10.1016/S0079-6700(02)00149-1

Cho, S.-J., Choi, K.-H., Yoo, J.-T., Kim, J.-H., Lee, Y.-H., Chun, S.-J., Park, S.-B., Choi, D.-H., Wu, Q., Lee, Sun-Young, Lee, Sang-Young, 2015. Hetero-Nanonet Rechargeable Paper Batteries: Toward Ultrahigh Energy Density and Origami Foldability. Advanced Functional Materials 25, 6029–6040. https://doi.org/10.1002/adfm.201502833

Choi, Y.-J., Jung, E.-K., Park, H.-J., Paik, S.R., Jung, S.-H., Kim, S.-H., 2004. Construction of Microbial Fuel Cells Using Thermophilic Microorganisms, Bacillus licheniformis and Bacillus thermoglucosidasius. Bulletin of the Korean Chemical Society 25, 813–818. https://doi.org/10.5012/bkcs.2004.25.6.813

Choy, K.L., 2003. Chemical vapour deposition of coatings. Progress in Materials Science 48, 57–170. https://doi.org/10.1016/S0079-6425(01)00009-3

Come Zebra, E.I., van der Windt, H.J., Nhumaio, G., Faaij, A.P.C., 2021. A review of hybrid renewable energy systems in mini-grids for off-grid electrification in developing countries. Renewable and Sustainable Energy Reviews 144, 111036. https://doi.org/10.1016/j.rser.2021.111036

Cornet, A.J., Homborg, A.M., Anusuyadevi, P.R., 't Hoen-Velterop, L., Mol, J.M.C., 2024. Unravelling corrosion degradation of aged aircraft components protected by chromate-based coatings. Engineering Failure Analysis 159, 108070. https://doi.org/10.1016/j.engfailanal.2024.108070

Costa, G.F., Winkler, M., Mariano, T., Pinto, M.R., Messias, I., Souza, J.B., Neckel, I.T., Santos, M.F.C., Tormena, C.F., Singh, N., Nagao, R., 2024. Identifying the active site of Cu/Cu2O for electrocatalytic nitrate reduction reaction to ammonia. Chem Catalysis 4, 100850. https://doi.org/10.1016/j.checat.2023.100850

Couto, A.B., Baldan, M.R., Ferreira, N.G., 2012. Copper photoelectrodeposition onto boron doped diamond electrodes at different doping level to enhance nitrate electroreduction. Presented at the Materials Research Society Symposium Proceedings, pp. 45–50. https://doi.org/10.1557/opl.2012.338

Couto, A.B., Oishi, S.S., Sardinha, A.F., Ferreira, N.G., 2017. Electrocatalytic performance of three dimensional electrode Cu/reduced graphene oxide/carbon fiber for nitrate reduction. Presented at the ECS Transactions, pp. 1081–1087. https://doi.org/10.1149/08010.1081ecst

Couto, A.B., Santos, L.C.D., Matsushima, J.T., Baldan, M.R., Ferreira, N.G., 2011. Hydrogen and oxygen plasma enhancement in the Cu electrodeposition and consolidation processes on BDD electrode applied to nitrate reduction. Applied Surface Science 257, 10141–10146. https://doi.org/10.1016/j.apsusc.2011.07.006

Cox, J.A., Litwinski, G.R., 1979. Voltammetric ion selective electrode for the determination of nitrate. Anal. Chem. 51, 554–556. https://doi.org/10.1021/ac50040a024

Cross, J., Murray, D., 2018. The afterlives of solar power: Waste and repair off the grid in Kenya. Energy Research & Social Science 44, 100–109. https://doi.org/10.1016/j.erss.2018.04.034

Curry, C., 2017. Lithium-ion battery costs and market. Bloomberg New Energy Finance 5, 43.

Dahal, S., Yilma, W., Sui, Y., Atreya, M., Bryan, S., Davis, V., Whiting, G.L., Khosla, R., 2020. Degradability of Biodegradable Soil Moisture Sensor Components and Their Effect on Maize (Zea mays L.) Growth. Sensors 20, 6154. https://doi.org/10.3390/s20216154

Das, G., Kang, D., Yoon, H.H., 2019. A Proton Conducting Composite Membrane based on Polyvinyl Alcohol and Polyaniline-intercalated Graphene Oxide. J. Korean Phys. Soc. 74, 384–388. https://doi.org/10.3938/jkps.74.384

Daskalakis, S.-N., Kimionis, J., Collado, A., Tentzeris, M.M., Georgiadis, A., 2017. Ambient FM backscattering for smart agricultural monitoring, in: 2017 IEEE MTT-S International Microwave Symposium (IMS). Presented at the 2017 IEEE MTT-S International Microwave Symposium (IMS), pp. 1339–1341. https://doi.org/10.1109/MWSYM.2017.8058860

Davis, A.N., Parui, K., Hasan, A.M.M., Pineda, L.A., Langhout, J.D., Treaster, K.A., Butala, M.M., Evans, A.M., 2024. Cross-linking organic cathodes enhances stability at the expense of ionic accessibility. J. Mater. Chem. A 12, 28874–28881. https://doi.org/10.1039/D4TA03617D

de Groot, M.T., Koper, M.T.M., 2004. The influence of nitrate concentration and acidity on the electrocatalytic reduction of nitrate on platinum. Journal of Electroanalytical Chemistry 562, 81–94. https://doi.org/10.1016/j.jelechem.2003.08.011

de Melo, D.A., Silva, P.C., da Costa, A.R., Delmond, J.G., Ferreira, A.F.A., de Souza, J.A., de Oliveira-Júnior, J.F., da Silva, J.L.B., da Rosa Ferraz Jardim, A.M., Giongo, P.R., Ferreira, M.B., de Assunção Montenegro, A.A., de Oliveira, H.F.E., da Silva, T.G.F., da Silva, M.V., 2023. Development and Automation of a Photovoltaic-Powered Soil Moisture Sensor for Water Management. Hydrology 10. https://doi.org/10.3390/hydrology10080166

De Vooys, A.C.A., Van Santen, R.A., Van Veen, J.A.R., 2000. Electrocatalytic reduction of NO-3 on palladium/copper electrodes. Journal of Molecular Catalysis A: Chemical 154, 203–215. https://doi.org/10.1016/S1381-1169(99)00375-1

Dejang, N., Klinbumrung, A., Sirirak, R., 2025. Effective CuSO4 Concentration on Phase Formation and Optical Characteristics of Electrodeposited Ni-Cu Alloy. Trends in Sciences 22, 8897–8897. https://doi.org/10.48048/tis.2025.8897

Della Rocca, C., Belgiorno, V., Meriç, S., 2007. Overview of in-situ applicable nitrate removal processes. Desalination 204, 46–62.

Deng, F., Zuo, P., Wen, K., Wu, X., 2020. Novel soil environment monitoring system based on RFID sensor and LoRa. Computers and Electronics in Agriculture 169, 105169. https://doi.org/10.1016/j.compag.2019.105169

Deng, Q., Li, X., Zuo, Jiane., Ling, A., Logan, B.E., 2010. Power generation using an activated carbon fiber felt cathode in an upflow microbial fuel cell. Journal of Power Sources 195, 1130–1135. https://doi.org/10.1016/j.jpowsour.2009.08.092

Depuydt, S., Van der Bruggen, B., 2024. Green Synthesis of Cation Exchange Membranes: A Review. Membranes (Basel) 14, 23. https://doi.org/10.3390/membranes14010023

Devapal, D., 2020. Smart Agro Farm Solar Powered Soil and Weather Monitoring System for Farmers. Presented at the MATERIALS TODAY-PROCEEDINGS, pp. 1843–1854.

Dey, S., Kalansuriya, P., Karmakar, N.C., 2015. A novel time domain reflectometry based chipless RFID soil moisture sensor. Presented at the 2015 IEEE MTT-S International Microwave Symposium, IMS 2015. https://doi.org/10.1109/MWSYM.2015.7166925

Dharmadhikari, S., Ghosh, P., Ramachandran, M., 2018. Synthesis of proton exchange membranes for dual-chambered microbial fuel cells. Journal of the Serbian Chemical Society 83, 611–623.

Dima, G.E., De Vooys, A.C.A., Koper, M.T.M., 2003. Electrocatalytic reduction of nitrate at low concentration on coinage and transition-metal electrodes in acid solutions. Journal of Electroanalytical Chemistry 554, 15–23.

Ding, J., Chandra, R., 2019. Towards Low Cost Soil Sensing Using Wi-Fi, in: The 25th Annual International Conference on Mobile Computing and Networking. Presented at the MobiCom '19: The 25th Annual International Conference on Mobile Computing and Networking, ACM, Los Cabos Mexico, pp. 1–16. https://doi.org/10.1145/3300061.3345440

Doglioni, M., Nardello, M., Brunelli, D., 2024. Plant Microbial Fuel Cells: Energy Sources and Biosensors for battery-Free Smart Agriculture. IEEE Transactions on AgriFood Electronics 2, 460–470. https://doi.org/10.1109/TAFE.2024.3417644

Donovan, C., Dewan, A., Heo, D., Beyenal, H., 2008. Batteryless, Wireless Sensor Powered by a Sediment Microbial Fuel Cell. Environ. Sci. Technol. 42, 8591–8596. https://doi.org/10.1021/es801763g

Dorel, S., Gmal Osman, M., Strejoiu, C.-V., Lazaroiu, G., 2023. Exploring Optimal Charging Strategies for Off-Grid Solar Photovoltaic Systems: A Comparative Study on Battery Storage Techniques. Batteries 9, 470. https://doi.org/10.3390/batteries9090470

Dorigo, W.A., Wagner, W., Hohensinn, R., Hahn, S., Paulik, C., Xaver, A., Gruber, A., Drusch, M., Mecklenburg, S., van Oevelen, P., Robock, A., Jackson, T., 2011. The International Soil Moisture Network: a data hosting facility for global in situ soil moisture measurements. Hydrology and Earth System Sciences 15, 1675–1698. https://doi.org/10.5194/hess-15-1675-2011

Du, Z., Li, H., Gu, T., 2007. A state of the art review on microbial fuel cells: A promising technology for wastewater treatment and bioenergy. Biotechnology Advances 25, 464–482. https://doi.org/10.1016/j.biotechadv.2007.05.004

Dureisseix, D., 2012. An overview of mechanisms and patterns with origami. International Journal of Space Structures 27, 1–14.

Durga, N., Schmitter, P., Ringler, C., Mishra, S., Magombeyi, M.S., Ofosu, A., Pavelic, P., Hagos, F., Melaku, D., Verma, S., Minh, T., Matambo, C., 2024. Barriers to the uptake of solar-powered irrigation by smallholder farmers in sub-saharan Africa: A review. Energy Strategy Reviews 51, 101294. https://doi.org/10.1016/j.esr.2024.101294

Dziegielowski, J., Bregu, G., Hulse, L., Di Lorenzo, M., 2022. Assessing the effect of the electrode orientation on the performance of soil microbial fuel cells. Presented at the E3S Web of Conferences. https://doi.org/10.1051/e3sconf/202233408003

Economou, A., Kokkinos, C., Prodromidis, M., 2018. Flexible plastic, paper and textile lab-on-a chip platforms for electrochemical biosensing. Lab on a Chip 18, 1812–1830. https://doi.org/10.1039/C8LC00025E

Ehsani, M., Kalugin, D., Doan, H., Lohi, A., Abdelrasoul, A., 2022. Bio-Sourced and Biodegradable Membranes. Applied Sciences 12, 12837. https://doi.org/10.3390/app122412837

Eiler, K., Krawiec, H., Kozina, I., Sort, J., Pellicer, E., 2020. Electrochemical characterisation of multifunctional electrocatalytic mesoporous Ni-Pt thin films in alkaline and acidic media. Electrochimica Acta 359, 136952. https://doi.org/10.1016/j.electacta.2020.136952

El Midaoui, A., Elhannouni, F., Taky, M., Chay, L., Menkouchi Sahli, M.A., Echihabi, L., Hafsi, M., 2002. Optimization of nitrate removal operation from ground water by electrodialysis. Separation and Purification Technology 29, 235–244. https://doi.org/10.1016/S1383-5866(02)00092-8

Elgrishi, N., Rountree, K.J., McCarthy, B.D., Rountree, E.S., Eisenhart, T.T., Dempsey, J.L., 2018. A Practical Beginner's Guide to Cyclic Voltammetry. J. Chem. Educ. 95, 197–206. https://doi.org/10.1021/acs.jchemed.7b00361

Eljaddi, T., Giordano, L., Roizard, D., 2021. Towards the synthesis of greener membranes: Interest of PVA as porous support for membrane application in gas and liquid separations. Separation and Purification Technology 263, 118357. https://doi.org/10.1016/j.seppur.2021.118357

Ellabban, O., Abu-Rub, H., Blaabjerg, F., 2014. Renewable energy resources: Current status, future prospects and their enabling technology. Renewable and Sustainable Energy Reviews 39, 748–764. https://doi.org/10.1016/j.rser.2014.07.113

Epron, F., Gauthard, F., Barbier, J., 2002. Influence of oxidizing and reducing treatments on the metal-metal interactions and on the activity for nitrate reduction of a Pt-Cu bimetallic catalyst. Applied Catalysis A: General 237, 253–261. https://doi.org/10.1016/S0926-860X(02)00331-9

Epron, F., Gauthard, F., Pinéda, C., Barbier, J., 2001. Catalytic Reduction of Nitrate and Nitrite on Pt-Cu/Al2O3 Catalysts in Aqueous Solution: Role of the Interaction between Copper and Platinum in the Reaction. Journal of Catalysis 198, 309–318. https://doi.org/10.1006/jcat.2000.3138

Faheem, M., Ashraf, M.W., Butt, R.A., Raza, B., Ngadi, Md.A., Gungor, V.C., 2019. Ambient Energy Harvesting for Low Powered Wireless Sensor Network based Smart Grid Applications, in: 2019 7th International Istanbul Smart Grids and Cities Congress and Fair (ICSG). Presented at the 2019 7th International Istanbul Smart Grids and Cities Congress and Fair (ICSG), pp. 26–30. https://doi.org/10.1109/SGCF.2019.8782404

Fan, M., Gong, L., Sun, J., Wang, D., Bi, F., Gong, Z., 2018. Killing Two Birds with One Stone: Coating Ag NPs Embedded Filter Paper with Chitosan for Better and Durable Point-of-Use Water Disinfection. ACS Appl. Mater. Interfaces 10, 38239–38245. https://doi.org/10.1021/acsami.8b13985

Farooqui, M.F., Kishk, A.A., 2018. Low-Cost 3D-Printed Wireless Soil Moisture Sensor. Presented at the Proceedings of IEEE Sensors. https://doi.org/10.1109/ICSENS.2018.8589802

Feng, A., Hu, Y., Yang, X., Lin, H., Wang, Q., Xu, J., Liu, A., Wu, G., Li, Q., 2024. ZnO Nanowire Arrays Decorated with Cu Nanoparticles for High-Efficiency Nitrate to Ammonia Conversion. ACS Catal. 14, 5911–5923. https://doi.org/10.1021/acscatal.3c04398

Feng, Yiyang, Liu, X., Yi, Z., Tan, H., Wang, L., Hou, F., Liang, J., 2022. Ni-nanoparticle-modified Cu nanowires for enhanced electrocatalytic nitrate removal. Surface Innovations 10, 402–410. https://doi.org/10.1680/jsuin.22.00040

Feng, Yuda, Xie, Y., Ganesan, D., Xiong, J., 2022. LTE-Based Low-Cost and Low-Power Soil Moisture Sensing. Presented at the Proceedings of the 20th ACM Conference on Embedded Networked Sensor Systems, pp. 421–434.

Ferdous, R.Md., Reza, A.W., Siddiqui, M.F., 2016. Renewable energy harvesting for wireless sensors using passive RFID tag technology: A review. Renewable and Sustainable Energy Reviews 58, 1114–1128. https://doi.org/10.1016/j.rser.2015.12.332

Ferrarezi, R.S., Dove, S.K., van Iersel, M.W., 2015. An automated system for monitoring soil moisture and controlling irrigation using low-cost open-source microcontrollers. HortTechnology 25, 110–118.

Filipović, A., 2020. Water Plant and Soil Relation under Stress Situations, in: Soil Moisture Importance. IntechOpen. https://doi.org/10.5772/intechopen.93528

Fraiwan, A., Choi, S., 2014. Bacteria-powered battery on paper. Phys. Chem. Chem. Phys. 16, 26288–26293. https://doi.org/10.1039/C4CP04804K

Fraiwan, A., Kwan, L., Choi, S., 2016. A disposable power source in resource-limited environments: A paper-based biobattery generating electricity from wastewater. Biosensors and Bioelectronics 85, 190–197. https://doi.org/10.1016/j.bios.2016.05.022

Fraiwan, A., Mukherjee, S., Sundermier, S., Choi, S., 2013. A microfabricated paper-based microbial fuel cell, in: 2013 IEEE 26th International Conference on Micro Electro Mechanical

Systems (MEMS). Presented at the 2013 IEEE 26th International Conference on Micro Electro Mechanical Systems (MEMS), pp. 809–812. https://doi.org/10.1109/MEMSYS.2013.6474366

Fraiwan, Arwa, Mukherjee, S., Sundermier, S., Lee, H.-S., Choi, S., 2013. A paper-based microbial fuel cell: Instant battery for disposable diagnostic devices. Biosensors and Bioelectronics 49, 410–414. https://doi.org/10.1016/j.bios.2013.06.001

G. M. Iyer, A. -M. Zaccarin, R. H. Olsson, K. T. Turner, 2022. Fabrication and Characterization of Cellulose-Based Materials for Biodegradable Soil Moisture Sensors, in: 2022 IEEE Sensors. Presented at the 2022 IEEE Sensors, pp. 1–4. https://doi.org/10.1109/SENSORS52175.2022.9967089

Gagliardi, G.G., Borello, D., Cosentini, C., Barra Caracciolo, A., Aimola, G., Ancona, V., Ieropoulos, I.A., Garbini, G.L., Rolando, L., Grenni, P., 2024. Microbial fuel cells with polychlorinated biphenyls contaminated soil as electrolyte: energy performance and decontamination potential in presence of compost. Journal of Power Sources 613, 234878. https://doi.org/10.1016/j.jpowsour.2024.234878

Galiano, F., Briceño, K., Marino, T., Molino, A., Christensen, K.V., Figoli, A., 2018. Advances in biopolymer-based membrane preparation and applications. Journal of Membrane Science 564, 562–586. https://doi.org/10.1016/j.memsci.2018.07.059

Gambhir, S., Jalili, R., Officer, D.L., Wallace, G.G., 2015. Chemically converted graphene: scalable chemistries to enable processing and fabrication. NPG Asia Mater 7, e186–e186. https://doi.org/10.1038/am.2015.47

Ganchev, M., Gergova, R., Terziyska, P., Popkirov, G., Vitanov, P., 2021. Direct thermal evaporation of thin films copper (I) bromide. Materials Today: Proceedings 37, A16–A20. https://doi.org/10.1016/j.matpr.2021.05.244

Gao, J., Huang, X., Xue, H., Tang, L., Li, R.K.Y., 2017. Facile preparation of hybrid microspheres for super-hydrophobic coating and oil-water separation. Chemical Engineering Journal 326, 443–453. https://doi.org/10.1016/j.cej.2017.05.175

Gao, W., Gao, L., Li, D., Huang, K., Cui, L., Meng, J., Liang, J., 2018. Removal of nitrate from water by the electrocatalytic denitrification on the Cu-Bi electrode. Journal of Electroanalytical Chemistry 817, 202–209. https://doi.org/10.1016/j.jelechem.2018.04.006

Gao, W., Gao, L., Meng, J., Li, D., Guan, Y., Cui, L., Shen, X., Liang, J., 2019. Preparation of a novel Cu-Sn-Bi cathode and performance on nitrate electroreduction. Water Science and Technology 79, 198–206. https://doi.org/10.2166/wst.2019.049

Gao, X., Liu, K., Su, C., Zhang, W., Dai, Y., Parkin, I.P., Carmalt, C.J., He, G., 2024. From bibliometric analysis: 3D printing design strategies and battery applications with a focus on zinc-ion batteries. SmartMat 5, e1197. https://doi.org/10.1002/smm2.1197

Gao, Y., Cho, J.H., Ryu, J., Choi, S., 2020. A scalable yarn-based biobattery for biochemical energy harvesting in smart textiles. Nano Energy 74, 104897. https://doi.org/10.1016/j.nanoen.2020.104897

Gao, Y., Choi, S., 2017. Versatile 3-D stacking of 2-D paper-based biobatteries. Presented at the Proceedings of the IEEE International Conference on Micro Electro Mechanical Systems (MEMS), pp. 448–451. https://doi.org/10.1109/MEMSYS.2017.7863439

Gao, Y., Mohammadifar, M., Choi, S., 2019. From Microbial Fuel Cells to Biobatteries: Moving toward On-Demand Micropower Generation for Small-Scale Single-Use Applications. Advanced Materials Technologies 4, 1900079. https://doi.org/10.1002/admt.201900079

García, B., Saiz-Poseu, J., Gras-Charles, R., Hernando, J., Alibés, R., Novio, F., Sedó, J., Busqué, F., Ruiz-Molina, D., 2014. Mussel-inspired hydrophobic coatings for water-repellent textiles and oil removal. ACS Applied Materials and Interfaces 6, 17616–17625. https://doi.org/10.1021/am503733d

Ghamsarizade, R., Ramezanzadeh, B., Mohammadloo, H.E., 2023. Chapter 12 - Corrosion measurements in coatings and paintings, in: Aslam, J., Verma, C., Mustansar Hussain, C. (Eds.), Electrochemical and Analytical Techniques for Sustainable Corrosion Monitoring. Elsevier, pp. 217–264. https://doi.org/10.1016/B978-0-443-15783-7.00008-6

Ghanbarzadeh, B., Almasi, H., Ghanbarzadeh, B., Almasi, H., 2013. Biodegradable Polymers, in: Biodegradation - Life of Science. IntechOpen. https://doi.org/10.5772/56230

Gianessi, S., Polo, M., Stevanato, L., Lunardon, M., Ahmed, H.S., Weltin, G., Toloza, A., Budach, C., Biro, P., Francke, T., Heistermann, M., Oswald, S.E., Fulajtar, E., Dercon, G., Heng, L.K., Baroni, G., 2021. Assessment of a new non-invasive soil moisture sensor based on cosmic-ray neutrons. Presented at the 2021 IEEE International Workshop on Metrology for Agriculture and Forestry, MetroAgriFor 2021 - Proceedings, pp. 290–294. https://doi.org/10.1109/MetroAgriFor52389.2021.9628451

Giles, M., Morley, N., Baggs, E.M., Daniell, T.J., 2012. Soil nitrate reducing processes – drivers, mechanisms for spatial variation, and significance for nitrous oxide production. Front Microbiol 3, 407. https://doi.org/10.3389/fmicb.2012.00407

Gill, R., Hasan Albaadani, A.N., 2021. Developing a Low Cost Sensor Node using IoT Technology with Energy Harvester for Precision Agriculture. Presented at the Proceedings - 2nd International Conference on Smart Electronics and Communication, ICOSEC 2021, pp. 187–194. https://doi.org/10.1109/ICOSEC51865.2021.9591849

Gomaa, M.M., Requena-Leal, I., Elsharkawy, M.R.M., Rodrigo, M.A., Lobato, J., 2024. Eco-friendly non-fluorinated membranes for renewable energy storage. International Journal of Hydrogen Energy 90, 328–341. https://doi.org/10.1016/j.ijhydene.2024.09.431

Gonzalez-Gallardo, C.L., Morales-Hernández, J., Álvarez-Contreras, L., Arjona, N., Guerra-Balcázar, M., 2024. Electrochemical detection of creatinine on Cu/carbon paper electrodes obtained by physical vapor deposition. Journal of Applied Electrochemistry 54, 115–126. https://doi.org/10.1007/s10800-023-01943-7

Gonzalez-Guerrero, M., Gomez, F.A., 2019. An all-printed 3D-Zn/Fe3O4 paper battery. Sensors and Actuators B: Chemical 289, 226–233. https://doi.org/10.1016/j.snb.2019.03.097

González-Pabón, M., Cardeña, R., Cortón, E., Buitrón, G., 2021. Hydrogen production in two-chamber MEC using a low-cost and biodegradable poly(vinyl) alcohol/chitosan membrane. BIORESOURCE TECHNOLOGY 319. https://doi.org/10.1016/j.biortech.2020.124168

González-Pabón, M.J., Figueredo, F., Martínez-Casillas, D.C., Cortón, E., 2019. Characterization of a new composite membrane for point of need paper-based micro-scale microbial fuel cell analytical devices. PLoS One 14, e0222538. https://doi.org/10.1371/journal.pone.0222538

Gonzalez-Teruel, J., Jones, S., Robinson, D., Gimenez-Gallego, J., Zornoza, R., Torres-Sanchez, R., 2022. Measurement of the broadband complex permittivity of soils in the frequency domain with a low-cost Vector Network Analyzer and an Open-Ended coaxial probe. COMPUTERS AND ELECTRONICS IN AGRICULTURE 195. https://doi.org/10.1016/j.compag.2022.106847

González-Teruel, J.D., Torres-Sánchez, R., Blaya-Ros, P.J., Toledo-Moreo, A.B., Jiménez-Buendía, M., Soto-Valles, F., 2019. Design and calibration of a low-cost SDI-12 soil moisture sensor. Sensors (Switzerland) 19. https://doi.org/10.3390/s19030491

Gopalakrishnan, S., Waimin, J., Raghunathan, N., Bagchi, S., Shakouri, A., Rahimi, R., 2021. Battery-Less Wireless Chipless Sensor Tag for Subsoil Moisture Monitoring. IEEE Sensors Journal 21, 6071–6082. https://doi.org/10.1109/JSEN.2020.3039363

Gopalakrishnan, S., Waimin, J., Zareei, A., Sedaghat, S., Raghunathan, N., Shakouri, A., Rahimi, R., 2022. A biodegradable chipless sensor for wireless subsoil health monitoring. Scientific reports 12, 8011.

Goranova, D., Rashkov, R., Avdeev, G., Tonchev, V., 2016. Electrodeposition of Ni–Cu alloys at high current densities: details of the elements distribution. J Mater Sci 51, 8663–8673. https://doi.org/10.1007/s10853-016-0126-y

Greenman, J., Thorn, R., Willey, N., Ieropoulos, I., 2024. Energy harvesting from plants using hybrid microbial fuel cells; potential applications and future exploitation. Front Bioeng Biotechnol 12, 1276176. https://doi.org/10.3389/fbioe.2024.1276176

Guang, L., Koomson, D.A., Jingyu, H., Ewusi-Mensah, D., Miwornunyuie, N., 2020. Performance of Exoelectrogenic Bacteria Used in Microbial Desalination Cell Technology. Int J Environ Res Public Health 17, 1121. https://doi.org/10.3390/ijerph17031121

Guo, J., Brimley, P., Liu, M.J., Corson, E.R., Muñoz, C., Smith, W.A., Tarpeh, W.A., 2023. Mass Transport Modifies the Interfacial Electrolyte to Influence Electrochemical Nitrate Reduction. ACS Sustainable Chemistry and Engineering 11, 7882–7893. https://doi.org/10.1021/acssuschemeng.3c01057

Guo, Jing, Wang, Y., Li, S., Qin, Y., Meng, Y., Jiang, L., Huang, H., Shen, L., 2023. Chitosan hydrogel polyelectrolyte-modified cotton pad as dendrite-inhibiting separators for stable zinc anodes in aqueous zinc-ion batteries. Journal of Power Sources 580, 233392. https://doi.org/10.1016/j.jpowsour.2023.233392

Guo, W., Zhang, K., Liang, Z., Zou, R., Xu, Q., 2019. Electrochemical nitrogen fixation and utilization: theories, advanced catalyst materials and system design. Chemical Society Reviews 48, 5658–5716. https://doi.org/10.1039/C9CS00159J

Gupta, S., Patro, A., Mittal, Y., Dwivedi, S., Saket, P., Panja, R., Saeed, T., Martínez, F., Yadav, A.K., 2023. The race between classical microbial fuel cells, sediment-microbial fuel cells, plant-microbial fuel cells, and constructed wetlands-microbial fuel cells: Applications and

technology readiness level. Science of The Total Environment 879, 162757. https://doi.org/10.1016/j.scitotenv.2023.162757

Gupta, S.K., Singh, S.K., Kanga, S., Kumar, P., Meraj, G., Sahariah, D., Debnath, J., Chand, K., Sajan, B., Singh, S., 2024. Unearthing India's soil moisture anomalies: impact on agriculture and water resource strategies. Theor Appl Climatol. https://doi.org/10.1007/s00704-024-05088-1

Haldrup, S., Catalano, J., Hinge, M., Jensen, G.V., Pedersen, J.S., Bentien, A., 2016. Tailoring Membrane Nanostructure and Charge Density for High Electrokinetic Energy Conversion Efficiency. ACS Nano 10, 2415–2423. https://doi.org/10.1021/acsnano.5b07229

Halima, N.B., 2016. Poly(vinyl alcohol): review of its promising applications and insights into biodegradation. RSC Adv. 6, 39823–39832. https://doi.org/10.1039/C6RA05742J

Han, J.-H., Yun, K.-S., 2024. Real-Time Soil Moisture Monitoring Using a Graphene Oxide Sensor Powered by a Solar Cell-Based Energy Harvester. J. Electr. Eng. Technol. 19, 3331–3337. https://doi.org/10.1007/s42835-024-01790-2

Hansen, U.E., Nygaard, I., Dal Maso, M., 2022. The dark side of the sun: solar e-waste and environmental upgrading in the off-grid solar PV value chain, in: The Dark Side of Innovation. Routledge, pp. 35–55.

Hao, D., Chen, Z., Figiela, M., Stepniak, I., Wei, W., Ni, B.-J., 2021. Emerging alternative for artificial ammonia synthesis through catalytic nitrate reduction. Journal of Materials Science & Technology 77, 163–168. https://doi.org/10.1016/j.jmst.2020.10.056

Hardie, M., 2020. Review of Novel and Emerging Proximal Soil Moisture Sensors for Use in Agriculture. SENSORS 20. https://doi.org/10.3390/s20236934

Hart, R.W., White, H.S., Dunn, B., Rolison, D.R., 2003. 3-D Microbatteries. Electrochemistry Communications 5, 120–123. https://doi.org/10.1016/S1388-2481(02)00556-8

Hasırcı, V., Lewandrowski, K., Gresser, J.D., Wise, D.L., Trantolo, D.J., 2001. Versatility of biodegradable biopolymers: degradability and an in vivo application. Journal of Biotechnology, Tailored Biopolymers 86, 135–150. https://doi.org/10.1016/S0168-1656(00)00409-0

Hasnat, M.A., Ben Aoun, S., Rahman, M.M., Asiri, A.M., Mohamed, N., 2015. Lean Cu-immobilized Pt and Pd films/–H+ Conducting Membrane Assemblies: Relative Electrocatalytic Nitrate Reduction Activities. Journal of Industrial and Engineering Chemistry 28, 131–137. https://doi.org/10.1016/j.jiec.2015.02.008

Hassanzadeh, N., Langdon, T.G., 2023. Invited viewpoint: biodegradable Mg batteries. J Mater Sci 58, 13721–13743. https://doi.org/10.1007/s10853-023-08828-2

Haupt, D.R., Landwehr, L., Schumann, R., Hahn, L., Issa, M., Coskun, C., Kunz, U., Sievers, M., 2022. A New Reactor Concept for Single-Chamber Microbial Fuel Cells and Possible Anti-Fouling Strategies for Long-Term Operation. Microorganisms 10, 2421. https://doi.org/10.3390/microorganisms10122421

He, L., Yao, F., Zhong, Y., Tan, C., Hou, K., Pi, Z., Chen, S., Li, X., Yang, Q., 2022. Achieving high-performance electrocatalytic reduction of nitrate by N-rich carbon-encapsulated Ni-Cu

bimetallic nanoparticles supported nickel foam electrode. Journal of Hazardous Materials 436. https://doi.org/10.1016/j.jhazmat.2022.129253

Hoehler, T.M., 2011. Redox Potential, in: Encyclopedia of Astrobiology. Springer, Berlin, Heidelberg, pp. 1440–1441. https://doi.org/10.1007/978-3-642-11274-4_1356

Hong, M., Wang, Q., Sun, J., Wu, C., 2022. A highly active copper-nanoparticle-based nitrate reduction electrocatalyst prepared by in situ electrodeposition and annealing. Science of The Total Environment 827, 154349. https://doi.org/10.1016/j.scitotenv.2022.154349

Hou, M., Pu, Y., Qi, W., Tang, Y., Wan, P., Yang, X.J., Song, P., Fisher, A., 2018. Enhanced electrocatalytic reduction of aqueous nitrate by modified copper catalyst through electrochemical deposition and annealing treatment. Chemical Engineering Communications 205, 706–715. https://doi.org/10.1080/00986445.2017.1413357

Hou, T., Shan, T., Rong, H., Zhang, J., 2025. Nitrate Electroreduction to Ammonia Over Copper-based Catalysts. ChemSusChem 18, e202402331. https://doi.org/10.1002/cssc.202402331

Howell, T.A., 2001. Enhancing Water Use Efficiency in Irrigated Agriculture. Agronomy Journal 93, 281–289. https://doi.org/10.2134/agronj2001.932281x

Hsu, L., Mohamed, A., Ha, P.T., Bloom, J., Ewing, T., Arias-Thode, M., Chadwick, B., Beyenal, H., 2017. The Influence of Energy Harvesting Strategies on Performance and Microbial Community for Sediment Microbial Fuel Cells. J. Electrochem. Soc. 164, H3109. https://doi.org/10.1149/2.0171703jes

Hu, T., Wang, C., Wang, M., Li, C.M., Guo, C., 2021. Theoretical Insights into Superior Nitrate Reduction to Ammonia Performance of Copper Catalysts. ACS Catal. 11, 14417–14427. https://doi.org/10.1021/acscatal.1c03666

Hu, X., Tian, X., Lin, Y.-W., Wang, Z., 2019. Nickel foam and stainless steel mesh as electrocatalysts for hydrogen evolution reaction, oxygen evolution reaction and overall water splitting in alkaline media. RSC Adv. 9, 31563–31571. https://doi.org/10.1039/C9RA07258F

Huang, J., Zhang, Y., 2022. Essays on Conceptual Electrochemistry: I. Bridging Open-Circuit Voltage of Electrochemical Cells and Charge Distribution at Electrode–Electrolyte Interfaces. Front. Chem. 10. https://doi.org/10.3389/fchem.2022.938064

Hubbe, M.A., Sjöstrand, B., Lestelius, M., Håkansson, H., Swerin, A., Henriksson, G., 2024. Swelling of cellulosic fibers in aqueous systems: A review of chemical and mechanistic factors. BioResources 19, 6859–6945.

Hummes, D.N., Hunt, J., Hervé, B.B., Schneider, P.S., Montanari, P.M., 2023. A comparative study of different battery geometries used in electric vehicles. Latin American Journal of Energy Research 10, 94–114.

Hung, C.-H., Allu, S., Cobb, C.L., 2021. Modeling Current Density Non-Uniformities to Understand High-Rate Limitations in 3D Interdigitated Lithium-ion Batteries. J. Electrochem. Soc. 168, 100512. https://doi.org/10.1149/1945-7111/ac2ac5

Hwang, S., 2012. Nanocomposite monolayer of copper and lead on gold and its effect on nitrate electroreduction. International Journal of Electrochemical Science 7, 1820–1826.

Hyun, G., Ham, Y., Harding, J., Jeon, S., 2024. Towards optimal 3D battery electrode architecture: Integrating structural engineering with AI-driven optimization. Energy Storage Materials 69, 103395. https://doi.org/10.1016/j.ensm.2024.103395

Hyusein, C., Tsakova, V., 2023. Nitrate detection at Pd-Cu-modified carbon screen printed electrodes. Journal of Electroanalytical Chemistry 930, 117172.

Ince, R., Alper, F.M.P., Yukselici, M.H., Asikoglu, A., Allahverdi, C., 2012. CdTe nanocrystals studied through in-situ electro-modulation spectroscopy. Presented at the International Conference on Oxide Materials for Electronic Engineering, OMEE 2012, pp. 75–76. https://doi.org/10.1109/OMEE.2012.6464793

Ingrao, C., Strippoli, R., Lagioia, G., Huisingh, D., 2023. Water scarcity in agriculture: An overview of causes, impacts and approaches for reducing the risks. Heliyon 9, e18507. https://doi.org/10.1016/j.heliyon.2023.e18507

Iqbal, U., Bakhsh, A., Shahid, M.A., Shah, S.H.H., Ali, S., 2020. Development of low cost indigenized soil moisture sensors for precision irrigation. Pakistan Journal of Agricultural Sciences 57, 205–217. https://doi.org/10.21162/PAKJAS/20.9154

Iribarren Anacona, P., Luján, J.P., Azócar, G., Mazzorana, B., Medina, K., Durán, G., Rojas, I., Loarte, E., 2023. Arduino data loggers: A helping hand in physical geography. The Geographical Journal 189, 314–328. https://doi.org/10.1111/geoj.12480

Isacsson, P., Björk, E., Capanema, E., Granberg, H., Engquist, I., 2024. Electrochemical characteristics of lignin in CTMP for paper battery electrodes. ChemSusChem e202400222.

Islam, Md.M., Abu Nayem, S.M., Shah, S.S., Islam, Md.Z., Aziz, Md.A., Saleh Ahammad, A.J., 2025. Electrochemical Selective Nitrate Reduction: Pathways to Nitrogen and Ammonia Production. The Chemical Record 25, e202400206. https://doi.org/10.1002/tcr.202400206

Ivars-Barceló, F., Zuliani, A., Fallah, M., Mashkour, M., Rahimnejad, M., Luque, R., 2018. Novel Applications of Microbial Fuel Cells in Sensors and Biosensors. Applied Sciences 8, 1184. https://doi.org/10.3390/app8071184

Iyer, G.M., Zaccarin, A.-M., Olsson, R.H., Turner, K.T., 2022. Fabrication and Characterization of Cellulose-Based Materials for Biodegradable Soil Moisture Sensors. Presented at the Proceedings of IEEE Sensors. https://doi.org/10.1109/SENSORS52175.2022.9967089

Jadhav, D.A., Pandit, S., Sonawane, J.M., Gupta, P.K., Prasad, R., Chendake, A.D., 2021. Effect of membrane biofouling on the performance of microbial electrochemical cells and mitigation strategies. Bioresource Technology Reports 15, 100822. https://doi.org/10.1016/j.biteb.2021.100822

Jain, P., Choudhury, S.B., Bhatt, P., Sarangi, S., Pappula, S., 2020. Maximising Value of Frugal Soil Moisture Sensors for Precision Agriculture Applications. Presented at the 2020 IEEE / ITU International Conference on Artificial Intelligence for Good, AI4G 2020, pp. 63–70. https://doi.org/10.1109/AI4G50087.2020.9311008

Jain, P., Vijaygopalan, K., 2010. RFID and wireless sensor networks. Proceedings of ASCNT–2010, CDAC, Noida, India 1–11.

Jamroen, C., Komkum, P., Fongkerd, C., Krongpha, W., 2020. An intelligent irrigation scheduling system using low-cost wireless sensor network toward sustainable and precision agriculture. IEEE Access. https://doi.org/10.1109/ACCESS.2020.3025590

Janakiraman, V., Sowmya, S., Thenmozhi, M., 2024. Biopolymer based membrane technology for environmental applications. Physical Sciences Reviews 9, 2051–2076. https://doi.org/10.1515/psr-2022-0222

Jawad, H.M., Nordin, R., Gharghan, S.K., Jawad, A.M., Ismail, M., 2017. Energy-Efficient Wireless Sensor Networks for Precision Agriculture: A Review. Sensors 17, 1781. https://doi.org/10.3390/s17081781

Jenani, R., Karishmaa, S., Babu Ponnusami, A., Senthil Kumar, P., Rangasamy, G., 2024. A recent development of low-cost membranes for microbial fuel cell applications. Desalination and Water Treatment 320, 100698. https://doi.org/10.1016/j.dwt.2024.100698

Jenkins, P., Tuurala, S., Vaari, A., Valkiainen, M., Smolander, M., Leech, D., 2012. A comparison of glucose oxidase and aldose dehydrogenase as mediated anodes in printed glucose/oxygen enzymatic fuel cells using ABTS/laccase cathodes. Bioelectrochemistry, International Symposium on Bioelectrochemistry and Bioenergetics, 21st BES 2011 87, 172–177. https://doi.org/10.1016/j.bioelechem.2011.11.011

Jia, X., Hou, D., Wang, L., O'Connor, D., Luo, J., 2020. The development of groundwater research in the past 40 years: A burgeoning trend in groundwater depletion and sustainable management. Journal of Hydrology 587, 125006. https://doi.org/10.1016/j.jhydrol.2020.125006

Jiang, J., Liu, X.X., Han, J., Hu, K., Chen, J.S., 2021. Self-Supported Sheets-on-Wire CuO@Ni(OH)2/Zn(OH)2 Nanoarrays for High-Performance Flexible Quasi-Solid-State Supercapacitor. Processes 9, 680. https://doi.org/10.3390/pr9040680

Jiang, Y.-B., Zhong, W.-H., Han, C., Deng, H., 2016. Characterization of Electricity Generated by Soil in Microbial Fuel Cells and the Isolation of Soil Source Exoelectrogenic Bacteria. Front. Microbiol. 7. https://doi.org/10.3389/fmicb.2016.01776

Jiao, W., Wang, J., He, Y., Xi, X., Chen, X., 2022. Detecting Soil Moisture Levels Using Battery-Free Wi-Fi Tag.

Jilani, A., Abdel-Wahab, M.S., Hammad, A.H., 2017. Advance deposition techniques for thin film and coating. Modern Technologies for Creating the Thin-film Systems and Coatings 2, 137–149.

Jin, M., Liu, J., Zhang, X., Zhang, S., Li, W., Sun, D., Zhang, Y., Wang, G., Zhang, H., 2024. Heterostructure Cu3P−Ni2P/CP catalyst assembled membrane electrode for high-efficiency electrocatalytic nitrate to ammonia. Nano Research 17, 4872–4881. https://doi.org/10.1007/s12274-024-6474-z

Johnston, S., Chebiam, R., Simka, H., Fischer, P., Dubin, V., 2004. Direct Plating of Cu on Ruthenium for sub-45nm Technology Node Interconnects Gapfill. Presented at the Advanced Metallization Conference (AMC), pp. 539–544.

Josephson, C., Barnhart, B., Katti, S., Winstein, K., Chandra, R., 2020. Demo abstract: RF soil moisture sensing via radar backscatter tags. Presented at the Proceedings - 2020 19th ACM/IEEE International Conference on Information Processing in Sensor Networks, IPSN 2020, pp. 365–366. https://doi.org/10.1109/IPSN48710.2020.000-4

Joshi, J.S., Langwald, S.V., Ehrmann, A., Sabantina, L., 2024. Algae-Based Biopolymers for Batteries and Biofuel Applications in Comparison with Bacterial Biopolymers—A Review. Polymers 16, 610. https://doi.org/10.3390/polym16050610

Juqu, T., Willenberg, S.C., Pokpas, K., Ross, N., 2022. Advances in paper-based battery research for biodegradable energy storage. Advanced Sensor and Energy Materials 1, 100037. https://doi.org/10.1016/j.asems.2022.100037

Kabiraz, M.K., Kim, J., Lee, H.J., Park, S., Lee, Y.W., Choi, S.-I., 2024. Nickel Nanoplates Enclosed by (111) Facets as Durable Oxygen Evolution Catalysts in Anion Exchange Membrane Water Electrolyzers. Advanced Functional Materials 34, 2406175. https://doi.org/10.1002/adfm.202406175

Kacmaz, G.K., Eczacioglu, N., 2024. The mechanism of bioelectricity generation from organic wastes: soil/plant microbial fuel cells. Environmental Technology Reviews 13, 76–95. https://doi.org/10.1080/21622515.2023.2283814

Kadir, M.F.Z., Arof, A.K., 2011. Application of PVA–chitosan blend polymer electrolyte membrane in electrical double layer capacitor. Materials Research Innovations 15, s217–s220. https://doi.org/10.1179/143307511X13031890749299

Kalita, H., Palaparthy, V.S., Baghini, M.S., Aslam, M., 2016. Graphene quantum dot soil moisture sensor. Sensors and Actuators B: Chemical 233, 582–590. https://doi.org/10.1016/j.snb.2016.04.131

Kandile, N.G., Nasr, A.S., 2023. Poly(vinyl alcohol) membranes-inspired heterocyclic compounds for different applications: synthesis and characterization. Polym. Bull. 80, 2367–2387. https://doi.org/10.1007/s00289-022-04143-z

Kang, X., Zuo, Q., Yuan, C., Chen, S., Zhao, Y., 2013. Low stress TaN thin film development for Mems/Sensor electrode application. Journal of Circuits, Systems and Computers 22. https://doi.org/10.1142/S0218126613400173

Karamad, M., Goncalves, T.J., Jimenez-Villegas, S., Gates, I.D., Siahrostami, S., 2023. Why copper catalyzes electrochemical reduction of nitrate to ammonia. Faraday Discussions.

Karthikeyan, C., Sathishkumar, Y., Lee, Y.S., Kim, A.R., Yoo, D.J., kumar, G.G., 2017. The Influence of Chitosan Substrate and Its Nanometric Form Toward the Green Power Generation in Sediment Microbial Fuel Cell. Journal of Nanoscience and Nanotechnology 17, 558–563. https://doi.org/10.1166/jnn.2017.12090

Kasuga, T., Mizui, A., Koga, H., Nogi, M., 2024. Wirelessly Powered Sensing Fertilizer for Precision and Sustainable Agriculture. Advanced Sustainable Systems 8, 2300314. https://doi.org/10.1002/adsu.202300314

Kehrer, M., Duchoslav, J., Hinterreiter, A., Cobet, M., Mehic, A., Stehrer, T., Stifter, D., 2019. XPS investigation on the reactivity of surface imine groups with TFAA. Plasma Processes and Polymers 16, 1800160. https://doi.org/10.1002/ppap.201800160

Kerr, C., Rogers, J., 2023. Low-Cost Portable High-Speed Data Logging. Presented at the ASME 2022 International Mechanical Engineering Congress and Exposition, American Society of Mechanical Engineers Digital Collection. https://doi.org/10.1115/IMECE2022-94016

Khan, A., Asmatulu, R., Hwang, G., 2015. Proton Conductivity of Graphene-Based Polymer Electrolyte Membrane. ECS Trans. 69, 569. https://doi.org/10.1149/06917.0569ecst

Khan, S.M., Nassar, J.M., Hussain, M.M., 2021. Paper as a Substrate and an Active Material in Paper Electronics. ACS Appl. Electron. Mater. 3, 30–52. https://doi.org/10.1021/acsaelm.0c00484

Kim, S., Le, T., Tentzeris, M.M., Harrabi, A., Collado, A., Georgiadis, A., 2014. An RFID-enabled inkjet-printed soil moisture sensor on paper for “smart” agricultural applications. Presented at the Proceedings of IEEE Sensors, pp. 1507–1510. https://doi.org/10.1109/ICSENS.2014.6985301

Kiv, D., Allabadi, G., Kaplan, B., Kravets, R., 2022. smol: Sensing soil moisture using lora. Presented at the Proceedings of the 1st ACM Workshop on No Power and Low Power Internet-of-Things, pp. 21–27.

Klair, D., Chin, K.-W., Raad, R., Lowe, D., 2008. A spatially aware RFID-enhanced wireless sensor network.

Knobeloch, L., Salna, B., Hogan, A., Postle, J., Anderson, H., 2000. Blue babies and nitrate-contaminated well water. Environmental health perspectives 108, 675–678.

Kobune, M., Takizawa, D., Nojima, J., Otomo, R., Kamiya, Y., 2020. Catalytic reduction of nitrate in water over alumina-supported nickel catalyst toward purification of polluted groundwater. Catalysis Today 352, 204–211.

Koç, Y., Morali, U., Erol, S., Avci, H., 2021. Investigation of electrochemical behavior of potassium ferricyanide/ferrocyanide redox probes on screen printed carbon electrode through cyclic voltammetry and electrochemical impedance spectroscopy. Turkish Journal of Chemistry 45, 1895–1915.

Koech, R., Langat, P., 2018. Improving Irrigation Water Use Efficiency: A Review of Advances, Challenges and Opportunities in the Australian Context. Water 10, 1771. https://doi.org/10.3390/w10121771

Kojima, Y., Shigeta, R., Miyamoto, N., Shirahama, Y., Nishioka, K., Mizoguchi, M., Kawahara, Y., 2016. Low-cost soil moisture profile probe using thin-film capacitors and a capacitive touch sensor. Sensors 16, 1292.

Kolajo, O.O., Pandit, C., Thapa, B.S., Pandit, S., Mathuriya, A.S., Gupta, P.K., Jadhav, D.A., Lahiri, D., Nag, M., Upadhye, V.J., 2022. Impact of cathode biofouling in microbial fuel cells and mitigation techniques. Biocatalysis and Agricultural Biotechnology 43, 102408. https://doi.org/10.1016/j.bcab.2022.102408

Korotcenkov, G., 2023. Paper-Based Humidity Sensors as Promising Flexible Devices: State of the Art: Part 1. General Consideration. Nanomaterials 13, 1110. https://doi.org/10.3390/nano13061110

Kosasih, W.C., Setiono, D.H., Calvin, A., Kretapradana, A.P., Suwarno, N.A.V., Saputra, D.E., 2023. Comparison on the Performance of Low-Cost Soil Moisture Sensors in Beach Sand Soil. Presented at the 10th International Conference on ICT for Smart Society, ICISS 2023 - Proceeding. https://doi.org/10.1109/ICISS59129.2023.10292066

Kosimaningrum, W.E., 2018. Modification of carbon felt for contruction of air-breathing cathode and its application in microbial fuel cell.

Kukal, M.S., Irmak, S., Sharma, K., 2019. Development and application of a performance and operational feasibility guide to facilitate adoption of soil moisture sensors. Sustainability 12, 321.

Kulmany, I.M., Bede-Fazekas, A., Beslin, A., Giczi, Z., Milics, G., Kovacs, B., Kovacs, M., Ambrus, B., Bede, L., Vona, V., 2022. Calibration of an Arduino-based low-cost capacitive soil moisture sensor for smart agriculture. Journal of Hydrology and Hydromechanics. https://doi.org/10.2478/johh-2022-0014

Kumar, A., Kamal, K., Arshad, M.O., Mathavan, S., Vadamala, T., 2014. Smart irrigation using low-cost moisture sensors and XBee-based communication. Presented at the Proceedings of the 4th IEEE Global Humanitarian Technology Conference, GHTC 2014, pp. 333–337. https://doi.org/10.1109/GHTC.2014.6970301

Kushwaha, A., Sharma, A., Bhatt, B.B., Mukhopadhyay, A., Gupta, D., 2023. Inkjet-Printed Graphene-Modified Aluminum Current Collector for High-Voltage Lithium-Ion Battery. ACS Appl. Energy Mater. 6, 4168–4178. https://doi.org/10.1021/acsaem.2c03870

Landers, M., Elhadad, A., Rezaie, M., Choi, S., 2022. Integrated Papertronic Techniques: Highly Customizable Resistor, Supercapacitor, and Transistor Circuitry on a Single Sheet of Paper. ACS Appl. Mater. Interfaces 14, 45658–45668. https://doi.org/10.1021/acsami.2c13503

Lange, R., Maisonhaute, E., Robin, R., Vivier, V., 2013. On the kinetics of the nitrate reduction in concentrated nitric acid. Electrochemistry Communications 29, 25–28. https://doi.org/10.1016/j.elecom.2013.01.005

Laschuk, N.O., Easton, E.B., Zenkina, O.V., 2021. Reducing the resistance for the use of electrochemical impedance spectroscopy analysis in materials chemistry. RSC Adv. 11, 27925–27936. https://doi.org/10.1039/D1RA03785D

Le, M.T., Pham, C.D., Nguyen, T.P.T., Nguyen, T.L., Nguyen, Q.C., Hoang, N.B., Nghiem, L.D., 2023. Wireless Powered Moisture Sensors for Smart Agriculture and Pollution Prevention: Opportunities, Challenges, and Future Outlook. Curr Pollution Rep 9, 646–659. https://doi.org/10.1007/s40726-023-00286-3

Leaković, S., Mijatović, I., Cerjan-Stefanović, Š., Hodžić, E., 2000. Nitrogen removal from fertilizer wastewater by ion exchange. Water Research 34, 185–190. https://doi.org/10.1016/S0043-1354(99)00122-0

Lee, C.-Y., Huang, Y.-N., 2013. The effects of electrode spacing on the performance of microbial fuel cells under different substrate concentrations. Water Science and Technology 68, 2028–2034. https://doi.org/10.2166/wst.2013.446

Lee, H., Choi, S., 2015. An origami paper-based bacteria-powered battery with an air-cathod, in: 2015 Transducers - 2015 18th International Conference on Solid-State Sensors, Actuators and Microsystems (TRANSDUCERS). Presented at the 2015 Transducers - 2015 18th International Conference on Solid-State Sensors, Actuators and Microsystems (TRANSDUCERS), pp. 1009–1012. https://doi.org/10.1109/TRANSDUCERS.2015.7181096

Lee, Hankeun, Choi, S., 2015. An origami paper-based bacteria-powered battery. Nano Energy 15, 549–557. https://doi.org/10.1016/j.nanoen.2015.05.019

Lee, M., Kim, S., Kim, H.-Y., Mahadevan, L., 2016. Bending and buckling of wet paper. Physics of Fluids 28, 042101. https://doi.org/10.1063/1.4944659

Lee, S.H., Ban, J.Y., Oh, C.-H., Park, H.-K., Choi, S., 2016. A solvent-free microbial-activated air cathode battery paper platform made with pencil-traced graphite electrodes. Sci Rep 6, 28588. https://doi.org/10.1038/srep28588

Lei, X., Liu, F., Li, M., Ma, X., Wang, X., Zhang, H., 2018. Fabrication and characterization of a Cu-Pd-TNPs polymetallic nanoelectrode for electrochemically removing nitrate from groundwater. Chemosphere 212, 237–244.

Li, B., Pan, X., Zhang, D., Lee, D.-J., Al-Misned, F.A., Mortuza, M.G., 2015. Anaerobic nitrate reduction with oxidation of Fe(II) by Citrobacter Freundii strain PXL1 – a potential candidate for simultaneous removal of As and nitrate from groundwater. Ecological Engineering 77, 196–201. https://doi.org/10.1016/j.ecoleng.2015.01.027

Li, H.-L., Liu, W., Chen, X.-F., 2017. Preparation of Separator Paper Used in Zinc-Silver Battery. Chung-kuo Tsao Chih/China Pulp and Paper 36, 1–6. https://doi.org/10.11980/j.issn.0254-508X.2017.06.001

Li, J., Gao, J., Feng, T., Zhang, H., Liu, D., Zhang, C., Huang, S., Wang, C., Du, F., Li, C., 2021. Effect of supporting matrixes on performance of copper catalysts in electrochemical nitrate reduction to ammonia. Journal of Power Sources 511, 230463.

Li, M., Huang, H., Low, J., Gao, C., Long, R., Xiong, Y., 2019. Recent Progress on Electrocatalyst and Photocatalyst Design for Nitrogen Reduction. Small Methods 3, 1800388. https://doi.org/10.1002/smtd.201800388

Li, T.-T., Yan, M., Zhong, Y., Ren, H.-T., Lou, C.-W., Huang, S.-Y., Lin, J.-H., 2019. Processing and characterizations of rotary linear needleless electrospun polyvinyl alcohol(PVA)/Chitosan(CS)/Graphene(Gr) nanofibrous membranes. Journal of Materials Research and Technology 8, 5124–5132. https://doi.org/10.1016/j.jmrt.2019.08.035

Li, X., Liu, Y., Feng, Y., Tong, Y., Qin, Z., Wu, Z., Deng, Y., Hu, W., 2023. Research prospects of graphene-based catalyst for seawater electrolysis. Mater. Futures 2, 042104. https://doi.org/10.1088/2752-5724/acf2fd

Li, X., Wang, X., Zhao, Q., Wan, L., Li, Y., Zhou, Q., 2016. Carbon fiber enhanced bioelectricity generation in soil microbial fuel cells. Biosensors and Bioelectronics 85, 135–141. https://doi.org/10.1016/j.bios.2016.05.001

Li, Xiaoqiang, Guo, Y., Meng, J., Li, Xinke, Li, M., Gao, D., 2022. Self-Powered Carbon Ink/Filter Paper Flexible Humidity Sensor Based on Moisture-Induced Voltage Generation. Langmuir 38, 8232–8240. https://doi.org/10.1021/acs.langmuir.2c00566

Li, Y., Lv, W., Huang, H., Yan, W., Li, X., Ning, P., Cao, H., Sun, Z., 2021. Recycling of spent lithium-ion batteries in view of green chemistry. Green Chemistry 23, 6139–6171. https://doi.org/10.1039/D1GC01639C

Li, Z., Qiu, F., Yue, X., Tian, Q., Yang, D., Zhang, T., 2021. Eco-friendly self-crosslinking cellulose membrane with high mechanical properties from renewable resources for oil/water emulsion separation. Journal of Environmental Chemical Engineering 9, 105857. https://doi.org/10.1016/j.jece.2021.105857

Li, Z., Shen, H., Alsaify, B., 2008. Integrating RFID with Wireless Sensor Networks for Inhabitant, Environment and Health Monitoring, in: 2008 14th IEEE International Conference on Parallel and Distributed Systems. Presented at the 2008 14th IEEE International Conference on Parallel and Distributed Systems, pp. 639–646. https://doi.org/10.1109/ICPADS.2008.66

Liang, X., Zhu, H., Yang, X., Xue, S., Liang, Z., Ren, X., Liu, A., Wu, G., 2022. Recent advances in designing efficient electrocatalysts for electrochemical nitrate reduction to ammonia. Small Structures 2200202.

Liang, Y., Zeng, Y., Tang, X., Xia, W., Song, B., Yao, F., Yang, Y., Chen, Y., Peng, C., Zhou, C., Lai, C., 2023. One-step synthesis of Cu(OH)2-Cu/Ni foam cathode for electrochemical reduction of nitrate. Chemical Engineering Journal 451, 138936. https://doi.org/10.1016/j.cej.2022.138936

Lim, J., Chen, Y., Cullen, D.A., Lee, S.W., Senftle, T.P., Hatzell, M.C., 2023. PdCu Electrocatalysts for Selective Nitrate and Nitrite Reduction to Nitrogen. ACS Catalysis 13, 87–98. https://doi.org/10.1021/acscatal.2c04841

Lima, A.S., Salles, M.O., Ferreira, T.L., Paixão, T.R.L.C., Bertotti, M., 2012. Scanning electrochemical microscopy investigation of nitrate reduction at activated copper cathodes in acidic medium. Electrochimica Acta 78, 446–451. https://doi.org/10.1016/j.electacta.2012.06.075

Lin, J.-X., Liu, X.-M., Cui, C.-W., Bai, C.-Y., Lu, Y.-M., Fan, F., Guo, Y.-Q., Liu, Z.-Y., Cai, C.-B., 2017. A review of thickness-induced evolutions of microstructure and superconducting performance of REBa2Cu3O7−δ coated conductor. Adv. Manuf. 5, 165–176. https://doi.org/10.1007/s40436-017-0173-x

Liu, B., Zou, B.-X., 2014. Electrocatalytic sensing of nitrate at Cu nanosheets electrodeposited on WO3/polyaniline modified electrode. Advanced Materials Research 881–883, 159–164. https://doi.org/10.4028/www.scientific.net/AMR.881-883.159

Liu, H., Qin, J., Lv, Y., Li, Z., Zhang, W., Xu, Q., Su, H., 2024. In Situ Construction of a Nanostructured Ultrathin Catalyst Layer on Both Sides of a Membrane toward Fuel Cell Application. ACS Appl. Energy Mater. 7, 1340–1347. https://doi.org/10.1021/acsaem.3c03107

Liu, J.-X., Richards, D., Singh, N., Goldsmith, B.R., 2019. Activity and selectivity trends in electrocatalytic nitrate reduction on transition metals. Acs Catalysis 9, 7052–7064.

Liu, X., Duan, Y., Cheng, X.-T., Zhao, H.-L., Liu, Z., Wang, Y.-Q., 2023. Cu/NiO nanorods for efficiently promoting the electrochemical nitrate reduction to ammonia. Dalton Trans. 52, 17470–17476. https://doi.org/10.1039/D3DT03352J

Liu, X., He, N., Ni, H., Wang, S., Yang, J., Guo, G., Kang, Y., Liu, Y., Zhou, C., Tong, L., Lu, B., Wang, Q., Yang, M., Han, S., Li, W., Han, Z., 2024. Revolutionizing nitrogen electrocatalysis: Atomically dispersed ruthenium catalyzed by manganese for unmatched performance. Applied Catalysis A: General 688, 119990. https://doi.org/10.1016/j.apcata.2024.119990

Liu, X., Liu, J., Li, G.-R., Liu, S., Gao, X.-P., 2022. Dimensionally Stable Composite Li Electrode with Cu Skeleton and Lithophilic Li–Mg Alloy Microstructure. ACS Appl. Mater. Interfaces 14, 56801–56807. https://doi.org/10.1021/acsami.2c17084

Liu, Y., Aoki, K.J., Chen, J., 2023. The Difference in the Effects of IR-Drop from the Negative Capacitance of Fast Cyclic Voltammograms. Electrochem 4, 460–472. https://doi.org/10.3390/electrochem4040030

Liu, Y., Peng, W., Zhang, J., Li, S., Hu, R., Yuan, B., Chen, G., 2022. Tuning the electronic properties of NiO anode by *in-situ* introducing metallic Cu for high capacity and long life-span lithium-ion batteries. Journal of Alloys and Compounds 918, 165693. https://doi.org/10.1016/j.jallcom.2022.165693

Lloret, J., Sendra, S., Garcia, L., Jimenez, J.M., 2021. A wireless sensor network deployment for soil moisture monitoring in precision agriculture. Sensors 21, 7243.

Lockhart, K., King, A., Harter, T., 2013. Identifying sources of groundwater nitrate contamination in a large alluvial groundwater basin with highly diversified intensive agricultural production. Journal of contaminant hydrology 151, 140–154.

Löffler, F., Siewert, C., 2004. Homogeneous coatings inside cylinders. Surface and Coatings Technology 177–178, 355–359. https://doi.org/10.1016/j.surfcoat.2003.09.026

Logan, B.E., Hamelers, B., Rozendal, R., Schröder, U., Keller, J., Freguia, S., Aelterman, P., Verstraete, W., Rabaey, K., 2006. Microbial Fuel Cells: Methodology and Technology. Environ. Sci. Technol. 40, 5181–5192. https://doi.org/10.1021/es0605016

Long, F., Ghani, D., Huang, R., Zhao, C., 2025. Versatile electrode materials applied in the electrochemical advanced oxidation processes for wastewater treatment: A systematic review. Separation and Purification Technology 354, 128725. https://doi.org/10.1016/j.seppur.2024.128725

Long, J.W., Dunn, B., Rolison, D.R., White, H.S., 2004. Three-Dimensional Battery Architectures. Chem. Rev. 104, 4463–4492. https://doi.org/10.1021/cr020740l

Long Doan, T.N., A. Hoang, T.K., Chen, P., 2015. Recent development of polymer membranes as separators for all-vanadium redox flow batteries. RSC Advances 5, 72805–72815. https://doi.org/10.1039/C5RA05914C

Lóránt, B., Lóka, M., Tardy, G.M., 2015. Substrate concentration dependency of electricity production in microbial fuel cells, in: 2015 5th International Youth Conference on Energy (IYCE). Presented at the 2015 5th International Youth Conference on Energy (IYCE), pp. 1–7. https://doi.org/10.1109/IYCE.2015.7180786

Lou, Y.-Y., Zheng, Q.-Z., Zhou, S.-Y., Fang, J.-Y., Akdim, O., Ding, X.-Y., Oh, R., Park, G.-S., Huang, X., Sun, S.-G., 2024. Phase-dependent Electrocatalytic Nitrate Reduction to Ammonia on Janus Cu@Ni Tandem Catalyst. ACS Catal. 14, 5098–5108. https://doi.org/10.1021/acscatal.4c00479

Lu, J., Lv, S., Park, H.S., Chen, Q., 2024. Electrocatalytically active and charged natural chalcopyrite for nitrate-contaminated wastewater purification extended to energy storage Zn-NO3− battery. Journal of Hazardous Materials 477, 135287. https://doi.org/10.1016/j.jhazmat.2024.135287

Lu, T.-F., Hsu, K.-N., Hsu, C.-C., Hsu, C.-Y., Wu, Y.S., 2024. Effect of Cu Film Thickness on Cu Bonding Quality and Bonding Mechanism. Materials 17, 2150. https://doi.org/10.3390/ma17092150

Lu, Y., Marshall, N.M., 2013. Redox Potential, in: Encyclopedia of Biophysics. Springer, Berlin, Heidelberg, pp. 2207–2211. https://doi.org/10.1007/978-3-642-16712-6_19

Lyu, Z., Lim, G.J.H., Koh, J.J., Li, Y., Ma, Y., Ding, J., Wang, Jinlan, Hu, Z., Wang, John, Chen, W., Chen, Y., 2021. Design and Manufacture of 3D-Printed Batteries. Joule 5, 89–114. https://doi.org/10.1016/j.joule.2020.11.010

Ma, J., Zheng, S., Fu, Y., Wang, X., Qin, J., Wu, Z.-S., 2024. The status and challenging perspectives of 3D-printed micro-batteries. Chemical Science 15, 5451–5481. https://doi.org/10.1039/D3SC06999K

Ma, Z., Wang, C., Yang, T., Wei, G., Huang, J., Liu, M., Zhang, K., Zhang, Z., Liu, Y., Gao, S., 2024. A 3D porous P-doped Cu–Ni alloy for atomic H* enhanced electrocatalytic reduction of nitrate to ammonia. J. Mater. Chem. A 12, 7654–7662. https://doi.org/10.1039/D3TA08086B

Madito, M.J., Matshoba, K.S., Ochai-Ejeh, F.U., Mongwaketsi, N., Mtshali, C.B., Fabiane, M., Manyala, N., 2020. Nickel-copper graphene foam prepared by atmospheric pressure chemical vapour deposition for supercapacitor applications. Surface and Coatings Technology 383, 125230. https://doi.org/10.1016/j.surfcoat.2019.125230

Magar, H.S., Hassan, R.Y.A., Mulchandani, A., 2021. Electrochemical Impedance Spectroscopy (EIS): Principles, Construction, and Biosensing Applications. Sensors (Basel) 21, 6578. https://doi.org/10.3390/s21196578

Mahmoud, R.H., Gomaa, O.M., Hassan, R.Y., 2022. Bio-electrochemical frameworks governing microbial fuel cell performance: technical bottlenecks and proposed solutions. RSC advances 12, 5749–5764.

Maiti, J., Kakati, N., Lee, S.H., Jee, S.H., Viswanathan, B., Yoon, Y.S., 2012. Where do poly(vinyl alcohol) based membranes stand in relation to Nafion® for direct methanol fuel cell applications? Journal of Power Sources 216, 48–66. https://doi.org/10.1016/j.jpowsour.2012.05.057

Manevski, K., Andersen, M.N., 2024. Field-Level Irrigation, in: Oxford Research Encyclopedia of Environmental Science. https://doi.org/10.1093/acrefore/9780199389414.013.614

Manjakkal, L., Mitra, S., Petillot, Y.R., Shutler, J., Scott, E.M., Willander, M., Dahiya, R., 2021. Connected sensors, innovative sensor deployment, and intelligent data analysis for online water quality monitoring. IEEE Internet of Things Journal 8, 13805–13824.

Marín, F., Santos, M., Diánez, F., Carretero, F., Gea, F.J., Yau, J.A., Navarro, M.J., 2013. Characters of compost teas from different sources and their suppressive effect on fungal phytopathogens. World Journal of Microbiology and Biotechnology 29, 1371–1382.

Mattarozzi, L., Cattarin, S., Comisso, N., Gerbasi, R., Guerriero, P., Musiani, M., Verlato, E., 2017. Electrodeposition of compact and porous Cu-Pd alloy layers and their application to nitrate reduction in alkali. Electrochimica Acta 230, 365–372. https://doi.org/10.1016/j.electacta.2017.02.012

McGrath, M.J., Scanaill, C.N., McGrath, M.J., Scanaill, C.N., 2013. Sensing and sensor fundamentals. Sensor technologies: Healthcare, wellness, and environmental applications 15–50.

McNabb, D.E., 2019. Agriculture and Inefficient Water Use, in: Global Pathways to Water Sustainability. Palgrave Macmillan, Cham, pp. 99–115. https://doi.org/10.1007/978-3-030-04085-7_7

Md Khudzari, J., Gariépy, Y., Kurian, J., Tartakovsky, B., Raghavan, G.S.V., 2019. Effects of biochar anodes in rice plant microbial fuel cells on the production of bioelectricity, biomass, and methane. Biochemical Engineering Journal 141, 190–199. https://doi.org/10.1016/j.bej.2018.10.012

Meghana, M.C., Nandhini, C., Benny, L., George, L., Varghese, A., 2023. A road map on synthetic strategies and applications of biodegradable polymers. Polym. Bull. 80, 11507–11556. https://doi.org/10.1007/s00289-022-04565-9

Mei, B.-A., Munteshari, O., Lau, J., Dunn, B., Pilon, L., 2018. Physical Interpretations of Nyquist Plots for EDLC Electrodes and Devices. J. Phys. Chem. C 122, 194–206. https://doi.org/10.1021/acs.jpcc.7b10582

Melchior, J.-P., Bräuniger, T., Wohlfarth, A., Portale, G., Kreuer, K.-D., 2015. About the Interactions Controlling Nafion's Viscoelastic Properties and Morphology. Macromolecules 48, 8534–8545. https://doi.org/10.1021/acs.macromol.5b01559

Melchor-Martínez, E.M., Macias-Garbett, R., Malacara-Becerra, A., Iqbal, H.M.N., Sosa-Hernández, J.E., Parra-Saldívar, R., 2021. Environmental impact of emerging contaminants from battery waste: A mini review. Case Studies in Chemical and Environmental Engineering 3, 100104. https://doi.org/10.1016/j.cscee.2021.100104

Meng, S., Ling, Y., Yang, M., Zhao, X., Osman, A.I., Al-Muhtaseb, A.H., Rooney, D.W., Yap, P.-S., 2023. Recent research progress of electrocatalytic reduction technology for nitrate wastewater: A review. Journal of Environmental Chemical Engineering 11, 109418. https://doi.org/10.1016/j.jece.2023.109418

Meshram, S.M.M., Gonugunta, P., Taheri, P., Jourdin, L., Pande, S., 2025a. Investigating the influence of a thin copper film coated on nickel plates through physical vapor deposition for electrocatalytic nitrate reduction. Front. Mater. 12. https://doi.org/10.3389/fmats.2025.1527753

Meshram, S.M.M., Gonugunta, P., Taheri, P., Jourdin, L., Pande, S., 2025b. Preparation of biodegradable membrane utilizing chitosan and polyvinyl alcohol, and assessment of its performance after coating with graphene conductive ink. Front. Membr. Sci. Technol. 4. https://doi.org/10.3389/frmst.2025.1552368

Mishu, M.K., Rokonuzzaman, M., Pasupuleti, J., Shakeri, M., Rahman, K.S., Hamid, F.A., Tiong, S.K., Amin, N., 2020. Prospective Efficient Ambient Energy Harvesting Sources for IoT-Equipped Sensor Applications. Electronics 9, 1345. https://doi.org/10.3390/electronics9091345

Miyamoto, K., 2024. Tailor-Made Design of Three-Dimensional Batteries Using a Simple, Accurate Geometry Optimization Scheme. ACS Phys. Chem Au 4, 546–554. https://doi.org/10.1021/acsphyschemau.4c00039

Miyamoto, K., Sasaki, T., Nishi, T., Itou, Y., Takechi, K., 2020. 3D-Microbattery Architectural Design Optimization Using Automatic Geometry Generator and Transmission-Line Model. iScience 23, 101317. https://doi.org/10.1016/j.isci.2020.101317

Mobilian, C., Craft, C.B., 2022. Wetland soils: physical and chemical properties and biogeochemical processes.

Moffat, A.S., 1998. Global nitrogen overload problem grows critical. Science 279, 988–989.

Mohammadifar, M., Choi, S., 2019. A solid phase bacteria-powered biobattery for low-power, low-cost, internet of Disposable Things. Journal of Power Sources 429, 105–110. https://doi.org/10.1016/j.jpowsour.2019.05.009

Mohammadifar, M., Choi, S., 2018. On-Demand Micro-Power Generation from an Origami-Inspired Paper Biobattery Stack. Batteries 4, 14. https://doi.org/10.3390/batteries4020014

Mohammadifar, M., Gao, Y., Choi, S., 2016a. An origami-inspired multicell biobattery stack, in: 2016 IEEE SENSORS. Presented at the 2016 IEEE SENSORS, pp. 1–3. https://doi.org/10.1109/ICSENS.2016.7808946

Mohammadifar, M., Zhang, J., Yazgan, I., Kariuki, V., Sadik, O., Choi, S., 2016b. High performance paper-based microbial fuel cells using nanostructured polymers, in: 2016 IEEE SENSORS. Presented at the 2016 IEEE SENSORS, pp. 1–3. https://doi.org/10.1109/ICSENS.2016.7808982

Mohammed, M., Jawad, A.J.M., Mohammed, A.M., Oleiwi, J.K., Adam, T., Osman, A.F., Dahham, O.S., Betar, B.O., Gopinath, S.C.B., Jaafar, M., 2023. Challenges and advancement

in water absorption of natural fiber-reinforced polymer composites. Polymer Testing 124, 108083. https://doi.org/10.1016/j.polymertesting.2023.108083

Mohd Said, N.A., 2014. Electrochemical biosensor based on microfabricated electrode arrays for life sciences applications.

Molodkina, E.B., Ehrenburg, M.R., Polukarov, Y.M., Danilov, A.I., Souza-Garcia, J., Feliu, J.M., 2010. Electroreduction of nitrate ions on Pt(1 1 1) electrodes modified by copper adatoms. Electrochimica Acta 56, 154–165. https://doi.org/10.1016/j.electacta.2010.08.105

Mondol, P., Panthi, D., Ayala, A.J.A., Odoh, S.O., Barile, C.J., 2022. Membrane-modified electrocatalysts for nitrate reduction to ammonia with high faradaic efficiency. J. Mater. Chem. A 10, 22428–22436. https://doi.org/10.1039/D2TA06938E

Morales-Jiménez, M., Palacio, D.A., Palencia, M., Meléndrez, M.F., Rivas, B.L., 2023. Bio-Based Polymeric Membranes: Development and Environmental Applications. Membranes (Basel) 13, 625. https://doi.org/10.3390/membranes13070625

Morgan, K.A., Tang, T., Zeimpekis, I., Ravagli, A., Craig, C., Yao, J., Feng, Z., Yarmolich, D., Barker, C., Assender, H., 2019. High-throughput physical vapour deposition flexible thermoelectric generators. Scientific reports 9, 4393.

Morris, M., Energy, N., 2006. Soil moisture monitoring: low-cost tools and methods. National Center for Appropriate Technology (NCAT) 1–12.

Mrozik, W., Ali Rajaeifar, M., Heidrich, O., Christensen, P., 2021. Environmental impacts, pollution sources and pathways of spent lithium-ion batteries. Energy & Environmental Science 14, 6099–6121. https://doi.org/10.1039/D1EE00691F

Mubarak, A.M.A., Hamzah, E.H.E., Tofr, M.T.M., 2005. Review of physical vapour deposition (PVD) techniques for hard coating. Jurnal Mekanikal.

Muhamaruesa, N.H.M., Isa, M.I.N.M., 2020. Chapter 19 - Biopolymer membranes for battery applications, in: de Moraes, M.A., da Silva, C.F., Vieira, R.S. (Eds.), Biopolymer Membranes and Films. Elsevier, pp. 477–502. https://doi.org/10.1016/B978-0-12-818134-8.00019-5

Muhmed, S.A., Jaafar, J., Ahmad, S.N.A., Mohamed, M.H., Ismail, A.F., Ilbeygi, H., Othman, M.H.D., Rahman, M.A., 2023. Incorporating functionalized graphene oxide in green material-based membrane for proton exchange membrane fuel cell application. Journal of Environmental Chemical Engineering 11, 109547. https://doi.org/10.1016/j.jece.2023.109547

Muhmed, S.A., Nor, N.A.M., Jaafar, J., Ismail, A.F., Othman, M.H.D., Rahman, M.A., Aziz, F., Yusof, N., 2020. Emerging chitosan and cellulose green materials for ion exchange membrane fuel cell: a review. Energ. Ecol. Environ. 5, 85–107. https://doi.org/10.1007/s40974-019-00127-4

Mukhlisin, M., Astuti, H.W., Wardihani, E.D., Matlan, S.J., 2021. Techniques for ground-based soil moisture measurement: a detailed overview. Arab J Geosci 14, 2032. https://doi.org/10.1007/s12517-021-08263-0

Mukoma, P., Jooste, B.R., Vosloo, H.C.M., 2004. Synthesis and characterization of cross-linked chitosan membranes for application as alternative proton exchange membrane materials in fuel cells. Journal of Power Sources 136, 16–23. https://doi.org/10.1016/j.jpowsour.2004.05.027

Mundewadi, G., Wolski, R., Krintz, C., 2023. Data Acquisition and Analysis for Improving the Utility of Low Cost Soil Moisture Sensors, in: 2023 IEEE International Conference on Smart Computing (SMARTCOMP). Presented at the 2023 IEEE International Conference on Smart Computing (SMARTCOMP), pp. 367–372. https://doi.org/10.1109/SMARTCOMP58114.2023.00087

Munro, P.G., Samarakoon, S., Hansen, U.E., Kearnes, M., Bruce, A., Cross, J., Walker, S., Zalengera, C., 2023. Towards a repair research agenda for off-grid solar e-waste in the Global South. Nat Energy 8, 123–128. https://doi.org/10.1038/s41560-022-01103-9

Murmu, R., Roy, D., Patra, S.C., Sutar, H., Choudhary, B., 2022. Preparation and Characterization of Red Mud Modified Chitosan-PVA Composite Membrane for Direct Methanol Fuel Cell. Journal of Electrochemical Energy Conversion and Storage 20. https://doi.org/10.1115/1.4055693

Nagahage, E., Nagahage, I., Fujino, T., 2019. Calibration and Validation of a Low-Cost Capacitive Moisture Sensor to Integrate the Automated Soil Moisture Monitoring System. AGRICULTURE-BASEL 9. https://doi.org/10.3390/agriculture9070141

Nagao, Y., 2024. Proton-Conducting Polymers: Key to Next-Generation Fuel Cells, Electrolyzers, Batteries, Actuators, and Sensors. ChemElectroChem 11, e202300846. https://doi.org/10.1002/celc.202300846

Nakamoto, T., Nakamoto, D., Tamenori, K., Taguchi, K., 2024. Soil Moisture Content Sensor: Utilizing Bacterial Cells as Living Sensors. E3S Web Conf. 514, 01003. https://doi.org/10.1051/e3sconf/202451401003

Neto, E.C., Barroso, D.A., Filho, P.P.R., Coelho, D.N., 2022. Novel low cost soil moisture sensor. Presented at the International Scientific and Technical Conference on Computer Sciences and Information Technologies, pp. 214–217. https://doi.org/10.1109/CSIT56902.2022.10000574

Ng, L.S., Mohamad, A.A., 2008. Effect of temperature on the performance of proton batteries based on chitosan–NH4NO3–EC membrane. Journal of Membrane Science 325, 653–657. https://doi.org/10.1016/j.memsci.2008.08.029

Nguyen, D.-T., Nguyen, H.-U.-D., Taguchi, K., 2022. Portable Membrane-Less Soil Microbial Fuel Cell: Using Multiwalled CNT Paper Electrodes. Journal of Electronic Materials 51, 5946–5955. https://doi.org/10.1007/s11664-022-09806-1

Nguyen, T.A.K., Huang, Y., Dang, N.M., Lin, C.-H., Chen, W.-C., Wang, Z.-Y., Lin, M.-T., 2024. Effect of sputtering power and thickness ratios on the materials properties of Cu–W and Cu–Cr bilayer thin films using high power impulse magnetron and DC magnetron sputtering. Journal of Vacuum Science & Technology A 42, 053410. https://doi.org/10.1116/6.0003795

Nguyen, V., Nitisoravut, R., 2019. Bioelectricity Generation in Plant Microbial Fuel Cell Using Forage Grass under Variations of Circadian Rhythm, Ambient Temperature, and Soil Water

Contents. Presented at the 2019 Asia Power and Energy Engineering Conference, APEEC 2019, pp. 240–244. https://doi.org/10.1109/APEEC.2019.8720344

Nikolov, G.T., Ganev, B.T., Marinov, M.B., Galabov, V.T., 2021. Comparative Analysis of Sensors for Soil Moisture Measurement, in: 2021 XXX International Scientific Conference Electronics (ET). Presented at the 2021 XXX International Scientific Conference Electronics (ET), pp. 1–5. https://doi.org/10.1109/ET52713.2021.9580162

Nobili, F., Dsoke, S., Mancini, M., Marassi, R., 2009. Interfacial properties of copper-coated graphite electrodes: Coating thickness dependence. Fuel Cells 9, 264–268. https://doi.org/10.1002/fuce.200800087

Oates, M.J., Ramadan, K., Molina-Martínez, J.M., Ruiz-Canales, A., 2017. Automatic fault detection in a low cost frequency domain (capacitance based) soil moisture sensor. Agricultural Water Management 183, 41–48. https://doi.org/10.1016/j.agwat.2016.12.002

Obileke, K., Onyeaka, H., Meyer, E.L., Nwokolo, N., 2021. Microbial fuel cells, a renewable energy technology for bio-electricity generation: A mini-review. Electrochemistry Communications 125, 107003. https://doi.org/10.1016/j.elecom.2021.107003

Okasha, A.M., Ibrahim, H.G., Elmetwalli, A.H., Khedher, K.M., Yaseen, Z.M., Elsayed, S., 2021. Designing low-cost capacitive-based soil moisture sensor and smart monitoring unit operated by solar cells for greenhouse irrigation management. Sensors 21, 5387.

Okoye, P.C., Azi, S.O., Qahtan, T.F., Owolabi, T.O., Saleh, T.A., 2023. Synthesis, properties, and applications of doped and undoped CuO and Cu2O nanomaterials. Materials Today Chemistry 30, 101513. https://doi.org/10.1016/j.mtchem.2023.101513

Osman, A.I., Chen, Z., Elgarahy, A.M., Farghali, M., Mohamed, I.M.A., Priya, A. k., Hawash, H.B., Yap, P.-S., 2024. Membrane Technology for Energy Saving: Principles, Techniques, Applications, Challenges, and Prospects. Advanced Energy and Sustainability Research 5, 2400011. https://doi.org/10.1002/aesr.202400011

O'Sullivan, J., Burgess, S., Rimmer, N., 2002. Metal lift-off using physical vapour deposition. Microelectronic engineering 64, 473–478.

Paidar, M., Roušar, I., Bouzek, K., 1999. Electrochemical removal of nitrate ions in waste solutions after regeneration of ion exchange columns. Journal of Applied Electrochemistry 29, 611–617.

Pal, P., Tripathi, S., Kumar, C., 2022. Single Probe Imitation of Multi-Depth Capacitive Soil Moisture Sensor Using Bidirectional Recurrent Neural Network. IEEE TRANSACTIONS ON INSTRUMENTATION AND MEASUREMENT 71. https://doi.org/10.1109/TIM.2022.3156179

Palanisamy, G., Muhammed, A.P., Thangarasu, S., Oh, T.H., 2023. Investigating the Sulfonated Chitosan/Polyvinylidene Fluoride-Based Proton Exchange Membrane with fSiO2 as Filler in Microbial Fuel Cells. Membranes 13, 758. https://doi.org/10.3390/membranes13090758

Pan, A., Shi, C., Jia, M., He, L., 2021. Novel fluoroalkyl polyhedral oligomeric silsesquioxane (FPOSS) macromers for fabricating diblock copolymer as self-cleaning coatings. Progress in Organic Coatings 151. https://doi.org/10.1016/j.porgcoat.2020.106097

Pan, Y., Zeng, W., Hu, R., Li, B., Wang, G., Li, Q., 2019. Investigation of Cu doped flake-NiO as an anode material for lithium ion batteries. RSC Adv 9, 35948–35956. https://doi.org/10.1039/c9ra05618a

Panawong, C., Tasarin, S., Saejueng, P., Budsombat, S., 2022. Composite proton conducting membranes from crosslinked poly(vinyl alcohol)/chitosan and silica particles containing poly(2-acrylamido-2-methyl-1-propansulfonic acid). Journal of Applied Polymer Science.

Pandey, I., Tiwari, J.D., Saha, T.K., Khosla, A., Furukawa, H., Sekhar, P.K., 2022. Black carbon paper based polyanthraquinone coated exfoliated graphite for flexible paper battery. Microsyst Technol 28, 59–67. https://doi.org/10.1007/s00542-019-04378-3

Papillon, J., Ondel, O., Maire, É., 2021. Scale up of single-chamber microbial fuel cells with stainless steel 3D anode: Effect of electrode surface areas and electrode spacing. Bioresource Technology Reports 13, 100632. https://doi.org/10.1016/j.biteb.2021.100632

Park, J.Y., Yoo, Y.J., 2009. Biological nitrate removal in industrial wastewater treatment: which electron donor we can choose. Appl Microbiol Biotechnol 82, 415–429. https://doi.org/10.1007/s00253-008-1799-1

Park, M.-H., Kim, T.-H., Yang, C.-W., 2012. Thickness contrast of few-layered graphene in SEM. Surface and Interface Analysis 44, 1538–1541. https://doi.org/10.1002/sia.4995

Parra, M., Parra, L., Lloret, J., Mauri, P.V., Llinares, J.V., 2019. Low-cost Soil Moisture Sensors Based on Inductive Coils Tested on Different Sorts of Soils. Presented at the 2019 6th International Conference on Internet of Things: Systems, Management and Security, IOTSMS 2019, pp. 616–622. https://doi.org/10.1109/IOTSMS48152.2019.8939258

Parra, M., Parra, L., Rocher, J., Lloret, J., Mauri, P.V., Llinares, J.V., 2020. A novel low-cost conductivity based soil moisture sensor. Advances in Intelligent Systems and Computing 1103 AISC, 27–35. https://doi.org/10.1007/978-3-030-36664-3_4

Pasternak, G., de Rosset, A., Tyszkiewicz, N., Widera, B., Greenman, J., Ieropoulos, I., 2022. Prevention and removal of membrane and separator biofouling in bioelectrochemical systems: a comprehensive review. iScience 25, 104510. https://doi.org/10.1016/j.isci.2022.104510

Patra, N., Ramesh, P., Donthu, V., Ahmad, A., 2024. Biopolymer-based composites for sustainable energy storage: recent developments and future outlook. Journal of Materials Science: Materials in Engineering 19, 34. https://doi.org/10.1186/s40712-024-00181-9

Patrizi, G., Bartolini, A., Ciani, L., Gallo, V., Sommella, P., Carratù, M., 2022. A virtual soil moisture sensor for smart farming using deep learning. IEEE Transactions on Instrumentation and Measurement 71, 1–11.

Paz Silva, L.A., Brito Filho, F. de A., de Andrade, H.D., 2023. Soil Moisture Monitoring System Based on Metamaterial-Inspired Microwave Sensor for Precision Agriculture Applications. IEEE Sensors Journal 23, 23713–23720. https://doi.org/10.1109/JSEN.2023.3307652

Peng, P., Yang, F., Wang, Z., Wei, D., 2023. Integratable Paper-Based Iontronic Power Source for All-In-One Disposable Electronics. Advanced Energy Materials 13, 2302360. https://doi.org/10.1002/aenm.202302360

Pérez-Gallent, E., Figueiredo, M.C., Katsounaros, I., Koper, M.T.M., 2017. Electrocatalytic reduction of Nitrate on Copper single crystals in acidic and alkaline solutions. Electrochimica Acta 227, 77–84. https://doi.org/10.1016/j.electacta.2016.12.147

Petrovic, S., 2021. Basic Electrochemistry Concepts, in: Electrochemistry Crash Course for Engineers. Springer, Cham, pp. 3–10. https://doi.org/10.1007/978-3-030-61562-8_2

Pirrone, N., Garcia-Ballesteros, S., Hernández, S., Bella, F., 2024. Membrane/electrolyte interplay on ammonia motion inside a flow-cell for electrochemical nitrogen and nitrate reduction. Electrochimica Acta 493, 144415. https://doi.org/10.1016/j.electacta.2024.144415

Placidi, P., Morbidelli, R., Fortunati, D., Papini, N., Gobbi, F., Scorzoni, A., 2021. Monitoring soil and ambient parameters in the iot precision agriculture scenario: An original modeling approach dedicated to low-cost soil water content sensors. Sensors 21, 5110.

Placidi, P., Vergini, C.V.D., Papini, N., Cecconi, M., Mezzanotte, P., Scorzoni, A., 2023. Low-Cost and Low-Frequency Impedance Meter for Soil Water Content Measurement in the Precision Agriculture Scenario. IEEE Transactions on Instrumentation and Measurement 72. https://doi.org/10.1109/TIM.2023.3302898

Poosapati, A., Negrete, K., Thorpe, M., Hutchison, J., Zupan, M., Lan, Y., Madan, D., 2021. Safe and flexible chitosan-based polymer gel as an electrolyte for use in zinc-alkaline based chemistries. Journal of Applied Polymer Science 138, 50813. https://doi.org/10.1002/app.50813

Prambauer, M., Paulik, C., Burgstaller, C., 2015. The influence of paper type on the properties of structural paper – Polypropylene composites. Composites Part A: Applied Science and Manufacturing 74, 107–113. https://doi.org/10.1016/j.compositesa.2015.04.004

Raaif, M., Mohamed, S.H., 2017. The effect of Cu on the properties of CdO/Cu/CdO multilayer films for transparent conductive electrode applications. Applied Physics A: Materials Science and Processing 123. https://doi.org/10.1007/s00339-017-1050-y

Rafiee, M., Abrams, D.J., Cardinale, L., Goss, Z., Romero-Arenas, A., Stahl, S.S., 2024. Cyclic voltammetry and chronoamperometry: mechanistic tools for organic electrosynthesis. Chem. Soc. Rev. 53, 566–585. https://doi.org/10.1039/D2CS00706A

Rafiee, Z., Elhadad, A., Choi, S., 2024. Revolutionizing Papertronics: Advanced Green, Tunable, and Flexible Components and Circuits. Advanced Sustainable Systems 8, 2400049. https://doi.org/10.1002/adsu.202400049

Raja, M.W., Basu, R.N., Pramanik, N.C., Das, P.S., Das, M., 2022. Paperator: The Paper-Based Ceramic Separator for Lithium-Ion Batteries and the Process Scale-Up Strategy. ACS Appl. Energy Mater. 5, 5841–5854. https://doi.org/10.1021/acsaem.2c00188

Rajmohan, K.S., Chetty, R., 2017. Enhanced nitrate reduction with copper phthalocyanine-coated carbon nanotubes in a solid polymer electrolyte reactor. J Appl Electrochem 47, 63–74. https://doi.org/10.1007/s10800-016-1020-7

Rajmohan, K.S., Chetty, R., 2014. Nitrate reduction at electrodeposited copper on copper cathode. ECS Transactions 59, 397.

Ramirez-Nava, J., Martínez-Castrejón, M., García-Mesino, R.L., López-Díaz, J.A., Talavera-Mendoza, O., Sarmiento-Villagrana, A., Rojano, F., Hernández-Flores, G., 2021. The Implications of Membranes Used as Separators in Microbial Fuel Cells. Membranes (Basel) 11, 738. https://doi.org/10.3390/membranes11100738

Ramos, A., Miranda-Hernández, M., González, I., 2001. Influence of Chloride and Nitrate Anions on Copper Electrodeposition in Ammonia Media. Journal of the Electrochemical Society 148, C315–C321. https://doi.org/10.1149/1.1357176

Randviir, E.P., 2018. A cross examination of electron transfer rate constants for carbon screen-printed electrodes using Electrochemical Impedance Spectroscopy and cyclic voltammetry. Electrochimica Acta 286, 179–186. https://doi.org/10.1016/j.electacta.2018.08.021

Rane, A.V., Kanny, K., Abitha, V.K., Thomas, S., 2018. Chapter 5 - Methods for Synthesis of Nanoparticles and Fabrication of Nanocomposites, in: Mohan Bhagyaraj, S., Oluwafemi, O.S., Kalarikkal, N., Thomas, S. (Eds.), Synthesis of Inorganic Nanomaterials, Micro and Nano Technologies. Woodhead Publishing, pp. 121–139. https://doi.org/10.1016/B978-0-08-101975-7.00005-1

Rasheed, M.W., Tang, J., Sarwar, A., Shah, S., Saddique, N., Khan, M.U., Imran Khan, M., Nawaz, S., Shamshiri, R.R., Aziz, M., Sultan, M., 2022. Soil Moisture Measuring Techniques and Factors Affecting the Moisture Dynamics: A Comprehensive Review. Sustainability 14, 11538. https://doi.org/10.3390/su141811538

Rastogi, V.K., Samyn, P., 2017. Synthesis of polyhydroxybutyrate particles with micro-to-nanosized structures and application as protective coating for packaging papers. Nanomaterials 7. https://doi.org/10.3390/nano7010005

Reddy, M.S.B., Ponnamma, D., Choudhary, R., Sadasivuni, K.K., 2021. A Comparative Review of Natural and Synthetic Biopolymer Composite Scaffolds. Polymers (Basel) 13, 1105. https://doi.org/10.3390/polym13071105

Reyter, D., 2014. Electrochemical Reduction of Nitrate, in: Kreysa, G., Ota, K., Savinell, R.F. (Eds.), Encyclopedia of Applied Electrochemistry. Springer, New York, NY, pp. 585–593. https://doi.org/10.1007/978-1-4419-6996-5_135

Reyter, D., Chamoulaud, G., Bélanger, D., Roué, L., 2006. Electrocatalytic reduction of nitrate on copper electrodes prepared by high-energy ball milling. Journal of Electroanalytical Chemistry 596, 13–24.

Rezaei Niya, S.M., Hoorfar, M., 2013. Study of proton exchange membrane fuel cells using electrochemical impedance spectroscopy technique – A review. Journal of Power Sources 240, 281–293. https://doi.org/10.1016/j.jpowsour.2013.04.011

Rezaei-Sameti, M., Zarei, P., 2018. NBO, AIM, HOMO–LUMO and thermodynamic investigation of the nitrate ion adsorption on the surface of pristine, Al and Ga doped BNNTs: A DFT study. Adsorption 24, 757–767. https://doi.org/10.1007/s10450-018-9977-7

Rhim, J.-W., Lee, J.-H., Hong, S.-I., 2006. Water resistance and mechanical properties of biopolymer (alginate and soy protein) coated paperboards. LWT - Food Science and Technology 39, 806–813. https://doi.org/10.1016/j.lwt.2005.05.008

Ribeiro, M.C.E., Couto, A.B., Ferreira, N.G., Baldan, M.R., 2014. Nitrate Removal by Electrolysis Using Cu/BDD Electrode Cathode. ECS Trans. 58, 21–26. https://doi.org/10.1149/05819.0021ecst

Ridwan, F., Febriyan, N., Husin, M.A., Aulia, F., 2024. A Study on the Effect of Cellulose Nanocrystalline Paper on PVA-KOH Electrolyte Membranes for Increasing Ionic Conductivity. International Journal of Energy Production and Management. 2024. Vol. 9. Iss. 2 9, 113–120.

Roberts, M., Johns, P., Owen, J., Brandell, D., Edstrom, K., Enany, G.E., Guery, C., Golodnitsky, D., Lacey, M., Lecoeur, C., Mazor, H., Peled, E., Perre, E., Shaijumon, M.M., Simon, P., Taberna, P.-L., 2011. 3D lithium ion batteries—from fundamentals to fabrication. J. Mater. Chem. 21, 9876–9890. https://doi.org/10.1039/C0JM04396F

Rosseto, M., Rigueto, C.V.T., Krein, D.D.C., Balbé, N.P., Massuda, L.A., Dettmer, A., Rosseto, M., Rigueto, C.V.T., Krein, D.D.C., Balbé, N.P., Massuda, L.A., Dettmer, A., 2019. Biodegradable Polymers: Opportunities and Challenges, in: Organic Polymers. IntechOpen. https://doi.org/10.5772/intechopen.88146

Rossi, M., Tosato, P., Gemma, L., Torquati, L., Catania, C., Camalò, S., Brunelli, D., 2017. Long range wireless sensing powered by plant-microbial fuel cell. Presented at the Proceedings of the 2017 Design, Automation and Test in Europe, DATE 2017, pp. 1651–1654. https://doi.org/10.23919/DATE.2017.7927258

Rossnagel, S.M., 2003. Thin film deposition with physical vapor deposition and related technologies. Journal of Vacuum Science & Technology A 21, S74–S87. https://doi.org/10.1116/1.1600450

Roy, C., Deschamps, J., Martin, M., Bertin, E., Reyter, D., Garbarino, S., Roué, L., Guay, D., 2016. Identification of Cu surface active sites for a complete nitrate-to-nitrite conversion with nanostructured catalysts. Applied Catalysis B: Environmental 187, 399–407.

Roy, H., Rahman, T.U., Tasnim, N., Arju, J., Rafid, Md.M., Islam, Md.R., Pervez, Md.N., Cai, Y., Naddeo, V., Islam, Md.S., 2023. Microbial Fuel Cell Construction Features and Application for Sustainable Wastewater Treatment. Membranes (Basel) 13, 490. https://doi.org/10.3390/membranes13050490

Rumora, A., Hopkins, L., Yim, K., Baykus, M.F., Martinez, L., Jimenez, L., 2024. 16S rRNA Analysis of Electrogenic Bacterial Communities from Soil Microbial Fuel Cells. Applied Microbiology 4, 918–933. https://doi.org/10.3390/applmicrobiol4020062

Rumora, A., Hopkins, L., Yim, K., Baykus, M.F., Martinez, L., Jimenez, L., 2023. Detection and Characterization of Electrogenic Bacteria from Soils. BioTech 12, 65. https://doi.org/10.3390/biotech12040065

Saeed, I.A., Qinglan, S., Wang, M., Butt, S.L., Zheng, L., Tuan, V.N., Wanlin, G., 2019. Development of a low-cost multi-depth real-time soil moisture sensor using time division multiplexing approach. IEEE Access 7, 19688–19697. https://doi.org/10.1109/ACCESS.2019.2893680

Safronova, E.Yu., Voropaeva, D.Yu., Lysova, A.A., Korchagin, O.V., Bogdanovskaya, V.A., Yaroslavtsev, A.B., 2022. On the Properties of Nafion Membranes Recast from Dispersion in N-Methyl-2-Pyrrolidone. Polymers (Basel) 14, 5275. https://doi.org/10.3390/polym14235275

Saghafi, M., Chinnathambi, S., Lemay, S.G., 2023. High-frequency phenomena and electrochemical impedance spectroscopy at nanoelectrodes. Current Opinion in Colloid & Interface Science 63, 101654. https://doi.org/10.1016/j.cocis.2022.101654

Sahu, P., Gupta, M., 2022. Water absorption behavior of cellulosic fibres polymer composites: A review on its effects and remedies. Journal of Industrial Textiles 51, 7480S-7512S. https://doi.org/10.1177/1528083720974424

Saidina, D.S., Eawwiboonthanakit, N., Mariatti, M., Fontana, S., Hérold, C., 2019. Recent Development of Graphene-Based Ink and Other Conductive Material-Based Inks for Flexible Electronics. J. Electron. Mater. 48, 3428–3450. https://doi.org/10.1007/s11664-019-07183-w

Saito, T., Oishi, T., Inoue, M., Iida, S., Mihota, N., Yamada, A., Shimizu, K., Inumochi, S., Inosako, K., 2022. Low-Error Soil Moisture Sensor Employing Spatial Frequency Domain Transmissometry. Sensors 22, 8658. https://doi.org/10.3390/s22228658

Sajib, M.M.H., Sayem, A.S.M., 2025. Innovations in Sensor-Based Systems and Sustainable Energy Solutions for Smart Agriculture: A Review. Encyclopedia 5, 67. https://doi.org/10.3390/encyclopedia5020067

Salahinejad, E., Hadianfard, M.J., Macdonald, D.D., Sharifi-Asl, S., Mozafari, M., Walker, K.J., Rad, A.T., Madihally, S.V., Tayebi, L., 2013. In Vitro Electrochemical Corrosion and Cell Viability Studies on Nickel-Free Stainless Steel Orthopedic Implants. PLOS ONE 8, e61633. https://doi.org/10.1371/journal.pone.0061633

Salazar, J., Tadeo, F., Prada, C., 2015. Modelling of Diesel Generator Sets That Assist OFF-Grid Renewable Energy Micro-grids. Renewable Energy and Sustainable Development 1, 72–80.

Salazar, P., Rico, V., González-Elipe, A.R., 2016. Nickel–copper bilayer nanoporous electrode prepared by physical vapor deposition at oblique angles for the non-enzymatic determination of glucose. Sensors and Actuators B: Chemical 226, 436–443. https://doi.org/10.1016/j.snb.2015.12.003

Saleh, M., Elhajj, I.H., Asmar, D., Bashour, I., Kidess, S., 2016. Experimental evaluation of low-cost resistive soil moisture sensors. Presented at the 2016 IEEE International Multidisciplinary Conference on Engineering Technology, IMCET 2016, pp. 179–184. https://doi.org/10.1109/IMCET.2016.7777448

Samir, A., Ashour, F.H., Hakim, A.A.A., Bassyouni, M., 2022. Recent advances in biodegradable polymers for sustainable applications. npj Mater Degrad 6, 1–28. https://doi.org/10.1038/s41529-022-00277-7

Sancho, M., Álvarez-Blanco, S., Kombo, G., García-Fayos, B., 2016. Experimental determination of nanofiltration models: application to nitrate removal. Desalination and Water Treatment 57, 22852–22859.

Sangeetha, E., Narayanan, A., Dhamodharan, R., 2022. Super water-absorbing hydrogel based on chitosan, itaconic acid and urea: preparation, characterization and reversible water absorption. Polym. Bull. 79, 3013–3030. https://doi.org/10.1007/s00289-021-03641-w

Satokawa, Y., Shikata, T., 2008. Hydration Structure and Dynamic Behavior of Poly(vinyl alcohol)s in Aqueous Solution. Macromolecules 41, 2908–2913. https://doi.org/10.1021/ma702793t

Savale, P., 2016. Physical vapor deposition (PVD) methods for synthesis of thin films: A comparative study. Arch. Appl. Sci. Res 8, 1–8.

Schaffer, J.V., Lupatini, K.N., Machado, B., Silva, E.S., Ferracin, R.J., Alves, H.J., 2018. Parameters effect on proton conductivity to obtain chitosan membranes for use as electrolytes in PEMFC. International Journal of Energy Research 42, 1381–1385. https://doi.org/10.1002/er.3933

Schmeisser, J.M., 2007. Proton transport in proton exchange membranes.

Schmidt-Rohr, K., 2018. How Batteries Store and Release Energy: Explaining Basic Electrochemistry. J. Chem. Educ. 95, 1801–1810. https://doi.org/10.1021/acs.jchemed.8b00479

Schwamback, D., Persson, M., Berndtsson, R., Bertotto, L.E., Kobayashi, A.N.A., Wendland, E.C., 2023. Automated Low-Cost Soil Moisture Sensors: Trade-Off between Cost and Accuracy. Sensors 23, 2451.

Selinger, J., Islam, M.T., Abbas, Q., Schaubeder, J.B., Zoder, J., Bakhshi, A., Bauer, W., Hummel, M., Spirk, S., 2024. Form-stable, crosslinked cellulose-based paper separators for charge storage applications. Carbohydrate Polymers 343, 122354. https://doi.org/10.1016/j.carbpol.2024.122354

Sen Gupta, R., Samantaray, P.K., Bose, S., 2023. Going beyond Cellulose and Chitosan: Synthetic Biodegradable Membranes for Drinking Water, Wastewater, and Oil–Water Remediation. ACS Omega 8, 24695–24717. https://doi.org/10.1021/acsomega.3c01699

Serra, J.P., Uranga, J., Gonçalves, R., Costa, C.M., de la Caba, K., Guerrero, P., Lanceros-Mendez, S., 2023. Sustainable lithium-ion battery separators based on cellulose and soy protein membranes. Electrochimica Acta 462, 142746. https://doi.org/10.1016/j.electacta.2023.142746

Shah, A., Izman, S., Ismail, S.N.F., Ayu, M., Daud, H., Abdul-Kadir, M., 2018. Physical Vapour Deposition on corrosion resistance: A review. ARPN J. Eng. Appl. Sci 13, 3515–3523.

Shahab Marf, A., M. Abdullah, R., B. Aziz, S., 2020. Structural, Morphological, Electrical and Electrochemical Properties of PVA: CS-Based Proton-Conducting Polymer Blend Electrolytes. Membranes 10, 71. https://doi.org/10.3390/membranes10040071

Sharma, A., Đelević, L., Herkendell, K., 2024. Next-Generation Proton-Exchange Membranes in Microbial Fuel Cells: Overcoming Nafion's Limitations. Energy Technology. https://doi.org/10.1002/ente.202301346

Sharma, Akshat, Đelević, L., Herkendell, K., 2024. Next-Generation Proton-Exchange Membranes in Microbial Fuel Cells: Overcoming Nafion's Limitations. Energy Technology 2301346.

Shen, J., He, R., Han, W., Sun, X., Li, J., Wang, L., 2009. Biological denitrification of high-nitrate wastewater in a modified anoxic/oxic-membrane bioreactor (A/O-MBR). Journal of Hazardous Materials 172, 595–600.

Shen, L.-L., Zhang, G.-R., Biesalski, M., M. Etzold, B.J., 2019. Paper-based microfluidic aluminum–air batteries: toward next-generation miniaturized power supply. Lab on a Chip 19, 3438–3447. https://doi.org/10.1039/C9LC00574A

Shen, W., Chen, X., Qiu, J., Hayward, J.A., Sayeef, S., Osman, P., Meng, K., Dong, Z.Y., 2020. A comprehensive review of variable renewable energy levelized cost of electricity. Renewable and Sustainable Energy Reviews 133, 110301.

Sheth, P., Patil, D., Kandasubramanian, B., Mayilswamy, N., 2024. Advancements in chitosan membranes for promising secondary batteries. Polym. Bull. 81, 15319–15348. https://doi.org/10.1007/s00289-024-05448-x

Shi, X., Deng, T., Zhang, B., Zhang, W., Sui, L., Yang, H., Wang, D., Shi, W., Chen, C.-M., Zheng, W., 2017. Accessible 3D Integrative Paper Electrode Shapes: All-Carbon Dual-Ion Batteries with Optimum Packaging Performances. ChemElectroChem 4, 3238–3243. https://doi.org/10.1002/celc.201700752

Shih, Y.-J., Wu, Z.-L., Huang, Y.-H., Huang, C.-P., 2020a. Electrochemical nitrate reduction as affected by the crystal morphology and facet of copper nanoparticles supported on nickel foam electrodes (Cu/Ni). Chemical Engineering Journal 383, 123157. https://doi.org/10.1016/j.cej.2019.123157

Shih, Y.-J., Wu, Z.-L., Lin, C.-Y., Huang, Y.-H., Huang, C.-P., 2020b. Manipulating the crystalline morphology and facet orientation of copper and copper-palladium nanocatalysts supported on stainless steel mesh with the aid of cationic surfactant to improve the electrochemical reduction of nitrate and N2 selectivity. Applied Catalysis B: Environmental 273, 119053.

Shimohata, H., Nakamoto, T., Taguchi, K., 2023. Proposal for a practical MFC using vertical electrodes with improved air cathode function. Energy Reports, The 8th International Conference on Sustainable and Renewable Energy Engineering 9, 280–283. https://doi.org/10.1016/j.egyr.2023.10.004

Shukur, M.F., Kadir, M.F.Z., 2015. Hydrogen ion conducting starch-chitosan blend based electrolyte for application in electrochemical devices. Electrochimica Acta 158, 152–165. https://doi.org/10.1016/j.electacta.2015.01.167

Smiljanić, M., Panić, S., Bele, M., Ruiz-Zepeda, F., Pavko, L., Gašparič, L., Kokalj, A., Gaberšček, M., Hodnik, N., 2022. Improving the HER Activity and Stability of Pt Nanoparticles by Titanium Oxynitride Support. ACS Catal. 12, 13021–13033. https://doi.org/10.1021/acscatal.2c03214

Solberg, A., Zehner, J., Somorowsky, F., Rose, K., Korpela, A., Syverud, K., 2023. Material properties and water resistance of inorganic–organic polymer coated cellulose paper and nanopaper. Cellulose 30, 1205–1223. https://doi.org/10.1007/s10570-022-04925-8

Song, Y., Zhao, G., Zhang, S., Xie, C., Yang, R., Li, X., 2024. Chitosan nanofiber paper used as separator for high performance and sustainable lithium-ion batteries. Carbohydrate Polymers 329. https://doi.org/10.1016/j.carbpol.2023.121530

Song, Z., Ma, T., Tang, R., Cheng, Q., Wang, X., Krishnaraju, D., Panat, R., Chan, C.K., Yu, H., Jiang, H., 2014. Origami lithium-ion batteries. Nat Commun 5, 3140. https://doi.org/10.1038/ncomms4140

Srbinovska, M., Gavrovski, C., Dimcev, V., Krkoleva, A., Borozan, V., 2015. Environmental parameters monitoring in precision agriculture using wireless sensor networks. Journal of Cleaner Production 88, 297–307. https://doi.org/10.1016/j.jclepro.2014.04.036

Srikanth, S., Kumar, M., Puri, S., 2018. Bio-electrochemical system (BES) as an innovative approach for sustainable waste management in petroleum industry. Bioresource Technology 265, 506–518.

S.U., S.L., Singh, D.N., Shojaei Baghini, M., 2014. A critical review of soil moisture measurement. Measurement 54, 92–105. https://doi.org/10.1016/j.measurement.2014.04.007

Sudarmaji, A., Saparso, Supriyo, H., Widodo, A., 2020. Simple Parallel Probe as Soil Moisture Sensor for Sandy Land in Tropical-Coastal Areas. PERTANIKA JOURNAL OF SCIENCE AND TECHNOLOGY 28, 829–838.

Sui, Y.K., Atreya, M., Dahal, S., Gopalakrishnan, A., Khosla, R., Whiting, G.L., 2021. Controlled Biodegradation of an Additively Fabricated Capacitive Soil Moisture Sensor. Acs Sustainable Chemistry & Engineering. https://doi.org/10.1021/acssuschemeng.0c07615

Sulthoni, M., Anugrah, B., Wicaksono, N., IEEE, 2016. Development of Economical Microcontroller-based Soil Moisture Sensor Using Time Domain Reflectometry. Presented at the 2016 INTERNATIONAL SYMPOSIUM ON ELECTRONICS AND SMART DEVICES (ISESD), pp. 360–364.

Sun, H., Xu, S., Zhuang, G., Zhuang, X., 2016. Performance and recent improvement in microbial fuel cells for simultaneous carbon and nitrogen removal: A review. Journal of Environmental Sciences, 40th Anniversary of RCEES 39, 242–248. https://doi.org/10.1016/j.jes.2015.12.006

Sun, H.-T., Wang, X.-P., Kou, Z.-Q., Wang, L.-J., Wang, J.-Y., Sun, Y.-Q., 2015. Optimization of TiO2/Cu/TiO2 multilayers as a transparent composite electrode deposited by electron-beam evaporation at room temperature. Chinese Physics B 24. https://doi.org/10.1088/1674-1056/24/4/047701

Sun, M., Shi, Z., Han, Q., 2025. Structure-function integrated carbon fiber reinforced composites with enhanced mechanical robustness and electrochemical stability. Chemical Engineering Journal 517, 164297. https://doi.org/10.1016/j.cej.2025.164297

Sun, Y., Zhang, X., Wang, C., Bai, X., Fan, L., Fan, J., Xu, S., Li, H., 2023. Effect of poly(3,4-ethylenedioxythiophene): poly(styrenesulfonate) on low-iridium catalyst layer for proton exchange membrane water electrolysis. Journal of Power Sources 586, 233678. https://doi.org/10.1016/j.jpowsour.2023.233678

Surti, P.V., Kailasa, S.K., Mungray, A.K., 2024. Development of a Novel Composite Polymer Electrolyte Membrane for Application as a Separator in a Dual Chamber Microbial Fuel Cell. Industrial and Engineering Chemistry Research 63, 5182–5194. https://doi.org/10.1021/acs.iecr.3c04280

Tabata, K., Nohara, T., Nakazaki, H., Makino, T., Saito, T., Arita, T., Masuhara, A., 2022. Proton conductivity dependence on the surface polymer thickness of core–shell type nanoparticles in a proton exchange membrane. Nanoscale Adv. 4, 4714–4723. https://doi.org/10.1039/D2NA00450J

Takahashi, T., 1998. Physical Vapor Deposition. Ultraclean Surface Processing of Silicon Wafers: Secrets of VLSI Manufacturing 352–360.

Tan, X., Wang, X., Zhou, T., Chen, T., Liu, Y., Ma, C., Guo, H., Li, B., 2022. Preparation of three dimensional bimetallic Cu–Ni/NiF electrodes for efficient electrochemical removal of nitrate nitrogen. Chemosphere 295, 133929. https://doi.org/10.1016/j.chemosphere.2022.133929

Tan, Y.K., Panda, S.K., 2010. Review of energy harvesting technologies for sustainable wireless sensor network. Sustainable wireless sensor networks 2010, 15–43.

Tessmer, A., Aschenbruck, N., 2023. Using Dynamic Time Warping to Calibrate Low-Cost Soil Moisture Sensors, in: 2023 IEEE 20th International Conference on Mobile Ad Hoc and Smart Systems (MASS). Presented at the 2023 IEEE 20th International Conference on Mobile Ad Hoc and Smart Systems (MASS), pp. 616–621. https://doi.org/10.1109/MASS58611.2023.00086

Thom, N.K., Yeung, K., Pillion, M.B., Phillips, S.T., 2012. “Fluidic batteries” as low-cost sources of power in paper-based microfluidic devices. Lab Chip 12, 1768–1770. https://doi.org/10.1039/C2LC40126F

Tian, H., Gao, C., Zhang, X., Yu, C., Xie, T., 2022. Smart Soil Water Sensor with Soil Impedance Detected via Edge Electromagnetic Field Induction. MICROMACHINES 13. https://doi.org/10.3390/mi13091427

Tian, S., Liu, C., Hu, H., Zhao, H., Yao, A., Lan, J., Liu, L., Shang, J., Huang, X., Lin, S., 2024. Construction of Waste Paper-Chitosan-Based Membranes with pH-Tunable Surface Charge for Efficient Separation of Oil-in-Water Emulsion and Dye. ACS Sustainable Chem. Eng. 12, 10854–10868. https://doi.org/10.1021/acssuschemeng.4c02540

Tiwari, A., Kumar Singh, R., 2024. Biopolymers for Energy Applications, in: Bio-Based Polymers: Farm to Industry. Volume 3: Emerging Trends and Applications, ACS Symposium Series. American Chemical Society, pp. 1–12. https://doi.org/10.1021/bk-2024-1487.ch001

Tiwari, A., Yadav, N., Jadhav, D.A., Saxena, D., Anghan, K., Sandhwar, V.K., Saxena, S., 2024. A Critical Review on the Advancement of the Development of Low-Cost Membranes to Be Utilized in Microbial Fuel Cells. Water 16, 1597. https://doi.org/10.3390/w16111597

Toczyłowska-Mamińska, R., Mamiński, M.Ł., Kwasowski, W., 2025. Microbial Fuel Cell Technology as a New Strategy for Sustainable Management of Soil-Based Ecosystems. Energies 18, 970. https://doi.org/10.3390/en18040970

Tomer, M.D., Porter, S.A., James, D.E., Boomer, K.M., Kostel, J.A., McLellan, E., 2013. Combining precision conservation technologies into a flexible framework to facilitate agricultural watershed planning. Journal of Soil and Water Conservation 68, 113A-120A.

Topp, G.C., Parkin, G., Ferré, T.P., Carter, M., Gregorich, E., 2008. Soil water content. Soil sampling and methods of analysis 2, 939–962.

Topsakal, M., Şahin, H., Ciraci, S., 2012. Graphene coatings: An efficient protection from oxidation. Phys. Rev. B 85, 155445. https://doi.org/10.1103/PhysRevB.85.155445

Trabia, S., Hwang, T., Kim, K.J., 2016. A fabrication method of unique Nafion® shapes by painting for ionic polymer–metal composites. Smart Mater. Struct. 25, 085006. https://doi.org/10.1088/0964-1726/25/8/085006

Tran, D.H., Ulbricht, M., 2023. Cellulose-cellulose composite membranes for ultrafiltration. Journal of Membrane Science 672, 121426. https://doi.org/10.1016/j.memsci.2023.121426

Tran, N.T., Nguyen, G.T., Le, T.M., Huynh, A.T.N., 2025. Chitosan/Graphene Oxide/Ag Nanocomposites Loaded in Polyvinyl Alcohol Films as Biodegradable, UV-Blocking, and Antibacterial Film for Fruit Packaging. Journal of Applied Polymer Science 142, e56677. https://doi.org/10.1002/app.56677

Turossi, T.C., Júnior, H.L.O., Monticeli, F.M., Dias, O.T., Zattera, A.J., 2025. Cellulose-Derived Battery Separators: A Minireview on Advances Towards Environmental Sustainability. Polymers 17, 456. https://doi.org/10.3390/polym17040456

Ucar, D., Zhang, Y., Angelidaki, I., 2017. An Overview of Electron Acceptors in Microbial Fuel Cells. Front. Microbiol. 8. https://doi.org/10.3389/fmicb.2017.00643

Ukoba, K., Yoro, K.O., Eterigho-Ikelegbe, O., Ibegbulam, C., Jen, T.-C., 2024. Adaptation of solar energy in the Global South: Prospects, challenges and opportunities. Heliyon 10, e28009. https://doi.org/10.1016/j.heliyon.2024.e28009

Ullah, A., Zubair, M., Zulfiqar, M.H., Kamsong, W., Karuwan, C., Massoud, Y., Mehmood, M.Q., 2024. Highly sensitive screen-printed soil moisture sensor array as green solutions for sustainable precision agriculture.

Umar, L., Setiadi, R.N., 2015. Low cost soil sensor based on impedance spectroscopy for in-situ measurement. Presented at the AIP Conference Proceedings. https://doi.org/10.1063/1.4917112

Uneputty, A., Dávila-Lezama, A., Garibo, D., Oknianska, A., Bogdanchikova, N., Hernández-Sánchez, J.F., Susarrey-Arce, A., 2022. Strategies applied to modify structured and smooth surfaces: A step closer to reduce bacterial adhesion and biofilm formation. Colloid and Interface Science Communications 46, 100560. https://doi.org/10.1016/j.colcom.2021.100560

Vandôme, P., Leauthaud, C., Moinard, S., Sainlez, O., Mekki, I., Zairi, A., Belaud, G., 2023. Making technological innovations accessible to agricultural water management: Design of a low-cost wireless sensor network for drip irrigation monitoring in Tunisia. Smart Agricultural Technology 4. https://doi.org/10.1016/j.atech.2023.100227

Vannieuwenborg, F., Verbrugge, S., Colle, D., 2018. Choosing IoT-connectivity? A guiding methodology based on functional characteristics and economic considerations. Transactions on Emerging Telecommunications Technologies 29, e3308. https://doi.org/10.1002/ett.3308

Varapragasam, S.J.P., Andriolo, J.M., Skinner, J.L., Grumstrup, E.M., 2021. Photocatalytic Reduction of Aqueous Nitrate with Hybrid Ag/g-C3N4 under Ultraviolet and Visible Light. ACS Omega 6, 34850–34856. https://doi.org/10.1021/acsomega.1c05523

Veerubhotla, R., Das, D., Pradhan, D., 2017. A flexible and disposable battery powered by bacteria using eyeliner coated paper electrodes. Biosensors and Bioelectronics 94, 464–470. https://doi.org/10.1016/j.bios.2017.03.020

Vera, J., Mosquera-Vargas, E., Diosa, J.E., 2022. Thermal, electrical and structural study of polymeric membranes based on poly(vinyl alcohol), chitosan and phosphoric acid. Appl. Phys. A 128, 1–5. https://doi.org/10.1007/s00339-022-05526-9

Vicente-Saez, R., Martinez-Fuentes, C., 2018. Open Science now: A systematic literature review for an integrated definition. Journal of business research 88, 428–436.

Vilela, C., Silvestre, A.J.D., Figueiredo, F.M.L., Freire, C.S.R., 2019. Nanocellulose-based materials as components of polymer electrolyte fuel cells. J. Mater. Chem. A 7, 20045–20074. https://doi.org/10.1039/C9TA07466J

W. A. K. Afridi, I. Vitoria, K. Jayasundera, S. C. Mukhopadhyay, Z. Liu, 2023. Development and Field Installation of Smart Sensor Nodes for Quantification of Missing Water in Soil. IEEE Sensors Journal 23, 26495–26502. https://doi.org/10.1109/JSEN.2023.3317418

Wagner, L.T., Hashemi, Niloofar, Hashemi, Nastaran, 2013. A Compact Versatile Microbial Fuel Cell From Paper. Presented at the ASME 2013 11th International Conference on Fuel Cell Science, Engineering and Technology collocated with the ASME 2013 Heat Transfer Summer Conference and the ASME 2013 7th International Conference on Energy Sustainability, American Society of Mechanical Engineers Digital Collection. https://doi.org/10.1115/FuelCell2013-18322

Walter, X.A., Gajda, I., Forbes, S., Winfield, J., Greenman, J., Ieropoulos, I., 2016. Scaling-up of a novel, simplified MFC stack based on a self-stratifying urine column. Biotechnology for Biofuels 9, 93. https://doi.org/10.1186/s13068-016-0504-3

Wang, yu-min, Seydou, T., Kerh, T., 2010. Applying Evapotranspiration Reference Model and RainfallContribution Index for Agricultural Water Management Plan in Burkina Faso. African Journal of Agricultural Research 4, 1493–1504.

Wang, C., Fu, B., Zhang, L., Xu, Z., 2019. Soil moisture–plant interactions: an ecohydrological review. J Soils Sediments 19, 1–9. https://doi.org/10.1007/s11368-018-2167-0

Wang, C., Liu, J.-M., Wang, Y.-H., Lu, X.-Y., 2023. Study on the electrochemical reduction of nitrate using a modified Cu-Pd bimetallic electrode. Zhongguo Huanjing Kexue/China Environmental Science 43, 5196–5207.

Wang, D.-C., Lei, S.-N., Zhong, S., Xiao, X., Guo, Q.-H., 2023. Cellulose-Based Conductive Materials for Energy and Sensing Applications. Polymers 15, 4159. https://doi.org/10.3390/polym15204159

Wang, H., Huang, J., Cai, J., Wei, Y., Cao, A., Liu, B., Lu, S., 2023. In Situ/Operando Methods for Understanding Electrocatalytic Nitrate Reduction Reaction. Small Methods 7, 2300169. https://doi.org/10.1002/smtd.202300169

Wang, H., Pilon, L., 2012. Physical interpretation of cyclic voltammetry for measuring electric double layer capacitances. Electrochimica Acta 64, 130–139. https://doi.org/10.1016/j.electacta.2011.12.118

Wang, Jun, Deng, H., Wu, S.-S., Deng, Y.-C., Liu, L., Han, C., Jiang, Y.-B., Zhong, W.-H., 2019. Assessment of abundance and diversity of exoelectrogenic bacteria in soil under different land use types. CATENA 172, 572–580. https://doi.org/10.1016/j.catena.2018.09.028

Wang, Jingfeng, Liu, Y., Fan, Z., Wang, W., Wang, B., Guo, Z., 2019. Ink-based 3D printing technologies for graphene-based materials: a review. Adv Compos Hybrid Mater 2, 1–33. https://doi.org/10.1007/s42114-018-0067-9

Wang, J., Zhang, Z., Ding, S., 2022. Cu supported on the graphene oxide modified graphite felt electrode for highly efficient nitrate electroreduction. Journal of Environmental Chemical Engineering 10, 108092. https://doi.org/10.1016/j.jece.2022.108092

Wang, L., Jin, M., Cai, Y., Lian, Y., Zhao, X., Wang, R., Qiao, S., Chen, L., Yan, X., 2023. Construction of electrochemical model for high C-rate conditions in lithium-ion battery based on experimental analogy method. Energy 279, 128073. https://doi.org/10.1016/j.energy.2023.128073

Wang, L., Zuo, X., Raut, A., Isseroff, R., Xue, Y., Zhou, Y., Sandhu, B., Schein, T., Zeliznyak, T., Sharma, P., Sharma, S., Hsiao, B.S., Rafailovich, M.H., 2019. Operation of proton exchange membrane (PEM) fuel cells using natural cellulose fiber membranes. Sustainable Energy Fuels 3, 2725–2732. https://doi.org/10.1039/C9SE00381A

Wang, X.-Y., Wang, J., Zhao, C., Ma, L., Rousseau, D., Tang, C.-H., 2023. Facile fabrication of chitosan colloidal films with pH-tunable surface hydrophobicity and mechanical properties. Food Hydrocolloids 137, 108429. https://doi.org/10.1016/j.foodhyd.2022.108429

Wang, Y., He, B., Zhao, L., 2017. Fabrication of Hydrophobic Coating on Filter Paper from Self-emulsifying Carnauba Wax-alcohol Emulsions with Nano-TiO2 Particles for Water/Diesel Separation. BioResources 12, 7774–7783. https://doi.org/10.15376/biores.12.4.7774-7783

Wang, Yang, Long, J., Hu, J., Sun, Z., Meng, L., 2020. Polyvinyl alcohol /Lyocell dual-layer paper-based separator for primary zinc-air batteries. Journal of Power Sources 453, 227853. https://doi.org/10.1016/j.jpowsour.2020.227853

Wang, Y., Qu, J., Liu, H., 2007. Effect of liquid property on adsorption and catalytic reduction of nitrate over hydrotalcite-supported Pd-Cu catalyst. Journal of Molecular Catalysis A: Chemical 272, 31–37. https://doi.org/10.1016/j.molcata.2007.02.028

Wang, Y., Wang, C., Li, M., Yu, Y., Zhang, B., 2021. Nitrate electroreduction: mechanism insight, in situ characterization, performance evaluation, and challenges. Chem. Soc. Rev. 50, 6720–6733. https://doi.org/10.1039/D1CS00116G

Wang, Yuting, Zhou, W., Jia, R., Yu, Y., Zhang, B., 2020. Unveiling the activity origin of a copper-based electrocatalyst for selective nitrate reduction to ammonia. Angewandte chemie international edition 59, 5350–5354.

Wang, Z., Ni, J., Li, L., Lu, J., 2020. Theoretical Simulation and Modeling of Three-Dimensional Batteries. Cell Reports Physical Science 1, 100078. https://doi.org/10.1016/j.xcrp.2020.100078

Wang, Z., Pan, R., Sun, R., Edström, K., Strømme, M., Nyholm, L., 2018. Nanocellulose Structured Paper-Based Lithium Metal Batteries. ACS Appl. Energy Mater. 1, 4341–4350. https://doi.org/10.1021/acsaem.8b00961

Wei, M., Li, S., Wang, X., Zuo, G., Wang, H., Meng, X., Wang, J., 2024. A Perspective on Cu-Based Electrocatalysts for Nitrate Reduction for Ammonia Synthesis. Advanced Energy and Sustainability Research 5, 2300173. https://doi.org/10.1002/aesr.202300173

Wei, P., Sui, Y., Meng, X., Zhou, Q., 2023. The advances development of proton exchange membrane with high proton conductivity and balanced stability in fuel cells. Journal of Applied Polymer Science 140, e53919. https://doi.org/10.1002/app.53919

Welch, C.M., Hyde, M.E., Banks, C.E., Compton, R.G., 2005. The detection of nitrate using in-situ copper nanoparticle deposition at a boron doped diamond electrode. Analytical Sciences 21, 1421–1430. https://doi.org/10.2116/analsci.21.1421

Wen, M., Wang, H., Ma, B., Xiong, F., 2024. Photothermal Performance of Lignin-Based Nanospheres and Their Applications in Water Surface Actuators. Polymers 16. https://doi.org/10.3390/polym16070927

Wenwu, Z., Xuening, F., Daryanto, S., Zhang, X., Yaping, W., 2018. Factors influencing soil moisture in the Loess Plateau, China: A review. Earth and Environmental Science Transactions of the Royal Society of Edinburgh 109, 501–509.

Widtsoe, J.A., McLaughlin, W.W., 1912. The movement of water in irrigated soils. Utah Agricultural College Experiment Station.

Wilberforce, T., Alaswad, A., Palumbo, A., Dassisti, M., Olabi, A.-G., 2016. Advances in stationary and portable fuel cell applications. International journal of hydrogen energy 41, 16509–16522.

Wu, L., Ko, E., Dulkin, A., Park, K.J., Fields, S., Leeser, K., Meng, L., Ruzic, D.N., 2010. Flux and energy analysis of species in hollow cathode magnetron ionized physical vapor deposition of copper. Review of Scientific Instruments 81. https://doi.org/10.1063/1.3504371

Wu, X., Liu, M., 2012. In-situ soil moisture sensing: measurement scheduling and estimation using compressive sensing, in: Proceedings of the 11th International Conference on Information Processing in Sensor Networks. Presented at the IPSN '12: The 11th International Conference on Information Processing in Sensor Networks, ACM, Beijing China, pp. 1–12. https://doi.org/10.1145/2185677.2185679

Xiao, W., Zhao, L., Gong, Y., Liu, J., Yan, C., 2015. Preparation and performance of poly(vinyl alcohol) porous separator for lithium-ion batteries. Journal of Membrane Science 487, 221–228. https://doi.org/10.1016/j.memsci.2015.04.004

Xie, Z., Yu, S., Yang, G., Li, K., Ding, L., Wang, W., Zhang, F.-Y., 2021. Optimization of catalyst-coated membranes for enhancing performance in proton exchange membrane electrolyzer cells. International Journal of Hydrogen Energy 46, 1155–1162. https://doi.org/10.1016/j.ijhydene.2020.09.239

Xu, H., Chen, J., Zhang, Z., Hung, C.-T., Yang, J., Li, W., 2023. In Situ Confinement of Ultrasmall Metal Nanoparticles in Short Mesochannels for Durable Electrocatalytic Nitrate Reduction with High Efficiency and Selectivity. Advanced Materials 35, 2207522. https://doi.org/10.1002/adma.202207522

Xu, Y., Zhu, Y., Han, F., Luo, C., Wang, C., 2015. 3D Si/C Fiber Paper Electrodes Fabricated Using a Combined Electrospray/Electrospinning Technique for Li-Ion Batteries. Advanced Energy Materials 5, 1400753. https://doi.org/10.1002/aenm.201400753

Yammine, P., El-Nakat, H., Kassab, R., Mansour, A., El Khoury, B., Koumeir, D., Matar, Z., Chmayssem, A., 2024. Recent Advances in Applied Electrochemistry: A Review. Chemistry 6, 407–434. https://doi.org/10.3390/chemistry6030024

Yang, C., Han, N., Wang, Y., Yuan, X.-Z., Xu, J., Huang, H., Fan, J., Li, H., Wang, H., 2020. A Novel Approach to Fabricate Membrane Electrode Assembly by Directly Coating the Nafion Ionomer on Catalyst Layers for Proton-Exchange Membrane Fuel Cells. ACS Sustainable Chem. Eng. 8, 9803–9812. https://doi.org/10.1021/acssuschemeng.0c02386

Yang, P., Li, J., Lee, S.W., Fan, H.J., 2021. Printed Zinc Paper Batteries. Adv Sci (Weinh) 9, 2103894. https://doi.org/10.1002/advs.202103894

Yang, S., Liu, Y., Jiang, Z., Gu, J., Zhang, D., 2018. Thermal and mechanical performance of electrospun chitosan/poly(vinyl alcohol) nanofibers with graphene oxide. Adv Compos Hybrid Mater 1, 722–730. https://doi.org/10.1007/s42114-018-0060-3

Yang, S., Wang, X., Song, Z., Liu, C., Li, Z., Wang, J., Song, L., 2022. Efficient electrocatalytic nitrate reduction in neutral medium by Cu/CoP/NF composite cathode coupled with Ir-Ru/Ti anode. Chemosphere 307, 136132. https://doi.org/10.1016/j.chemosphere.2022.136132

Yang, X., Huang, L., Deng, Q., Dong, W., 2024. A Sustainable and Eco-Friendly Membrane for PEM Fuel Cells Using Bacterial Cellulose. Polymers 16, 3017. https://doi.org/10.3390/polym16213017

Yang, X., Wu, W., Liu, Y., Lin, Z., Sun, X., 2022. Chitosan modified filter paper separators with specific ion adsorption to inhibit side reactions and induce uniform Zn deposition for aqueous Zn batteries. Chemical Engineering Journal 450, 137902. https://doi.org/10.1016/j.cej.2022.137902

Yanguas-Gil, A., Yanguas-Gil, A., 2017. Physical and Chemical Vapor Deposition Techniques. Growth and Transport in Nanostructured Materials: Reactive Transport in PVD, CVD, and ALD 19–37.

Yao, X., Yu, B., Xue, Y., Ran, X., Zuo, J., Qiu, K., 2021. Selective conversion of nitrate to nitrogen by CuNi alloys embedded mesoporous carbon with breakpoint chlorination. Journal of Water Process Engineering 42, 102174. https://doi.org/10.1016/j.jwpe.2021.102174

Yin, D., Liu, Y., Song, P., Chen, P., Liu, X., Cai, L., Zhang, L., 2019. In situ growth of copper/reduced graphene oxide on graphite surfaces for the electrocatalytic reduction of nitrate. Electrochimica Acta 324, 134846. https://doi.org/10.1016/j.electacta.2019.134846

Yingnakorn, T., Hartley, J., Keal, M.E., Gordon, R., Florido, D.M., Abbott, A.P., Yang, J.M., 2025. Catalyst coated membranes for fuel cell and water electrolyser delamination induced by organic solution soaking and water ultrasonication. RSC Sustainability 3, 1900–1908. https://doi.org/10.1039/D4SU00795F

Yogesh, R., Srivastava, N., 2022. A detailed insight towards the role of microbial fuel cells for pharmaceutical wastewater treatment, in: Microbial Fuel Cell: Electricity Generation and Environmental Remediation. pp. 157–191.

Yoon, S.G., Yang, Y., Jin, H., Lee, W.H., Sohn, A., Kim, S.-W., Park, J., Kim, Y.S., 2019. A Surface-Functionalized Ionovoltaic Device for Probing Ion-Specific Adsorption at the Solid–Liquid Interface. Advanced Materials 31, 1806268. https://doi.org/10.1002/adma.201806268

Younas, M., Maryam, A., Khan, M., Nawaz, A.A., Jaffery, S.H.I., Anwar, M.N., Ali, L., 2019. Parametric analysis of wax printing technique for fabricating microfluidic paper-based analytic devices (μPAD) for milk adulteration analysis. Microfluid Nanofluid 23, 1–10. https://doi.org/10.1007/s10404-019-2208-z

Yu, B., Tian, J., Feng, L., 2017. Remediation of PAH polluted soils using a soil microbial fuel cell: Influence of electrode interval and role of microbial community. Journal of Hazardous Materials 336, 110–118. https://doi.org/10.1016/j.jhazmat.2017.04.066

Yu, K.M., Kim, S.-H., Park, J.-W., Sim, E.-S., Boampong, A.A., Kim, M.-H., 2020. Controllable liquid water sensitivity of polymer-encapsulated oxide thin-film transistors. Semiconductor Science and Technology 35. https://doi.org/10.1088/1361-6641/abad75

Yu, L., Gao, W., R Shamshiri, R., Tao, S., Ren, Y., Zhang, Y., Su, G., 2021. Review of research progress on soil moisture sensor technology.

Yuan, M., Sun, J., Wu, Y., Zheng, M., Sheng, C., Wu, C., Wang, Q., 2024. Enhanced electroreduction of low-concentration nitrate using a Cu-Pd bimetallic cathode system: Performance evaluation, mechanism analysis, and potential applications. Journal of Environmental Chemical Engineering 12, 113031. https://doi.org/10.1016/j.jece.2024.113031

Yue, X., Wang, Y., Zhao, Y., Xiang, H., Shu, S., Zhang, P., Zhang, J., Xue, J., Liu, J., Yu, D., 2024. A novel self-supported catalytic electrode preparation method: Synthesizing & printing Cu-based nanoparticles on nickel foam by cold plasma jet. Applied Surface Science 662, 160079. https://doi.org/10.1016/j.apsusc.2024.160079

Zaccarin, A., Iyer, G.M., Olsson, R.H., Turner, K.T., 2023. Fabrication and Characterization of Soil Moisture Sensors on a Biodegradable, Cellulose-Based Substrate. IEEE Sensors Journal 1–1. https://doi.org/10.1109/JSEN.2023.3299430

Zare, M.Y., 2010. Coupling RFID with supply chain to enhance productivity. Business Strategy Series 11, 107–123. https://doi.org/10.1108/17515631011026434

Zeng, X., Liu, Y., He, R., Li, T., Hu, Y., Wang, C., Xu, J., Wang, L., Wang, H., 2022. Tissue paper-based composite separator using nano-SiO2 hybrid crosslinked polymer electrolyte as

coating layer for lithium ion battery with superior security and cycle stability. Cellulose 29, 3985–4000. https://doi.org/10.1007/s10570-022-04499-5

Zeni, M., Ondula, E., Mbitiru, R., Nyambura, A., Samuel, L., Fleming, K., Weldemariam, K., 2015. Low-power low-cost wireless sensors for real-time plant stress detection. Presented at the ACM DEV-6 2015 - Proceedings of the 2015 Annual Symposium on Computing for Development, pp. 51–59. https://doi.org/10.1145/2830629.2830641

Zhang, C., Zhang, P., Wang, Y., Zhang, L., Hu, J., Zhang, W., 2022. Support Vector Machine Based Lithium-ion Battery Electrolyte Leakage Fault Diagnosis Method, in: 2022 4th International Conference on Smart Power & Internet Energy Systems (SPIES). Presented at the 2022 4th International Conference on Smart Power & Internet Energy Systems (SPIES), pp. 1880–1886. https://doi.org/10.1109/SPIES55999.2022.10082286

Zhang, F., Zhang, Z., Liu, Y., Leng, J., 2014. Shape memory properties of electrospun nafion nanofibers. Fibers Polym 15, 534–539. https://doi.org/10.1007/s12221-014-0534-z

Zhang, H., Wang, S., Tian, Y., Liu, Y., Wen, J., Huang, Y., Hang, C., Zheng, Z., Wang, C., 2020. Electrodeposition fabrication of Cu@Ni core shell nanowire network for highly stable transparent conductive films. Chemical Engineering Journal 390, 124495. https://doi.org/10.1016/j.cej.2020.124495

Zhang, X., Feng, G., Sun, X., 2024. Advanced technologies of soil moisture monitoring in precision agriculture: A Review. Journal of Agriculture and Food Research 18, 101473. https://doi.org/10.1016/j.jafr.2024.101473

Zhang, X., Ma, G., Shui, L., Zhou, G., Wang, X., 2022. Ni3N nanoparticles on porous nitrogen-doped carbon nanorods for nitrate electroreduction. Chemical Engineering Journal 430, 132666. https://doi.org/10.1016/j.cej.2021.132666

Zhang, X., Wang, Y., Liu, C., Yu, Y., Lu, S., Zhang, B., 2021. Recent advances in non-noble metal electrocatalysts for nitrate reduction. Chemical Engineering Journal 403, 126269.

Zhao, G., Chen, Y., Li, X.-F., Zhang, S., Situ, Y., 2020. Fabrication of highly proton-conductive chitosan whole-bio-membrane materials functionalized with adenine and adenosine monophosphate. Green Chemistry 22, 2426–2433. https://doi.org/10.1039/c9gc04104d

Zhao, J., Xu, J., Shi, L., 2024. Electrodeposition of a 3D dendritic Cu–Sn bimetallic alloy for electrocatalytic nitrate reduction to ammonia. New Journal of Chemistry 48, 13233–13237. https://doi.org/10.1039/D4NJ02343A

Zhao, X., Geng, Q., Dong, F., Zhao, K., Chen, S., Yu, H., Quan, X., 2023. Boosting the selectivity and efficiency of nitrate reduction to ammonia with a single-atom Cu electrocatalyst. Chemical Engineering Journal 466, 143314. https://doi.org/10.1016/j.cej.2023.143314

Zhao, Y., Liu, Y., Zhang, Z., Mo, Z., Wang, C., Gao, S., 2022. Flower-like open-structured polycrystalline copper with synergistic multi-crystal plane for efficient electrocatalytic reduction of nitrate to ammonia. Nano Energy 97, 107124. https://doi.org/10.1016/j.nanoen.2022.107124

Zhou, W., Xu, Z., Ross, D., Dignan, J., Fan, Y., Huang, Y., Wang, G., Bagtzoglou, A.C., Lei, Y., Li, B., 2019. Towards water-saving irrigation methodology: Field test of soil moisture

profiling using flat thin mm-sized soil moisture sensors (MSMSs). Sensors and Actuators B: Chemical 298, 126857.

Zhu, G., Ge, M., 2021. Study on efficient degradation of polyvinyl alcohol in aqueous solution. Environmental Challenges 4, 100176. https://doi.org/10.1016/j.envc.2021.100176

Zhu, Q., Lin, H., 2011. Influences of soil, terrain, and crop growth on soil moisture variation from transect to farm scales. Geoderma 163, 45–54.

Zhu, T., Chen, Q., Liao, P., Duan, W., Liang, S., Yan, Z., Feng, C., 2020. Single-Atom Cu Catalysts for Enhanced Electrocatalytic Nitrate Reduction with Significant Alleviation of Nitrite Production. Small 16, 2004526. https://doi.org/10.1002/smll.202004526

Zong, C., Yang, X., Chen, D., Chen, Y., Zhou, H., Jin, W., 2021. Rational tuning of the viscosity of membrane solution for the preparation of sub-micron thick PDMS composite membrane for pervaporation of ethanol-water solution. Separation and Purification Technology 255, 117729. https://doi.org/10.1016/j.seppur.2020.117729

Zurita, N., Garcia, S., 2022. Influence of supporting electrolyte on electrochemical formation of copper nanoparticles and their electrocatalytic properties. Journal of Electrochemical Science and Engineering 12, 253–264.

Zurita, N., García, S.G., 2023. Comparative study of electrodeposited copper nanoparticles on different substrates for their use in the reduction of nitrate ions. Results in Engineering 17. https://doi.org/10.1016/j.rineng.2022.100800

ACKNOWLEDGEMENTS

I begin by expressing my profound respect for Dr. Babasaheb Bhimrao Ramji Ambedkar, whose life, intellect, and unwavering commitment to equality and knowledge have been a guiding influence in my academic journey. His advocacy for scientific temper, education as a means of empowerment, and the dignity of labor has significantly shaped the motivation behind this work. This dissertation is dedicated to his vision of a just, rational, and self-reliant India.

The completion of this Ph.D. thesis has been made possible through the support, guidance, and encouragement of numerous individuals and institutions, to whom I express my sincere gratitude. I extend my heartfelt thanks to you, Nick. Although you were not directly involved in my project, your suggestions during the annual meetings were invaluable and insightful. I am grateful to you, Saket, for providing me with the opportunity to contribute to the farming community. I recall the day when you interviewed me, and I expressed my desire to help farmers in India, particularly in light of the distressing issue of farmer suicides in my region. You responded immediately, sharing your ongoing work with cotton farmers in the Vidarbha region, which strongly encouraged me to pursue research under your guidance. I am thankful to you for allowing me to work on and design the technical aspects of the project, which, once fully developed, may aid farmers in developing countries in managing water resources on their farms. Your encouragement and guidance, even when results did not meet expectations, were instrumental in maintaining my focus on this multidisciplinary research. Your strict yet supportive nature was akin to that of an elder brother, helping me navigate both academic and personal challenges during my Ph.D. journey.

I am also indebted to you, Ludovic, for your expert advice and guidance, without which this Ph.D. would have remained a distant aspiration. Despite not being from my department, you personally visited us during the annual meetings to provide insights into the project, offering both confidence and support. The mentorship of both Saket and Ludovic provided me with direction as well as the freedom to innovate, enabling me to explore this interdisciplinary research with confidence.

I express my sincere gratitude to the committee members for dedicating their valuable time to review my dissertation and provide a positive evaluation. I extend my thanks to Lydia and Betty, my departmental secretaries, for their assistance with scholarship forms throughout my Ph.D. journey. I am also grateful to Linda for her support with the visa extension process. My appreciation extends to TU Delft's International Office for their assistance with accommodation during the COVID-19 pandemic.

I am thankful to all the Water Lab staff for their support during my experiments, especially Armand and Bright for their help with ordering equipment and chemicals, as well as their assistance in the laboratory. I also want to acknowledge the Mechanical Engineering Lab staff, Julia and Matrick, for their support with my experiments. I am grateful to Plant-e for demonstrating the MFC setup and providing the exo-electrogenic bacteria. I express my gratitude to the Social Justice and Special Assistance Department, Government of Maharashtra, India, for awarding me the scholarship to pursue my Ph.D. at TU Delft, without which this endeavor would have been difficult. I also acknowledge BANAE, Nagpur, for the financial assistance during the pandemic.

I am thankful to Anjana, whose valuable suggestions and guidance as a senior helped me navigate various challenges during my Ph.D. journey. I am also appreciative of Diana, whose discussions and shared experiences provided relief during moments of frustration. I thank David for organizing departmental activities that facilitated socialization and relaxation amidst a busy Ph.D. schedule. I extend my gratitude to you, Soham. You were not just an IIT alumnus but also an academic senior and a friend. Your support as a co-author and colleague was instrumental in the publication of my first paper, which significantly enhanced my confidence and belief in my ability to complete my Ph.D.

I am also thankful to Peyman for giving me the opportunity to collaborate with the Mechanical Department and use its facilities. I am grateful to Prasad for his assistance with characterization experiments and for granting me access to the laboratories for various other experiments. I recall the day when I met Prasad at Prasaanth's residence, where he read my hand and assured me that I would complete my Ph.D., albeit with considerable effort. I am equally appreciative of Prasaanth for his positive outlook and for encouraging me to have faith in my efforts (karma), which helped me persist in this journey.

I extend my sincere gratitude to Ali for his assistance and guidance during my experiments. I also wish to thank Asif for our informal discussions related to laboratory work and other topics of interest. Furthermore, I am grateful to Tejas and Akhilesh for their support and engaging discussions during our lab work. I also appreciate the support of my colleagues Mrinal, Yuke, and Shou in the laboratory.

I extend my sincere gratitude to my colleagues for cultivating a supportive and serene work environment. I am particularly indebted to Ko for the invaluable assistance with accommodation during the pandemic, despite our brief association. I also wish to express my appreciation to Banafsheh, who has been more than a colleague, serving as a confidante with whom I could discuss a wide range of topics, from Ph.D.-related issues to personal matters. I fondly recall our office interactions, which often encompassed cultural exchanges, personal challenges, and academic difficulties. It is well known that discussing problems can ease their burden, and her guidance throughout my Ph.D. journey, particularly in addressing academic challenges, has been immensely beneficial. I am grateful to Shan for being a silent colleague and providing a peaceful environment in the office. I also appreciate my newly joined colleagues Joshua and Ana for contributing to a lively atmosphere.

I extend my sincere gratitude to my friends and colleagues - Sreenath, Mario, Reza, Sanjeeb, Jerom, Luuk, Bas, Chelsea, Bart, Judith, Ali, Alireza, Ibrahim, Changrang, Dengxiao, Alexandra, and Monica—for their invaluable contributions to my professional development and for enhancing my understanding through their diverse perspectives. I am also grateful to Sowmya and Vineet for sharing their experiences and providing guidance during my Ph.D. I especially appreciate the financial support received from Vineet and Sowmya during permit extensions. Furthermore, I am thankful to Vineet, Vivek, Aastha, Krishna, and Pooja for making this journey unforgettable. I also express my gratitude to Pankaj, Aparna, Pradeep, Vaishali, Amol, Karen, and Marco for their financial assistance during the permit extension period.

I extend my gratitude to my cousins - Harshwardhan, for assisting in times of need, Rahul, for arranging tickets; and Sujata, for providing emotional support. I also acknowledge Mamaji and Mami, Aakka and Mamaji, as well as other relatives who directly and indirectly contributed to my Ph.D. journey. Furthermore, I wish to express my appreciation to my

extended family, in-laws, and relatives, whose encouragement, practical support, and belief in my work were invaluable, even when the goal seemed distant.

I extend my profound gratitude to Shilpa for her understanding, sacrifices, and unwavering motivation, without which this work would not have been feasible. I recall the times when I experienced stress the day before weekly meetings and how you would deliberately tease me to help me relax.

Beyond the academic sphere, this journey would not have been possible without the unwavering love, sacrifices, and blessings of my family. I am deeply grateful to my grandparents, the late Madhav and the late Manjula Meshram, as well as my father, the late Moreshwar Meshram, and my mother, Maya Meshram. My father and mother have been the strong foundation of my values. They instilled in me the importance of education, discipline, and perseverance. During moments of doubt and difficulty, their calm yet steadfast support sustained me. Despite numerous financial and emotional challenges, I remain indebted to them for supporting my education.

I recall that while he was alive, my father would often inquire about the progress of my Ph.D. and the number of research papers I had published. Today, I have published research papers and have earned the highest academic degree (Ph.D.) from one of the world's leading universities, Delft University of Technology, however, my father is not here to witness his son using the title "Dr." before his name. I will always regret that I could not complete my Ph.D. during his lifetime.

I remember that some neighbours and relatives would question my parents, asking what would come of educating their son in good schools whether he would become a renowned engineer or doctor, or secure a government job. Yet, without expecting any immediate returns and regardless of financial hardships, they never wavered in their determination to provide me with a quality education. Today, I can proudly say that through their blessings and hard work, I have reached this stage of my life and have become both an engineer and a doctor. I also extend my special gratitude to my mother, who stood by me in every decision I made, whether right or wrong. I remember when I decided to resign from my government job to pursue a Ph.D. at that time, my father and many others opposed my decision. However, my mother convinced my father, stood firmly by my side, and supported my choice. She instilled in me the confidence that whatever I chose to do would be better than the past, for which I will always remain deeply grateful.

शैक्षणिक क्षेत्राच्या पलीकडे पाहिले असता, माझ्या कुटुंबाच्या अखंड प्रेमाशिवाय, त्यागाशिवाय आणि आशीर्वादांशिवाय हा प्रवास शक्य झाला नसता. माझे आजी-आजोबा दिवंगत माधव आणि दिवंगत मंजुळा मेश्राम, तसेच माझे वडील दिवंगत मोरेश्वर मेश्राम आणि माझी आई माया मेश्राम यांच्याप्रती मी मनापासून कृतज्ञ आहे. माझे बाबा आणि आई हे माझ्या मूल्यांचे भक्कम अधिष्ठान राहिले आहेत. शिक्षणाचे महत्त्व, शिस्त आणि चिकाटी यांची शिकवण त्यांनी मला दिली. शंका आणि अडचणींच्या क्षणी त्यांची शांत पण दृढ साथ मला लाभली. विविध आर्थिक व भावनिक अडचणी असूनही मला शिक्षण देण्यासाठी त्यांनी दिलेल्या पाठिंब्याबद्दल मी त्यांचा ऋणी आहे.

मला आठवते, हयात असताना बाबा नेहमी माझ्या पीएच.डी.ची प्रगती आणि मी किती संशोधन लेख (पेपर) प्रकाशित केले आहेत याची चौकशी करायचे. आज मी संशोधन लेख प्रकाशित केले आहेत आणि जगातील आघाडीच्या विद्यापीठांपैकी एक असलेल्या डेल्फ्ट युनिव्हर्सिटी ऑफ टेक्नॉलॉजी येथून सर्वोच्च शैक्षणिक पदवी (पीएच.डी.) प्राप्त केली आहे, मात्र "डॉ." ही उपाधी नावापुढे लावलेला त्यांचा मुलगा पाहण्यासाठी बाबा आज माझ्यासोबत नाहीत. त्यांच्या हयातीत मी पीएच.डी. पूर्ण करू शकलो नाही, याची खंत मला नेहमी राहील.

मला आठवते, काही शेजारी आणि नातेवाईक माझ्या पालकांना म्हणायचे की इंग्लिश शाळेत शिकवून काय होणार आहे? तुमचा मुलगा काय मोठा इंजिनिअर किंवा डॉक्टर होणार आहे का, किंवा त्याला कुठे शासकीय नोकरी मिळणार आहे का? मात्र फळाची अपेक्षा न ठेवता आणि

आर्थिक अडचणींची पर्वा न करता तुम्ही मला दर्जेदार शिक्षण देण्याचा निर्धार कधीही सोडला नाही. आज मी अभिमानाने सांगू शकतो की त्यांच्या आशीर्वादामुळे आणि कष्टामुळे मी आज इथपर्यंत पोहोचलो असून आज एक इंजिनिअर तसेच एक डॉक्टर झालो आहे.

माझ्या आईचेही मी विशेष आभार मानतो, कारण मी घेतलेल्या प्रत्येक निर्णयात तो योग्य असो वा अयोग्य तिने मला कायम साथ दिली. मला आठवते, जेव्हा मी पीएच.डी. करण्यासाठी माझ्या शासकीय नोकरीचा राजीनामा देण्याचा निर्णय घेतला, तेव्हा बाबा आणि इतर अनेक जण या निर्णयाच्या विरोधात होते. मात्र तिने बाबांना समजावले, ठामपणे माझ्या पाठीशी उभी राहिली आणि माझ्या निवडीला पाठिंबा दिला. मी जे काही करेन ते पूर्वीपेक्षा नक्कीच अधिक चांगलेच असेल, असा आत्मविश्वास तू माझ्यात निर्माण केलास, त्याबद्दल मी तुझा सदैव ऋणी राहीन.

I also sincerely thank my siblings my elder sister, the late Mrunalini (Taai), my younger sister Apeksha, and my younger brother Vaibhav for their unwavering emotional support, for which I will always remain indebted.

This achievement is not solely mine but serves as a humble tribute to my Aai and Baba, for their unwavering patience, encouragement, and dedication. Without your support, this milestone would not have been attainable. Finally, I would like to say: *"Every achievement demands sacrifice; nothing truly valuable comes without it."*

Sumit Moreshwar Meshram
Delft, Netherlands, February 2026

CURRICULUM VITAE

Sumit Maya Moreshwar Meshram

S.M.Meshram@tudelft.nl www.linkedin.com/in/sumitmeshram16/ 06 1708 0668

Profile

A water resources engineer and researcher with 8.5 years of experience - 5.5 years of research and in-house development of a biodegradable soil moisture sensor, and 3 years of field experience as a government irrigation engineer & manager of water and infrastructure projects.

Work Experience

- **2015-2018: Assistant Engineer (**Water resources Department)
  Government of Maharashtra, India.

- **2019-2019**: **Assistant Professor (**Civil Engineering Department)
  Wainganga College of Engineering and Management, Nagpur, India.

Education

- **2019 - 2025**: **PhD (**Water Resources Department)
  Delft University of Technology, Delft, South Holland, The Netherlands

- **2012 - 2014**: **MTech** (Geomatics Engineering)
  Indian Institute of Technology, Roorkee, Uttarakhand, India

- **2007 - 2011**: **BE** (Civil Engineering)
  Rashtrasant Tukadoji Maharaj Nagpur University, Nagpur, India

Research Projects

- **PhD Thesis** - Design of biodegradable soil moisture sensor powered by bacteria charged paper batteries.
- **MTech Thesis** - Comparing the Reliability of Single Frequency GPS Receivers: A Field Study

Workshops

- Process Development and Process Evaluation in Biorefinery Industry
- Giving plants a voice

Skills

- **Experimental skills**: Experimental design, Sample preparation, Chemical analysis
- **Soft Skills**: Product development, Image editing, Video editing

Softwares and Tools

- Arduino GIS, AutoCAD, Origin, Potentiostat, data logger, H-type fuel cell

Languages

Hindi - Native English - Proficient
Marathi - Native Dutch - Elementary

LIST OF PUBLICATIONS

RESEARCH PAPER

1. **Maya Moreshwar Meshram, S**., Gonugunta, P., Taheri, P., Jourdin, L., Pande, S. (2025). Preparation of biodegradable membrane utilizing chitosan and polyvinyl alcohol, and assessment of its performance after coating with graphene conductive ink. Frontiers in Membrane Science and Technology, Volume 4 – 2025

2. **Maya Moreshwar Meshram, S**., Gonugunta, P., Taheri, P., Jourdin, L., Pande, S. (2025). Investigating the influence of a thin copper film coated on nickel plates through physical vapor deposition for electrocatalytic NO_3^- reduction. Frontiers in Materials, Volume 12 - 2025.
3. **Maya Moreshwar Meshram, S.,** Adla, S., Jourdin, L., Pande, S. (2024).Review of low-cost, off-grid, biodegradable, in situ autonomous soil moisture sensing systems: Is there a perfect solution? Computers and Electronics in Agriculture 225, 109289.

4. van Hateren T.C., Jongen H. J., Al-Zawaidah H., Beemster J. G.W., Boekee J., Aerts J. P.M., Agoungbome S.M.D., **Maya Moreshwar Meshram, S.**, et.al (2023). Where should hydrology go? An early-career perspective on the next IAHS Scientific Decade: 2023–2032. Hydrological Sciences Journal 2023.

5. **Maya Moreshwar Meshram, S**., Pande, S. (2025). Design of origami-inspired paper batteries as a power source for soil moisture sensing system. (Submitted)

ABSTRACTS AND CONFERENCE PRESENTATIONS

1. **Maya Moreshwar Meshram, S.,** Jourdin L., Pande S. (2022). Design of soil moisture sensor powered by bacteria charged paper battery, EGU General Assembly Conference Abstracts, EGU22-10140

2. **Maya Moreshwar Meshram, S.**, Jourdin L., Pande S. (2021). Design of soil moisture sensor powered by bacteria charged paper battery, Delft International Conference on Sociohydrology, 6-8 September 2021, The Netherlands
3. **Maya Moreshwar Meshram, S.**, Jourdin L., Pande S. (2021). Design of soil moisture sensor powered by bacteria charged paper battery, International Symposium on Water Sustainability: Challenges, Technologies & Opportunities, March 22-25, 2021